ANNÉE 2017

THÈSE / UNIVERSITÉ DE RENNES 1
sous le sceau de l'Université Bretagne Loire

pour le grade de

DOCTEUR DE L'UNIVERSITÉ DE RENNES 1

Mention : Biologie

École doctorale
Biologie-Santé

Théo Lebeaupin

Préparée à l'unité de recherche UMR6290, IGDR
Institut de Génétique et Développement de Rennes
Université de Rennes 1, UFR SVE

Intitulé de la thèse : Multiscale analysis of poly-ADP-ribosylation dependent chromatin remodeling mechanisms at DNA breaks

Thèse soutenue à Rennes le 18 Octobre 2017

devant le jury composé de :

Sébastien HUET
MCU, UR1 / *directeur de thèse*

Olivier GADAL
DR2, CNRS / *rapporteur*

Françoise DANTZER
DR2, CNRS / *rapporteur*

Anna CAMPALANS
Chercheur E5, CEA / *examinateur*

Denis MICHEL
PU, UR1 / *président du jury*

Gyula TIMINSZKY
Group leader, LMU / *examinateur*

Table of contents

ACKNOWLEDGMENTS

First of all, I would like to thank Gyula and Sébastien. First time I met with you was right after I got my master's degree and couldn't keep working on my M2 internship project. You guys came to me, out of nowhere, and offered me the wonderful opportunity to work on this project. Thank you for putting your faith in me back then, and thank you for your trust in me throughout this PhD. Gyula, I regret that we did not spend more time working together, as it was originally planned, but I really enjoyed the little time we did and the chats we had these last years trying to make sense out of my weird results. I keep a very fond memory of my time in Munich, as short as it was. I was a bit anxious to go work in another country, in another language, without knowing anybody, but you made it all so easy for me over there, I ended up having a great time. So, thank you, and I wish you the best of luck in your future endeavors.

Sébastien, you taught me almost everything I know about microscopy and image analysis, always finding time in your busy schedule to answer my questions or simply chat about results and possible future experiments. Thank you for having given me a perfect combination of freedom and guidance throughout these three years. You might be one of the best teachers I have met, always cool and patient, always finding solutions even to the most improbable problems, and caring enough that you are willing to explain ten times over the same maths or physics stuff that don't come logically to me. For this, your kindness and understanding, and incidentally the fact that you were willing to spend all your remaining lab money so that I could still finish my PhD under these weird circumstances, thank you.

I would like to thank Olivier Gadal and Françoise Dantzer for accepting to review my work, as well as Denis Michel and Anna Campalans for being part of my examination jury. I would also like to thank Badia, and Nathalie Théret from VAS, who agreed to go along with my weird situation and made my PhD submission possible.

I would also like to thank members of the team. Starting with Hafida, you took a big sistery-role from the start, I have to admit it scared me a little at the beginning, but we ended up becoming good friends and my PhD wouldn't have been the same if it wasn't for you. I think we complemented each other nicely and I always valued your opinion and enjoyed our little chats in the office. Thank you for your good mood, and your not so good mood when it came to cursing at the microscopes crashing in the middle of an experiment, it's always nice to have someone backing you up when cursing at the microscope! I wish you all the best for your future career. Catherine, you're an invaluable part of the team and you make it

all so easy for us it's unfair for other Phd students. You're always taking the time whenever I have questions or need your help while making seem effortlessly all the different things you manage to do, thank you for all your help. Thanks also to Benjamin, we did not spend that much time working together but those afternoon at the microscope were fun, and your help for translation in your second mother tongue, the MatLab language, was really helpful.

Special thanks also to the members, past and present, of the labs of Marc Tramier and Jacques Pécréaux. These 3-teams lab meetings that you put in place with many different people coming from various backgrounds are, in my opinion, way more instructive than any other I have been a part of. For helpful discussions and hindsight during or outside these lab meetings, thank you. I would also like to thank Stéphanie and Clément from the MRic platform. The spinning disk, as well as the SP8 in the end, were like second offices to me, you both created a happy work environment there and were always available whenever I had a problem or a specific question regarding the microscopes and my experiments, thank you.

I would also like to thank Géraldine, the executive assistant of the institute. You are so much more than that, you might just be the glue holding the whole IGDR together. You always had time for me, answering my diverse, and sometimes stupid questions, always caring and harboring a reassuring smile. Thank you. Lastly, many thanks to all the people that, both inside and outside of the institute, whether at coffee breaks or outside work, contributed at making these three years as enjoyable as possible!

I have to finish these acknowledgments by thanking my wife, Christelle. You do not always get what I do, and I know that my work taking so much time in our lives is not easy for you. Yet, you are always there for me, sharing the lows and the highs, enduring my bad moods whenever my experiments went wrong, patiently coping with my late evenings at the microscope or in front of the computer working, helping me out with administrative stuff or proof-reading at 2 a.m. because I finished writing at the last possible moment. I have absolutely no doubt that I wouldn't be there if it wasn't for you. Thank you for everything.

ABBREVIATIONS LIST

3C: Chromatin conformation capture
53BP1: p53-binding protein 1
ADP: Adenosine diphosphate
Alc1: Amplified in liver cancer 1
APLF: Aprataxin and PNK-like factor
ARH: ADP-ribosylhydrolase
ART domain: ADP-ribosyltransferase domain
ARTD: ADP-ribosyltransferase diphtheria toxin-like
ATM: Ataxia telangiectasia mutated
ATP: Adenosine triphosphate
ATR: ATM- and RAD3-related
BRCA1: Breast cancer 1
BRCT domain: BRCA1 C-terminal domain
BZip domain: Basic leucine zipper domain
CAP: Chromatin-associated protein
CAT domain: Catalytic domain
CEBP: CCAAT enhancer-binding protein
CHD domain: Chromodomain helicase DNA-binding domain
CHD4: Chromodomain helicase DNA-binding protein 4
Chdk1: Checkpoint kinase 1
CHFR: Checkpoint with FHA and RING finger
CRISPR/Cas9: Clustered Regularly Interspaced Short Palindromic Repeats / CRISPR-associated protein-9 nuclease
CTCF: CCCTC-binding factor
C-ter: C-terminal region
DDR: DNA damage response
DNA: Deoxyribonucleic acid
DNA-PK: DNA-dependent protein kinase
DNMT: DNA methyltransferase
DSB: DNA double-strand break
(E)GFP: (Enhanced) Green Fluorescent Protein
ERRC1: Excision repair cross-complementation group 1
ES cells: Embryonic stem cells
FACS: Fluorescence-activated cell sorting
FCS: Fluorescence correlation spectroscopy
FDA: Food and drug administration
FHA domain: forkhead-associated domain
FISH: Fluorescence in situ hybridization
FRAP: Fluorescence recovery after photo-bleaching
HAT: histone acetyltransferase
HMG: High mobility group
HNF-3: Hepatocyte nuclear factor 3
HP1: Heterochromatin protein 1
HR: Homologous recombination
INO80: Inositol requiring mutant 80

ISWI: Imitation switch
MARylation: Mono-ADP-ribosylation
MBD: Methyl-CpG binding domain
MeCP2: Methyl-CpG binding protein 2
MRE11: Meiotic recombination 11
MRN complex: Mre11-Rad50-Nbs1 complex
MSD: Mean square displacement
NAD: Nicotinamide adenine dinucleotide
NBS1: Nijmegen breakage syndrome 1
NER: Nucleotide-excision-repair
NF-KB: Nuclear factor-kappa B
NHEJ: Non-homologous end-joining
NTR: N-terminal region
OB-fold domain: Oligonucleotide/Oligosaccharide-binding-fold domain
p300/CBP: p300/ CREB-binding protein
PAGFP: Photoactivatable green fluorescent protein
PAR chains: Poly-ADP-ribose chains
PARG: PAR glycohydrolase
PARP: Poly(ADP-ribose) polymerase
PARylation: Poly(ADP-ribosyl)ation
PATagRFP: Photoactivatable tag red fluorescent protein
PBM: PAR-binding motif
PBZ: PAR-binding zinc finger
PCNA: Proliferating cell nuclear antigen
PIKK family: Phosphatidylinositol 3-kinase-related kinase family
PIN domain: PilT N-terminus domain
PTM: Post-translational modification
RFC: Replication factor C
RG/RGG motifs: Regions rich in arginine and glycine
RNA: Ribonucleic acid
RNF: Ring finger protein
RPA: Replication protein A
RRM: RNA recognition motif
RRM: RNA recognition motif
SACS: Small-angle X-ray scattering
SEM: Standard error of the mean
SWI/SNF: Switch/sucrose non-fermentable
TAD: Topologically associating domain
TARG1: Terminal ADP-ribose protein glycohydrolase 1
Tet (enzymes): Ten Elevated Translocation
TF-II complex: Transcription factor 2 complex
U2OS: Human osteosarcoma
UBF: Upstream binding factor
XLF: XRCC4-like factor
XPA/XPF/XPG: xeroderma pigmentosum group A/F/G
XRCC4: X-ray repair cross-complementing protein 4

FIGURES LIST

ABSTRACT

For a long time, chromatin was only described as a mean to fit the two-meters long DNA molecule into a nucleus of only a few microns. It is admitted today that chromatin actually represents a key element in the regulation of all nuclear functions dependent on DNA. In the context of UV-induced DNA damage, chromatin undergoes a rapid and transient relaxation which leads to an expansion of the damaged area to 1.5 times its original size. While this chromatin response to damage is associated with a higher DNA accessibility, the link between those two phenomena, as well as the mechanisms driving them, are still poorly understood.

Using live-cell imaging and laser micro-irradiation to induce DNA damage on specific nuclear areas, this work allowed to gain hindsight on the predominant role played by PARP1 in the DNA damage-induced chromatin relaxation. Indeed, showing that PARP1 at DNA damage sites can both induce chromatin compaction through its recruitment at DNA breaks or chromatin decondensation through its PARylation activity helped reconcile its apparent opposite effects described in the literature. A focus was also made on the linker histone H1, as it displays a peculiar behavior upon DNA damage, being rapidly released from the site of DNA lesions. Even if the driving force behind H1 release from damaged chromatin areas has not been identified yet, its behavior suggests that H1 might play a part in chromatin relaxation or in increasing DNA accessibility upon DNA damage. Lastly, combining photo-activation techniques and fluorescence correlation spectroscopy, experiments were performed in order to understand the physical environment that damaged, relaxed chromatin constitutes. We report here that, while enhanced binding of random DNA binding factors is observed in the damaged chromatin area, no significant change is observed in the macromolecular crowding levels that could potentially explain this enhanced binding, as well as a higher DNA accessibility.

RÉSUMÉ

Au sein des noyaux de chacune de nos cellules, l'ADN, porteur de l'information génétique de l'organisme, n'est pas nu. Il est en permanence associé à de nombreuses protéines, formant ainsi une structure à l'architecture complexe et dynamique : la chromatine. La chromatine n'est pas uniquement une forme de compaction nécessaire afin d'inclure une molécule d'ADN d'environ deux mètres de long dans un noyau de quelques micromètres de diamètre, mais est aujourd'hui reconnue comme étant un élément majeur de contrôle et de régulation de toutes les fonctions de la cellule dépendantes de l'ADN. Son architecture s'étend sur plusieurs niveaux. En premier lieu, l'ADN s'enroule autour d'un octamère formé par l'association de paires de quatre histones de cœur, H2A, H2B, H3 et H4, formant ainsi l'unité structurelle de la chromatine : le nucléosome. L'association de multiples nucléosomes tout au long de la fibre d'ADN est renforcée par l'addition d'un cinquième histone, l'histone H1, qui s'associe à l'extérieur de cette structure, interagissant à la fois avec l'ADN nucléosomique et inter-nucléosomique. À l'échelle supérieure, la conformation de cette fibre de chromatine est encore sujet de débats et plusieurs modèles ont été proposés. Le niveau d'organisation suivant fait appel à la formation de boucles qui se regroupent pour faire apparaître des domaines fonctionnels appelés TADs (topologically associating domains). Ces domaines vont s'associer en compartiments au sein de chaque chromosome, puis ces compartiments vont se regrouper pour former les territoires chromosomiques qui se répartissent au sein du noyau des cellules.

Au sein de cette structure, l'intégrité de l'ADN est constamment menacée. En effet, des dommages au sein de l'ADN, induits par des processus endogènes comme des erreurs de réplication ou l'action de produits du métabolisme néfastes pour l'ADN, ou des agressions exogènes comme l'exposition aux rayons UV ou l'action de polluants environnementaux, surviennent en permanence dans nos cellules. De nombreux mécanismes cellulaires existent pour reconnaitre et réparer ces dommages de l'ADN. Parmi les premières réponses de la cellule face à de telles agressions, une décondensation rapide de la chromatine se produit au niveau des zones endommagées. On observe également dans ces zones décondensées une plus grande accessibilité de l'ADN pour les protéines de réparation. Ces deux effets ne sont, à l'heure actuelle, toujours pas liés, car les mécanismes les produisant sont encore mal décrits.

Afin d'obtenir une meilleure compréhension du phénomène de décondensation de la chromatine suite aux dommages de l'ADN, une technique a été développée au sein de notre équipe pour visualiser la chromatine à l'aide d'histones H2B liés à une protéine fluorescente photo-activable. Cette technique nous permet, après traitement des cellules au Hoechst, de photo-activer la chromatine et d'endommager l'ADN dans des zones spécifiques avec une même micro-irradiation laser pour étudier la décondensation de la chromatine en cellules vivantes. En couplant cette technique à une autre technique de photo-manipulation de protéine attachée à un fluorophore, j'ai également étudié la dynamique de l'histone H1 au sein des zones d'ADN endommagé. Étant le plus mobile des histones, je me suis demandé s'il pouvait jouer un rôle dans la décondensation de la chromatine suite aux dommages de l'ADN car sa présence est souvent liée à une compaction plus forte de la chromatine. Pour finir, j'ai utilisé une approche de spectroscopie de corrélation de fluorescence pour étudier la dynamique locale de différentes protéines à l'intérieur des zones d'ADN endommagé afin d'obtenir une meilleure compréhension de l'environnement chromatinien que constitue la chromatine décondensée.

Ces travaux ont permis d'élucider le rôle spécifique de la protéine PARP1 (poly(ADP-ribose) polymerase 1) dans la décondensation de la chromatine. En effet, nous avons démontré que PARP1 possède un double rôle dans la régulation du niveau de compaction de la chromatine et que ce lui-ci est régulé par la présence ou non de dommages de l'ADN. PARP1 est recruté rapidement et en grande quantité au niveau des zones d'ADN endommagées. La présence de dommages de l'ADN va entraîner son activation catalytique et la production massive de chaînes de PAR (poly(ADP-ribose)). Ceci va, à la suite du recrutement de protéines spécifiques reconnaissant les chaînes de PAR, entraîner la décondensation de la chromatine. À l'inverse, lorsque l'on utilise l'inhibiteur spécifique de la PARylation AG-14361, PARP1 est recruté aux dommages mais incapable de synthétiser des chaînes de PAR, ce qui va entraîner une surcondensation de la chromatine au niveau des zones endommagées.

Par la suite, je me suis intéressé à la dynamique de la protéine H1 au sein et hors des zones de dommages de l'ADN. En photo-activant les histones H2B et H1 simultanément à l'induction des dommages, j'ai pu constater que l'histone H1 présent au niveau de l'ADN au moment de l'induction des dommages se dissocie rapidement de la chromatine, pouvant expliquer en partie la décondensation de la chromatine. Considérant la rapidité avec laquelle H1 quitte la zone endommagée, ma première hypothèse a été que son départ était lié à l'action de PARP1. En effet, PARP1 est recruté très rapidement aux zones de cassures et est connu pour PARylé H1 dans d'autres contextes, ou encore le remplacer par compétition au niveau de son site de liaison au nucléosome dans certaines régions chromatiniennes. J'ai démontré que le départ de l'histone H1 des zones de cassures est en fait indépendant de la PARylation, car celui-ci s'effectue même sous l'effet de l'inhibiteur de la PARylation. De plus, j'ai pu constater, en utilisant une lignée cellulaire PARP1 KO, que la dissociation de H1 ne dépend pas non plus de la protéine PARP1 en elle-même et qu'elle ne nécessite pas d'énergie possiblement fournie par l'ATP. Cette exclusion est également indépendante de protéines clés des voies de réparation de l'ADN, ATM et DNA-PK, qui sont recrutées rapidement aux zones de dommages et connues pour interagir avec H1. De façon intéressante, cette exclusion se produit donc dans toutes les conditions testées dans mes expériences, et donc même en l'absence de décondensation obtenue par l'utilisation d'inhibiteurs de la PARylation. Ceci suggère que l'exclusion de H1 des zones de dommages n'est pas suffisante pour induire une décondensation, mais pourrait tout de même être un phénomène nécessaire pour qu'une decondensation de la chromatine puisse se produire. Même si les mécanismes entraînant cette exclusion restent, à ce jour, inconnus, l'exclusion de H1 des zones de dommages est un phénomène très intéressant, et devrait, à mon avis, faire l'objet d'études ultérieures pour déterminer précisément sa fonction et caractériser les mécanismes qui en sont responsables.

Pour finir, mon attention s'est portée sur la décondensation de la chromatine en elle-même et les modifications qu'elle pouvait induire considérant l'accessibilité de l'ADN aux zones endommagées. Pour ce faire, je me suis intéressé au modèle de l'encombrement moléculaire qui suggère que des protéines auront plus de mal à naviguer dans un environnement où de nombreuses autres molécules sont présentes. En effet, l'espace nucléaire est supposé être très encombré car la chromatine représente à elle seule 30% à 50% du volume nucléaire. Je me suis alors demandé si la decondensation de la chromatine pouvait être un moyen de réduire l'encombrement aux zones endommagées et permettre ainsi aux protéines de la réparation d'accéder plus facilement et plus rapidement à l'ADN endommagé. En couplant des techniques

de FRAP (Fluorescence Recovery After Photo-bleaching) et de FCS (Fluorescence Correlation Spectroscopy), j'ai pu constater que la faible augmentation du volume accessible pour la GFP aux zones de dommages, protéine qui n'interagit avec aucun élément présent dans le noyau des cellules, ne peut pas expliquer l'augmentation d'accessibilité de l'ADN. De plus, aucun changement n'est observé par FCS quant à la vitesse de diffusion de protéines au sein des zones de dommages. J'en ai conclu que la diminution du niveau d'encombrement observée est trop faible pour avoir un impact visible sur la dynamique de la GFP au sein des zones endommagées, probablement dû au fait que les chaînes de PAR produites par PARP1, ainsi que les protéines qui s'y attachent, comblent l'espace nouvellement libéré par la décondensation, et que la conformation spatiale de la chromatine joue un rôle plus important dans le cas de la diffusion des protéines que dans le cas du volume accessible. Par ailleurs, j'ai pu constater que des molécules non impliquées dans les voies de réparation de l'ADN, comme LacI, TetR, ou BZip, interagissent plus fortement avec l'ADN dans les zones endommagées. Ceci nous conforte dans l'idée que l'ADN est plus accessible pour les protéines de la réparation de l'ADN, même probablement pour toutes les protéines, après dommages et décondensation, même si les mécanismes moléculaires le permettant restent inconnus.

INTRODUCTION

During my Ph.D., my work has been focused on chromatin dynamics upon DNA damage. In order to study the impact of DNA damage on chromatin structure and function, one must first understand the architecture of chromatin and grasp the complexity of its multi-layered organization. Therefore, the first part of this introduction will be dedicated to the description of chromatin components and their association at different levels to form this complex structure. In the second part, looking at chromatin structure through time, I will present the latest data known on chromatin dynamics and the mechanisms driving those chromatin structure modifications. As chromatin displays an inhomogeneous and complex structure, as well as countless means to modify and adapt this structure to different stimuli, I will try in the next section to gather information on the possible functional roles of chromatin architecture and dynamics. In the last part, I will introduce the general context surrounding my work on chromatin, DNA damage, and describe the role of several molecular players that are at the center of this study.

Chromatin Structure

Chromatin has been the focus of intense research for over a hundred years and still is. Yet, all structural levels of its architecture in an undamaged, unstressed state, are not fully understood, or even described, demonstrating the complexity of its organization. Going from the deoxyribose nucleic acid double helix up to the mitotic chromosomes, I will here draw the picture of the structural organization of chromatin at different levels, as we currently understand it.

DNA

Research on DNA started more than a hundred years ago. Since the first discovery of a novel molecule that was neither protein nor lipid in the nucleus of leukocytes by Friedrich Miescher in 1868, many scientists have tried to elucidate the purpose of this "nuclein". It took fifty years and a lot of efforts before nucleic acids were recognized as the carriers of genetic information in all cells [Dahm, 2008]. In 1953, the structure of DNA was elucidated by Watson and Crick and most of DNA's secrets were cracked in the following decade to form the picture that we know today (fig. 1) [Dahm, 2008; Watson and Crick, 1953]. DNA is a macromolecule formed by two polynucleotides strands coiled around each other to form a double helix. Each nucleotide of these strands is constituted of a nucleobase (cytosine (C), guanine (G), adenine (A), or thymine (T)), a sugar (deoxyribose) and a phosphate group (fig). Due to its composition,

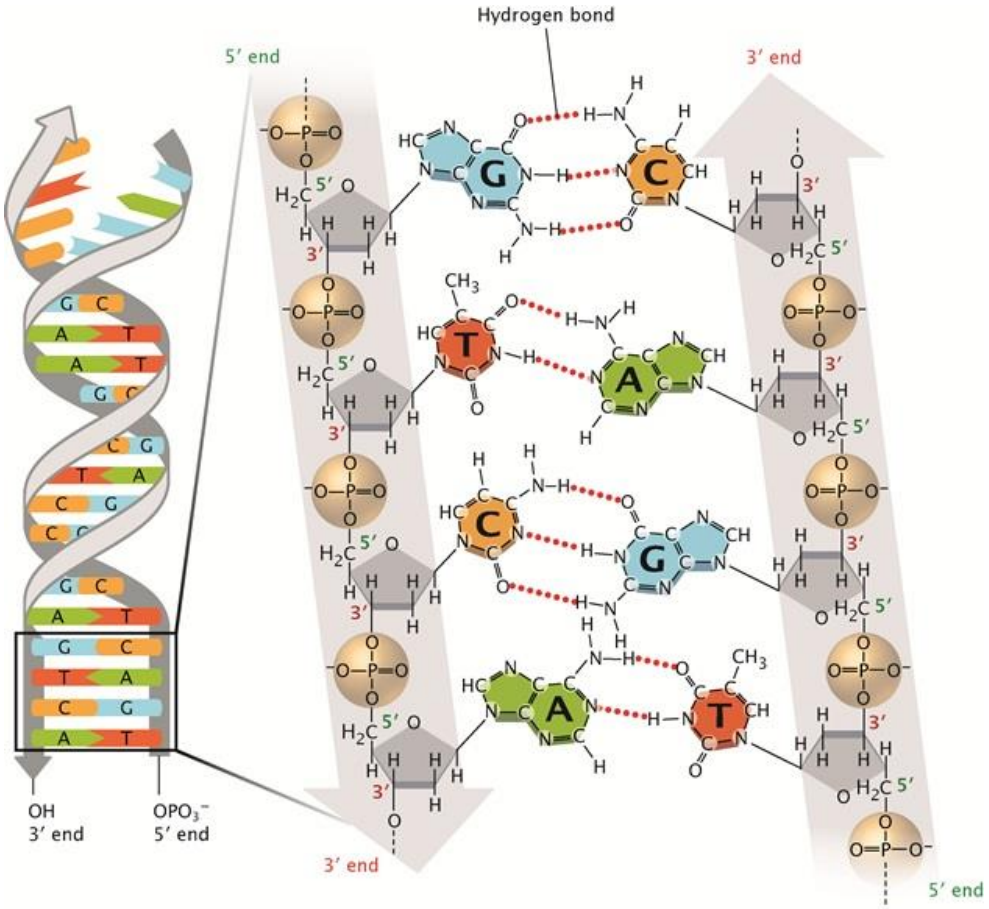

Figure 1: Structure of DNA.
Two sugar-phosphate backbones (gray) run anti-parallel from each other. Each sugar-phosphate group is linked to one of the four bases of DNA, glycine (blue), cytosine (orange), thymine (red), and adenine (green). Two hydrogen bonds connect T to A, and three hydrogen bonds connect G to C. From Pray, 2008.

DNA is an extremely resistant and stable molecule with a high negative charge. Moreover, DNA, in every cell, contains the whole genetic information of the organism, meaning that there is no loss of nonrelevant DNA for a specific cell-type during cellular differentiation, as it was initially proposed [Dahm, 2008]. This means that specific cellular functions come from the use or not of different genes in specific cell types.

In order to fit the 2-meters long DNA molecule in a nucleus of around 10 µm of diameter, and in order to specify which genes should be expressed or not within a given cell, DNA must adopt a highly organized 3-dimensional structure allowing the creation of particular transcriptionally active and inactive regions.

The structural unit of chromatin: the nucleosome

Early studies on chromatin conformation discovered a structural unit composed of a core particle, the nucleosome, and linker DNA [Kornberg, 1974]. The structure of the nucleosome core particle was rapidly solved at low resolution using x-ray crystallography [Richmond *et al.*, 1984], allowing the description of DNA wrapped around a disk-like shaped protein complex. It was then refined ten years later using the same technique, allowing for a high-resolution structure to be validated and the precise path of DNA to be characterized [Luger *et al.*, 1997]. The protein complex is assembled with 2 copies of each of the four core histone proteins H2A, H2B, H3, and H4. Around this octamer of histones are wrapped 146 base pairs of DNA on approximately 1.7 superhelical turns to form the nucleosome (fig. 2). Histones are highly positively charged proteins with a central globular domain placed towards the center of the nucleosome and two unstructured tails with one usually coming out of the nucleosome [Kouzarides 2007]. Therefore, strong electrostatic interactions between the positive histones and the negative DNA allow this structure to stay very stable [Ettig *et al.*, 2011]. Histone tails allow for specific modifications that are involved in the regulation of the chromatin compaction state and the recruitment of many chromatin interactors [Kouzarides 2007]. Nucleosomes decorating sparsely chromatin separated by linker DNA of a variable length, usually inferior to 100 bp, results in a "beads-on-a-string" fiber with a diameter of 11 nm [Davey *et al.*, 2002]. This nucleosomal array represents the first level of chromatin compaction. In order to stabilize this molecular array and promote the formation of higher chromatin compaction states, an additional key protein is associated with the nucleosomes: linker histone H1.

Linker histone H1: master regulator of the internal architecture of chromatin

H1 is the fifth histone, also called linker histone, as it will clamp the nucleosomal particle interacting simultaneously with core histones and the two ends of DNA coming in and out of the nucleosome (fig. 3). This model is supported by a lot of evidence [Allan *et al.*, 1980; Syed *et al.*, 2010]. However, since a high-

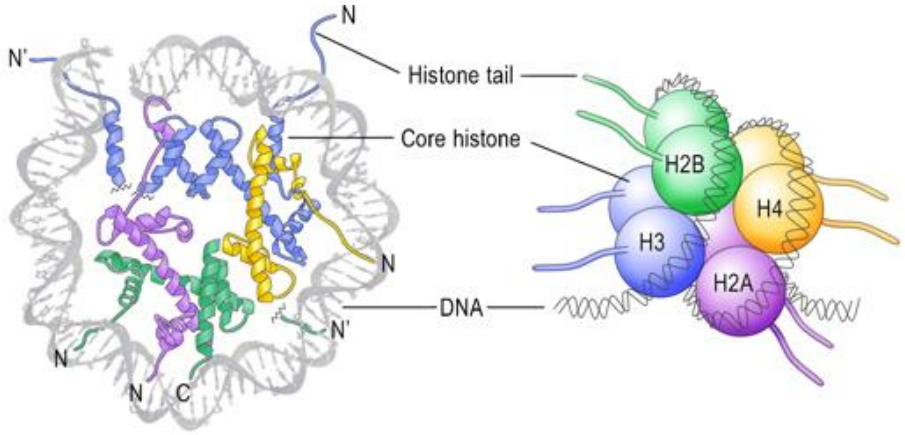

Figure 2: Structure of the nucleosome.
Two of each of the four histones are assembled into a protein octamer. Approximately 150 base pairs of DNA are wrapped around this structure in a bit less than two turns to form the nucleosome. At least one of each histone tails is coming out of the nucleosome and can be, depending on the conformation of chromatin, highly accessible for post-transcriptional modification enzymes.
From Gräff and Mansuy, 2008.

resolution structure of the chromatosome, meaning the nucleosome with the linker DNA and linker histone, is still lacking, the precise positioning of H1 both in the nucleosome particle and its involvement in higher order structures are still under debate [Robinson and Rhodes, 2006; Hamiche *et al.*, 1996; Pruss *et al.*, 1996]. Same as the other histones, H1 is highly positively charged and composed of a central globular domain and two unstructured tails, the C-terminal tail being the longest. All three domains are presumed to be important for the proper binding of H1 on the nucleosome [Hutchinson *et al.*, 2015; Syed *et al.*, 2010]. Being outside of the histone octamer, H1 is dramatically more dynamic than core histones and shows a residency time of no more than a few minutes on chromatin [Misteli, 2000], compared to core histones that display a residency time of several hours [Hergeth, 2015].

H1 incorporation into chromatin not only affects the conformation of individual nucleosomes, but also the chromatin fiber folding [Bednar *et al.*, 2015]. Indeed, H1 brings the two DNA ends, coming in and out of the nucleosome, closer together and compacts the structure [Hamiche *et al.*, 1996; Syed *et al.*, 2010], preventing access to the underlying DNA, as shown by the first DNAse experiments [Robinson and Rhodes, 2006; Whitlock and Simpson, 1976; Simpson, 1978], and preventing the possible spontaneous unwrapping of nucleosomal DNA, rendering it inaccessible to chromatin interactors. It is important to note, however, that some transcription factors, such as NF-KB, have been shown to be able to displace H1 [Lone *et al.*, 2013]. H1 also dictates the exit angles of DNA from the chromatosome [Bednar *et al.*, 1998; Bednar and Woodcock, 1999], hinting at its potential prominent role in higher order structures (see next section). Furthermore, the stoichiometry of H1 *in vivo* has been shown to dictate, at least to some extent, the chromatin condensation state [Kizilyaprak *et al.*, 2011]. The concentration of H1 has also been positively linked *in vivo* to the nucleosomal repeat length [Woodcock *et al.*, 2006], but the mechanisms behind this phenomenon remain unclear [Fan *et al.*, 2003]. Even if the mechanisms by which H1 regulates the nucleosomal behavior and the whole fiber topology are not fully characterized, there is no doubt that the linker histone is a key player in the regulation of chromatin conformation.

The second chromatin folding level: 30-nm fiber or melted polymer?

The second level of chromatin compaction has long been described to be a 30-nm chromatin fiber based on *in vitro* chromatin reconstitution or chromatin purification studies [Grigoryev and Woodcock, 2012], a structure formed by bringing nucleosomes closer together on the DNA fiber involving interactions between nucleosomes and a possible prominent role of the linker histone, as discussed above [Robinson and Rhodes, 2006; Hamiche *et al.*, 1996; Pruss *et al.*, 1996]. Early electron microscopy studies of native chromatin fibers have led to the proposal of two major models of interaction driven compaction into a 30-

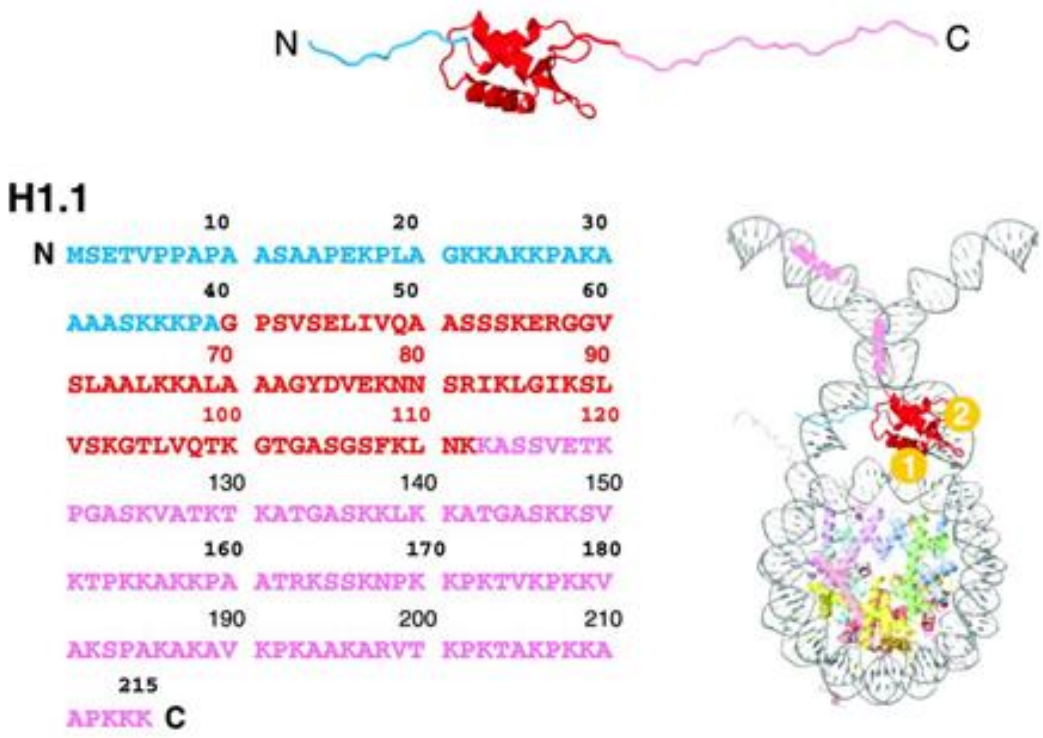

Figure 3: Sequence and structure of histone linker H1.
The sequence, the structure and the predicted binding of H1.1 to the nucleosome are presented. H1 is composed of three different domains, a short N-terminal tail (blue), a central globular domain (red), and a long C-terminal tail (pink).
Adapted from Hutchinson *et al.*, 2015.

nm fiber [Finch and Klug, 1976; Woodcock *et al.*, 1984]. Linker DNA is bent in between adjacent nucleosomes that follow a superhelical path with 6 to 8 nucleosomes per turn in the solenoid model, whereas a straight linker DNA separates adjacent nucleosomes organized in a zig-zag configuration to form the two-start helix model (fig. 4). Both those models have risen from theoretical predictions and are coherent with *in vitro* experiments [Grigoryev and Woodcock, 2012; Zhu and Li, 2016]. However, despite considerable efforts over the last decades, the 30-nm fiber structure has been primarily observed *in vitro* and under low ionic strength [Fussner *et al.*, 2012; Joti *et al.*, 2012; Nishino *et al.*, 2012; Maeshima *et al.*, 2014], meaning that it probably is a rare and transient state of chromatin compaction conformation in the cell if it can be found at all.

Following decades of debate on the structure of the 30-nm fiber conformation, new models have emerged suggesting that chromatin could actually consist of irregularly folded 11-nm fibers rather than 30-nm fibers [Fussner *et al.*, 2012; Maeshima *et al.*, 2014]. The first clue was obtained using cryo-electron microscopy to look at mitotic chromosomes. In those experiments, looking at the highest chromatin compaction state possible, chromosomes displayed a homogeneous texture with ~ 11-nm spacing without any higher-order or periodic structures [McDowall *et al.*, 1986; Eltsov *et al.*, 2008; Maeshima *et al.*, 2010]. The same conclusions were reached using small-angle-X-ray scattering [Joti *et al.*, 2012; Nishino *et al.*, 2012; Maeshima *et al.*, 2014], and super resolution microscopy which only revealed sparse heterogeneous nucleosome rich 'clutches', still in agreement with the irregularly folded 11-nm fiber chromatin model [Ricci *et al.*, 2015]. Taking these latest data into consideration, the 30-nm fiber configuration would seem to be only promoted in special conditions such as low ionic strength and well-separated short chromatin fibers reconstituted *in vitro*, while in the crowded nucleus, an interdigitated 'melted polymer' state would be favored (fig. 5) [Maeshima *et al.*, 2016]. It would seem that the high concentration of chromatin fibers in the nucleus would favor distal nucleosomal interactions rather than local ones that could only emerge in the case of isolated fibers. Yet, the question of the secondary structure of chromatin is still an open one.

Higher order structures: chromatin looping and TADs

As for the formation of the controversial 30-nm chromatin fiber, little is known about the mechanisms driving chromatin compaction into higher order structures. Whether chromatin is in a 30-nm fiber configuration or a melted polymer conformation, the next levels of compaction is relying on the formation

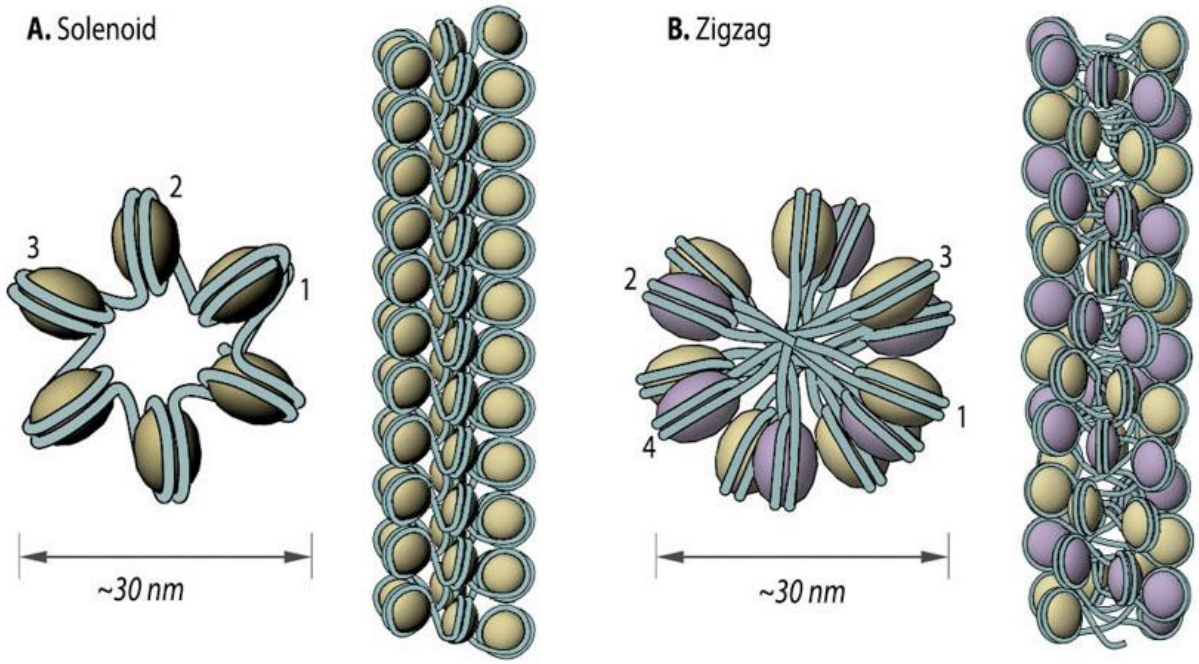

Figure 4: Solenoid (A) and zigzag (B) models of intermediate chromatin condensation.
Two major models are proposed to describe the topology of the 30-nm chromatin fiber. The solenoid, or one-start-helix, model proposes that nucleosomes follow each other along the same helical path, and that interactions between histone cores occur sequentially. In the zigzag, or two-start-helix model, linker DNA connects two opposing nucleosomes, creating a structure where the alternate histone cores become interacting partners, highlighted by the two different nucleosome colors.
From MBInfo contributors.

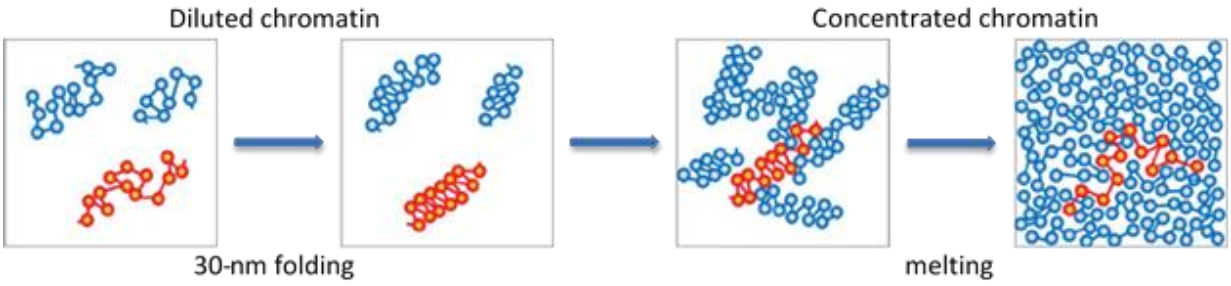

Figure 5: The "melted polymer" model of chromatin compaction.
In this model, chromatin would only adopt a 30-nm fiber conformation in dilute conditions where interactions within the polymer are favored. With a high concentration of chromatin, interactions between different chromatin fibers are favored and chromatin adopts an unstructured 11-nm conformation.
From Eltsov *et al.*, 2008.

of loops (fig. 6). Indeed, during transcription regulation, promoters and regulatory elements have been shown to interact directly while being separated by hundreds of kilo-bases [Nobrega *et al.*, 2003; Jin *et al.*, 2013]. The driving force behind the formation of those loops is still not fully understood. Some proteins, such as CTCF or cohesins, have been shown to be essential for the maintenance of those loops [Phillips and Corces, 2009; Phillips-Cremins *et al.*, 2013; Tark-Dame *et al.*, 2014], but their role in the formation of those structures is still under debate [Li *et al.*, 2013; Zuin *et al.*, 2014]. Theoretical studies also predict that loops can arise from entropy-driven mechanisms without the need for specific linker proteins [Heerman *et al.*, 2012]. It has been proposed that the position of the loops would be dictated by the flexibility of chromatin, and thus, the distribution of nucleosomes on the chromatin fiber [Li *et al.*, 2006].

The latest data regarding the conformation of chromatin at these scales come from the recent developments of the 3C technique (chromatin conformation capture) and its higher-dimension derivatives. Taking advantage of chromatin immunoprecipitation and crosslinking, this elegant technique allows the quantification of interactions between nearby genomic loci inside the 3-dimensional nuclear space [Simonis *et al.*, 2007; van Steensel and Dekker, 2010]. These experiments confirmed the important number of chromatin interactions reported between promoters and enhancers [Hakim et al, 2011], as well as long range interactions between genic regions of the same chromosome separated by up to 10 Mb of DNA [Simonis *et al.*, 2006; Lieberman-Aiden *et al.*, 2009] and even interactions between genic regions of two different chromosomes [Kaufmann *et al.*, 2015], although those seem to be less abundant. In fact, these observations led to the discovery of TADs (topologically associated domains). Those domains are characterized by a high level of chromatin interactions within a single TAD and a low level of interaction between different TADs [Dixon *et al.*, 2012; Nora *et al.*, 2012; Dixon *et al.*, 2015] and are proposed to be created associating several chromatin loops together. Approximately 70% of chromatin loops are presumed to actually occur within TADs [Sanyal *et al.*, 2012]. Their boundaries are often associated with DNA binding regions for the insulator protein CTCF [Dixon *et al.*, 2012; Nora *et al.*, 2012; Dixon *et al.*, 2015]. In addition to helping bring together regulatory elements with their target, this TAD organization allows for a global regulation as the TAD will be able to act as a co-regulated unit in terms of transcription activation or chromatin compaction state.

Higher order structures: compartments and chromosomes

Even if, once again, mechanisms and molecular players driving this organization are still unknown, TADs have been proposed to regroup to form higher entities called chromosomal compartments [Ea *et al.*,

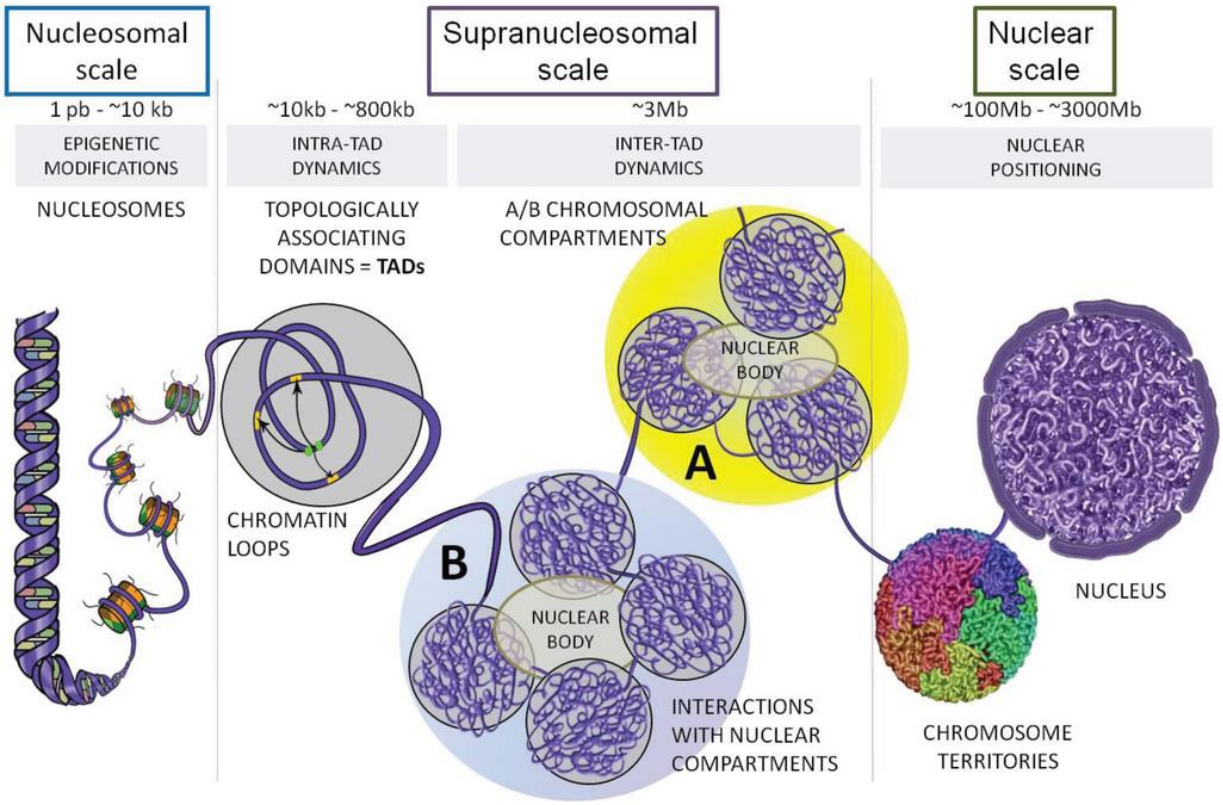

Figure 6: Chromatin higher order structures.

Here is presented a schematic representation of genome organization in mammals from the DNA double-helix to chromosome territories. Between those two extreme scales, chromatin loops, TADs and chromosomal compartments are proposed to be essential determinants of eukaryotic genome organization.

From Ea *et al.*, 2015.

2015]. Divided into two categories, A-compartments encompass more transcriptionally active TADs, while B-compartments form rather inactive chromatin regions (fig. 6) [Simonis et al, 2006, Lieberman-Aiden *et al.*, 2009]. Structurally and functionally, this organization makes sense as it is coherent with transcriptomics data, histone modification and protein binding-site maps [Shen *et al.*, 2012; Lesne *et al.*, 2014; Kundaje *et al.*, 2015]. Furthermore, DNA contacts between two A-compartments or two B-compartments are favored as compared to heterotypic contacts [Liberman-Aiden *et al.*, 2009]. Interestingly, while TADs are highly conserved and stable during differentiation, their association with one or the other compartment is cell-type specific [Sexton and Cavalli, 2015].

Knowing that chromatin, at all smaller scales, displays a highly structured, functionally relevant, conformation suggests that chromosomes must also follow the same rule and form organized entities. Indeed, taking advantage of FISH (fluorescence in situ hybridization), distinct chromosome territories can be observed in the interphase nucleus, stating that each chromosome occupies its own space inside the nucleus without much overlapping on its neighbors (fig. 7). This could suggest that the chromosomal location is tightly linked to its functional regulation [Peric-Hupkes *et al.*, 2010; Chaumeil *et al.*, 2006]. To help maintaining and possibly creating this nuclear landscape, chromatin has been shown to be attached to different chromatin landmarks. Several candidates have emerged as chromatin anchoring sites over the last decades and it appears that chromatin could be attached to some extent to the nuclear lamina surrounding the nucleus [Guelen et al, 2008; Peric-Hupkes et al, 2010], the nuclear pore complexes [Liang and Hetzer, 2010, Casolari et al, 2004; Capelson et al, 2010] and even the nucleoli [Nemeth et al, 2010; van Koningsbruggen et al, 2010] to tether this structure and help maintaining its complex architecture and a specific location for certain genomic regions.

Functional roles of the 3-dimensional organization of chromatin

Following the description of this complex macromolecular structure, it appears obvious that chromatin is not only a necessary mean to compact this huge amount of DNA in a small nucleus, but also an integrant part of the regulation of all cellular functions using DNA as a template. The multi-layered compartmentalization of chromatin allows for a more efficient gene expression and chromatin conformation regulation as DNA binding factors associated with a certain function will be addressed to a specific nuclear location. Hence, they will find their target faster and will be able to coordinate the expression of multiple genes involved in one specific biological pathway [Cremer *et al.*, 2004]. Moreover, our current and insufficient knowledge of the chromatin proteome tells us that more than a thousand

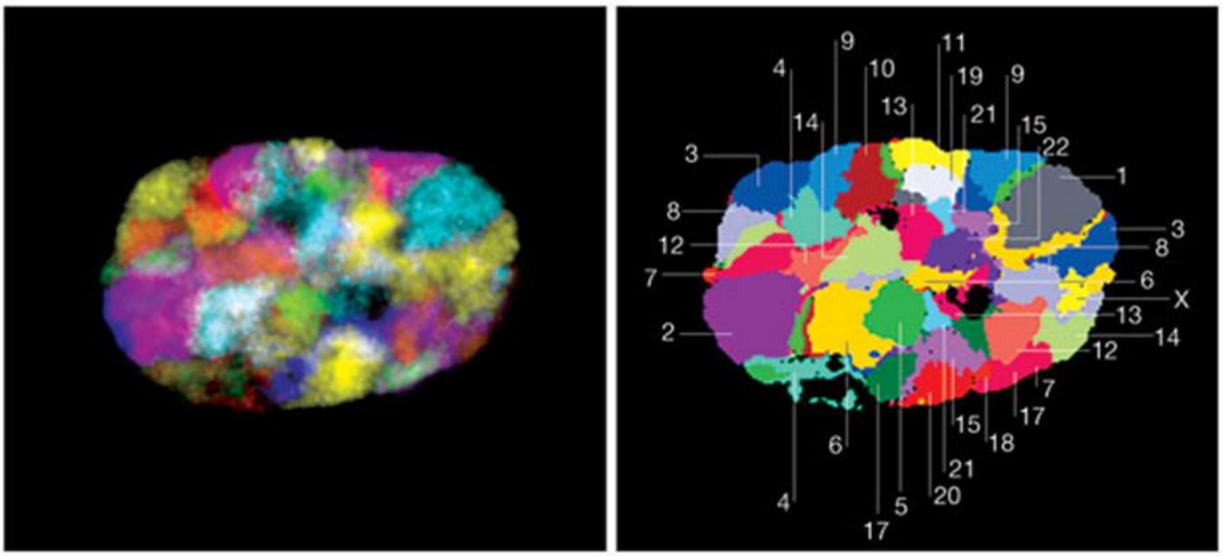

Figure 7: Chromosome territories.

Visualization of the 24 labeled human chromosomes in an intact interphase nucleus. The left image is obtained from deconvoluted mid-plane nuclear sections from a three-dimensional stack by superposition of 7 color channels. Recognizing each unique set of fluorophores characterizing each specific chromosome in automated analysis allows to obtain the picture on the right in which all chromosomes are delimited in territories and labeled by their number. Dark areas represent unstrained nucleoli.

From Speicher and Carter, 2005.

proteins interact with or are directly a part of chromatin structure [Vaquerizas *et al.*, 2009], stressing the need for a functional clustering of DNA.

As for the regulation of gene expression, the same can be said for all nuclear functions using DNA as a template. For instance, DNA replication involves multiple factors and complexes that must regroup to very specific locations on the genome [Prioleau and MacAlpine, 2016]. The choice of the location of these replication origins, as well as their efficiency, meaning the length of DNA replicated starting from this single point, has been proposed to be mainly driven by chromatin local conformation and interactors [Smith and Aladjem, 2014]. Going further than the classical view of euchromatin versus heterochromatin, a systematical study mapping more than fifty DNA binding factors of different families and several specific epigenetic marks on the entire genome of cultured drosophila cells revealed that five classes of chromatin, defined as colors, can be solidly established to see emerge a functional compartmentalization in terms of DNA accessibility and chromatin compaction state [Filion et al, 2010]. Scaling down to the chromatin fiber level, specific domains of tens of base pairs can also be visualized, such as transcription start sites, which exhibit changes in the nucleosome repeat length and different affinities for specific chromatin interactors [Nie *et al.*, 2014]. In the case of DNA damage, it has also been proposed that the first proteins responsible for the recognition of DNA alterations are actually sensitive to the altered physical topology of the DNA rather than the biological and chemical changes induced by the damage [Maréchal and Zou, 2013].

Altogether, chromatin architecture at all levels appears not only as a structural component but also as an integrant part of DNA functions regulation and cell physiology as it will regulate access to DNA both locally and globally. Locally, the position and possibly the tightening of nucleosomes prevent access to the underlying DNA. Globally, the overall multiscale chromatin architecture is thought to affect the way chromatin interactors diffuse, find and bind to their target [Normanno *et al.*, 2015]. However, the influence of chromatin architecture on reaction-diffusion dynamics of chromatin-interacting proteins remains poorly understood. In the following, I will describe how the molecular crowding model, which has been extensively used to predict biochemical reaction kinetics in the intracellular environment [Mourão *et al.*, 2014], can help us decipher the specific impact of the nuclear environment on protein diffusion and reaction kinetics.

The impact of the nuclear architecture on reaction-diffusion dynamics of proteins: the concept of macromolecular crowding

General principle, physiological relevance

Understanding chromatin physiology not only means grasping the complexity of its architecture but also implies understanding its impact on shaping the nuclear environment and vice versa. In order to do so, a lot of physical models, such as polymer physics or fractal behaviors, can be applied to chromatin and help gather valuable information that could lead us towards a broader understanding of the nuclear physiology. Among them, macromolecular crowding is a simple model, and probably the most obvious one. It states that any high concentration of macromolecules in a solution will alter the behavior of every component in this solution (fig. 8). Knowing that a media is considered crowded when more than 20% of the volume is occupied by background molecules [Ellis, 2001], and considering that chromatin alone occupies 30% to 50% of the entire nuclear volume [Lopez-Velazquez *et al.*, 1996; Rouquette *et al.*, 2009], it appears obvious that this crowded environment will have a great impact on the architecture, the dynamics, and the interactions of chromatin with other molecules. In fact, since macromolecular crowding will have an impact both on the properties of the molecule itself, and its interactions with others [Laurent, 1963], and since most reaction rates and macromolecule properties are still studied in solutions in which macromolecular crowding is negligible, one can assume that many calculated parameters differ by several orders of magnitude from their relevant, *in vivo*, equivalents [Minton, 1997; Minton, 2006]. Just like chromatin was seen for a long time as just a mean to fit DNA in the nucleus and now appears to be the principal player in terms of genetic regulation, the phenomenon of macromolecular crowding was blindly overlooked for decades. Yet, its effect on chromatin and on nuclear physiology can have a "life or death" impact for the cell. Moreover, macromolecular crowding could actually be more than just an obstacle to overcome when considering interactions within the nucleus and chromatin physiology. It could, just like chromatin, be an integrant part of the regulation of nuclear structures properties, and a necessary mean to dictate many chromatin interactions, and take part in a possible nuclear functional clustering.

Volume exclusion

The first predicted effect of macromolecular crowding inside the nucleus is straightforward. The volume occupied by chromatin, not to mention the additional space taken by RNA and other nuclear molecules not directly involved in chromatin architecture, is not accessible for any other diffusive particle navigating through the environment [Mourão *et al.*, 2014]. Thus, the volume fraction accessible for a diffusive particle

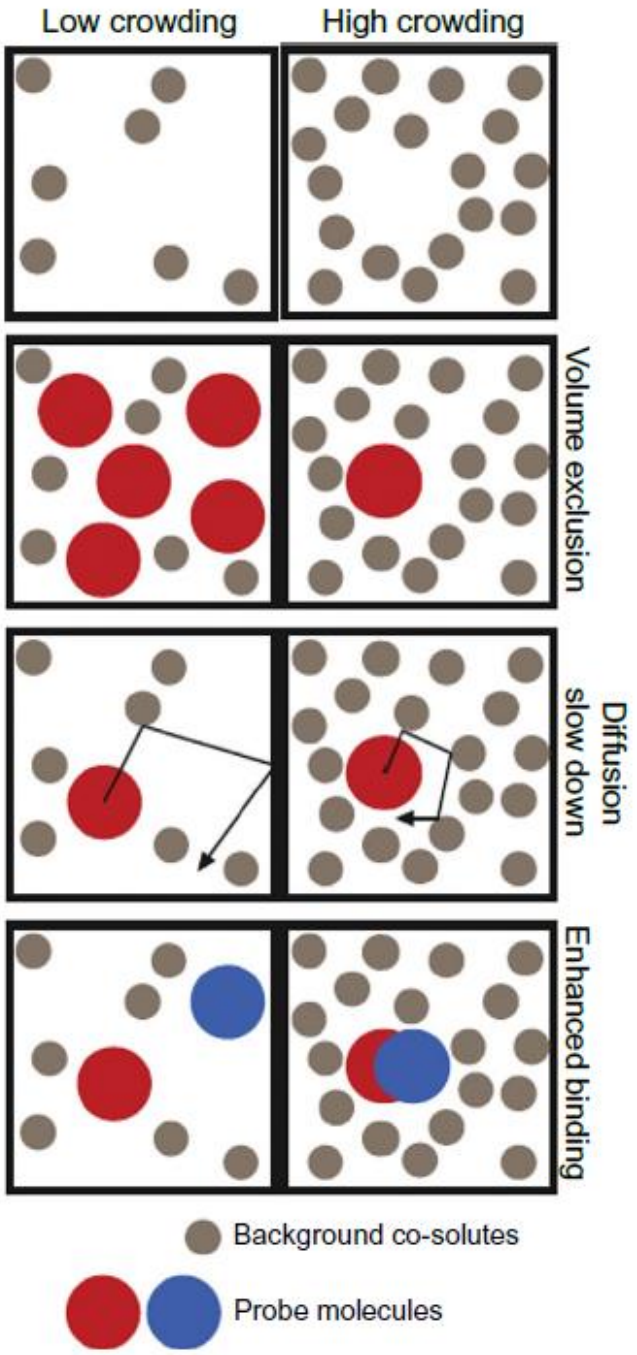

Figure 8: The impact of molecular crowding.
The presence of high amounts of background (right panel) species reduces the volume accessible to additional macromolecules, inducing volume exclusion (second row). Background species also act as obstacles impeding the diffusion of the molecules (third row), and they alter the thermodynamics of binding reactions, which tend to be shifted toward the bound state (fourth row).
From Huet *et al.*, 2014.

followed, referred to as the tracer, is dependent on the size of this particle and its co-solutes, referred to as background molecules (fig. 9). Moreover, this volume fraction can be further reduced when considering the shape of both the tracer and background molecules [Hall and Minton, 2003]. When only considering molecules as hard, incompressible particles and thus neglecting possible attractive or repulsive interactions, an infinitely small molecule will have access to the entire fraction that is not occupied by background molecules [Hall and Minton, 2003]. As the size of the molecular tracer increases, the volume fraction available decreases dramatically as it will only be able to approach obstacles up to their radial dimension only and will be progressively completely excluded from narrow areas if the crowding agents form a complex, heterogeneous structure like chromatin is supposed to [Minton, 2006; Mourão *et al.*, 2014; Huet *et al.*, 2014].

First experimental results regarding volume exclusion inside the nucleus were obtained by injecting FITC-dextrans of increasing size inside mammalian nuclei. In agreement with theoretical predictions, small-sized tracers were able to display a homogeneous distribution while heavier dextrans were excluded from more crowded regions such as dense heterochromatin areas or nucleoli [Görisch *et al.*, 2003; Verschure *et al.*, 2003]. Performing the same experiment with electrostatically charged tracers led to different conclusions, confirming that the physiochemical properties of both the background molecules and the molecular tracers will influence the observed effects of macromolecular crowding on molecules inside the nucleus [Görisch *et al.*, 2003; Verschure *et al.*, 2003]. In addition, modification of the chromatin compaction state by osmotic perturbations or molecular alterations of histone epigenetic marks has been shown to modify the level of exclusion of inert tracers inside nuclei, which confirms at the same time that chromatin is the main crowding agent in the nucleus [Martin and Cardoso, 2010; Walter *et al.*, 2013; Tóth *et al.*, 2004; Bancaud *et al.*, 2009].

Macromolecular crowding and diffusion

Another intuitive effect of high concentrations of particles in a solution will be a decrease in the diffusion capacity of molecules. Due to an important amount of collisions with background molecules, the tracer followed will display a slower diffusion in a crowded media [Muramatsu and Minton, 1988]. Unlike the volume exclusion effect which can be estimated quite precisely when knowing the properties of the tracer and background molecules [Hall and Minton, 2003], the impact of macromolecular crowding on the diffusion of particles is trickier to assess in theoretical studies [Phillies, 1985]. In addition to the diffusion speed reduction of tracers in crowded environments, a recurring debate is whether or not the macromolecular crowding inside the nucleus could influence the qualitative diffusive behavior of the

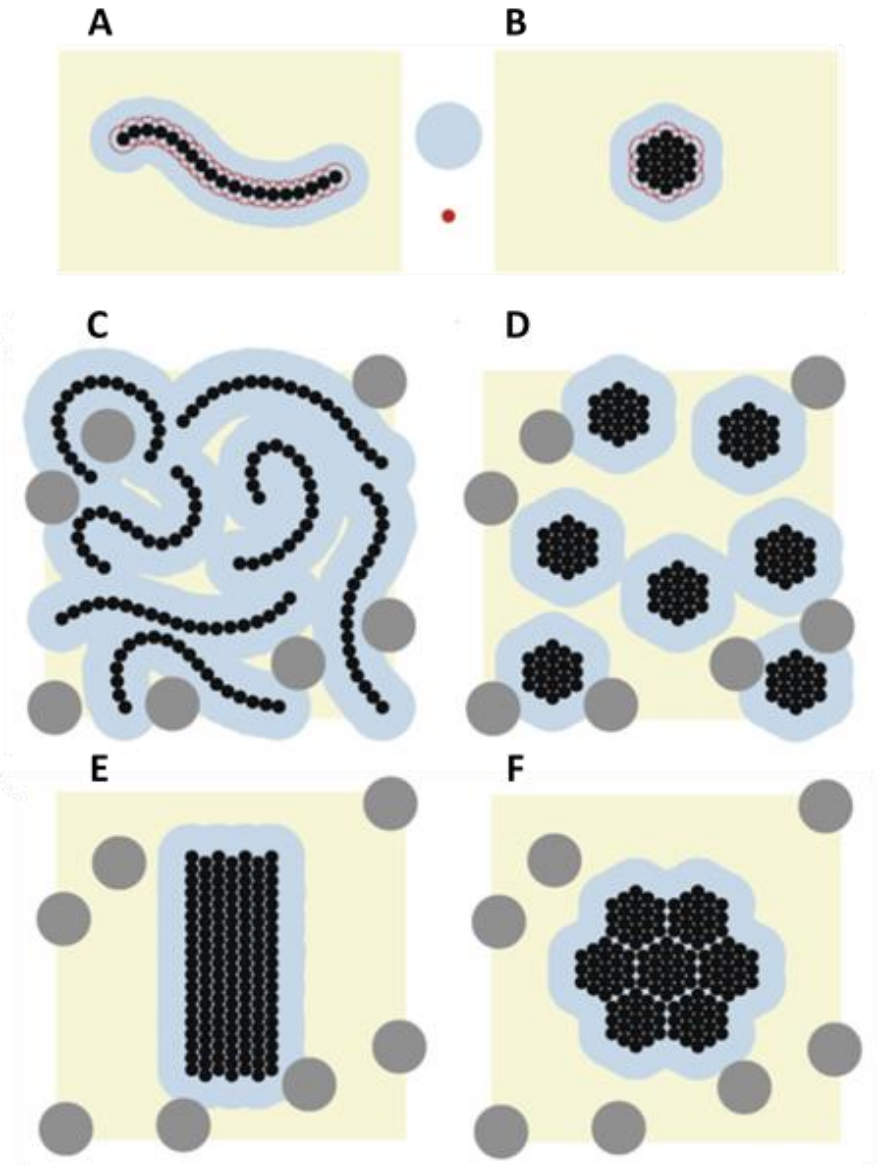

Figure 9: The volume exclusion effect depends on the size and shape of molecules.
(A, B) Shown is the volume fraction inaccessible to a large (blue) or a small (red) tracer in the presence of background molecules (black). The inaccessible volume fraction is higher for the large particle than it is for the small particle. If background molecules organize in a more compact manner, the accessible volume fraction increases. This gain of accessible volume is more important for the large tracer than for the small one. (C) Within a solution of polymer-filaments (black) and globular macro-solutes (gray) in water, the centers of the gray globules can populate a very restricted volume only, due to steric repulsion from the polymers (yellow: accessible volume; blue: volume excluded to the gray globules by the black filaments). (B - D) The accessible volume substantially increases, if the black filaments collapse into compact structures (B) align with each other (C), or do both (D).
From Richter *et al.*, 2008.

particle, going from the presumed pure diffusion model to a subdiffusive behavior [Saxton , 2012; Huet *et al.*, 2014; Höfling *et al.*, 2006; Banks and Fradin, 2005], adding a layer of complexity for the proper characterization of the effect of macromolecular crowding on diffusion. Indeed, if the molecular tracer exhibits a subdiffusive behavior in a crowded environment, its diffusive properties no longer rely on its diffusion coefficient and the diffusion hindrance in a crowded environment becomes more complicated to assess. This theory is still under debate and following results do not take it into account since the results were analyzed using a pure diffusion model for the tracers.

The impaired capacity of diffusion of molecules in living cells was confirmed using both fluorescence recovery after photo-bleaching (FRAP) and fluorescence correlation spectroscopy (FCS) to follow the dynamics of EGFP tracers. The tracers indeed displayed an apparent diffusion coefficient three to four times slower in the cell compared to their diffusion in solution (Seksek *et al.*, 1997; Görisch *et al.*, 2003]. Moreover, the diffusion hindrance was shown to be linked to the level of macromolecular crowding as it is higher inside the nucleoli than it is in the rest of the nucleoplasm [Bancaud *et al.*, 2009]. It has also been shown to be increased in the nucleoplasm as compared to the cytoplasm, hinting at the fact that the cytoplasm might be a less crowded cellular compartment [Pack *et al.*, 2006; Beaudouin *et al.*, 2006]. Inside the nucleus, a positive link is even established between the local concentration of chromatin, the main crowder of the nucleus, and diffusion hindrance [Walter *et al.*, 2013].

Reaction kinetics

The last presumed effect of macromolecular crowding, and perhaps the most relevant one in terms of nuclear physiology, is the predicted modification of reaction equilibria and kinetics. Indeed, due to volume exclusion, crowding will tend to favor the "bound state" in any reaction meaning that, depending on the type of reaction followed, crowding alone can shift the equilibrium towards the formation of the product [Minton, 1998]. In order to investigate this potential effect *in vivo*, Bancaud and colleagues probed the local dynamics of three different generic chromatin interactors inside the nucleus using FRAP [Bancaud *et al.*, 2009]. All three displayed a slower redistribution in heterochromatin compared to their redistribution in euchromatin, indicating that their interaction with chromatin was enhanced in a more crowded environment. Moreover, submitting nuclei to a hyperosmolar treatment which results in higher chromatin compaction, the histone H2B and the chromatin interacting factor HP1 displayed a superior residency time in those conditions and the estimation of the mobile fraction was lowered for those two proteins in over-condensed chromatin [Martin and Cardoso, 2010]. This all suggests that macromolecular crowding strongly impacts the physiology of chromatin and its interaction with its partners.

Physiological role of crowding

Considering the huge impact that macromolecular crowding can have in shaping the nuclear environment, one might wonder if crowding could actually be a physiological and necessary force driving a lot of process inside the nucleus. Going from protein folding to nuclear compartmentalization, a lot of cellular mechanisms could benefit from a crowded environment as opposed to a dilute one. As discussed previously, the architecture of chromatin itself might be relying a lot on the level of crowding inside the nucleus. Following the work of Maeshima and colleagues [Maeshima *et al.*, 2010; Maeshima *et al.*, 2016], and their melted polymer model, the reason why a 30-nm chromatin fiber would only be found very rarely and in specific conditions *in vivo* is the intermingling between different chromatin fibers due to crowding. Thus, entropic forces due to the level of crowding inside the nucleus could very well be one of the major factors driving the formation of the complex chromatin architecture [Hancock, 2008; Hancock, 2014]. At the nuclear scale, it is also known that modifying the size of the nucleus using hypo- or hypertonic treatments will alter the global chromatin compaction state, and thus, DNA accessibility and nuclear physiology [Walter *et al.*, 2013]. Hence, since the activation of gene transcription has been shown to be associated with local chromatin relaxation [Chambeyron and Bickmore, 2004; Hu *et al.*, 2009], and since it was demonstrated recently that mechanically or chemically modifying chromatin compaction state can tune transcription rates [Tajik *et al.*, 2016; Vaňková Hausnerová and Lanctôt, 2017], it appears clear that the level of macromolecular crowding inside the nucleus will directly affect the transcriptional program of the cell.

Moreover, another nuclear architecture trait could benefit from crowding. The formation of intranuclear structures has been proposed to arise from phase separation, the physical process by which molecules with different physiochemical properties will tend to spontaneously segregate, just like oil in water [Hyman *et al.*, 2014]. Phase separation, driven mostly by the physiochemical properties of the components followed [Nott *et al.*, 2015], has been shown to be strongly enhanced by macromolecular crowding [Hancock, 2004; Cho and Kim, 2012].

In addition, as already discussed, crowding will favor the "bound state" when considering reactions involving chromatin and its interactors [Bancaud *et al.*, 2009]. This means that the crowded nuclear environment will potentially influence the way chromatin interacting factors diffuse and scan for their targets [Meyer *et al.*, 2012]. Coupled with the principle of phase separation, crowding inside the nucleus could also be one of the main driving forces behind the assembly of the many multi-protein complexes that take part in the nuclear physiology and in regulating the level of local and global chromatin

compaction state. Altogether, crowding may be the source of specific functional clustering inside the nucleus whether it is at a basal level, during transcription or replication for instance [Meyer *et al.*, 2012; Tajik *et al.*, 2016], or upon the activation of specific signaling pathways, such as DNA damage repair or transcriptional program changes [Cravens and Stivers, 2016]. It is becoming more and more obvious that crowding will greatly affect a lot of nuclear functions, but the true extent of its effects, and their meaning in terms of nuclear physiology, still require more work to elucidate.

Chromatin Dynamics

The chromatin architecture described above only represents a glimpse of its complexity. Indeed, when adding time to the mix, it becomes clear that chromatin is also a highly dynamic structure. When looking at mitosis alone, representing one of the most fundamental functions of the cell, its multiplication, chromatin must undergo serious rearrangements of its structure to go from the interphase chromatin soup to the mitotic chromosomes, the highest form of chromatin compaction, in only a few minutes [Hahn *et al.*, 2009]. Moreover, during the S phase of the cell cycle, all of the genome is scanned and replicated by the cellular machinery in a matter of hours [Hahn *et al.*, 2009]. In addition to these global reorganizations can be added a precise and located regulation. When dealing with DNA damage for instance, as it will be discussed further on, a very precise regulation of the chromatin compaction state through space and time must occur for the damage to be handled properly. To face these endogenous and exogenous stimuli and allow chromatin to adapt dynamically, the cell has access to a great number of mechanisms involving chromatin remodeling processes both at the molecular level and at the structural level. Among them, the replacement of chromatin components can locally affect its structure and change its interactors, the same goes for post-translational modifications that can alter the physiochemical and biological properties of chromatin structural components and interactors.

Chromatin dynamics at the molecular level

Core histone variants

One way to alter the compaction state of chromatin is to replace some of its structural components by other molecules with similar, but different, physiochemical and molecular properties. Among structural chromatin proteins, histones play a major role in chromatin conformation and compaction state. Unlike canonical histones that are expressed exclusively during the S phase and incorporated into newly synthesized chromatin, most of the histone variants (fig. 10) follow a replication-independent transcription and incorporation into chromatin [Albig and Doenecke, 1997]. Histone variants have been shown to

interact with many different chromatin modifiers [Tagami *et al.*, 2004; Heo *et al.*, 2008; Luk *et al.*, 2010; Elsaesser and Allis, 2010] and their deposition into chromatin replacing canonical histones is the work of specific histone chaperones. Some are associated with more compacted, repressive chromatin state, such as macroH2A, while others, like H3.3 or H2AZ, correlate with a more open, transcriptionally active, chromatin [Chakravarthy and Luger, 2006; Thakar *et al.*, 2009; Li *et al.*, 2012]. The incorporation of histone variants can also be linked to a specific cellular process. It is the case for the H3 variant CENP-A which is incorporated specifically in centromeric regions and is essential for the maintenance and propagation of the centrosomal identity of the region [Yoda *et al.*, 2000]. Another example is the deposition of H2A.Z near transcription start sites associated with gene activation in differentiating cells [Li *et al.*, 2012]. To add to the subtlety of this regulation, histone variants genes, unlike canonical ones, encompass introns and can be subjected to alternative splicing [Rasmussen *et al.*, 1999; Marzluff *et al.*, 2002]. Of particular importance is to note that, even if core histone variants incorporation into chromatin and function have been extensively studied, a lot is still unknown considering linker histone variants or other proteins that could fulfill the same role, or the replacement of other chromatin structural proteins.

Linker histone variants

In humans, the linker histone family is composed of 11 members, 7 of which are somatic subtypes (fig. 10) [Izzo and Schneider, 2015]. There are also 3 testis-specific subtypes and 1 oocyte-specific subtype [Izzo *et al.*, 2008; Parseghian and Hamkalo, 2001]. Of the somatic subtypes, H1.1 to H1.5 are widely expressed in many different cell lines in a replication-dependent manner, while H1X and H1.0 are expressed independently of the cell cycle [Marzluff, 2005]. Those two differ from the other five sharing a poor percentage of primary sequence homology and are therefore presumed to possess specific functions. H1X has been shown to be located in nucleoli and involved in mitotic progression [Takata *et al.*, 2007], while H1.0 has been proposed to replace other subtypes in terminally differentiated cells [Zlatanova and Doenecke, 1994; Happel *et al.*, 2005]. H1.1 to H1.5 display a very high similarity and only differ from the composition and length of their N- and C-terminal tails [Hergeth and Schneider, 2015]. Even if differences between those variants have been shown in terms of their capacity to condense chromatin [Talasz *et al.*, 1998; Marion *et al.*, 1985], their affinity for chromatin [Misteli *et al.*, 2000], and the nucleosome repeat length resultant of their incorporation [Clausell *et al.*, 2009; Öberg *et al.*, 2012], the specific functional role of these H1 subtypes remain unknown. Interestingly, in mice, while a knockout of one H1 subtype failed to demonstrate a clear phenotype, drastic changes in chromatin compaction state and gene expression

were observed upon the simultaneous knockout of three different H1 variants [Fan *et al.*, 2005], hinting at the fact that H1 variants may both possess some redundant and some specific functions.

In addition to linker histone variants, some chromatin structural proteins have been shown to compete, or at least exhibit a mutually exclusive binding on chromatin, with H1. It is the case for MeCP2 (methyl-CpG binding protein 2) [Riedmann and Fondufe-Mittendorf, 2016], several members of the HMG (high-mobility group) family of proteins [Catez *et al.*, 2002; Catez *et al.*, 2004; Nalabothula *et al.*, 2014], and of particular importance in this project, PARP1 (poly(ADP-ribose) polymerase 1) [Kim *et al.*, 2004; Krishnakumar *et al.*, 2008]. This list could be enriched by the addition of multiple proteins in the future, possible candidates currently include the upstream binding factor UBF, the liver-enriched transcription factor HNF-3 and the glucocorticoid receptor [Zlatanova *et al.*, 2000]. All those chromatin-associated proteins, combined with H1 variants, could form a network of interchangeable elements continuously remodeling nucleosomes, and thus, the chromatin fiber conformation and the accessibility of DNA, increasing once more the complexity of chromatin architecture and dynamics [Phair *et al.*, 2004; Bustin *et al.*, 2005].

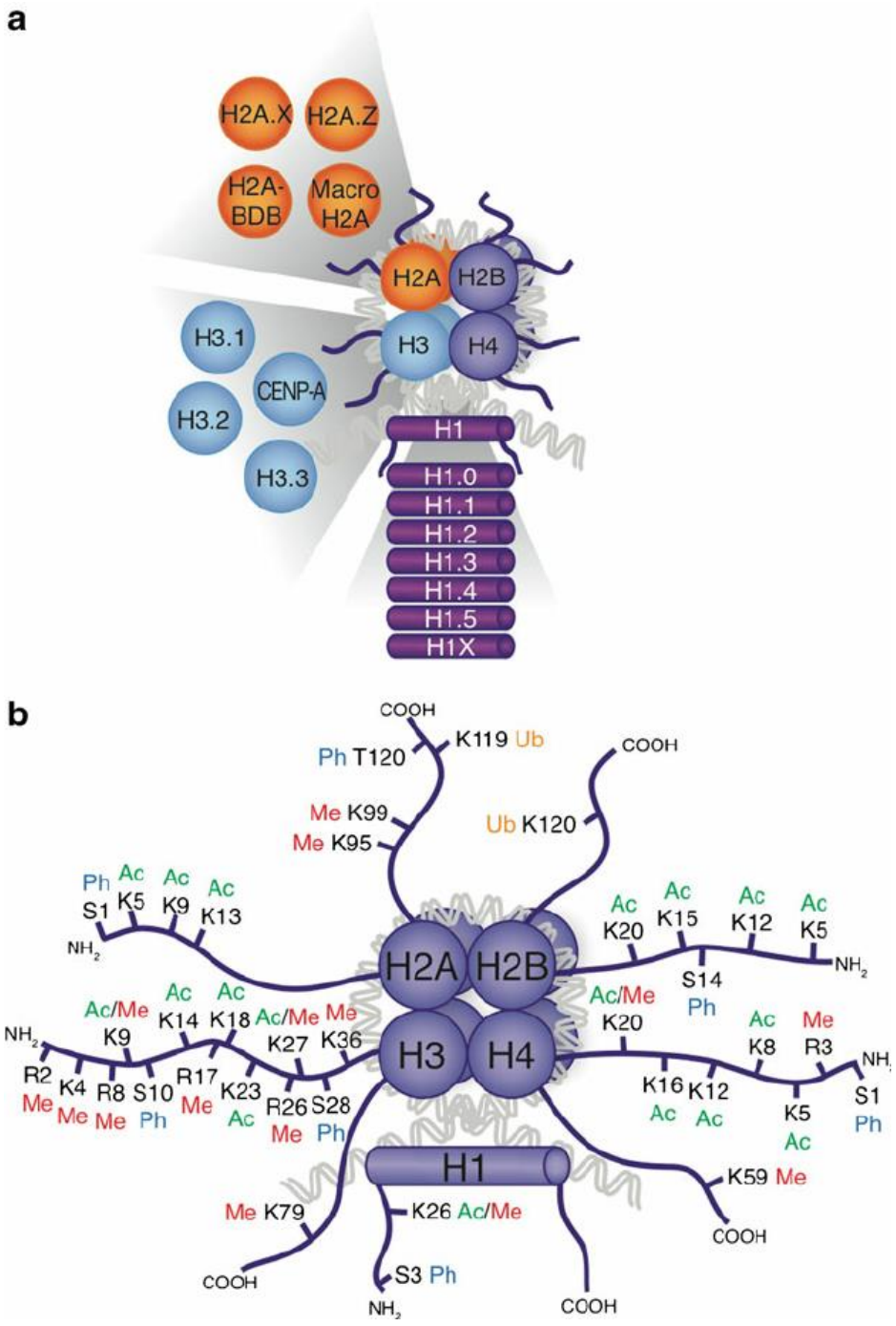

Figure 10: Histone post-translational modifications and variants.
(a) Schematic drawing of a nucleosome with the 4 canonical histones (H2A, H2B, H3, and H4), the linker histone H1 and their variants. (b) Currently known covalent histone post-translational modifications are highlighted on the N- and C- terminal tails of each histone. Me=methylation; Ac= acetylation; Ub=ubiquitination; Ph=phosphorylation.
From Zhao *et al.*, 2013.

Epigenetics and post-translational modifications

One way to modify chromatin structure globally or locally without replacing some of its parts is to modify directly chromatin components. The first and most essential chromatin component that can be modified is DNA itself. Indeed, DNA methylation, a reversible modification mostly occurring on cytosine residues and catalyzed by DNA methyltransferase (DNMT) enzymes, is described as a mechanism that would induce gene silencing and higher chromatin compaction [Deaton and Bird, 2011]. Methyl-CpG binding domain proteins (MBDs) will be recruited to methylated DNA sites and will, therefore, prevent transcription and, in some cases, induce a higher chromatin compaction [Iyer *et al.*, 2011]. The DNA methylation pattern of a cell will be transmitted from cell to cell along divisions, making it a form of cellular memory. Nonetheless, it is not absolute since this pattern can change in the life of an individual due to environmental changes, aging, or pathological causes [Zampieri *et al.*, 2015; Pacchierotti and Spanò, 2015; Jones and Baylin, 2007]. However, the molecular mechanisms driving these shifts remain, for the most part, unknown.

The other components of the structural unit of chromatin that are subject to a huge amount of different modifications are the histones. As stated above, histones are small basic proteins with a large globular domain and two unstructured tails encompassing a very high amount of post-translational modification (PTM) sites (fig. 10) [Kouzarides, 2007]. The incredible amount of different covalent modifications that can occur, their association and the integration of their possible complementary or opposite effects makes the "histone code" very difficult to crack [Strahl and Allis, 2000]. These modifications will alter DNA-protein or protein-protein interactions and thus alter chromatin structure and function [Choi and Howe, 2009; Strahl and Allis, 2000]. As for histone variants, some modifications are linked to a more opened chromatin state. It is the case for the acetylation of lysine 14 of histone H3 or the methylation of its lysine 4 [Jenuwein and Allis, 2001]. Others will tend to create a more compacted chromatin conformation, like the trimethylation of the lysine 9 of histone H3 [Rea *et al.*, 2000] which will create a high-affinity binding site for HP1 [Bannister *et al.*, 2001; Peters *et al.*, 2002]. Divided into two classes, those modifications will either have a physiochemical effect on their own, the addition of the negative charges of a phosphate group disrupting DNA-histone contacts for instance, or will act indirectly by creating binding sites for specific factors that will then alter chromatin compaction state [Cosgrove *et al.*, 2004]. In addition, a lot of those modifications will be involved in specific signaling pathways, transcription regulation or the DNA damage response [Rea *et al.*, 2010; Bannister *et al.*, 2001]. Again, most studies interested in chromatin PTMs have focused on histones, but little is known about other chromatin architectural proteins that would most likely also be subject to post-translational modifications that will modulate their interaction with chromatin and other

structural components, such as the poly(ADP-ribosyl)ation (PARylation) of CTCF by PARP1 [Yu *et al.*, 2004, Guastafierro *et al.*, 2008].

Linker histones are no exception to the rule and encompass a very high level of PTM sites. Even if a significant number can be found on its globular domain and its N-terminal short tail, most of them are located on its long C-terminal tail [Wisniewski *et al.*, 2007; Deterding *et al.*, 2008]. H1 has been shown to be subject to almost all known PTMs. The most extensively studied modification is, without a doubt, phosphorylation [Roth and Allis, 1992]. Mostly associated with the cell cycle progression [Gutiyama *et al.*, 2008; Talasz *et al.*, 1996; Baatout and Derradji, 2006], H1 phosphorylation has nevertheless also been linked to the chromatin compaction state [Roth and Allis, 1992; Th'ng, *et al.*, 1994]. Those results suggest that the phosphorylation of H1 will lead to an opening of the local chromatin compaction, but the high number of phosphorylation sites and the possible similar or opposite effects of those different modifications prevent us from drawing clear conclusions [Izzo and Schneider, 2015]. The linker histonehas also been shown to be the subject of methylation [Wisniewski *et al.*, 2007], acetylation [Vaquero *et al.*, 2004], citrullination [Christophorou *et al.*, 2014], ubiquitylation [Danielsen *et al.*, 2011], carbonylation [García-Giménez *et al.*, 2012], formylation [Wisniewski *et al.*, 2007], denitration [Haqqani *et al.*, 2001], crotonylation [Tan *et al.*, 2011], lysine 2-hydroxyisobutyrylation [Dai *et al.*, 2014] and ADP-ribosylation [Hottiger, 2011]. The function of most of these modifications on H1 remains to be solved, but several have been shown to be implicated in the chromatin compaction state, and this cannot be excluded for the others.

Of particular importance is to note that a strong link binds these different epigenetic marks, PTMs, and chromatin components together. Indeed, DNA and histone modifiers, as well as chaperones, are often found in the same chromatin regulating complexes [Geiman and Robertson, 2002], meaning that all these modifications form a complex, interconnected signaling network regulating chromatin conformation. For instance, DNA hypermethylation can act as a platform for recruitment for histone deacetylases and histone methyltransferases [Lachner and Jenuwein, 2002], which are also linked with a more closed, transcriptionally inactive, chromatin state [Geiman and Robertson, 2002]. DNA hypermethylation also strongly colocalize with HP1, a protein enriched in heterochromatin areas [Lachner *et al.*, 2001], and anti-correlates with the incorporation of histone variant H2AZ [Coleman-derr et Zilberman, 2016], associated with a more transcriptionally active state of chromatin [Li *et al.*, 2012].

Repositioning nucleosomes along DNA with the help of chromatin remodelers

In addition to modifications of DNA, histones, or the replacement of histones, the 11-nm nucleosomal array can also be modified by changing the position of the nucleosomes along the DNA, or simply removing entire nucleosomes from the fiber. It has been known since the first DNAse I footprinting experiments on nucleosomes that the accessibility of DNA to proteins involved in cellular functions using DNA as a template is not uniform along the chromatin fiber and in particular is impeded by the presence of nucleosomes [Staynov, 2008]. It becomes then essential for the cell to have mechanisms that enable the displacement of nucleosomes to permit access to the underlying DNA. To fulfill this complicated task, chromatin remodeling enzymes, which are highly abundant in the cell [Ghaemmaghami *et al.*, 2003], will assemble into multi-protein remodeling complexes encompassing one effector ATPase subunit that will catalyze the displacement of the nucleosome, and from 2 to 20 different regulating subunits [Längst and Manelyte, 2015]. Those regulatory components will be required for the targeting of the remodeling complex, taking advantage of the recognition of specific chromatin associated proteins, epigenetic marks, histone variants, DNA structures or sequences, or perhaps a combination of all of the above [Bowen *et al.*, 2004; Mohrmann and Verrijzer, 2005; Marfella and Imbalzano, 2007; Erdel *et al.*, 2011]. These chromatin remodeling complexes are all ATP-dependent and belong to four different families, the SWI/SNF, ISWI, CHD, and INO80 families. The interplay between those different families and the possible synergic or opposite effects that their simultaneous recruitment may have are not fully understood [Hota and Bartholomew, 2011; Längst and Manelyte, 2015; Runge *et al.*, 2016]. In addition to the catalytic and regulatory subunits, DNA and histone modifying enzymes, as well as histone chaperones, have also been shown to be involved in such multi-protein assemblies, hinting at a global regulation of DNA accessibility and chromatin compaction state involving many modifications and actors [Bowen *et al.*, 2004; Mohrmann and Verrijzer, 2005; Qiu *et al.*, 2016; Runge *et al.*, 2016].

Chromatin dynamics at the structural level

Considering the huge amount of changes in terms of components and conformation that chromatin can go through at a molecular level, one might wonder about the dynamics of chromatin looking at this structure at the nuclear level. The global architecture of chromatin is quite stable through the interphase, which makes the previous static description of its conformation inside the nucleus possible [Gerlich *et al.*, 2003; Walter *et al.*, 2003]. Nevertheless, chromatin loci, as well as larger chromatin regions, have been shown to display movements ranging from small, seemingly random, motion to large chromatin structure

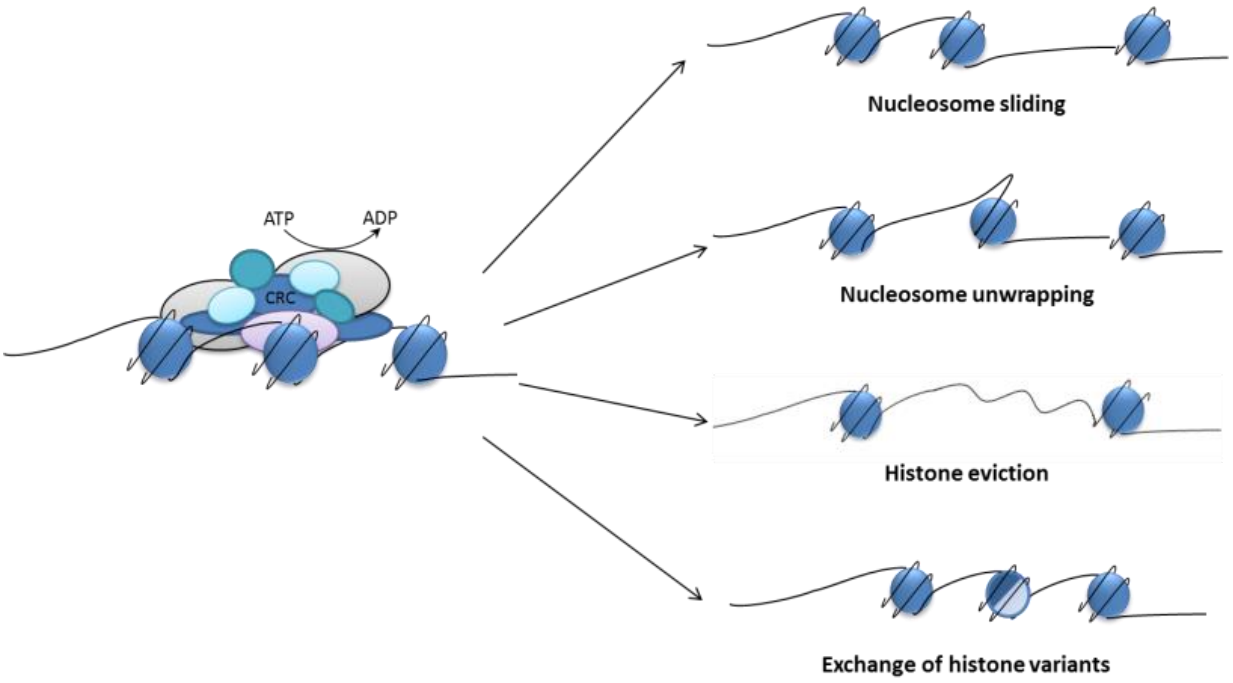

Figure 11: Mechanisms of ATP-dependent chromatin remodeling activity to alter the accessibility of nucleosomal DNA.

Three mechanisms of action for chromatin remodeling complexes have been described to alter nucleosomal structure using the energy provided by ATP hydrolysis, nucleosome sliding along the DNA, unwrapping by disrupting DNA-histones contacts, or nucleosome eviction from DNA. In some cases, ATP-dependent remodeling complexes can introduce histone variants into the nucleosome, such as H2A-H2B dimers or H2A variants-H2B dimers.

From Xu *et al.*, 2013.

alterations [Price and D'Andrea, 2013]. Even if small movements of chromatin loci could be explained by thermal fluctuations, both may arise from physiological processes, such as transcription modulation or DNA damage repair [Price and D'Andrea, 2013; Dion and Gasser, 2013].

Motion of chromatin loci

The study of the motion of chromatin loci was made possible both in yeast and mammalian cells by following the diffusion of a fluorescently-tagged protein bound to a specific integrated sequence in the genome of a cell [Robinett *et al.*, 1996]. Trajectories of multiple fluorescently-tagged chromatin loci can be then tracked through time-lapse acquisitions to calculate the mean square displacement (MSD) of these loci. Plotting the average squared distance covered by these loci over increasing time intervals allows for the characterization of their diffusional behavior [Berg, 1993]. In particular, the analysis of MSD curves can reveal whether the particle tracked is following a random walk, directed motion, or constrained Brownian motion, and determine the radius of constraint or the diffusion coefficient of the particle, if applicable (fig. 13).

Conducting such experiments in bacteria, yeast or mammalian cells, the motion of chromatin loci was shown to range from 10^{-5} to 10^{-3} µm²/s, and over distances up to 1 µm from their origin [Bornfleth *et al.*, 1999; Chubb *et al.*, 2002; Heun *et al.*, 2001; Marshall *et al.*, 1997; Neumann *et al.*, 2012; Weber *et al.*, 2012]. Those movements, considering their amplitude and their apparent randomness, both in yeast and mammalian cells, have been proposed to arise from thermal fluctuations [Marshall *et al.*, 1997; Bornfleth *et al.*, 1999; Pliss *et al.*, 2013; Hajjoul *et al.*, 2013]. If so, according to the Stockes-Einstien law, they should be directly proportional to the temperature. It was reported not to be the case, both in mammals [Weber *et al.*, 2012] and yeast [Neumann *et al.*, 2012], suggesting that thermal fluctuations are not solely responsible for the motion observed. However, this only holds true when considering pure Brownian motion, and while an extrachromosomal ring of yeast chromatin does display a constrained Brownian random walk [Neumann *et al.*, 2012], this diffusion model does not recapitulate the motion of chromosomal loci, leaving the question unanswered.

Indeed, chromatin loci followed during timescales ranging from 10^{-2} to 10^{2} s both in yeast and mammalian cells exhibit a subdiffusive behavior (fig. 13) [Bronstein *et al.*, 2009; Hajjoul *et al.*, 2013; Bornfleth *et al.*, 1999; Weber *et al.*, 2012]. This particular diffusional behavior could have many potential causes, like the tethering of chromatin to nuclear structures, the impact of crowding, as discussed above, or simply the properties of the chromatin polymer inside the nuclear heterogeneous medium. Interestingly, even if this

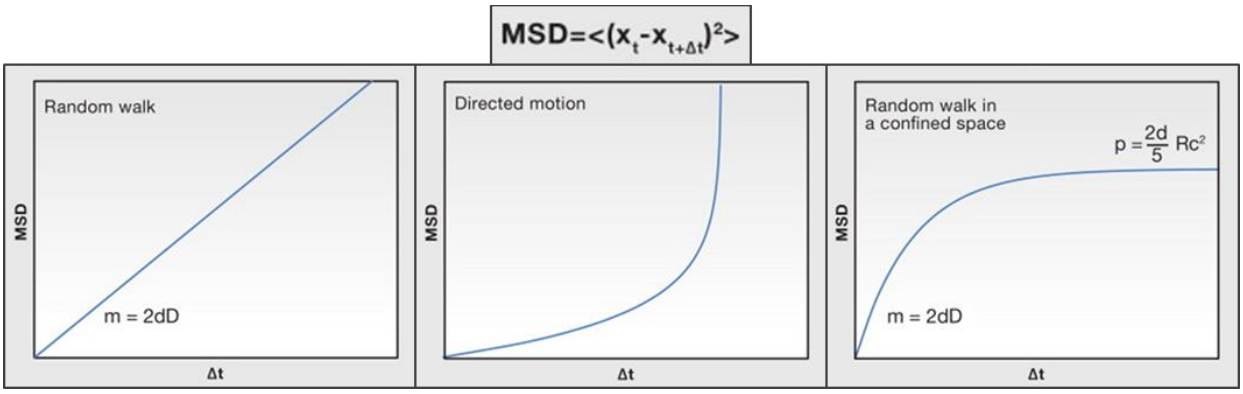

Figure 12: MSD Analysis.
MSD values are derived from determining the distance moved by a particle over increasing time intervals, Δt. In other words, (Xt – Xt+Δt), where X is the position at time t. The left panel depicts a characteristic MSD plot for a random walk where the slope (m) equals the diffusion coefficient (D) times twice the number of dimensions in which movement is measured (d). The center panel shows the shape of an MSD graph in the case of directional motion. The mobility of a particle moving according to Brownian motion within confined space will generate a curve that levels off at larger time intervals, as in the right panel. In this case, the plateau (p) is equal to the square root of 2/5 times the number of dimensions (d) times the radius of constraint (Rc) (Neumann *et al.*, 2012).
From Dion and Gasser, 2013.

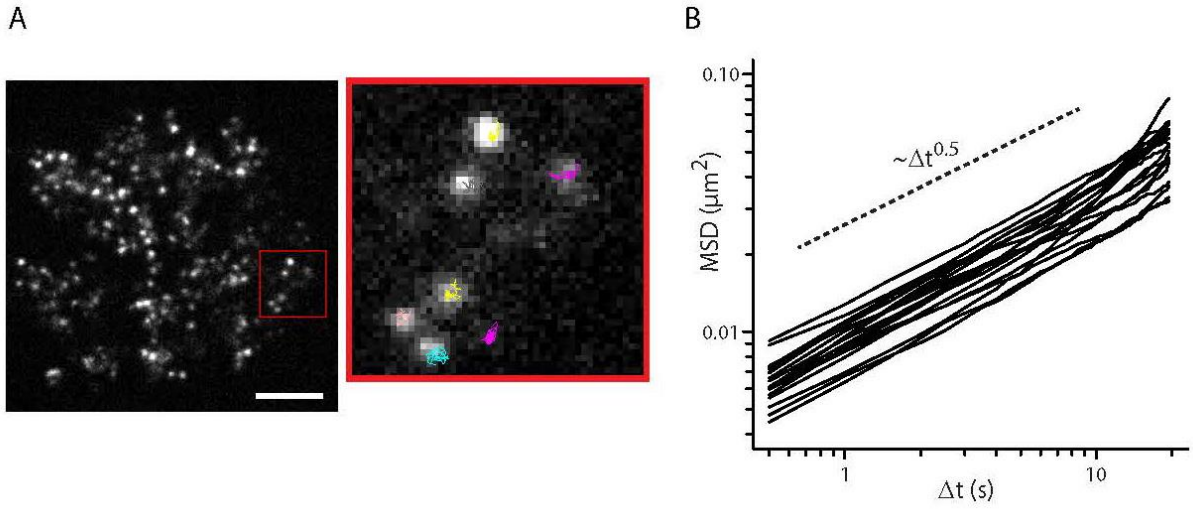

Figure 13: MSD analysis of the motion of chromatin loci.
(A) Shown is the nucleus of a U2OS cell with its DNA labeled using fluorescent nucleotides. Bar = 5μm. The inset shows examples of trajectories displayed by the labeled chromatin foci. The trajectories were recorded for 30 seconds at 2 frames per second. (B) Curves of the mean square displacement (MSD) calculated from the trajectories of the labeled foci. Each curve corresponds to the averaged chromatin dynamics within one nucleus (21 nuclei, 40 to 180 tracks per nucleus). The fact that the curves show a slope of ~0.5 in the log-log representation indicates that the chromatin dynamics is subdiffusive at the studied timescales.

phenomenon seems rare, directed motion of chromatin loci has also been reported, both in yeast [Lisby *et al.*, 2003] and mammalian cells [Khanna *et al.*, 2014].

Linking chromatin motion to physiological processes

The mechanisms responsible for chromatin motion are still the source of debate and their characterization has been the subject of intense research. Chromatin movements have been shown in yeast to be dependent on the level of glucose in the extracellular medium [Marshall *et al.*, 1997; Heun *et al.*, 2001]. Furthermore, movements of chromatin loci in mammalian cells have been shown to be dependent on the cellular level of ATP [Weber *et al.*, 2012; Zidovska *et al.*, 2013; Chubb *et al.*, 2002], strongly hinting at the fact that chromatin motion comes from an active mechanism. Interestingly, ATP is required at any time to maintain proper chromatin conformation as its depletion from the cell leads to a global chromatin over-compaction [Platani *et al.*, 2002; Cushman *et al.*, 2004; Llères *et al.*, 2009]. The impaired dynamics observed in the case of ATP depletion could then only be the mere reflection of the altered chromatin compaction level. As of now, a clear answer cannot be given regarding this question, but one should not forget that multiple forces together could drive these chromatin movements. An interesting model reconciling these different views proposes that chromatin motion does actually arise from thermal fluctuations and depend almost exclusively on the local flexibility of chromatin [Hajjoul *et al.*, 2013]. Since this flexibility is permanently altered by chromatin remodelers and epigenetic modifications [Neumann *et al.*, 2012], which includes a lot of ATP-dependent processes, chromatin motion could be linked to biological nuclear events while being only the result of thermal fluctuations [Soutoglou and Misteli, 2007].

Another puzzling question concerns the link between chromatin local mobility and transcription. While the relationship between chromatin motion and cell cycle progression seems clear with a higher mobility observed in the G1 phase both in yeast and mammals [Heun *et al.*, 2001; Walter *et al.*, 2003], mixed results were obtained when assessing the possible correlation between transcription rates and chromatin mobility [Dion and Gasser, 2013]. Indeed, a link was established between chromatin decompaction, transcriptional activation and directed motion of the locus when targeting a viral transactivator to a heterochromatic transgene both in yeast [Neumann *et al.*, 2012] and mammals [Chuang *et al.*, 2006]. Yet, other studies have shown that some highly-transcribed genes associate to nuclear pore complexes, and possess therefore a highly-hindered motion capacity [Cabal *et al.*, 2006; Taddei *et al.*, 2006]. Furthermore, in yeast, a silent chromatin ring was shown to diffuse freely inside the entire nucleus without any triggered transcriptional activation when the proteins necessary for its anchoring were missing [Gartenberg *et al.*, 2004]. Other studies failed to demonstrate a link between transcription rate and chromatin mobility [Pliss

et al., 2009; Mearini and Fackelmayer, 2006], hinting at the fact that chromatin motion might rely more on local chromatin conformation [Hajjoul *et al.*, 2013] and possible tethering to nuclear proteins and structures, such as lamin A [Bronshtein *et al.*, 2016], or the cytoskeleton [Chubb *et al.*, 2002], than transcriptional activity. Altogether, chromatin mobility seems to be resultant of the combination of both physiological and molecular mechanisms, and physical parameters, but the interplay between those two components still requires more work to be elucidated.

Modulation of chromatin compaction levels

The mobility of chromatin loci can help gather clues regarding the level of compaction of the chromatin fiber, as the positioning of nucleosomes and the length of linker DNA, as well as the conformation of the chromatin fiber might govern its flexibility. However, the diffusional capacity of chromatin loci does not recapitulate the local chromatin compaction level. Indeed, other factors will alter the diffusional capacity of specific loci, such as the tethering to nuclear structures [Chubb *et al.*, 2002], or the binding to chromatin interactors [Hajjoul *et al.*, 2013]. Assessing chromatin compaction levels *in vivo* at small scales then becomes quite complicated, even if some new techniques are emerging and will help shed light on this matter [Llères *et al.*, 2009]. Therefore, most studies have focused on large-scale chromatin compaction alterations. These modifications can occur both during physiological processes and pathological events.

The first event that comes to mind where tremendous chromatin reorganization must occur in the life of a cell is its differentiation. Indeed, embryonic stem (ES) cells display a highly different nucleus from differentiated cells [Talwar *et al.*, 2013]. Lacking lamin A [Gruenbaum *et al.*, 2005] and a well-defined cytoskeleton [Mazumder *et al.*, 2010], ES cells are characterized by a homogeneous compaction state all over the nucleus and chromatin has to go through extensive changes before showing the complex and well-defined architecture that differentiated cells possess [Talwar *et al.*, 2013]. Further on, differentiated cells will go through multiple cell cycles which are composed of chromatin compaction and decompaction processes while maintaining a stable architecture during the interphase [Deng *et al.*, 2016]. Cells will also need to respond to a lot of different internal and external stimuli by modifying their transcriptional programs. As mentioned above, chromatin is one of the major actors involved in transcriptional activation or repression and will go through extensive rearrangements in this context [Chuang *et al.*, 2006]. Also important to mention is the fact that many diseases are triggered through altered chromatin conformation both at specific loci or globally, like in the case of cancer where the entire nuclear chromatin conformation can be altered [Koschmann *et al.*, 2017].

Among all stimuli that can trigger changes in the chromatin compaction level, DNA damage, and especially in its most deleterious form, DNA double-strand breaks (DSBs), has been one of the most studied through the years and is the focus of the next section.

DNA damage

The link between DNA damage and chromatin

One of the most impactful events for the cell, that will trigger major chromatin reorganizations, is DNA damage. Assaults to the genome are actually quite common in the life of a cell, whether it arises from endogenous factors, such as reactive oxygen species produced by the cellular metabolism or replication errors, or exogenous events, such as UV radiation or environmental toxins [Soria *et al.*, 2012]. Those will induce various forms of DNA alterations from base lesions or mismatches to the most deleterious case of DNA damage: double-strand breaks (DSBs) [van Gent *et al.*, 2001]. Endangering the life of the cell, as its functions might be impaired, its genome integrity must then be restored [Mills *et al.*, 2003; Suzuki *et al.*, 2006]. Knowing the complex architecture of chromatin and its sheltering effect on DNA, one can think intuitively that chromatin reorganization should occur in order to allow access of DNA for repair proteins. Smerdon and Lieberman first showed that damaged DNA undergoing repair actually demonstrated a higher sensitivity to nucleases [Smerdon and Lieberman, 1978], which then became the foundation of the "access-repair-restore" model for DNA repair [Smerdon, 1991]. This model states that DNA repair in chromatin will occur sequentially during these three steps, first the recognition of the damage and release of factors that might hinder the repair, then the actual DNA repair, and finally the restoration of chromatin to its pre-damage state.

This model has been however recently questioned with the publication of studies showing that an over-condensation of chromatin might be required for the proper DNA damage repair, suggesting that most of the actual DNA repair could occur during the "restore" phase of this process [Khurana *et al.*, 2014; Ayrapetov *et al.*, 2014; Burgess *et al.*, 2014]. Nevertheless, those studies and previous ones all agree on the fact that chromatin is a major player in the DNA damage repair. In addition to these local reorganization mechanisms in the vicinity of the DNA breaks, DNA damage induction can also trigger genome-wide effects such as a global reduction of the regular transcription program and an enhancement of the transcription of repair associated factors [Adam and Polo, 2014; Meas and Mao, 2015; Suzuki *et al.*, 2006]. Although chromatin dynamics related to transcriptional regulation upon DNA damage has not

drawn as much attention as the regulation of chromatin compaction state in the vicinity of the lesion, one can assume this would also require major chromatin reorganization.

Even if the mechanisms behind chromatin specific dynamics upon DNA damage still require a lot of work, being a younger field of research, the knowledge gathered from decades of study on the DNA damage response allows us to draw an elaborated picture regarding the molecular actors involved in the different DNA repair pathways.

Molecular actors in DNA Repair

Among different types of DNA damage induced by laser micro-irradiation, double-strand breaks (DSBs) are the most challenging ones for the cell and are easily artificially induced. Thus, DSBs constitute the focus of many experiments on the subject [Stracker and Petrini, 2011; Soria *et al.*, 2012]. In fact, a single unrepaired DSB can lead to cell death or cancer formation [Mills *et al.*, 2003]. Considering all types of DNA damage, the classical generic DNA damage response (DDR) involves firstly the recognition of the damage by sensors, then the recruitment of effector proteins directly or through interactions with other proteins playing the role of scaffold, those will signal the presence of damage by modifying the DNA damage site components to finally allow the recruitment of DNA repair factors.

For example, naming only the core proteins implicated in the process, the nucleotide-excision-repair (NER) pathway (fig. 14) deals with many lesions with a structural common trait, a destabilized double-helix resultant from a bend in the DNA molecule [Schärer, 2013]. The NER pathway handles bulky DNA adducts by erasing a part of the damaged DNA strand and recopying the information from the other strand [Green and Almouzni, 2002]. First, it involves XPA and XPC for the recognition of the DNA damage [Sugasawa *et al.*, 1998; Tapias *et al.*, 2004]. Next, XPG, XPF-ERRC1, and proteins of the TF-II complex are recruited to the site of damage in order to reorganize locally the chromatin and the DNA double helix conformation [Volker *et al.*, 2001; Tapias *et al.*, 2004]. XPA and RPA are presumed to help in the process of opening the double helix and protecting single-stranded DNA [Krasikova *et al.*, 2010]. RFC and PCNA are then loaded on the DNA to allow for the DNA polymerase to copy the undamaged strand of DNA [Shivji *et al.* 1995]. A specific DNA ligase is finally required to seal the nicks and restore the DNA molecule [Schärer, 2013].

Regarding DSBs recognition and repair, the situation is a bit more complicated. Indeed, two major pathways have been described in human, the main one being non-homologous end-joining (NHEJ), in which loose DNA ends will be reattached together (fig. 15) [Lieber, 2010]. It is described as a more error-prone mechanism. It involves firstly the Ku heterodimer proteins [Blier *et al.*, 1993] that can recognize

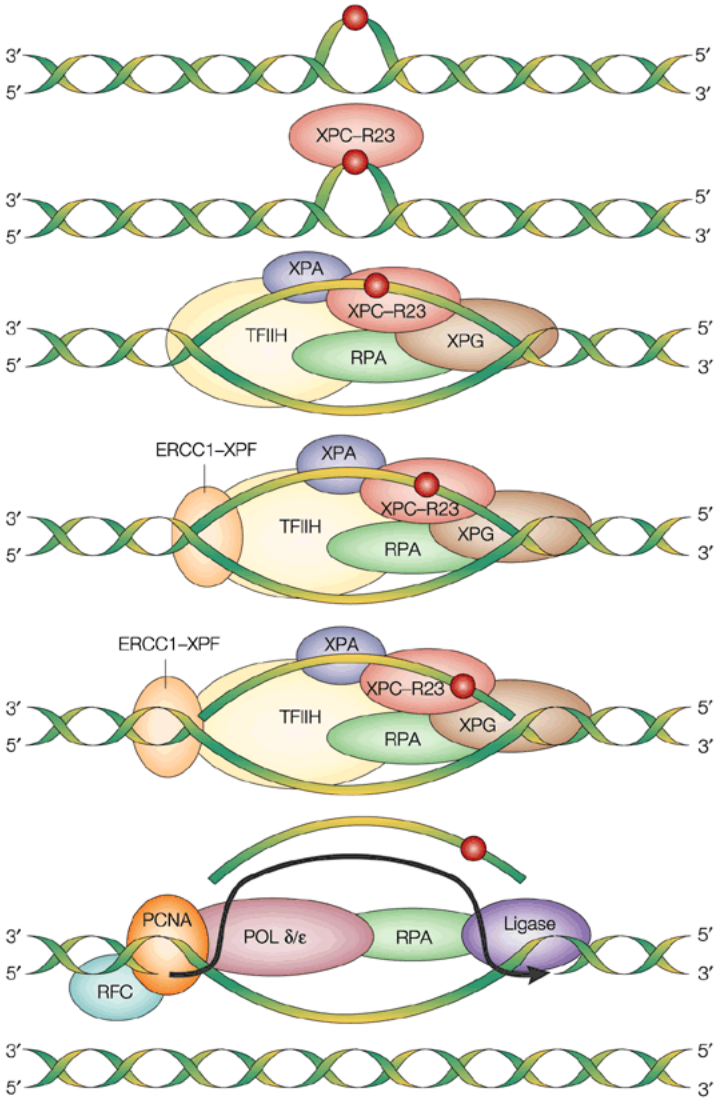

Figure 14: Molecular actors involved in the nucleotide-excision repair pathway.
Upon base damage caused by exogenous agents and altering the structure of the DNA duplex, the NER pathway is activated. Shown are the major factors involved in the recognition and repair of such damage, and restoration of the damaged DNA to its native chemistry and configuration.
From Friedberg, 2001.

and bind to the DSB. This is the crucial step of the process as it will presumably trigger its conformational change [Lieber, 2010; Yaneva *et al.*, 1997] that will allow the Ku-DSB complex to recruit the nuclease complex Artemis-DNA-PKcs to cut DNA overhangs [Chang *et al.*, 2015]. It will also allow for the recruitment, in some cases, of polymerases μ and λ to fill DNA gaps [Ma *et al.*, 2004], and the XLF-XRCC4-DNA ligase IV complex to reattach the two DNA ends together [Nick McElhinny *et al.*, 2000]. A lot of variations of this system can occur, and several, probably less common, other NHEJ pathways have been described [Lieber, 2010; Mahaney *et al.*, 2009; Ciccia and Elledge, 2010]. The second major pathway, homologous recombination (HR), takes advantage of the use of an undamaged copy of the broken area to restore its integrity (fig. 15) [Heyer *et al.*, 2010]. This more error-free mechanism is restricted to specific conditions, like the G2 phase of the cell cycle, when an undamaged copy of the damaged DNA is readily accessible for the repair factors [Brandsma and Gent, 2012]. Broken DNA ends are recognized by the MRN complex (MRE11-RAD50-NBS1) [Stracker and Petrini, 2011], which will promote the activation of ATM [Williams *et al.*, 2007]. Together, the MRN complex and ATM are then able to recruit all other proteins necessary for the processing of the damaged DNA to form extended regions of single-stranded DNA bound to RPA [Ma *et al.*, 2017]. Those proteins can include different nucleases and helicases [Mimitou and Symington, 2009]. With the help of BRCA1, RPA bound to the single-strand DNA is then replaced by RAD51, which will conduct the homology search, with other proteins, to find the homologous DNA sequence and perform the strand invasion [Ciccia and Elledge, 2010]. At least a polymerase and a DNA ligase are needed to complete this HR-mediated repair, but many other proteins can also be involved and their association will govern the resolution of this complicated four strand DNA junction. Three different outcomes are currently described, divergent in their level of intermingling between the broken DNA double-helix and its homologous counterpart, but the enzymatic requirements for each of them remain to be clarified [Heyer *et al.*, 2010].

In addition to these molecular components acting at the DNA breaks, multiples PTMs are also known to regulate the DNA repair processes due to their impact on the chromatin structure, their ability to recruit repair factors and to regulate their activity.

All known PTMs are involved in the DNA Damage Response

During the early stages of the DNA damage response, a lot of chromatin modifications and alterations in its structure have been reported at the site of the breaks [Price and D'Andrea, 2013; Shi and Oberdoerffer, 2012]. At the nucleosomal scale, the most studied modification is the phosphorylation of histone variant

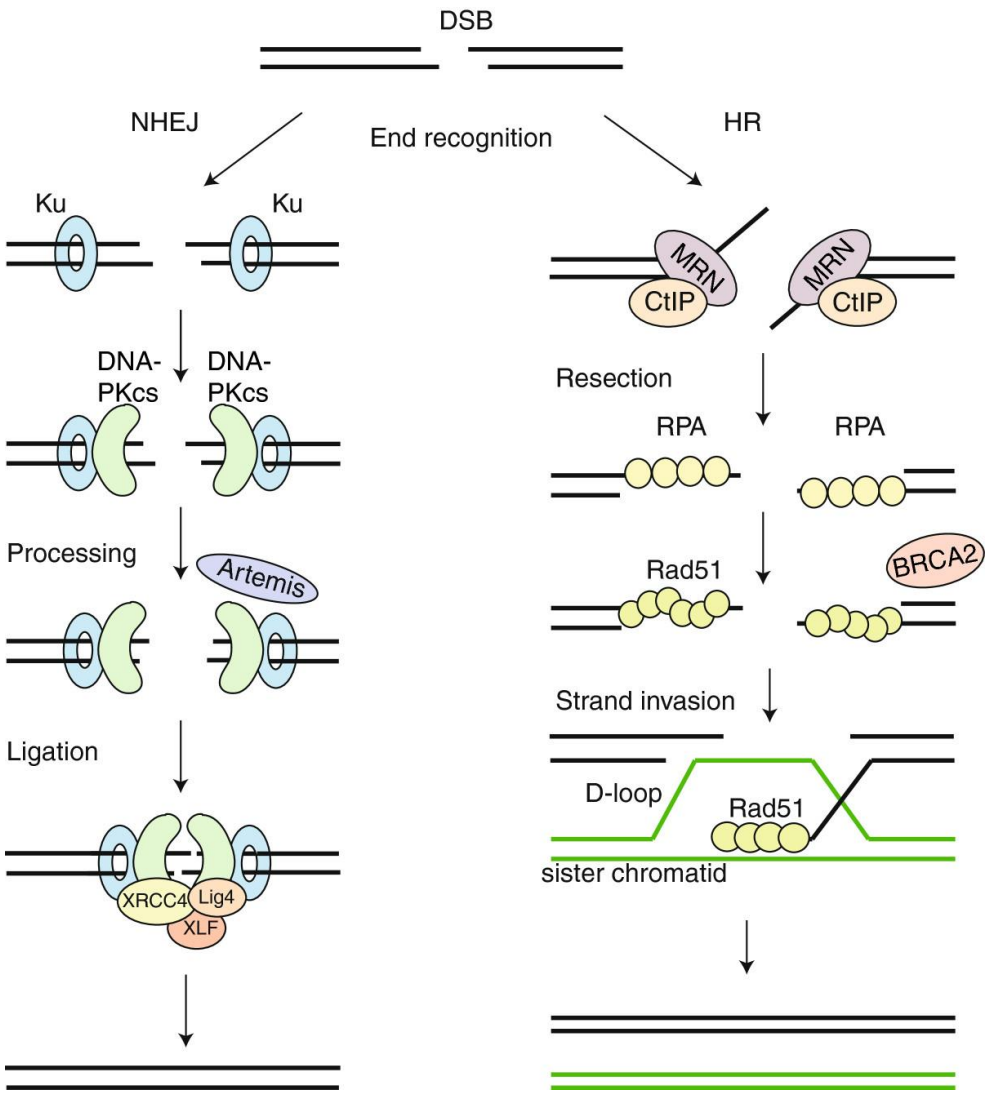

Figure 15: Molecular actors involved in non-homologous end-joining and homologous recombination.

Upon the formation of a double-strand break in the DNA molecule, two major pathways can be activated to handle the damage, NHEJ and HR. Shown are the major factors involved, both in NHEJ and HR, in the recognition and repair of DSBs, and restoration of the damaged DNA to its native chemistry and configuration.

From Brandsma and Gent, 2012.

H2AX by the PIKK family of kinases, including ATR, ATM, and DNA-PKs that will help in signaling the damage and in the recruitment of other factors [Rogakou *et al.*, 1999; Lukas *et al.*, 2004; Lou *et al.*, 2006]. This phosphorylation event, along with others, can lead to the recruitment of specific DDR factors that harbor phosphor-binding domains such as BRCT or FHA [Mohammad and Yaffe, 2009]. Ubiquitylation is another PTM that is supposed to play a role as soon as the first steps of DNA damage signaling, thanks to the recruitment of RNF8 and RNF168 among others [Doil *et al.*, 2009; Huen *et al.*, 2007]. It has been shown to help in the DNA damage induced repression of gene expression such as cyclin B1 and chdk1 which will ultimately lead to the cell cycle arrest to allow time for the repair to occur [Shimada *et al.*, 2008]. Independently, acetylation also occurs at early times during the DNA damage response, notably by the p300/CBP or the NuA4 histone acetyltransferase (HAT) complexes [Jiang *et al.*, 2010; Murr *et al.*, 2006]. HAT inhibitor treatment or depletion of either one of those complexes significantly impairs the DNA damage repair capacity of cells [Ogiwara *et al.*, 2011]. Methyl-transferases are also involved in the DDR, especially through their action on histones to later act as platform for recruitment of proteins with a chromodomain or a tudor domain for instance [Taverna *et al.*, 2007], such as 53BP1, HP1 or TIP60 [Cheutin *et al.*, 2003; Sun *et al.*, 2009]. In this process, and through those epigenetic marks are also recruited chromatin remodeling complexes. Even if their direct mechanism of action and their purpose at the site of breaks is still not a consensual topic, the ISWI [Erdel *et al.*, 2010], INO80 [Wu *et al.*, 2007], SWI/SNF [Smith-Roe *et al.*, 2015] complexes and members of the CHD family [Ahel *et al.*, 2009, Polo *et al.*, 2010] have all been associated with the DNA damage response.

While the study of the molecular players and PTMs involved in the DDR led to great advancements in the field, chromatin was disregarded for a long time. Nevertheless, all those events are bound to have a major impact on its structure and more recent studies have tried to investigate this matter.

Chromatin relaxation and mobility changes upon DNA Damage

While chromatin displays similar dynamics in yeast and human cells in undamaged conditions, as previously discussed, differences arise when assessing the behavior of chromatin upon the induction of DSBs in these two eukaryote species. These differences might come from the fact that NHEJ is predominantly used to deal with DSBs in mammalian cells lines while, in yeast, HR dominates [Sonoda *et al.*, 2006].

Chromatin dynamics upon DNA damage in yeast

Chromatin mobility was assessed in yeast in many studies by tracking fluorescently-tagged loci after DSB induction using either pharmacological treatment or restriction enzymes. As briefly touched on above, DSB repair by HR first involves the processing of DNA ends before the homology search and homologous recombination can occur [Seeber and Gasser, 2016]. During this first step, damaged chromatin loci actually display a hindered diffusion capacity [Saad *et al.*, 2014], probably due to the need to keep the two DNA ends close together for the proper subsequent homology search. During this next step, as one would expect, chromatin loci show an increased mobility [Dion *et al.*, 2012; Miné-Hattab and Rothstein, 2012]. Some molecular players have been successfully linked to this process, such as Mec1 or Rad9 [Dion *et al.*, 2012]. Furthermore, it has been shown that this higher chromatin mobility is not restricted to the damaged locus and that it spreads to the entire nucleus in diploid cells [Miné-Hattab and Rothstein, 2012]. Mec1, Rad53, and INO80 are known to be involved in this overall increased mobility effect [Seeber *et al.*, 2013]. It is important to note, however, that not all damage in yeast triggers enhanced chromatin mobility. Spontaneous damage or DNA adducts repaired by exchange with a sister chromatin or through NHEJ do not induce this effect [Dion *et al.*, 2012], hinting at the importance of this regulated process for proper DSB repair when a homology search through the nucleus is required.

Interestingly, large directed motion of damaged loci has also been reported in yeast. Indeed, a recurring debate regarding DSB repair is the possible formation of "repair factories" [Meister *et al.*, 2003], structures presumed to be formed by the recruitment of multiple DSBs and constituting a form of functional clustering inside the nucleus. Even if some studies have demonstrated such cluster formation [Lisby *et al.*, 2003] or relocation to the nuclear periphery [Nagai *et al.*, 2008; Kalocsay *et al.*, 2009], those movements seem to be restricted to specific, yet undefined, conditions.

Chromatin dynamics upon DNA damage in mammals

In coherence with the use of HR as a major DSB repair pathway in yeast, increased mobility of damaged chromatin loci is well documented and firmly established for this organism. The situation in mammalian cells seems, instead, more complicated. Indeed, consistent with the fact that the major DSB repair pathway in mammals is NHEJ and that increased mobility might not be beneficial in this case, a lot of studies reported that no apparent change in mobility was observed upon DNA damage induction using either UV-laser irradiation [Kruhlak *et al.*, 2006], X-ray irradiation [Nelms *et al.*, 1998], ion irradiation [Jakob *et al.*, 2009], or enzymes [Soutoglou *et al.*, 2007; Roukos *et al.*, 2013]. Nevertheless, some others found damaged

loci to have enhanced mobility compared to undamaged DNA [Krawczyk *et al.*, 2012; Lottersberger *et al.*, 2015], and even regroup to form clusters [Aten *et al.*, 2004], hinting once again at potentials "repair factories". Moreover, directed motion of damaged loci towards euchromatin areas was also reported specifically for DSBs occurring in dense heterochromatin areas [Jakob *et al.*, 2011; Ježková *et al.*, 2014]. This phenomenon has been proposed to occur to prevent possible harmful chromosomal rearrangements following illegitimate recombination within the highly repetitive chromatin environment. It was shown recently to be restricted to specific conditions, both in space, as pericentric heterochromatin seems more prone to relocate than centromeric heterochromatin, and in time as it is suggested to only occur during the S/G2 phases of the cell cycle when HR would be used to repair DSBs [Tsouroula *et al.*, 2016]. As opposed to the yeast model, no global change in chromatin mobility has been reported in human cells.

Besides this potential enhanced chromatin mobility, many reports stated that induction of DNA damage will affect the chromatin compaction state. In fact, it was shown in 1978 that UV-induced DNA damage leads to an increased sensitivity of chromatin to nucleases [Smerdon and Lieberman, 1978]. This higher accessibility has been since correlated with chromatin relaxation observed at the micrometer scale accessible by light microscopy [Kruhlak *et al.*, 2006; Ziv *et al.*, 2006]. This fast occurring process is followed by a slow re-condensation of chromatin until it reaches again its normal compaction state [Khurana *et al.*, 2014], or even possibly reaches higher compaction levels than its pre-damage state [Burgess *et al.*, 2014]. A lot is still unknown regarding the mechanisms driving this decondensation process upon DNA damage. Indeed, proteins involved, as well as signaling and demarcation through time and space of the area supposed to undergo relaxation, or even the purpose of this phenomenon still require more work to elucidate.

In extreme cases, when the amount of DNA damage is too important for the cell to handle, a complete cell cycle arrest followed by apoptosis will occur [Farrell *et al.*, 2011; Kulms and Schwarz, 2000]. Programmed cell death upon the accumulation of unrepaired DNA damage will involve the same signaling pathways as DNA damage and repair [Farrell *et al.*, 2011; Schou *et al.*, 2008], and the shift towards apoptosis has been proposed to be driven by the persistence of these signals, with a possible prominent role for the phosphorylation of H2AX by ATM [Schou *et al.*, 2008]. Chromatin is also at the center of this process as it will over-condense dramatically before being degraded and separated into individual bodies [Yuan, 1996].

Even if the subject of chromatin dynamics upon DNA damage is currently the focus of intense research and if great advancements were achieved over the last decades, we still lack an understanding of the bridge between molecular players described in the classical view of DNA repair and the chromatin

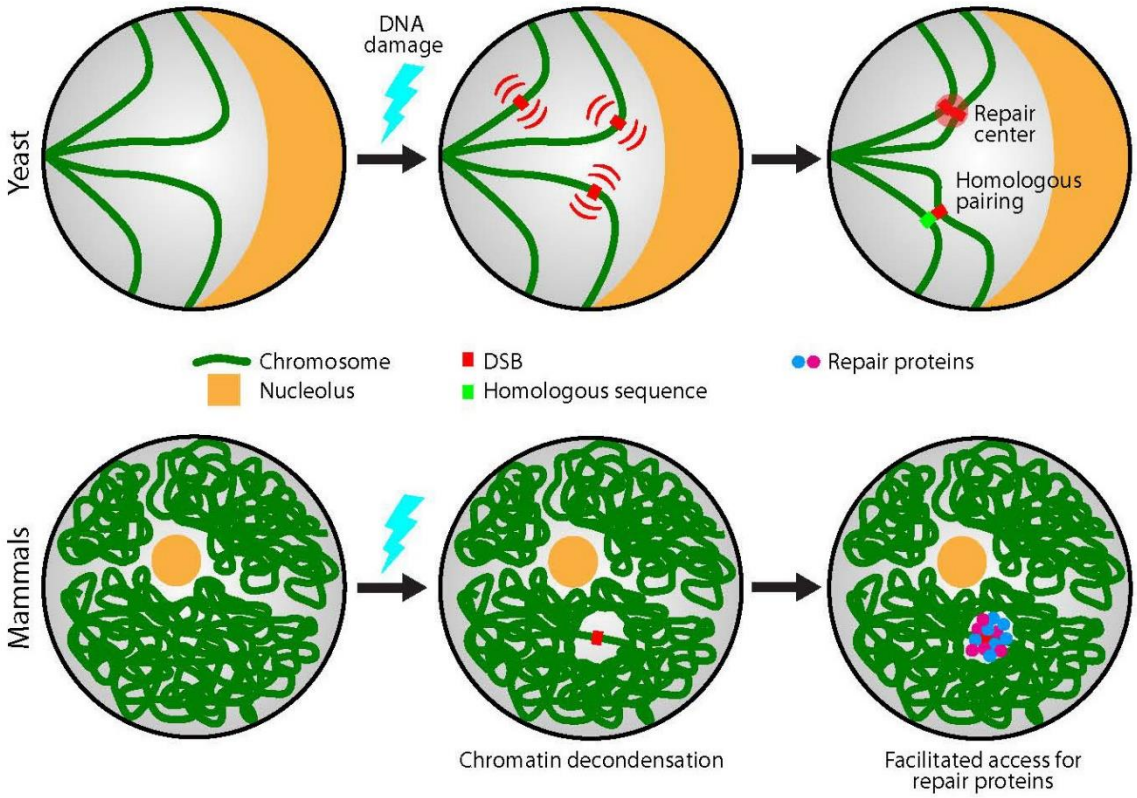

Figure 16: Chromatin dynamics upon DNA damage in yeast and mammals.
In yeast, induction of double-strand break triggers enhanced locus mobility, mechanism proposed to help in finding and pairing with the homologous sequence of the genome in order to repair the damage using homologous recombination. In mammals, non-homologous end-joining is the major pathway used to repair double-strand breaks and no enhanced locus mobility is observed. Instead, a local chromatin decondensation occurs, which has been proposed to help DNA repair factors access damaged DNA.

reorganization observed at the micrometer scale. PARP1, a central player in the DDR that has recently been the focus of many studies interested in the role of chromatin structure in DNA damage repair as it has been shown to be involved both in chromatin architecture and in the DNA damage response, may help fill this gap.

PARP1 and PARylation

Among the numerous chromatin PTMs observed in the early stages of the DNA damage response described above, one seems to play a key role in the regulation of chromatin structure at DNA breaks, poly(ADP-ribosyl)ation (PARylation). This modification was actually discovered more than fifty years ago [Chambon *et al.*, 1963], but has drawn more and more attention these last decades as it was shown to not be only involved in DNA damage, but also in a plethora of other nuclear processes [Bock and Chang, 2016]. Furthermore, its potential role in cancer development has led to promising results, drawing even more attention on this modification [O'Sullivan Coyne *et al.*, 2015]. Indeed, the level of PARP enzymes in cancer cells represents a valuable biomarker of prognosis and can help in the choice of further treatment for certain cancers, and the first PAR enzymes inhibitor has recently been approved by the FDA for the treatment of specific breast cancers, paving the way for many more [O'Sullivan Coyne *et al.*, 2015].

Writers of PAR: the PARP family

PARylation represents the addition of ADP-ribose units on a substrate over one another to generate poly(ADP-Ribose) (PAR) chains [D'Amours *et al.*, 1999]. Each ADP-ribose addition on a substrate requires one NAD^+ molecule to act as a donor molecule [D'Amours *et al.*, 1999]. Even if PARylation has been shown to occur primarily on acidic residues (aspartate and glutamate) [D'Amours *et al.*, 1999; Zhang *et al.*, 2013], it has also been shown to target lysine and cysteine residues [Altmeyer *et al.*, 2009; Vyas *et al.*, 2014], and more recently serine residues as well [Fontana *et al.*, 2017]. PARylation, like any PTM, will affect its target by either altering its binding affinities for its partners, modifying its enzymatic activity, or target it to a specific location [Bock and Chang, 2016]. Unlike other PTMs however, PARylation consists in the formation of a non-polypeptide polymeric structure, possibly branched [Miwa *et al.*, 1979], exhibiting a really high amount of negative charges [D'Amours *et al.*, 1999]. These unique features differentiate PARylation from the rest of PTMs since PAR chains will display more similarities with DNA or RNA than with any other PTM product. Thus, in addition to the impact of PARylation on a substrate, PAR molecules can also regulate protein activity and function through non-covalent binding [Kassner *et al.*, 2013].

PARylation is catalyzed by the PAR Polymerase (PARP) family of enzymes, also known as ADP-ribosyltransferase diphtheria toxin-like (ARTD) [Hottiger *et al.*, 2010]. Even if only four enzymes have a well-documented PARylation activity, namely PARP1 and 2 and two tankyrases, this family is composed of seventeen members (fig. 17) [Barkauskaite *et al.*, 2015], the others having either no detectable enzymatic activity or a mono-ADP-ribosylation (MARylation) activity [Barkauskaite *et al.*, 2015; Vyas *et al.*, 2014; Kleine *et al.*, 2008]. The structure of the catalytic domain of PARP1, the founding member of the family, has been unraveled twenty years ago [Ruf *et al.*, 1996]. Besides the presence of this ART domain that allows the interaction with NAD^+ and characterizes the family, PARP enzymes are quite diverse and frequently possess DNA- or RNA-binding motifs, as well as other regulatory domains [Steffen *et al.*, 2013]. This diversity translates in the diversity between PARP family members in terms of subcellular location, activity, and function [Steffen *et al.*, 2013]. In the case of PARP1, in addition to the ART domain linked to a helical subdomain, five others are described. Three zinc fingers motifs allow the recognition of specific DNA structures, while an auto-modification domain bears the major auto-modification sites of PARP1 [Langelier *et al.*, 2012]. The last domain is a "WGR" domain. Even if its function is not yet established, it has been shown to be essential [Altmeyer *et al.*, 2009].

Even considering the versatility of domains characterizing different PARP enzymes, categories can be established based on their prominent known function [Barkauskaite *et al.*, 2015]. In this way, PARP1, 2, and 3 represents DNA-dependent PARP, tankyrases (PARP5a and 5b) are defined by the presence of ankyrin repeats, CCCH zinc finger PARP (PARP7, 12, and 13) have the ability to bind viral DNA, and macro PARPs (PARP9, 14, and 15) possess a PAR-binding domain [Vyas *et al.*, 2014]. Due to lack of knowledge on their precise function, the six other PARPs remain, for now, unclassified.

In addition to the impact of PARylation on its target, and on the possible effect of free PAR chains on other molecules, PARP enzymes have also been shown to have a role independently of their catalytic activity. Indeed, some PARPs have been shown to bind and sequester proteins, or RNAs without involving PARylation (or MARylation) in the process [Hassa and Hottiger, 2008]. Furthermore, PARPs with RNA-binding motifs can also regulate the stability of specific RNAs and thus, the expression levels of specific proteins [Hassa and Hottiger, 2008]. Altogether, the PARP family appears to regulate a lot of cellular functions, and this through many possible ways.

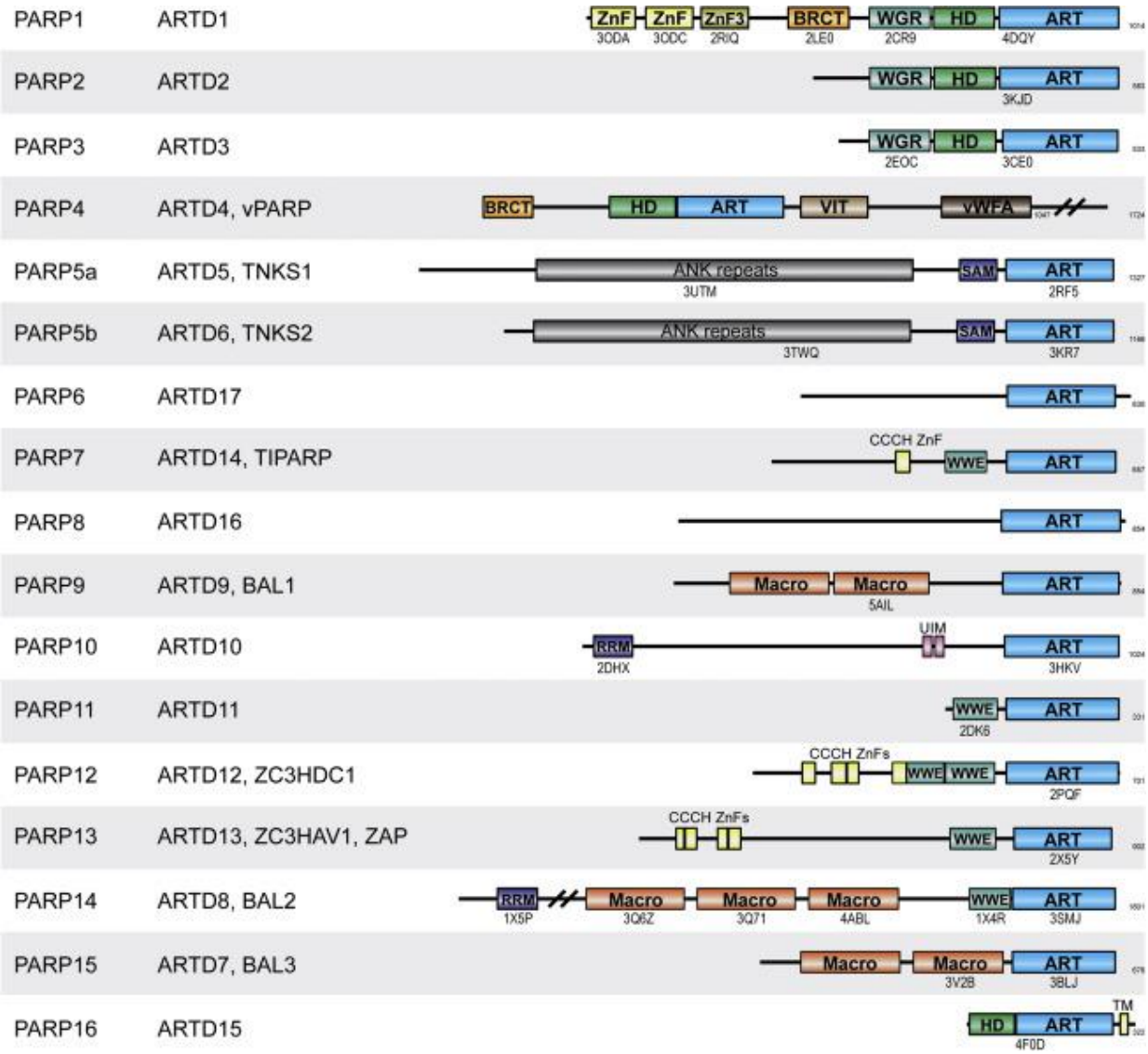

Figure 17: The PARP family.
Shown are the schematic representations of the 17 members of the PARP family with the location of their known domains.
From Barkauskaite *et al.*, 2015.

Readers of PAR: signaling through PAR-binding domains

Like any PTM, PARylation needs writers to apply the mark, but also readers to translate the signal. Excluding the possible roles of free PAR chains on surrounding molecules, PARylation on a target can have a structural or chemical effect on its own, regulating proteins interaction, function or location, but can also fulfill its purpose through the interaction with PAR-binding factors [Teloni and Altmeyer, 2016]. Indeed, recent advancements in proteome-wide analysis of the cellular PARylome has led to the conclusion that more than 800 proteins interact with PAR [Gagné *et al.* 2008], hinting at the fact that a high localized PARylation event can have tremendous effects on nuclear protein redistribution and influence many different cellular pathways. Therefore, finding PAR-interacting domains has been the focus of many studies over the last years, and great advancements were achieved in the field (fig. 18) [Teloni and Altmeyer, 2016].

The first domain discovered to bind PAR was named PBM (PAR-binding motif) and characterized less than 20 years ago [Pleschke *et al.*, 2000]. It is defined as a cluster of around 20 hydrophobic amino acids spaced by basic residues, and more than 800 proteins are presumed to bear this motif [Pleschke *et al.*, 2000; Gagné *et al.* 2008]. The vast majority of those proteins are involved either in DNA and RNA functions, or stress signaling and cell cycle regulation [Gagné *et al.* 2008]. Interestingly, a single protein can bear multiple PBMs, hinting at a possible higher regulation of PAR interactors taking into account the length and topology of PAR chains. The PAR-binding zinc finger (PBZ) domain is another sequence of 30 amino acids that can interact with PAR [Ahel *et al.*, 2008; Isogai *et al.*, 2010]. Two proteins only have been described to interact with PAR through zinc finger domains, APLF (aprataxin and PNK-like factor) and CHFR (checkpoint with forkhead and ring finger domains), both involved in the DNA damage response. Interestingly, PBZ domains of those two proteins were shown to be critical for their proper recruitment at the site of damage and subsequent function [Rulten *et al.*, 2008; Oberoi *et al.*, 2010]. Variations of this PBZ motif are described and may also enable interaction with PAR, but more work is needed for their proper characterization [Ahel *et al.*, 2008; Min *et al.*, 2013].

Other PAR interactors encompass 3-dimensional domains that can recognize this modification. Twelve human proteins possess a WWE domain, named after its most conserved amino acids, and are regrouped in only two families of proteins, PARPs and ubiquitin ligases [Wang *et al.*, 2012]. Macrodomains are other readers of PAR [Timinszky *et al.*, 2009; Gottschalk *et al.*, 2009]. The macrodomain possesses unique features as it is the only PAR-binding domain known to date to recognize single ADP-ribose moieties, granting its bearer possible interaction with both PARylated and MARylated proteins [Ahel *et al.*, 2009].

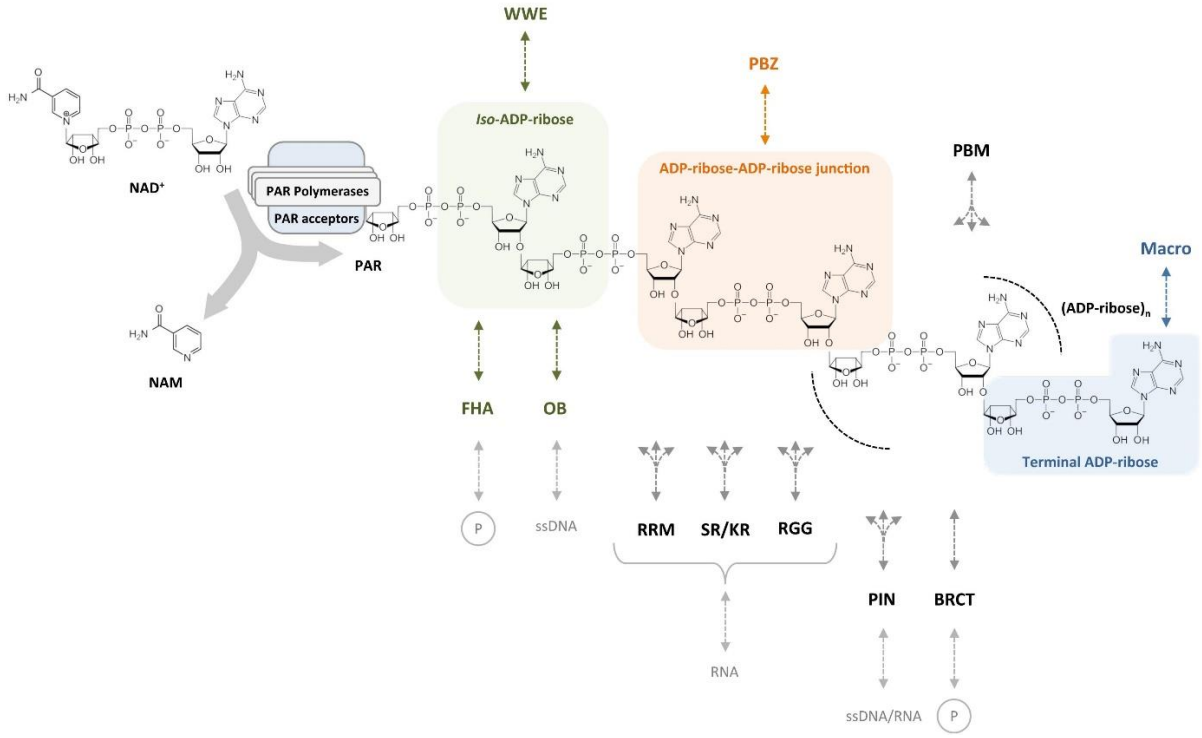

Figure 18: Readers of poly(ADP-ribose).
PAR polymerases use NAD+ to generate highly anionic linear and branched (not shown) PAR chains of different size and branching complexity. Besides the classical, well-characterized PAR reader modules WWE, PBZ, PBM, and macrodomains (top) also newly emerging PAR reader modules such as FHA, OB-fold, PIN domain, RRM, SR, and KR repeats, RGG repeats and BRCT (bottom) appear as PAR readers and effectors. Multi-branched arrows indicate that the exact binding sites have not been defined.
From Teloni and Altmeyer, 2016.

Eleven proteins possess one or several macrodomains, including PARPs and chromatin interactors [Timinszky *et al.*, 2009; Ahel *et al.*, 2009]. Interestingly, PARPs that encompass one or several PAR-binding motifs have not been shown to possess a PARylation catalytic activity, hinting at another possible different role and specialization among PARPs. The rest of the PAR-binding domains known to date were described previously for another function but have been shown recently to interact with proteins carrying this modification. This list includes FHA (Forkhead-associated) and BRCT (BRCA1 C-terminal) domains [Breslin *et al.*, 2015; Li and Yu, 2013] and a lot of DNA and RNA binding domains such as the RNA recognition motif (RRM) [Gagné *et al.*, 2003], the RG and RGG motifs (regions rich in arginine and glycine) [Haince *et al.*, 2008] or the PIN domain (PilT N-terminus) [Zhang *et al.*, 2015].

Erasers of PAR and the complexity of PAR signaling

PARylation also shares with other PTMs the fact that it is a reversible modification. However, while most PTMs are reversed through a single reaction involving a single specific type of enzyme, PARylation shows once more an increased complexity. Indeed, at least two different enzymes are needed to completely remove PAR from a target as the hydrolysis of the last ADP-ribose moiety requires a different enzymatic activity than for the rest of the PAR chain. The main eraser of PAR in the cell is PAR glycohydrolase (PARG) [Barkauskaite *et al.*, 2015]. This enzyme displays both exo- and endo-glycohydrolase activities [Dunstan *et al.*, 2012], but is unable to remove the last, or the only in the case of MARylated proteins, ADP-ribose bound to the target [Slade *et al.*, 2011]. Its macrodomain recognizing ADP-ribose moieties and its double enzymatic activity give this eraser the power to degrade PAR chains almost entirely and terminate the signal, or to free PAR chains of different length from their targets, potentially altering the signal on the target protein while allowing free PAR chains to retain their role as scaffolding polymers [Brochu *et al.*, 1994].

After the complete degradation of a PARylation signal on a protein by PARG, or in the case of MARylation, mono-ADP-ribose hydrolases are required to remove the last ADP-ribose unit. The three members of the ARH family (ARH1, 2, and 3) have been shown to be able to fulfill that purpose, as well as a few other proteins, namely TARG1 (terminal ADP-ribose protein glycohydrolase, also known as C6orf130), macroD1 and macroD2 [Rosenthal *et al.*, 2013]. Interestingly, ARH3 has been shown to also act as a PAR glycohydrolase, even if its affinity for PAR chains is far below the one of PARG [Oka *et al.*, 2006]. Also important to note is that TARG1 has been proposed to act on the ADP-ribose unit linked to the target even in the case of PARylation, suggesting the same kind of regulation described for PARG endo-glycohydrolase ability [Sharifi *et al.*, 2013].

The termination of the PARylation signal is supposed to be as important as its induction, as shown by the embryonic lethality of PARG knockout mice [Koh *et al.*, 2004] and the induction of a specific type of cell death, parthanatos, due to excessive PARylation in the nucleus [Wang *et al.*, 2011]. In fact, PARylation represents a highly transient and dynamic signal, since PAR was shown to be processed in a matter of seconds, and MAR in a timescale of minutes [Wielckens *et al.*, 1982].

PARP1 and PARylation in chromatin architecture and dynamics

Considering the diversity of PARP enzymes, and the complexity of PAR signaling and PAR levels regulation, both PARPs and PARylation are bound to have a major impact on the regulation of nuclear physiology through a wide range of effects, including the regulation of chromatin structure and dynamics. Since PARP1 was the first PARP enzyme discovered and seems to be the most active PARylator in the cell, it has been the focus of most studies and both its roles as a DNA-binding protein and as a PARP enzyme have been investigated.

PARP1 has been shown to act as a structural component of chromatin without any involvement of its catalytic activity. Indeed, in the absence of NAD^+, PARP1 is able to bind strongly to nucleosomes in a way similar to that of H1, and induce chromatin condensation *in vitro* [Kim *et al.*, 2004]. The binding of PARP1 to nucleosomes was shown to involve both entry and exit sites of linker DNA, like H1 [Clark *et al.*, 2012]. Nevertheless, even if the binding of both those proteins has been shown to promote heterochromatin formation, PARP1 seems to be associated with less condensed chromatin [Clark *et al.*, 2012] and large, non-overlapping, chromatin regions bound to PARP1 or H1 can be observed [Kim *et al.*, 2004]. This hints at the fact that PARP1 and H1 binding to chromatin is a regulated process that leads to the formation of structurally different heterochromatin. Interestingly, this competition between H1 and PARP1 for binding to the nucleosome has been shown to play a part in transcription regulation where an exclusion of H1 in promoter regions of PARP1-regulated genes is observed [Krishnakumar *et al.*, 2008]. In addition, the exclusion of H1 from promoter regions in the case of transactivation can also occur in a PARylation-dependent manner [Shan *et al.*, 2014].

Besides its role as a structural component of chromatin, PARP1 can also PARylate a lot of chromatin structural components. The vast range of its targets include all canonical core histones [Messner *et al.*, 2010], linker histone H1, as well as CTCF [Yu *et al.*, 2004] and a tremendous amount of proteins involved in DNA metabolism [Gagné *et al.*, 2008]. In the case of histone modifications, PARylation is presumed to destabilize DNA-histone or histone-histone interactions and promote chromatin relaxation [Mathis and

Althaus, 1987]. The case of CTCF is interesting as the presence of CTCF stimulates the activation of PARP1 which will, in turn, PARylate CTCF as well as inhibiting DNA methylation. Those two events contribute to the insulator behavior of the chromatin region [Yu *et al.*, 2004, Guastafierro *et al.*, 2008]. Also important to note is that PARylation is tightly linked to all other chromatin epigenetic modifications. Indeed, the loss of PAR through chemical inhibition or depletion has been shown to lead to genome-wide dramatic changes in terms of histone acetylation [Verdone *et al.*, 2015], methylation [Erener *et al.*, 2012], or DNA methylation [Caiafa *et al.*, 2009].

Altogether, PARP1 appears as a guardian of chromatin conformation in unstressed conditions, participating in the maintenance of epigenetic marks, insulator regions, and heterochromatin definition. However, the main event that triggers PARP1 activation, that has led to its discovery and has therefore been the subject of intense research, is DNA damage. It will be discussed in the following section. It is important to note that, while most studies interested in chromatin structure and dynamics have focused on PARP1, a lot is still unknown about possible roles of other PARPs in chromatin regulation and this question should be addressed in future studies.

PARP1 and PARylation in the DNA damage response

Along with PARP2 and PARP3, PARP1 is categorized as a DDR-PARP and seems to be the major player in this context as it is responsible for more than 90% of the overall PARylation triggered by the alterations of DNA [Rank *et al.*, 2016]. Moreover, PARP1 is the only protein that has been shown to be involved in almost every repair pathway described to date, demonstrating its importance in the recognition of multiple sorts of DNA alterations [Wei and Yu, 2016]. Indeed, upon DNA damage, PARP1 acts as a sensor and is recruited at the site of the breaks within seconds after their induction [Ahel *et al.*, 2009]. Binding of PARP1 to damaged DNA was proposed to occur in a very different way than its binding to chromatin in unstressed conditions [Langelier *et al.*, 2012]. Indeed, the recognition of altered DNA structures involving two DNA-binding domains, as well as its WGR domain, has been predicted to induce a conformational change in the molecule triggering its catalytic activation [Langelier *et al.*, 2012, Altmeyer *et al.*, 2009]. The recognition of damaged DNA by PARP1 will lead to a fast and high increase of PARylation levels at the site of DNA damage [Timinszky *et al.*, 2009]. Interestingly, the main acceptor of PAR upon DNA damage is PARP1 itself [Ogata *et al.*, 1981], and its auto-modification *in vitro* weakens its affinity for chromatin, but not for DNA [Muthurajan *et al.*, 2014], possibly hinting at the regulation of its dual role in chromatin structure.

This PARylation event is correlated with a fast and local chromatin relaxation at the site of DNA damage [Ahel *et al.*, 2009, Kruhlak *et al.*, 2006], observed at the micrometer scale accessible by light microscopy. This process is followed by a slow re-condensation event [Khurana *et al.*, 2014], presumably following the DNA damage repair. Since all histone proteins are targets of PAR, this process has been proposed to be dependent on their PARylation at DNA damage sites, loosening the tides between histones and DNA [Mathis and Althaus, 1987]. However, *in vivo* data is still lacking to prove this assumption. Another hypothesis is that PARylation at DNA damage sites could also induce chromatin relaxation through the recruitment of proteins encompassing PAR-binding modules. Indeed, several chromatin-remodeling enzymes have been shown to be recruited to the site of DNA damage in a PAR-dependent manner [Chou *et al.*, 2010; Polo *et al.*, 2010; Smeenk *et al.*, 2013]. Other proteins with chromatin PTM activities that are recruited at DNA damaged sites and involved in DNA repair could also play a role in the chromatin relaxation process. However, the link between possible nucleosome remodeling and chromatin PTM events happening at the molecular scale and the chromatin relaxation occurring at the nuclear scale remains to be elucidated.

MATERIAL AND METHODS

Cell Culture and Transfections

Plasmids

The core histone H2B, subcloned from the pH2B-mCherry vector (a gift from J. Ellenberg, [Neumann *et al.*, 2010], Euroscarf P30632), was cloned into pPATagRFP-N1 using NdeI and BamHI restriction sites. pPATagRFP-N1 was a gift from V. Verkhusha ([Subach *et al.*, 2010], Addgene plasmid # 31941). The histone H1.1-PAGFP, along with H1.2-5, was a gift from J. Ellenberg ([Beaudouin *et al.*, 2006], Euroscarf P30503). Another construct of H1.1-PAGFP was produced with the PAGFP tag on the other side of the protein to ensure that similar results could be obtained with both constructs [Hutchinson *et al.*, 2015]. H1.1 was PCR amplified from the H1.1-PAGFP plasmid and subcloned into pmEGFP-N1 using BglII and ApaI to obtain the H1.1-EGFP construct. The same thing was done with all other H1 isoforms. PARP1-mCherry, described previously [Timinszky *et al.*, 2009], was used to generate PARP1-EGFP by exchanging mCherry with EGFP. The sequence of PARP2 was a gift from Gyula Timinszky and PARP2-EGFP was generated by PCR using NheI/SmaI and placed into pmEGFPC1 (Clontech). PARP3-EGFP (short isoform) was a gift from C. Prigent [Rouleau *et al.*, 2007]. PAGFP was replaced by EGFP to produce the H1-tail-EGFP plasmid. The GFP protein alone was expressed using the pEGFP-C2 plasmid (Clontech). The plasmid pmEGFP5 was a gift from J. Ellenberg ([Bancaud *et al.*, 2009], Euroscarf P30624). The EGFP2 plasmid was purchased (Euroscarf P30623). The plasmid pEGFP-LacI was a gift from G. Timinszky, and the plasmids BZip-Ruby2 [Tsekouras *et al.*, 2015], TetR-GFP and RevTetR-GFP [Normanno *et al.*, 2015] came, respectively, from S. Pressé and from M. Dahan. Mammalian expression was under the control of CMV promoter. All constructs were sequence verified.

Cell culture

Wild-type U2OS or knock-out U2OS cell lines were routinely cultured in Dulbecco's modified Eagle's medium (with 4.5 g/L glucose) supplemented with 10% fetal bovine serum, 2 mM glutamine, 100 µg/mL penicillin, 100 U/mL streptomycin in 5% CO2 at 37 °C. For microscopy experiments, cells were plated on Lab-Tek II chambered coverglass (Thermo scientific) and the medium was replaced immediately prior to imaging by Leibovitz's L-15 medium (Life Technologies) supplemented with 20% fetal bovine serum, 2 mM glutamine, 100 µg/mL penicillin and 100 U/mL streptomycin.

Generation of the PARP1 knock-out cell line

The knock-out cell line was designed according to the protocol described by the Zhang lab [Ran *et al.*, 2013], and using their web-based CRISPR design tool (http://www.genome-engineering.org) to identify the target sequence for PARP1 (5'-GTCCAACAGAAGTACGTGCAA-3'). The sgRNA oligos were introduced into pX458 expressing Cas9 nuclease fused to GFP (Addgene #48138). pSpCas9(BB)-2A-GFP (PX458) was a gift from Feng Zhang (Addgene plasmid # 48138). Plasmids were transfected using XtremeGENE HP (Roche) according to manufacturer's protocol. Single GFP positive cells were sorted into 96-well plates using FACS. Cell lines grown up from single cells were identified by western blot using a specific antibody.

Transfections

Transient transfections were performed 24h after plating cells using XtremeGENE HP (Roche) or JetPRIME (Polyplus Transfection) according to manufacturer's instructions. Cells were imaged 48 to 72h after transfection.

Treatments

Cells were pre-sensitized for 1h prior to imaging in medium containing 0.3 µg/mL Hoechst 33342 (Life Technologies). PARP inhibitor AG-14361 (Euromedex) was used at 30 µM 10 minutes before and during acquisition. ATP depletion was achieved as described by Platani and colleagues [Platan I *et al.*, 2002]. The osmotic shock procedure was previously described by Walter and colleagues [Walter *et al.*, 2013]. ATM inhibition and DNA-PK inhibition were achieved using, respectively, KU-55933 (Euromedex) and NU7441 (KU-57788, Euromedex) at 10 µM 6h before and during the acquisitions. All experiments were performed on unsynchronized cells.

DNA labeling with fluorescent nucleotides

U2OS cells expressing H2B-PATagRFP were synchronized at the G1/S phase transition using aphidicolin (Sigma) at 5 µg/mL for 18h. After aphidicolin release, the cell layer, bathed with growing medium containing 10 µM of dUTP-ATTO633 (Jena-Bioscience), was scraped using a silicon stick to allow nucleotide loading and integration to the DNA during replication (Schermelleh *et al.*, 2001).

Microscopy

Photo-activation and FRAP experiments

Photo-activation and Fluorescence Recovery After Photobleaching (FRAP) experiments were performed on an inverted confocal spinning disk (imaging scan head CSU-X1 from Yokogawa and microscope body Ti-E from Nikon) equipped with a single-point scanning head to allow laser micro-irradiation and local photo-activation using a 405-nm laser, or photo-bleaching using a 488-nm laser. A Plan APO 63x oil immersion objective lens (O.N. 1.4) and an sCMOS ORCA Flash 4.0 camera (Hamamatsu) were used for imaging. The pixel resolution at the object plane was 108 nm. The fluorescence of EGFP and PAGFP was excited with a laser at 488 nm and the fluorescence of mCherry and PATagRFP was excited with a laser at 561 nm. Band pass filters adapted to the fluorophores were used for fluorescence detection. Laser power and acquisition time-lapse conditions were adjusted to minimize photobleaching and possible photo-toxicity during imaging. Photo-activation and DNA damage were induced simultaneously with a 405-nm laser. For FRAP experiments, DNA damage and photo-bleaching were induced simultaneously with a 405-nm laser and a 488-nm laser. Laser powers at 405 nm and 488 nm were measured at the sample level and adjusted before each experiment to stay in the same conditions throughout all experiments. Cells were always irradiated along a 16 µm-long vertical line crossing the nucleus. Cells were maintained at 37°C using a heating chamber during all experiments.

Fluorescence Correlation Spectroscopy (FCS) experiments

FCS experiments were performed on a Leica SP8 confocal microscope equipped with a Plan APO 63x/1.2 NA water immersion objective. The mEGFP fluorescence was excited with a 488-nm laser and selected by a bandpass filter at 500-550 nm. Laser power used for FCS measurements was adjusted to minimize photobleaching and avoid the induction of photo-damage in sensitized cells. Single photons were detected and counted using a τ-Single Photon Avalanche Photodiode and a PicoHarp module from PicoQuant. Each FCS acquisition lasted 45 seconds to reduce the noise on the autocorrelation curves. In those conditions, no recruitment of either 53BP1, PARP1, or Alc1 was detected in sensitized cells. To estimate the residence time of EGFP-tagged proteins in the focal volume, autocorrelation curves were fitted with a one-specie model assuming pure diffusion and neglecting the contribution of the photophysics of the EGFP using the FFS Data Measurements and Analysis suite (SSTC - Scientific Software Technologies Center). For each probed nucleus, FCS traces were acquired at three randomly chosen positions inside the pre-photo-irradiation region and the fitted residency times were averaged. Another round of three FCS traces was obtained 2 minutes after DNA damage induction, *i.e.* after the initial chromatin relaxation phase, at three

different locations inside the photo-damaged area and the fitted residency times were averaged. DNA damage and photo-activation were accomplished using a 405-nm laser. The power of the 405-nm laser was measured at the sample level and adjusted before each experiment to ensure similar irradiations throughout all experiments. Cells were maintained at 37°C using a heating chamber during all experiments.

Data Representation and statistics

Mean curves corresponding to chromatin decondensation, protein releases or recoveries are presented with SEM. The fluorescence intensity measured inside the photo-irradiated area is always divided by the one of the entire nucleus through all experiments to correct for photobleaching during the acquisition as well as possible focus drifts. Moreover, a step of normalization is applied to compare results between multiple cells and experiments. For chromatin decondensation and photoactivation experiments, data is normalized using the value of the fluorescence inside the irradiated area (divided by the one of the entire nucleus) at the first image after photo-irradiation. For recruitment and FRAP experiments, the reference taken is the last image before photo-irradiation. In this case, the mask created using the first image after photo-irradiation is applied to the image immediately preceding photo-irradiation.

Boxplots are generated using a web-based tool developed by the Tyers and Rappsilber labs ('http://boxplot.tyerslab.com/'). The box limits show the first and third quartiles and the median is displayed inside the box. Whiskers extend 1.5 times the interquartile range and outliers are represented as dots. Unless stated otherwise, p values are calculated using unpaired t-test assuming unequal variances. Respectively, *, **, ***, **** are displayed for $p<0.05$, $p<0.01$, $p<0.001$, $p<0.0001$, n.s. stands for 'non-significant'.

RESULTS

During my Ph.D., I focused my attention on three main topics. Firstly, I wanted to further our understanding of the mechanisms driving the PARylation-dependent chromatin relaxation upon DNA damage. To this end, I followed this chromatin decondensation using live cell imaging and photo-manipulation techniques in various conditions. Following the results obtained in this first part, I investigated the role of histone H1 in this process and studied precisely its dynamics upon DNA damage and its possible role in chromatin decondensation. Finally, I performed fluorescence correlation spectroscopy (FCS) experiments, as well as fluorescence recovery after photo-bleaching (FRAP) experiments to study the dynamics of several proteins at the site of the breaks and outside of the breaks. These advanced fluorescence microscopy techniques are used to probe the crowding conditions at the DNA breaks and understand the physical properties of the damaged chromatin environment and its impact on protein dynamics and interactions with chromatin.

An assay to follow chromatin relaxation at DNA damage sites in living cells

In order to follow chromatin dynamics upon DNA damage, an assay was developed in the team using U2OS cell lines in which histones H2B are tagged with a photoactivatable fluorescent protein. Two proteins were used in our experiments: PATagRFP and PAGFP. Both possess the advantage to be slightly visible even before photo-activation, allowing for the location of transfected cells and the estimation of proper expression levels, and a possible activation upon irradiation with a laser emitting at 405 nm. Pre-sensitizing cells with Hoechst at 0.3 µg/mL for 1h allows for the simultaneous DNA damage induction and photo-activation of dyes with the same 405-nm laser micro-irradiation (fig. 19.1). This way, only in the damaged area is the chromatin visible and relaxation upon DNA damage can be followed through time using live cell imaging (fig. 19.2 and 3). For each experiment, a control with the same conditions except for Hoechst treatment can be executed. By expressing a second fluorescently-tagged protein in the cell, one can follow, in parallel to chromatin remodeling, its recruitment to DNA damage sites (fig. 19.3 and 4). Moreover, exchange kinetics for this protein can also be assessed by performing a simultaneous FRAP experiment or another photo-activation experiment to study, respectively, its recovery to damaged chromatin, or its release from damaged chromatin. Photo-irradiation conditions and the power of the laser used for photo-damage have been chosen in order to induce damage in Hoechst-sensitized cells but not in non-sensitized cells. Moreover, the conditions and pattern of irradiation were unchanged throughout all experiments, and the laser power was rigorously measured at the sample level before each experiment.

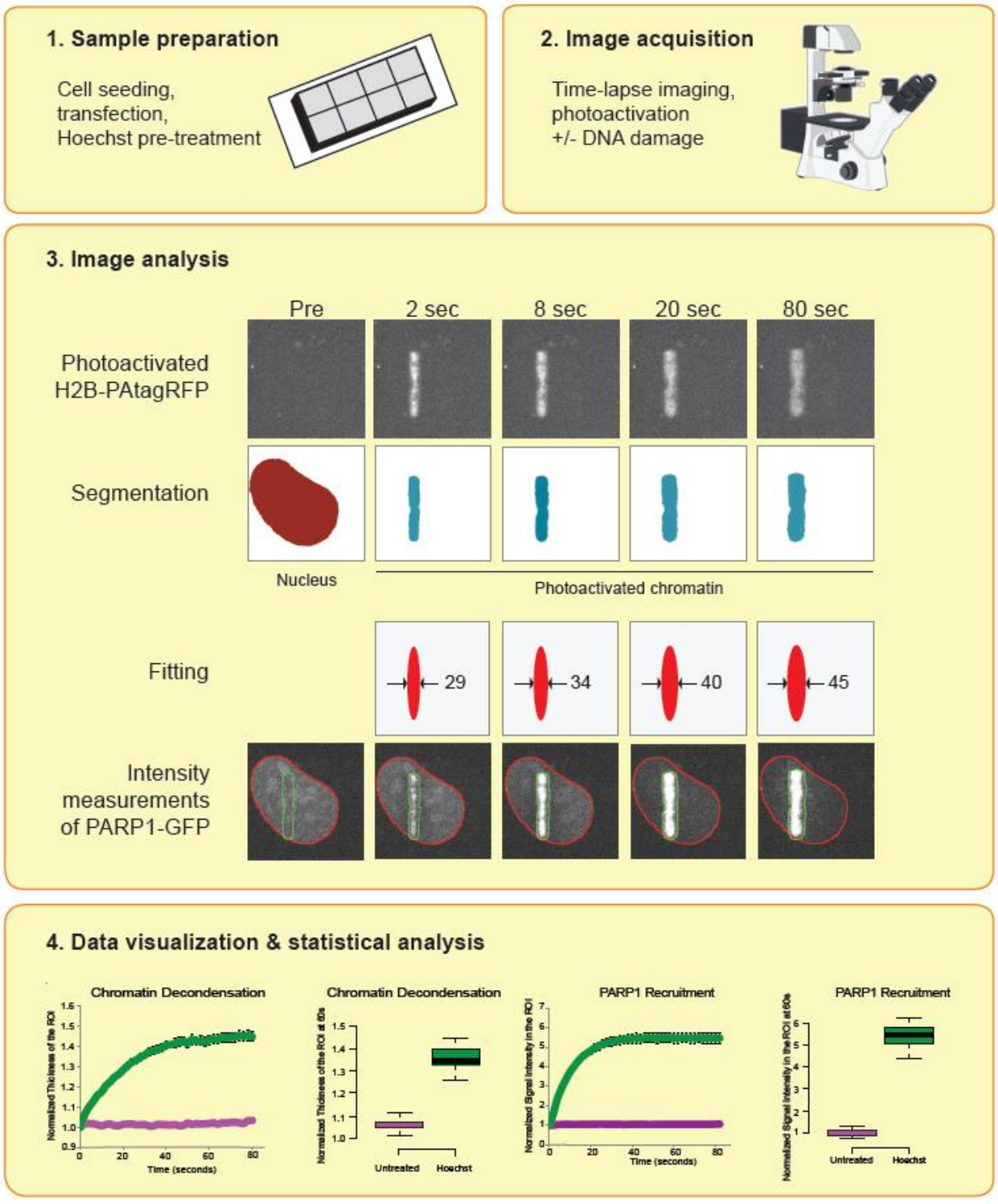

Figure 19: Workflow of the chromatin decondensation and protein recruitment assay.
Shown are the major steps of our H2B photo-activation-based assay developed to follow the relaxation of chromatin upon DNA damage induction, as well as the simultaneous release, recovery, or recruitment of another factor at or from the site of DNA damage. Results for the recruitment of PARP1-GFP are shown as an example.

Validation of the assay

The first needed validation for the assay was to confirm that DNA damage was indeed induced in our conditions, and more specifically, induced in Hoechst-treated cells and not in untreated cells. To this end, the recruitment of PARP1-GFP was assessed upon DNA damage in U2OS cells expressing H2B-PATagRFP, as well as the resultant chromatin relaxation. A strong recruitment of PARP1 can be observed within 10 seconds after photo-irradiation in Hoechst-treated cells, while no recruitment was seen after photo-irradiation in untreated cells (fig. 20, A). The same conclusions were reached while looking at the recruitment of 53BP1, a well-studied DDR actor that is rapidly recruited to DNA damage sites (Panier and Boulton, 2014; fig. 20, A). Moreover, the thickness of the photo-activated line of H2B molecules displayed a 50% increase over time in Hoechst-treated cells after 60 seconds (fig. 20, B), probably reflecting local chromatin relaxation, while no significant change was observed in untreated cells over the same time-lapse (fig. 20, C).

Secondly, in order to ensure that the increase in the size of the fluorescently-tagged H2B area was indeed reflecting chromatin relaxation and not the local release of H2B molecules from the damaged chromatin, another experiment following the behavior of fluorescently-tagged DNA loci upon DNA damage was performed. By incorporating fluorescent nucleotides during replication and after a few cell divisions, this technique allows generating cells with a discontinuous DNA labeling composed of trackable loci. Inducing DNA damage as described above within cells stably expressing H2B-PATagRFP, fluorescent DNA loci within the photo-activated H2B region displayed a directional motion away from the irradiated area (fig. 21, A, B). The calculated speed of this motion was similar to the speed of increase of the size of the photo-activated H2B area (fig. 21, C), validating the use of photo-activated H2B to follow chromatin dynamics upon DNA damage.

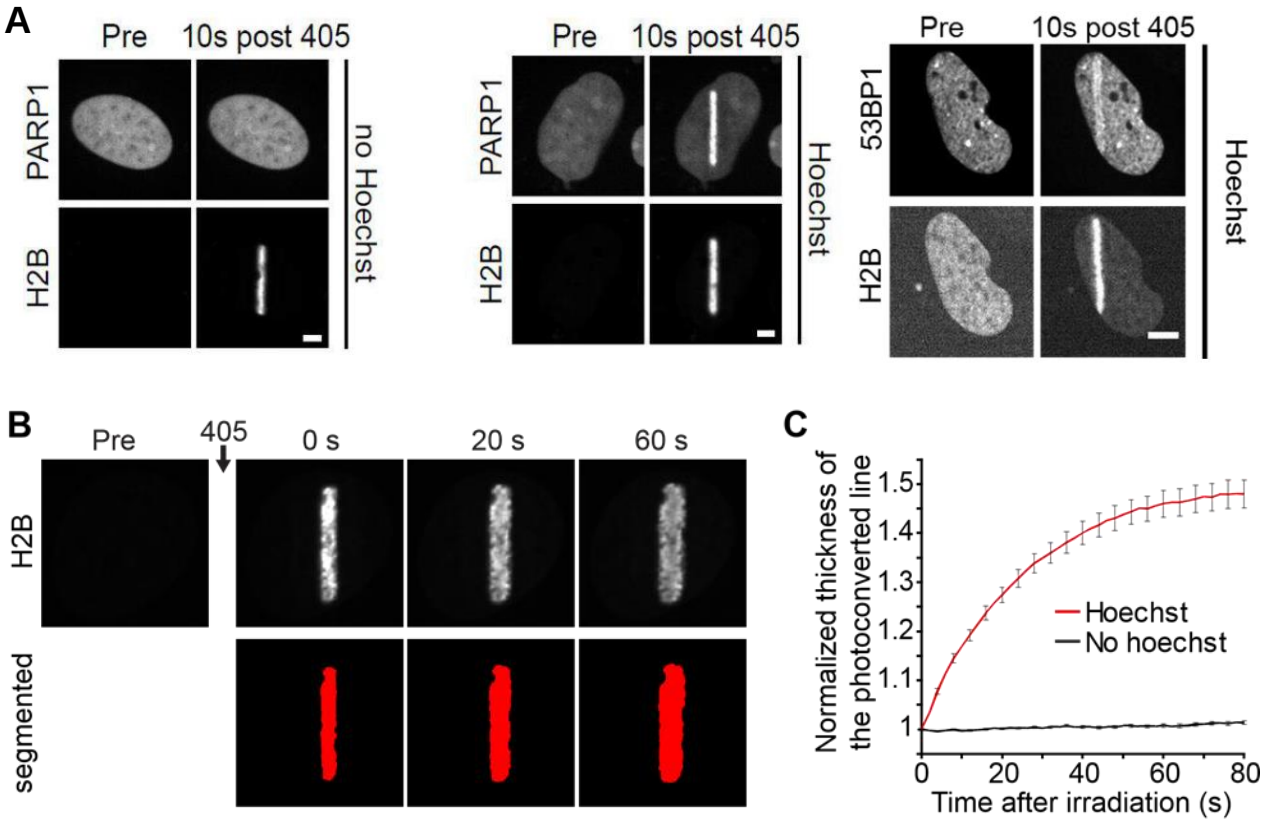

Figure 20: Laser irradiation upon Hoechst treatment induces PARP1 recruitment and chromatin relaxation.

(A) In cells not pre-sensitized with Hoechst, the 405-nm irradiation induces local photo-activation of the H2B-PAGFP but no recruitment of PARP1-mCherry. In contrast, in the case of Hoechst pre-sensitization, the 405-nm irradiation induces both photo-activation of the H2B-PAGFP and a marked recruitment of PARP1-mCherry, indicating the presence of DNA lesions. Similarly, the recruitment of 53BP1-GFP to the H2B-PATagRFP photo-activated area was only observed in Hoechst-sensitized cells. Bar = 4 µm. (B) Confocal image sequence of a human U2OS nucleus expressing H2B-PAGFP. The automatic segmentation of the histone H2B channel is shown in red below the raw images. The average thickness of the segmented line can be plotted as a function of time after irradiation, as shown in (C) for cells pre-sensitized (n=17) or not (n=23) with Hoechst (mean ± SEM). Based on this analysis, the ratio between the thicknesses of the photo-converted line at time = 60 s and time = 0 s can be calculated to estimate the relative relaxation of the irradiated region.

Analysis of the data

Image Analysis – ImageJ and MatLab

Whether looking only at chromatin relaxation upon DNA damage in different conditions or following at the same time the dynamics of another protein, this assay generates a lot of data. In order to analyze those data in a reliable and robust way, the analysis was automated and divided into several parts. First, visualization of Tiff images for quality control and individual cell cropping was done under ImageJ (http://rsb.info.nih.gov/ij/) using custom-made macros. Then, chromatin decondensation, protein recruitment, and release at or from the site of DNA damage was performed with a custom-made program running under MatLab (MathWorks). During this analysis, the nucleus of each cell is segmented using a two-clusters k-means segmentation on the images taken before photo-irradiation (fig. 19.3). This step is performed using the 'protein channel', meaning the second channel used when following the recruitment, recovery or release of a protein at DNA damage sites, if applicable, or the 'chromatin channel', meaning the H2B-tagged channel, if only looking at chromatin relaxation. The photo-activated area is then segmented, also using a two-clusters k-means segmentation, on each of the post-photo-activation images of the timelapse in the H2B channel. An ellipsoid is fitted onto this photo-activated area, frame by frame. Chromatin decondensation is assessed following the width of this ellipsoid through time (fig. 19.3 and fig. 20, C). To assess protein dynamics on another channel, a ratio of fluorescence intensities is calculated dividing the signal inside the photo-activated area by the signal gathered from the entire nucleus, frame by frame. Any measure of intensity presented has been background-subtracted. When considering a GFP or mCherry channel, the background is estimated by measuring the average intensity outside of the nucleus, this area being defined using the inverse of the mask of the nucleus. When looking at a photoactivatable protein, background represents the slightly visible fluorescence coming from non-activated fluorophores and is defined using the average fluorescence intensity inside the nucleus before photo-irradiation. I developed several variations of this program to assess the dynamics of other proteins upon simultaneous FRAP or photo-activation to follow their dynamics inside or outside the damaged chromatin area.

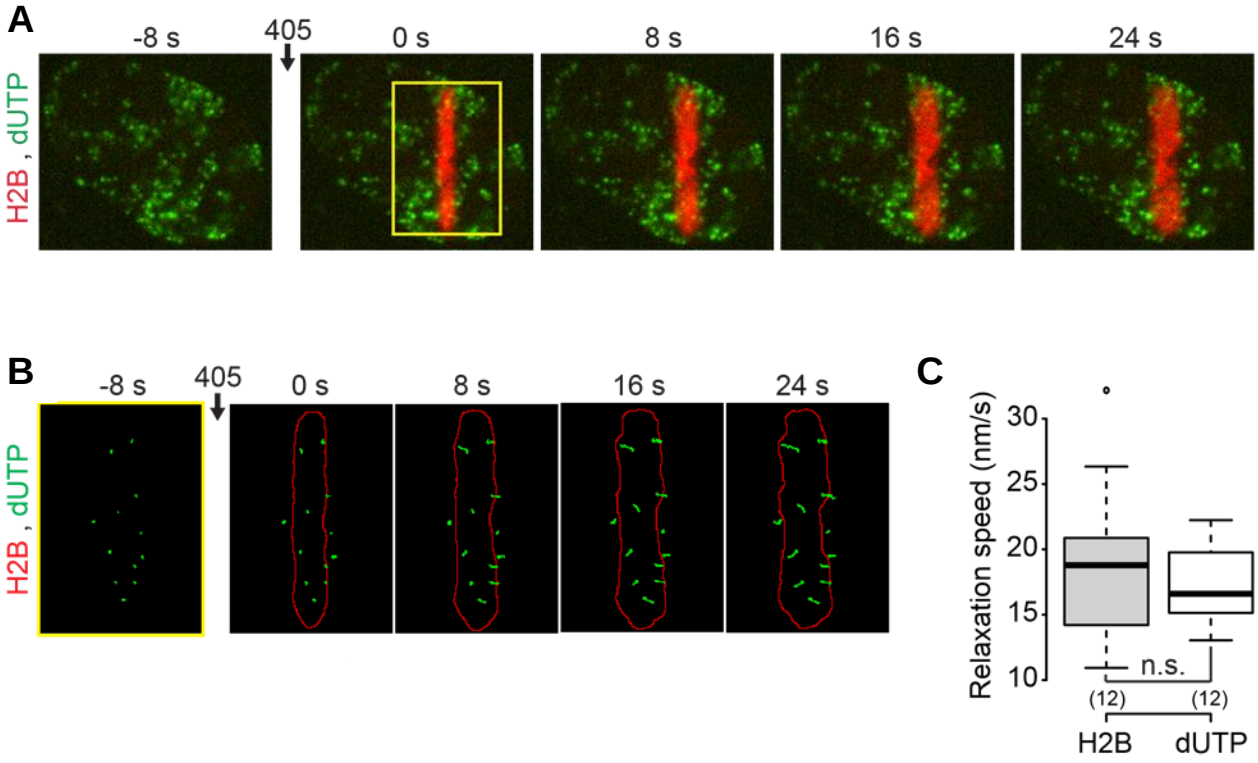

Figure 21: DNA foci exhibit the same directional motion as photo-activated H2B upon DNA damage.

(A) Confocal image sequence of a U2OS cell expressing H2B-PATagRFP (red) and labeled with fluorescent nucleotides dUTP-ATTO633 (green). (B) Enlarged view of the region overlaid in yellow on the previous panel. On the images are shown the segmentation of the photoconverted chromatin area (red outline) and trajectories of individual foci labeled with fluorescent nucleotides (green). (C) Comparison between the speed at which the width of the H2B labeled region is growing and the speed of the dUTP-labeled foci perpendicular to the irradiation line. We show the average speed for the 30 s subsequent to laser micro-irradiation. p values were calculated by paired t-test.

.

Validation of the analysis

The confocal microscope equipped with a spinning disk and a photo-manipulation module used to perform these experiments allows for a fast acquisition and low photo-toxicity while keeping a resolution sufficient to assess chromatin relaxation and proteins dynamics inside and outside of the damaged area (fig. 22, A). Nevertheless, both segmentation errors due to lack of sufficient signal and acquisition photo-bleaching in the case of low signal can compromise the results obtained. In order to easily detect segmentation errors, a value is calculated frame by frame and used to assess the quality of the results as it should remain constant throughout the experiment. This calculated parameter is, in the H2B channel, the integrated intensity of the signal inside the photo-activated region divided by the integrated intensity of the signal inside the whole nucleus (fig. 22, B and C). Any instability of this parameter indicates that segmentation of either the photo-irradiated area or the nucleus was not conducted properly throughout the timelapse and cells showing such features were discarded.

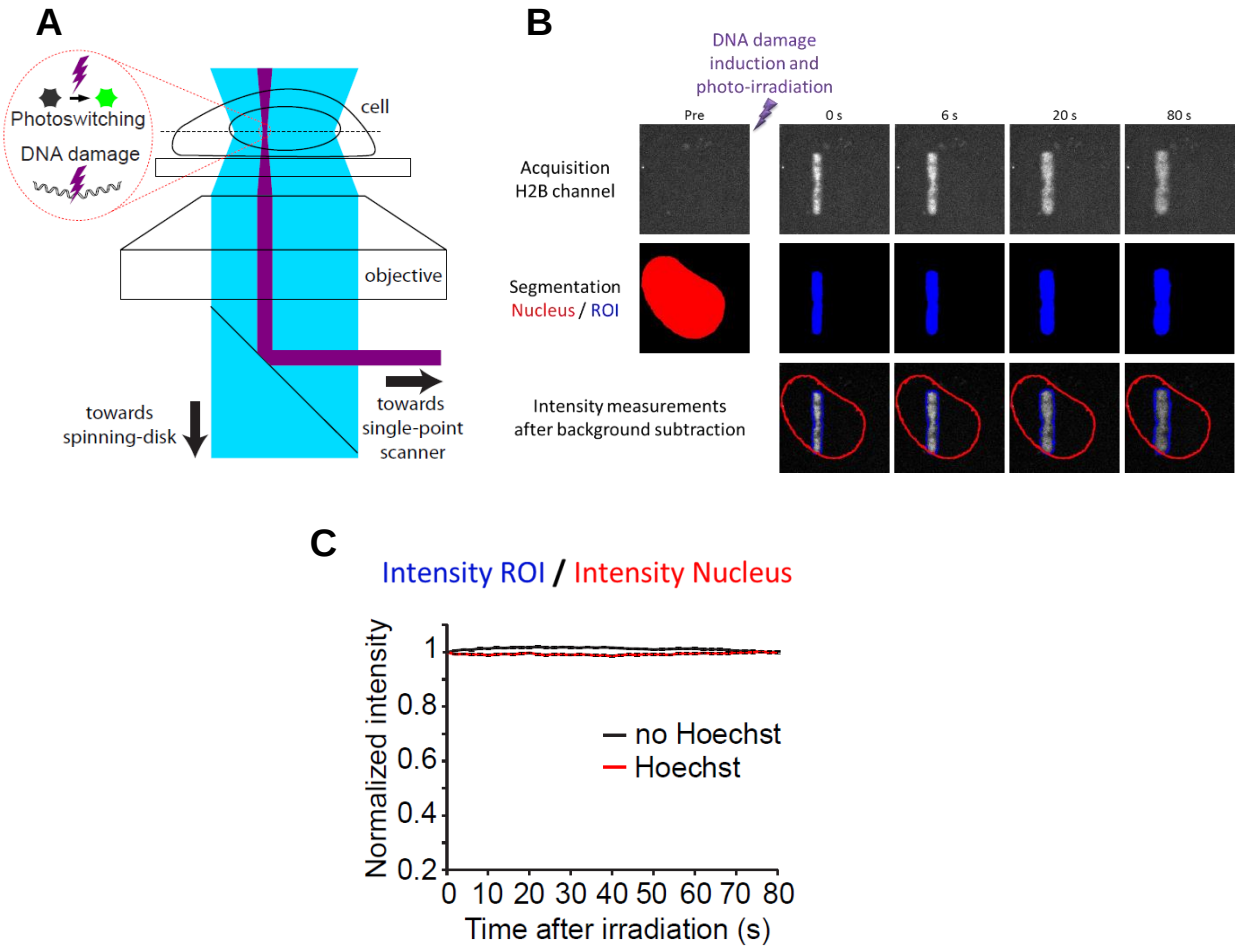

Figure 22: The quantification in the H2B channel serves as a validation during the analysis. (A) Schematic representation of the photo-irradiation of a cell in our system. The light pathway coming from the FRAP module (purple) allows for a focused and precise 405-nm laser irradiation to photo-activate the fluorophore(s) and induce DNA damage. The light pathway coming from the spinning-disk head (blue) allows for diffuse illumination during acquisition, keeping photo-toxicity and photo-bleaching at their minimum. (B) Confocal image sequence of a human U2OS nucleus expressing H2B-PATagRFP. The automatic segmentation of the nucleus (red) and the photo-damaged area (blue) in the histone H2B channel are shown below the raw images. In the third row are displayed the background-subtracted images used for signal quantification, as well as the outline of the two masks in their corresponding colors. (C) The integrated intensity of the signal inside the photo-activated H2B area is divided by the integrated intensity of the signal inside the whole nucleus, normalized using the first ratio after photo-perturbation, and plotted through time. Shown are experimental data obtained with wild-type U2OS cells expressing H2B-PATagRFP and pre-sensitized (n=18) or not (n=20) with Hoechst (mean ± SEM).

DNA Damage, Chromatin relaxation and PARylation

PARylation triggers chromatin relaxation at DNA damage sites

Using the assay described above, a strong and fast chromatin relaxation can be observed upon the induction of DNA damage in our conditions. Indeed, the photo-damaged chromatin area is already starting to expand 2 seconds after irradiation and reaches a maximum of about 150% its original size after 1 minute (fig. 20, C). Interestingly, this relaxation process is followed by a slower re-condensation phase restoring the initial size of the area in about 20 minutes (fig. 23, B). A specific inhibitor of PARylation, AG-14361, was used to assess the role of the PARylation signaling in this process. Importantly, treatment with AG-14361 allows to completely block PARylation, as seen by the absence of recruitment of the PAR-binding domain WWE, but does not affect the recruitment of PARP1 to DNA damage sites (fig. 23, A). Treatment with this inhibitor at 30 µM 15 minutes before photo-irradiation led to complete abolition of chromatin relaxation upon DNA damage. Interestingly, PARP inhibitor treatment not only abolished chromatin relaxation at DNA breaks but also induced a chromatin over-compaction after laser irradiation. Indeed, while cells untreated with Hoechst kept a stable chromatin compaction state, independently of PARylation activity, DNA damage induction led to a slight, yet significant, reduction of the thickness of the photo-activated chromatin line in cells treated with PARP inhibitor (fig. 23, B and C). As it is for chromatin relaxation, this over-compaction is followed by a slow decondensation process leading towards the previous undamaged chromatin compaction state (fig. 23, B). This result shows that PARylation upon DNA damage is necessary for chromatin relaxation, even counteracting an over-condensation phenomenon occurring when PARylation is blocked.

PARP1 binding on chromatin leads to over-condensation

Even if PARP1 has been reported to be responsible for more than 90% of the PARylation induced upon DNA damage [Rank *et al.*, 2016], PARP2 and PARP3 are also rapidly recruited to sites of DNA damage (fig. 24, A). Therefore, in order to characterize precisely the role of PARP1 in chromatin relaxation upon DNA damage, our collaborators in the team of Gyula Timinszky designed a PARP1 knockout (KO) cell line taking advantage of the CRISPR/Cas9 methodology. Performing the same experiment in this cell line resulted in a strongly impaired relaxation upon DNA damage and no over-compaction, as for WT cells, under PARP inhibition, was observed (fig. 23, C and D). Furthermore, in those PARP1 knockout cells, the PARP inhibitor treatment had no effect on chromatin relaxation (fig. 23, C). This experiment shows that, while PARP2 and PARP3, and maybe other PARPs, could still play a small role in chromatin relaxation upon DNA damage, PARylation by PARP1 seems to be the main driving force behind this process. Moreover, since no alteration of the chromatin compaction state is observed upon DNA damage and PARP inhibitor treatment in the PARP1 KO cells, it also suggests that PARP1 recruitment and binding to chromatin, without catalytic activity, is responsible for a local over-compaction of the chromatin.

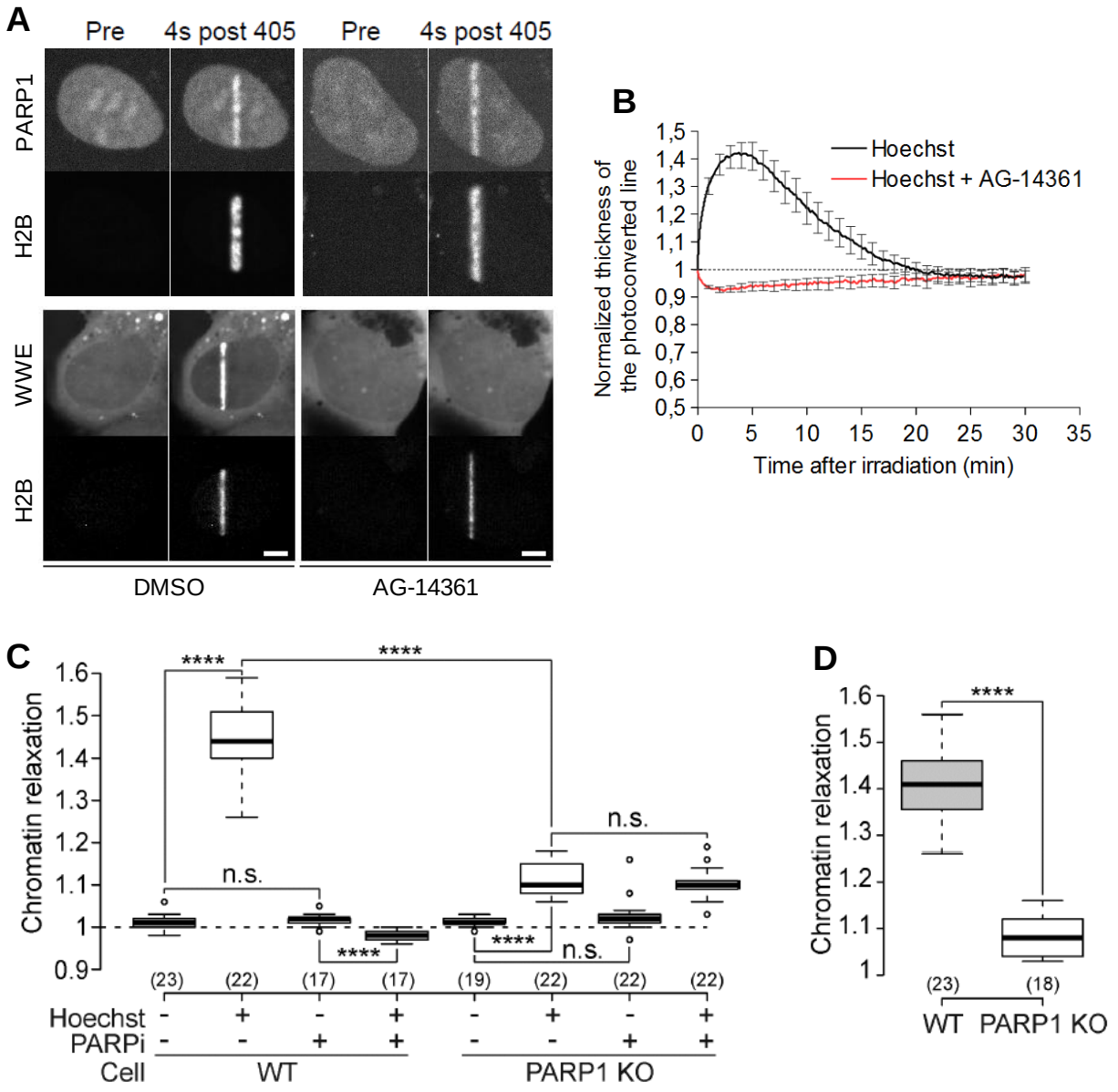

Figure 23: PARP1 activity controls chromatin relaxation at DNA damage sites.
(A) Recruitment at DNA damage sites of PARP1 and the PAR-binder WWE domain of RNF146 in cells co-expressing PARP1-EGFP, or WWE-EGFP, and H2B-PATagRFP, pre-sensitized with Hoechst and treated or not with the PARP inhibitors AG-14361 (30 µM, 1h). (B) Dynamics of the chromatin compaction state at DNA damage sites over long time scales (mean ± SEM) measured in wild-type U2OS cells expressing H2B-PATagRFP with (n=16) or without (n=14) treatment with AG-14361 (30 µM, 1h). (C) Relative chromatin relaxation at 60 seconds after laser micro-irradiation in *wild-type* and PARP1 knockout cells (clone C8) transfected with H2B-PAGFP and treated or not with the PARP inhibitor AG14361 (30 µM, 1h). (D) Similar results were obtained with a second PARP1 KO cell clone (clone C12).

The prominent role of PARP1 in chromatin relaxation upon DNA damage

In order to validate those results, PARP1 was re-expressed in PARP1 knockout cells in order to rescue the phenotype. However, only a partial rescue could be obtained as chromatin decondensation did not reach the levels obtained in wild-type cells (fig. 24, B). A possible explanation for this partial rescue lies with the dual role that PARP1 plays in modulating chromatin structure, at the same time inducing over-condensation through its binding, and promoting chromatin relaxation through PARylation. This all hints at the fact that decondensation upon DNA damage is a very well-regulated process, and the key element of this mechanism might just be the level of recruitment and activation of PARP1 at the site of DNA damage. Indeed, while the level of chromatin decondensation is increased with a higher level of DNA damage (fig. 25, a and B), chromatin relaxation is not amplified by a higher level of PARP1 inside the cell. Indeed, an over-expression of PARP1 in wild-type cells actually leads to an impaired chromatin relaxation (fig. 25, C and D), suggesting that any dysregulation in the level of expression or recruitment to DNA damage sites of PARP1 will have dire consequences for the following chromatin relaxation, and thus, possibly also for the subsequent DNA repair and survival of the cell.

Interestingly, both the recruitment to DNA damage (fig. 24, A) and the level of expression (fig. 24, C) of PARP2 and PARP3 seem unaffected by the knockout of PARP1, suggesting that no compensation mechanism between those different DDR-PARPs is taking place in the context of the DNA damage response. Moreover, the fact that a highly-hindered chromatin relaxation is still observed in PARP1 KO cells upon DNA damage with or without applying PARP inhibitory treatment suggests that PARylation by PARP2 and/or PARP3 is not likely to play a role in chromatin relaxation upon DNA damage.

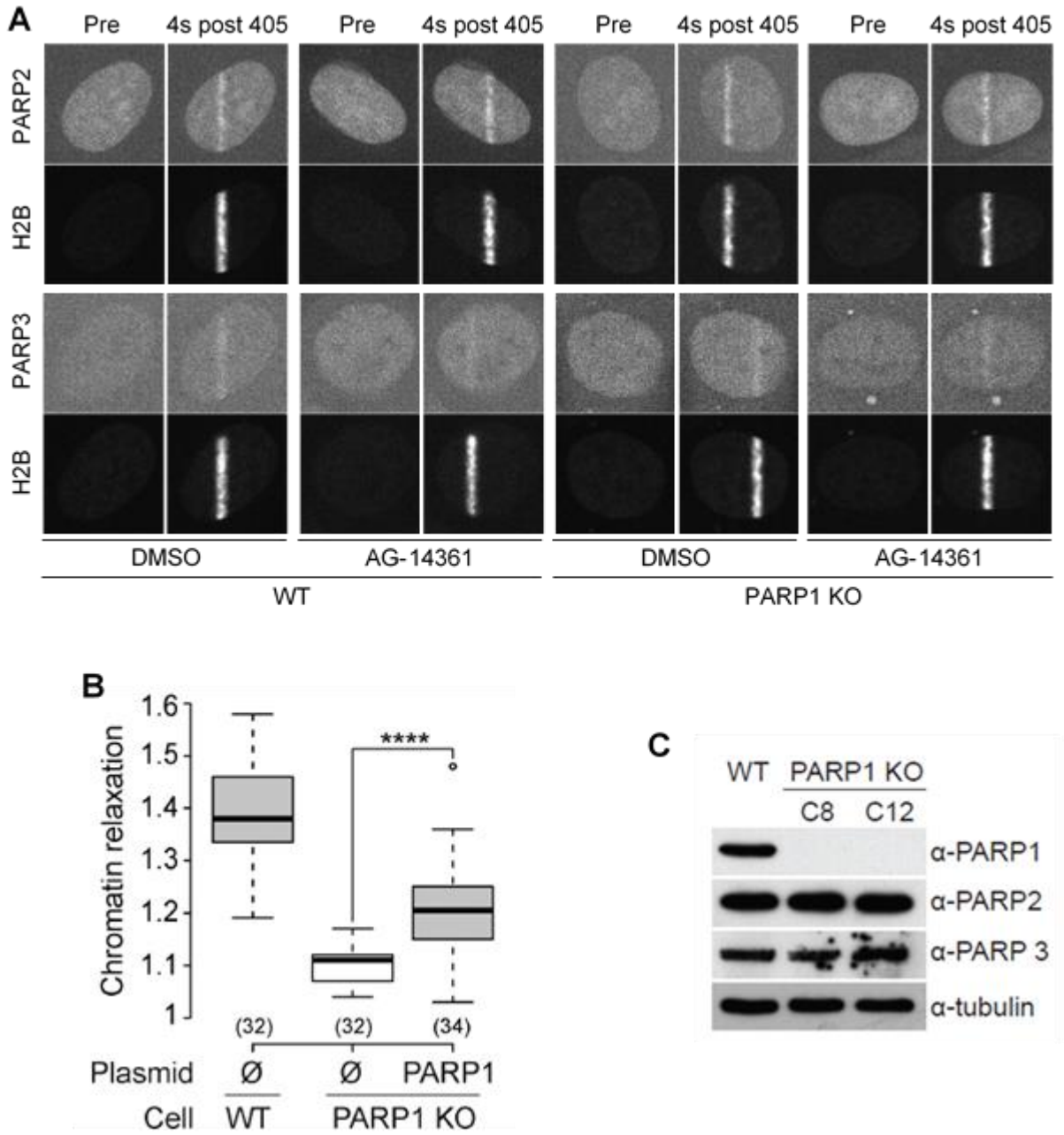

Figure 24: PARP1 is the key player regulating chromatin compaction state at DNA damage sites.

(A) Recruitment at DNA damage sites of PARP2 or PARP3 in U2OS wild-type or PARP1 KO cells co-expressing PARP2-EGFP, or PARP3-EGFP, and H2B-PATagRFP, pre-sensitized with Hoechst and treated or not with the PARP inhibitors AG-14361 (30 μM, 1h). (B) Partial rescue of the impairment of chromatin relaxation in PARP1 KO cells by re-expression of PARP1-mCherry. (C) Western-blot of wild-type U2OS cells and the two PARP1 KO cell lines showing the relative amount of PARP1, PARP2 and PARP3 in the different cell lines.

Decondensation relies on ATP- and PAR-dependent processes

In order to understand if chromatin relaxation upon DNA damage is the direct consequence of the PARylation event occurring at the site of lesions, or if PARylation only constitutes a mean to recruit factors responsible for this process, we decided to check for the requirement of other factors. Since ATP is necessary for the introduction of a lot of epigenetic marks that can modulate the chromatin compaction state, and used by all chromatin remodeling complexes, it appeared obvious to start by looking at decondensation upon ATP depletion. After bathing WT U2OS cells in the ATP depletion medium for 24h, chromatin decondensation upon DNA damage was strongly impaired (fig. 26, A), while the recruitment of the PAR-binding domain WWE of RNF146 remained unaffected (fig. 26, B). This suggests that the recruitment of PARP1 to DNA damage sites, as well as its activation and PARylation levels, are unaffected by the lack of available ATP, while the DNA damage-triggered decondensation is hindered.

However, since the absence of ATP inside the nucleus triggers an overall chromatin over-compaction (fig. 26, C), this alteration of the basal chromatin compaction state alone could affect the relaxation process occurring upon DNA damage without any direct impact of the lack of ATP. In order to rule out this possibility, a global chromatin over-compaction was achieved by bathing cells in a hypertonic medium, mimicking the effect of the depletion while keeping normal levels of ATP inside the cell (fig. 26, C). In those cells, chromatin relaxation upon DNA damage was actually slightly enhanced (fig. 26, D), suggesting that a basal higher level of chromatin compaction actually allows for a higher level of decondensation. In those cells, the recruitment of the WWE domain of RNF146 was comparable to the one in untreated cells, indicating that hypertonic treatment affects chromatin relaxation without modifying PARP1 activity (fig. 26, E). This experiment suggests that chromatin over-compaction before UV-irradiation, as observed in ATP depleted cells, is not, *per se*, sufficient to inhibit chromatin relaxation at DNA breaks, but could actually enhance it.

Altogether, this seems to indicate that, even if PARylation itself could directly contribute to chromatin relaxation upon DNA damage, as 40% of the initial chromatin relaxation remains after ATP depletion, it could also serve as a platform for recruitment for ATP-dependent factors that will be involved in chromatin decompaction at DNA damaged sites. I next focused my research trying to understand how processes other than PARylation, ATP-dependent or not, could induce chromatin relaxation upon DNA damage.

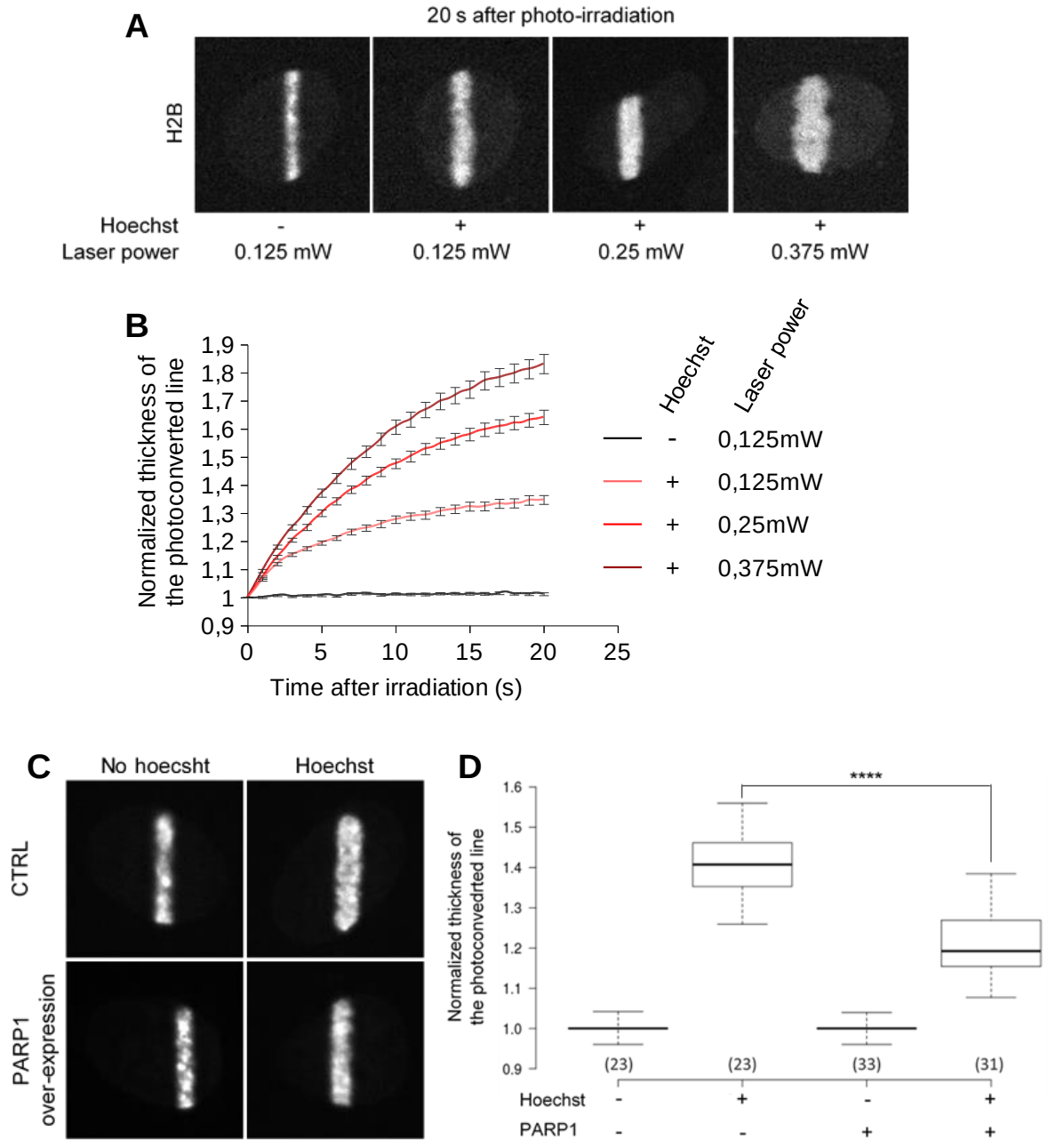

Figure 25: The extent of chromatin relaxation depends on the level of DNA damage and on the level of PARP1 expression.

(A) Confocal images of nuclei of WT U2OS cells transfected with H2B-PATagRFP and treated or not with Hoechst. Pictures are shown 20 seconds after photo-irradiation using different laser powers measured at the sample level. (B) Dynamics of the chromatin compaction state in those cells over 20 seconds (mean +/- SEM). (C) Confocal images of nuclei of wild-type cells treated or not with Hoechst and transfected with either H2BPATagRFP alone, or along with PARP1-EGFP. Pictures are shown 60 seconds after photo-irradiation using 0.125 mW of the 405-nm laser power. (D) Quantification of the chromatin relaxation 60 seconds after photo-damage in those cells.

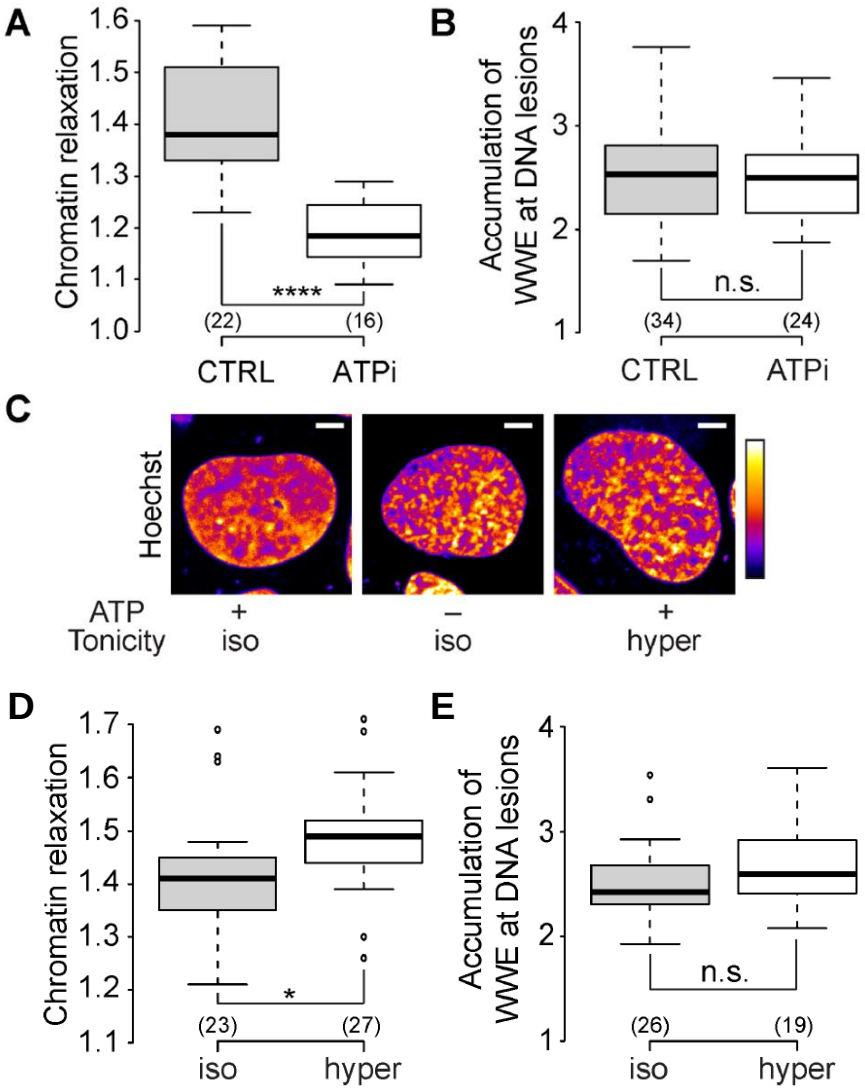

Figure 26: Chromatin relaxation at DNA damage sites partially depends on ATP.
(A) Relative chromatin relaxation at 60 seconds after laser micro-irradiation in wild-type cells expressing H2B-PAGFP and depleted or not for ATP. (B) Accumulation of the WWE domain of RNF146 at DNA lesions estimated 60 seconds after laser micro-irradiation in wild-type cells expressing an EGFP-tagged version of WWE and depleted or not for ATP. (C) Confocal image of U2OS cell nuclei stained with Hoechst and left untreated, depleted for ATP or bathed with hypertonic medium pseudocolored using the lookup table shown on the right of the images. (D) Relative chromatin relaxation at 60 seconds after laser micro-irradiation in wild-type cells expressing H2B-PAGFP and bathed in isotonic or hypertonic media. (E) Accumulation of the WWE domain of RNF146 at the DNA lesions estimated 60 seconds after laser micro-irradiation in wild-type cells bathed in isotonic or hypertonic media.

The Role of Histone H1

H1 is released faster from the DNA damage sites

In order to understand the molecular mechanisms responsible for chromatin relaxation at DNA breaks, I took a particular interest in H1 dynamic binding to chromatin. This fifth histone is supposed to play an important part in the formation and maintenance of compacted higher order chromatin structures [Bednar *et al.*, 2015]. The fact that no H2B molecule seems to be released from the site of the damage (fig. 20 and 21; fig. 22, C) suggests that no nucleosome disassembly is occurring. It would then appear necessary in order for the decondensation to occur to remove the linker histone or at least decrease H1 binding abilities at the site of DNA damage. Moreover, H1 has been shown to be PARylated [Shan *et al.*, 2014], which is supposed to decrease its affinity for DNA, and PARP1 has been shown to replace H1 on the nucleosome in specific areas [Kim *et al.*, 2004; Clark *et al.*, 2012]. Unlike canonical histones, H1 is highly dynamic displaying a residency time of no more than a few minutes on the nucleosome in normal conditions [Misteli, 2000]. Yet, the linker histone has been shown to display a low free pool of molecules, meaning that the vast majority of H1 proteins inside the cell is bound to chromatin at any given time [Misteli, 2000]. In order to understand the possible part played by H1 in the damaged chromatin relaxation process, I followed the dynamics of the fifth histone tagged to PAGFP while performing a decondensation assay. To analyze those data, I measured, frame by frame, the integrated fluorescence intensity inside the expanding region of interest defined by the "damaged chromatin mask" created with the signal coming from the chromatin channel. This method allows to look at all H1 molecules that were at the site of DNA damage when it was induced and follow them through time inside a growing, yet encompassing the same damaged chromatin, area.

The highly dynamic behavior of H1 was confirmed in our experiments in untreated conditions as H1 proteins photo-activated at the laser irradiation site rapidly spread outside of the area defined by the photo-activated H2B molecules (fig. 27, A; fig. 28). Interestingly, a clear increase of H1 release speed from the damaged chromatin area can be observed upon laser micro-irradiation (fig. 27, A). Similar accelerated release from DNA damage sites was also observed for other H1 isoforms (fig. 27). Those promising results led me to believe that H1 release from the site of DNA damage could be necessary, or even sufficient, for chromatin relaxation and I wanted next to investigate the driving force behind this behavior.

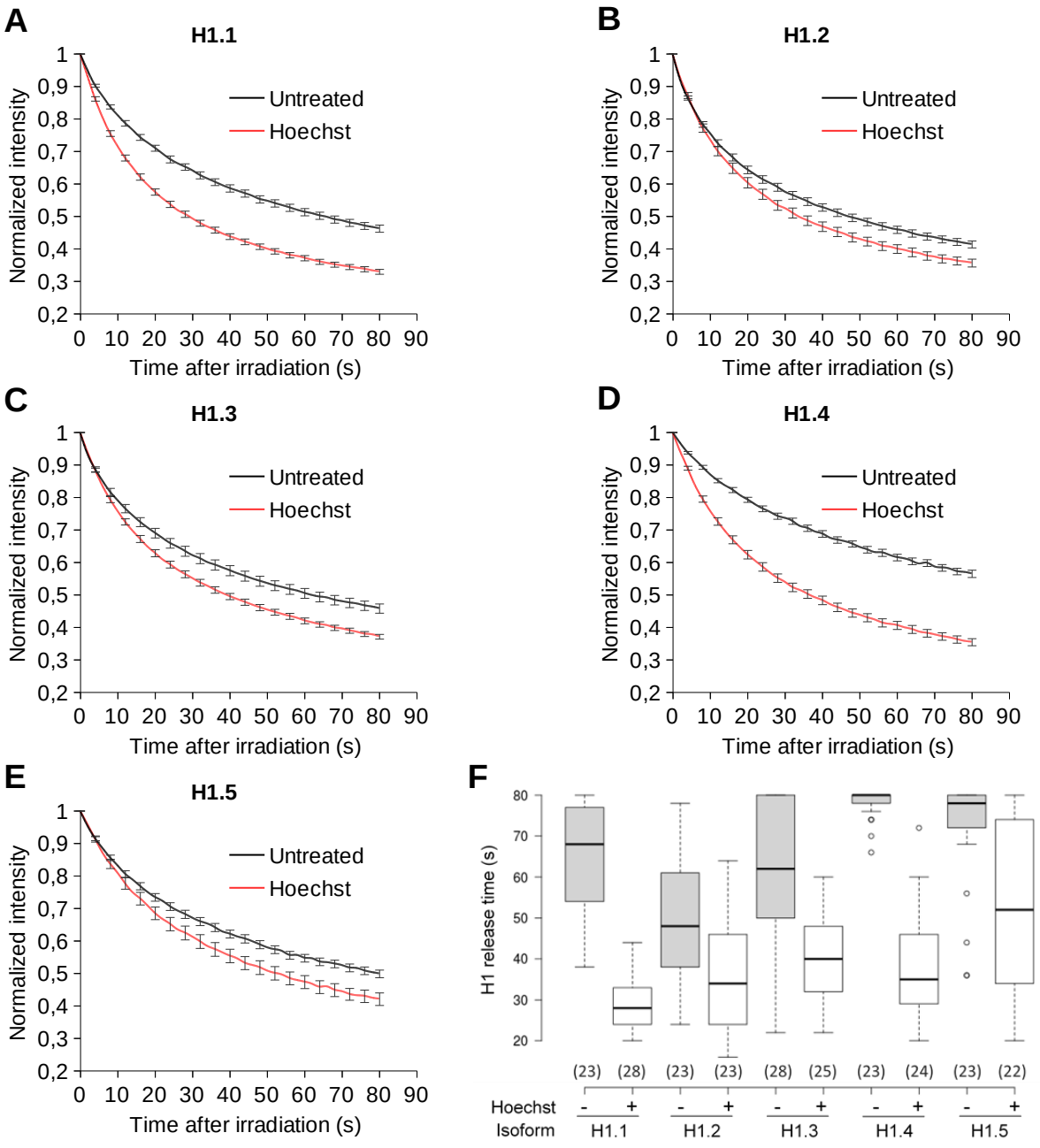

Figure 27: All canonical H1 isoforms display an accelerated release upon DNA damage.
(A - E) Kinetics of the release of the H1 proteins localized at the DNA lesions at the time of laser micro-irradiation in WT cells co-expressing H2B-PATagRFP and one of the five canonical H1 isoforms tagged to PAGFP and pre-sensitized or not with Hoechst (mean ± SEM). H1 isoform constructs were obtained linking PAGFP to the C-terminal end of H1 proteins (F) Characteristic release time for H1 isoforms, representing the time needed for half the initial fluorescence inside the region of interest to be redistributed outside of this region. This indicator is used to assess the variability between different cells within the same experimental condition and apply statistical analysis, when possible.

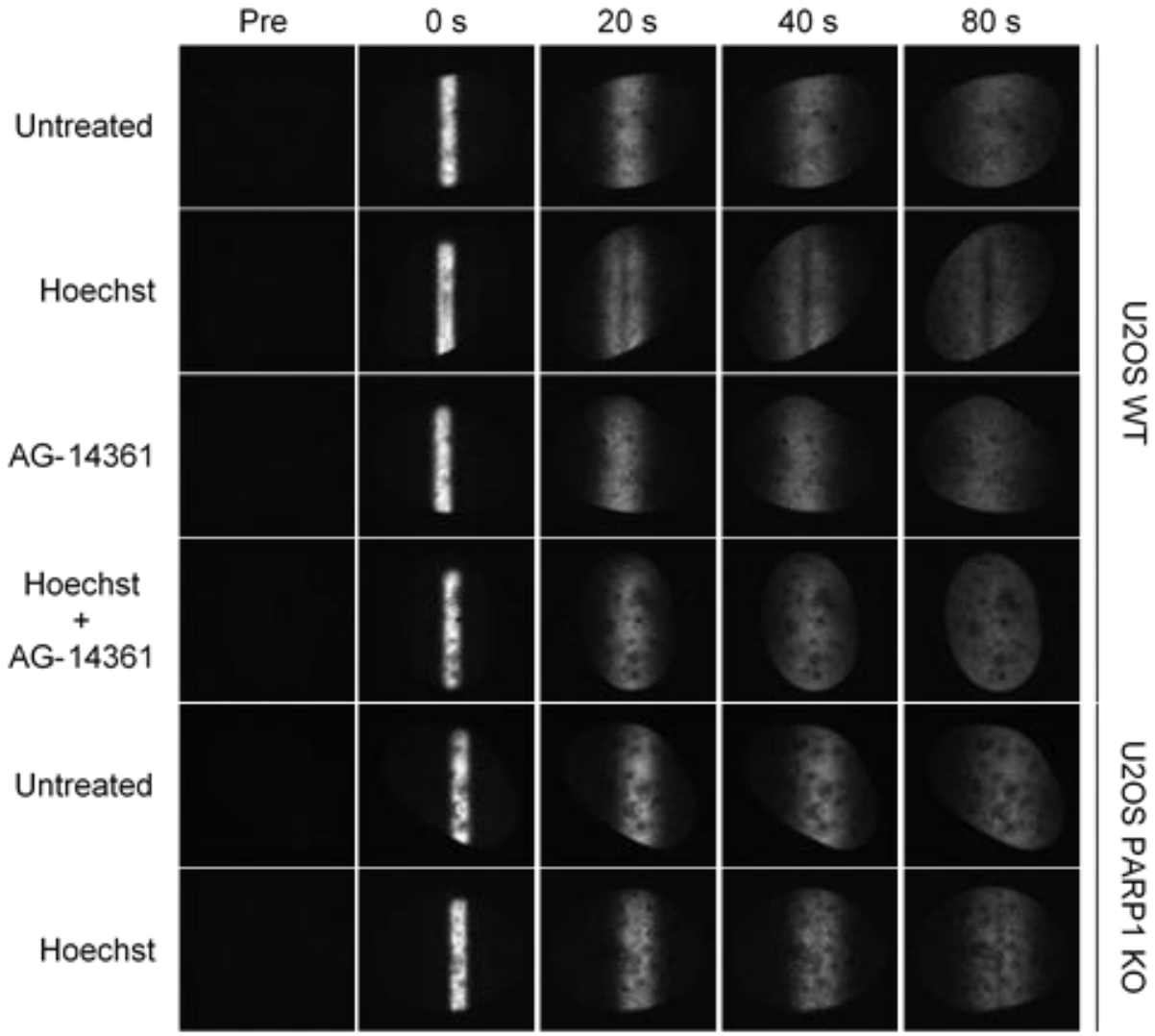

Figure 28: The dynamic binding kinetics of histone H1 is modified upon DNA damage.
Confocal image sequences of the dynamics of H1 photo-activated on a straight vertical line using the 405-nm laser in wild-type and PARP1 knockout cells. Cells were transfected with H1.1-PAGFP, along with H2BPATagRFP (pictures not shown) to assess decondensation and perform required segmentation of the photo-activated, or photo-damaged area. WT cells were either left untreated, pre-sensitized with Hoechst or treated with the PARP inhibitor AG-14361, or both. PARP1 knockout cells were left untreated or pre-sensitized with Hoechst.

H1 accelerated release is not driven by PARP1 recruitment or PARylation

To understand the driving force behind this H1 increased release speed from damaged chromatin, I first focused my attention on PARP1. Indeed, as mentioned above, PARP1 could participate in H1 release from the damaged area both through PARylation or through competition for binding. In order to see if PARylation at the site of DNA damage could impact H1 behavior, I followed the dynamics of H1 tagged to PAGFP upon DNA damage with or without applying PARP inhibitor treatment using AG-14361 (fig. 28; fig. 29, A). Interestingly, while inhibition of PARylation completely abolishes chromatin relaxation, it does not suppress the accelerated release of H1 at DNA breaks (fig. 29, B and D). Another interesting point is that PARylation inhibition leads to a small but significant decrease in H1 speed, both in the presence and the absence of DNA damage (fig. 29, D), probably reflecting the relationship between H1 and PARP enzymes in other cellular processes. This result demonstrates that H1 release from the site of DNA damage, even if it could be a necessary step towards chromatin decondensation upon DNA damage, is not sufficient to drive this process. At this point, the chromatin over-compaction observed in PARP inhibitory conditions still can, as well as the behavior of H1, result from a competition for binding between H1 and the concentrated PARP1 in the damaged area.

In order to see if the high amount of PARP1 recruited at the site of DNA damage could compete for binding on nucleosomes with H1, I performed the experiment in the PARP1 knockout cell line. In those cells, H1 still showed a faster release at DNA breaks compared to its dynamics in the absence of damage (fig. 29, C and D). Those experiments showed that H1 is released faster from the site of DNA damage, but this behavior appears to be independent of the binding or the activity of PARP1. Following those results, I wanted to take a broader approach to figure out the driving force behind H1 release and tested its possible ATP requirement and its possible relation to classical DNA repair signaling pathways.

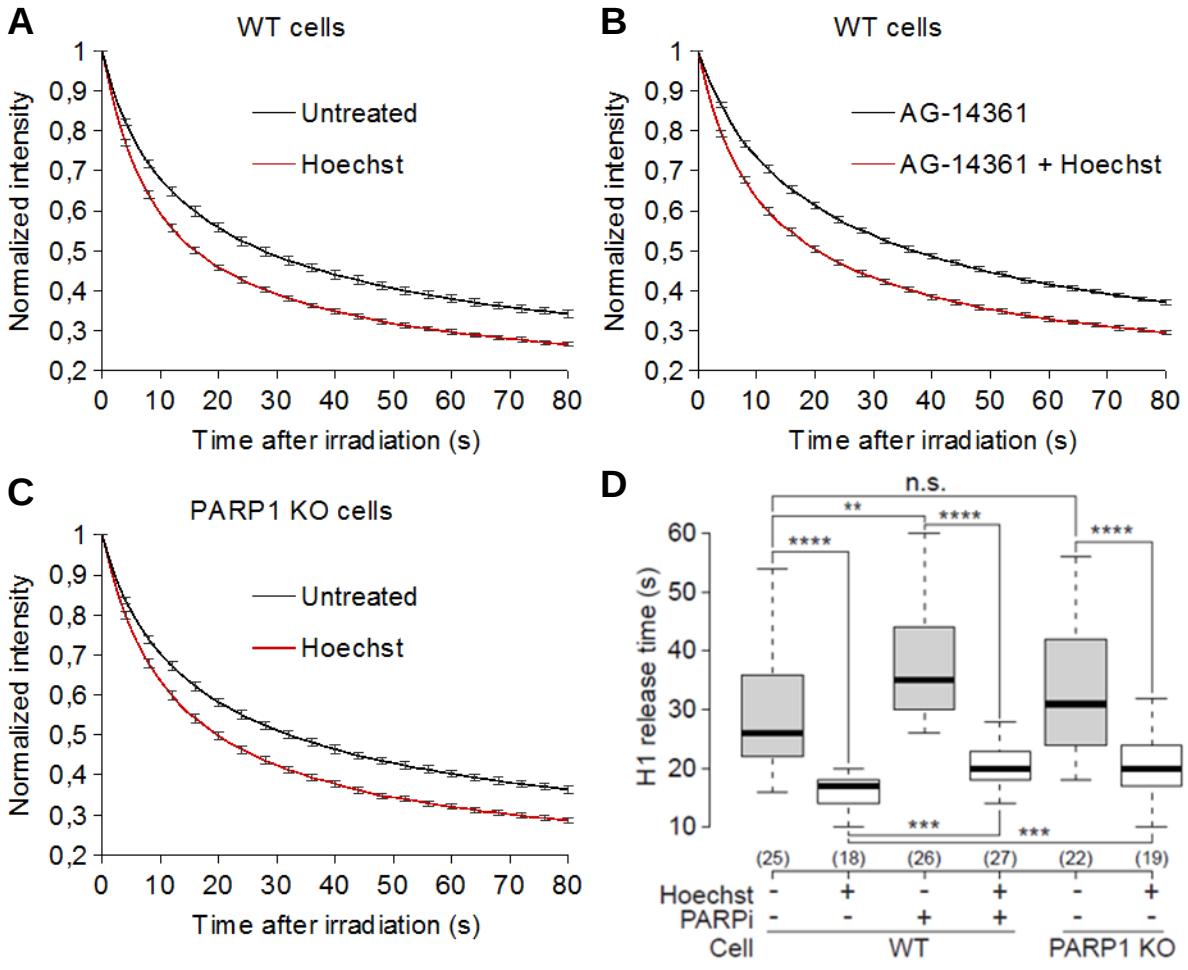

Figure 29: The speed of release of histone H1 is increased upon DNA damage.
(A - C) Kinetics of the release of the H1 proteins localized at the DNA lesions at the time of laser micro-irradiation in WT cells or PARP1 KO cells co-expressing H2B-PATagRFP and H1.1-PAGFP, pre-sensitized or not with Hoechst and treated or not with the PARP inhibitor AG-14361 (mean ± SEM). (D) Characteristic release time for H1, measured at half fluorescence decay, in WT and PARP1 KO cells.

H1 accelerated release from DNA damage sites is unaffected by the lack of ATP

Since H1 release seems independent from PARP1 and PARylation, and since ATP-dependent processes are involved in chromatin decondensation upon DNA damage (fig. 26), I next tested if H1 dynamics were affected by ATP depletion. Unsurprisingly considering its impact on chromatin conformation (fig. 26; fig. 30, B), the lack of ATP greatly alters H1 behavior as its redistribution speed is slowed down in undamaged conditions (fig. 30, A). However, the accelerated release from the photo-irradiated area is still observed after Hoechst treatment, suggesting that ATP is not required for the accelerated release of H1 from the site of DNA damage (fig. 30, A, C, and D).

As for the experiment focused on ATP and decondensation, a mean to differentiate the effect of the lack of ATP alone, and its impact on chromatin conformation, is necessary. This time, I wanted to look at H1 dynamics in ATP depleted conditions while keeping the chromatin compaction state as unaltered by the treatment as possible. Thus, I used hypotonic shock, which induces a global chromatin decompaction, under ATP depleted conditions in order to restore the basal chromatin compaction state (fig. 30, B) and performed again the H1 photo-activation experiment. Once again, H1 displayed an increased release speed in those conditions upon DNA damage, again hinting at the fact that ATP may not be required for H1 release from damaged chromatin (fig. 30, C, D, and E).

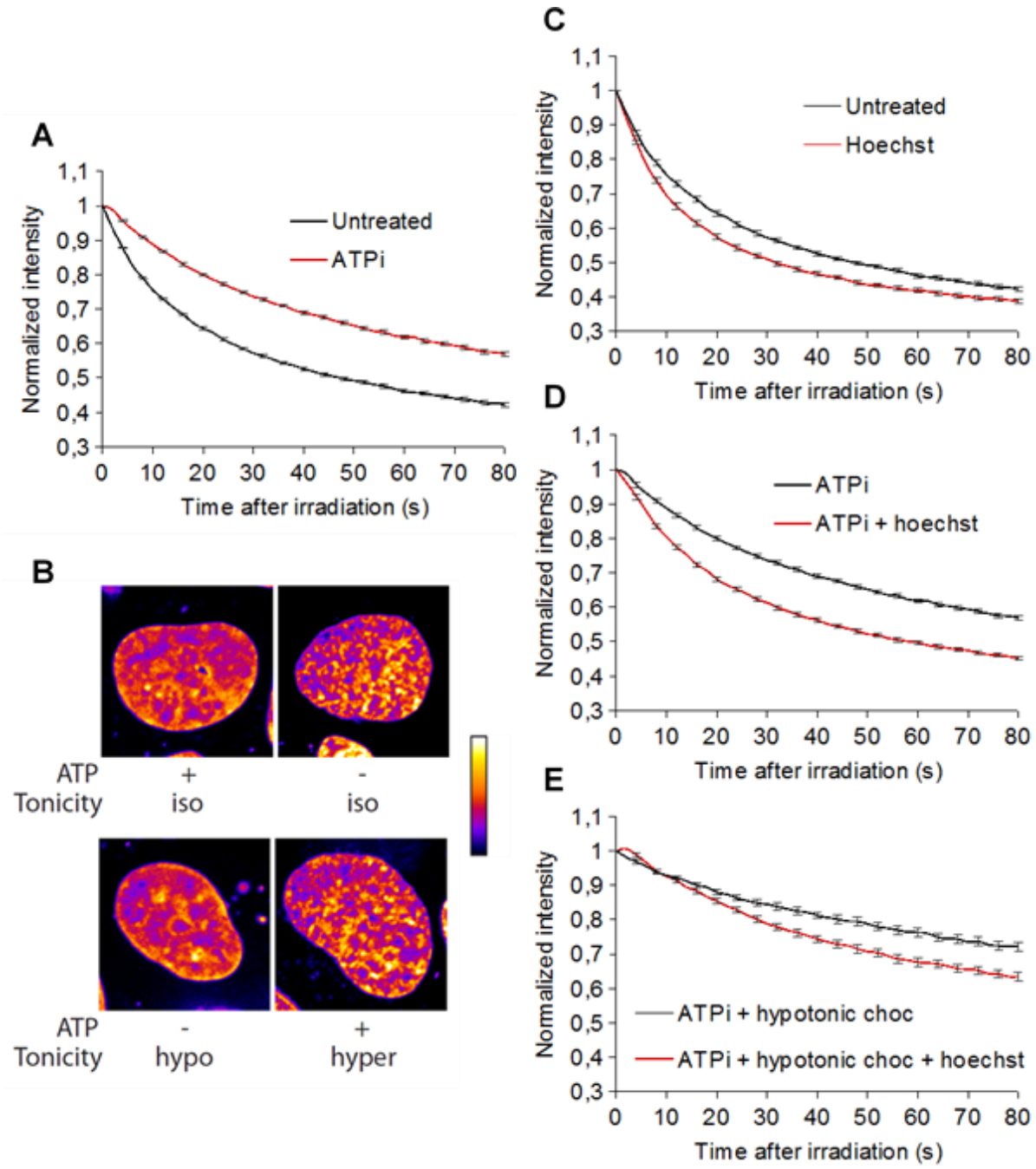

Figure 30: The accelerated release of H1 from DNA damage sites does not require ATP.
(A) Kinetics of the release of the H1 proteins localized at the DNA lesions at the time of laser micro-irradiation in WT cells co-expressing H2B-PATagRFP and H1.1-PAGFP, depleted or not for ATP (mean ± SEM). (B) Confocal image of U2OS cell nuclei stained with Hoechst and left untreated, depleted for ATP or bathed with hypotonic medium pseudocolored using the lookup table shown on the right of the images. (C - E) Kinetics of the release of the H1 proteins localized at the DNA lesions at the time of laser micro-irradiation in WT cells depleted for ATP and co-expressing H2B-PATagRFP and H1.1-PAGFP, pre-sensitized or not with Hoechst and or not with hypotonic medium (mean ± SEM).

H1 release speed from damaged chromatin seems independent from ATM or DNA-PK

Next, I wanted to see if the eviction of H1 from damaged chromatin could be dependent on the activation of classical repair pathways. I focused on two major molecular players with a central role in DNA repair that could potentially play a role, directly or indirectly, in H1 eviction from DNA damage sites: ATM and DNA-PK. Indeed, both those proteins were shown to be recruited and activated within seconds after damage induction, making them good candidates [Uematsu *et al.*, 2007]. Moreover, as key actors in the DDR, both exhibit a wide range of targets including histones and chromatin epigenetic modifiers [Caron *et al.*, 2015]. In addition, both can phosphorylate histone variant H2AX, modification known to weaken H1 affinity for the nucleosome [Caron *et al.*, 2015; Li *et al.*, 2010], and both have been shown to be involved directly in H1 phosphorylation and dephosphorylation, modulating H1 affinity for the nucleosome [Guo *et al.*, 1999; Kysela *et al.*, 2005].

Chemical inhibition of those two protein activities was achieved using KU-55933 (ATMi) and NU7441 (DNA-PKi) using experimental conditions previously tested (Golia *et al.*, 2017). After 6 hours of treatment with either inhibitor, H1 still displayed in both cases an accelerated release from the damaged area (fig. 31). At this point, the factor driving H1 eviction upon DNA damage remains unknown even if it might be an essential element for chromatin decondensation upon DNA damage. This question should be answered in the future to better understand the purpose of H1 release from DNA damage sites during chromatin relaxation and learn more about this cellular response to DNA damage.

H1 recovery is accelerated at the site of DNA damage

During the previous photo-activation experiments, only H1 proteins located at the site of DNA damage are visible and can be followed. However, since H1 is in constant dynamic exchange, I also wanted to investigate the behavior of H1 proteins located outside of the damaged area, looking at the repopulation, or possible exclusion, of H1 to or from the damaged area. Indeed, H1 proteins located at the site of DNA damage when it occurs may receive specific modifications responsible for H1 accelerated release from the site of the breaks, H1 located outside of the breaks would then not be affected and display “normal” kinetics. On the contrary, the change could come from the environment that damaged chromatin represents; in this case, H1 located outside of the damaged area should behave the same way as H1 located at the site of the breaks.

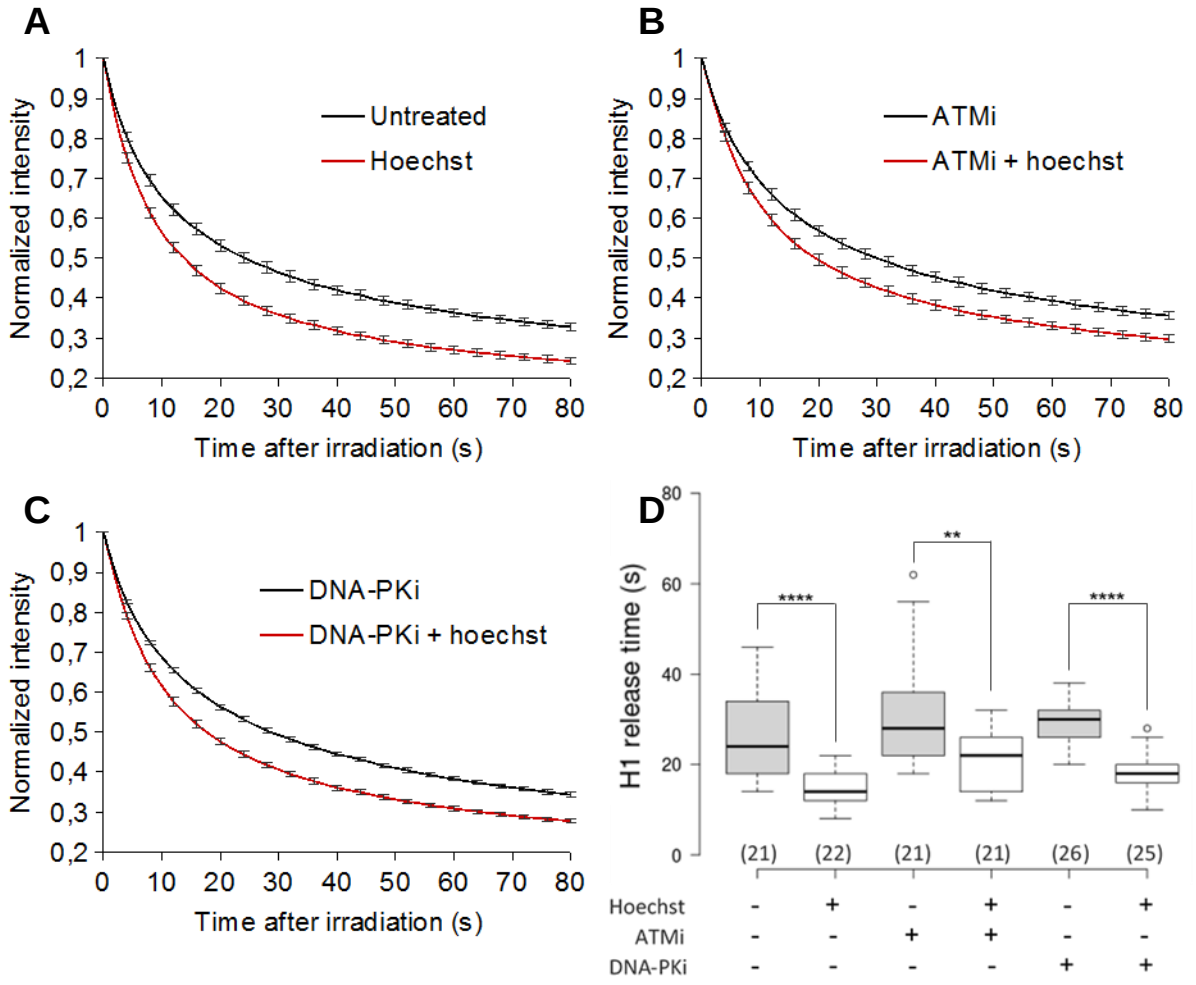

Figure 31: The accelerated release of H1 from DNA damage sites is independent of the signalization of the DNA repair proteins ATM or DNA-PK.

(A - C) Kinetics of the release of the H1 proteins localized at the DNA lesions at the time of laser micro-irradiation in WT cells co-expressing H2B-PATagRFP and H1.1-PAGFP, pre-sensitized or not with Hoechst and treated or not with the ATM inhibitor KU-55933 or the DNA-PK inhibitor NU7441 for 6h before imaging at 10 µM (mean ± SEM). (D) Characteristic release time for H1, measured at half fluorescence decay.

In this simultaneous FRAP and DNA damage induction experiment, cells are co-transfected with H2B-PATagRFP and H1-GFP and two lasers are used simultaneously for photo-irradiation, the 405-nm laser to photo-activate H2B proteins and induce damage upon Hoechst treatment, and the 488-nm laser to photo-bleach H1 proteins present at the site of the damage when damage is occurring (fig. 32). Surprisingly, H1 recovery speed is higher at DNA breaks than in the absence of damage (fig. 33, A and D). H1 then seems to have enhanced dynamics in a chromatin damaged area hinting towards an alteration of its binding abilities to damaged chromatin. However, even more surprising is the fact that this increased speed of recovery to the damaged area is dependent on PARylation. Indeed, performing the same experiment while blocking PARylation using AG-14361 results in a reverse phenomenon in which H1 recovery to DNA damage sites is slowed down compared to its recovery towards undamaged chromatin (fig. 33, B and D).

To assess the role of PARP1 itself, I performed the same experiment in the PARP1 KO cells. I found that the recovery speed of H1 is similar in the presence or in the absence of DNA damage when PARP1 is missing from the cells (fig. 33, C and D). These results suggest that the recruitment of PARP1 lacking its catalytic activity slows down H1 recovery to the site of damage, probably through its direct binding on nucleosomes taking the place of H1. However, PARylation by PARP1 and/or decondensation, as the two phenomena cannot be separated, leads to an enhancement of the speed of recovery of H1 to DNA damage sites.

Altogether, photoactivation experiments have shown that H1 release speed from damaged sites is increased in a PARylation- and decondensation-independent manner and FRAP experiments have shown that H1 recovery speed is increased to damaged sites in a PARylation- and decondensation-dependent manner. In order to try to reconcile those apparently contradictory results, I focused the third part of my work trying to understand the purpose of the DNA damage-induced chromatin relaxation and the implications of this phenomenon in regards to the modulation of interactions between chromatin and its partners.

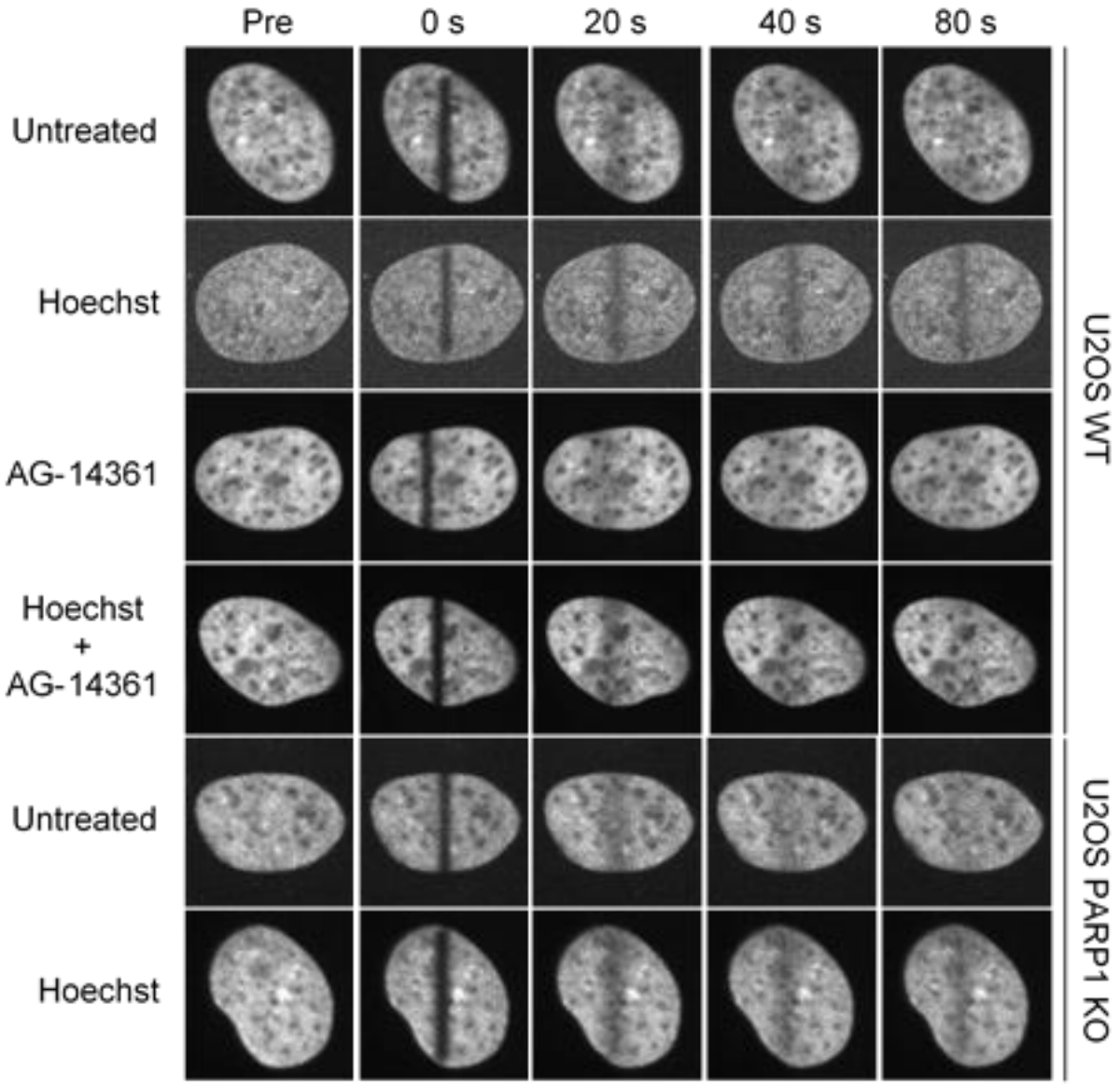

Figure 32: H1 recovery after photo-bleaching from DNA damage sites.
Confocal image sequences of the dynamics of H1 photo-activated on a straight vertical line using simultaneously the 405-nm and the 488-nm lasers in wild-type and PARP1 knockout cells. Cells were transfected with H1.1-GFP, along with H2BPATagRFP (pictures not shown) to assess decondensation and perform required segmentation of the photo-activated, or photo-damaged area. WT cells were either left untreated, pre-sensitized with Hoechst or treated with the PARP inhibitor AG-14361, or both. PARP1 knockout cells were left untreated or pre-sensitized with Hoechst.

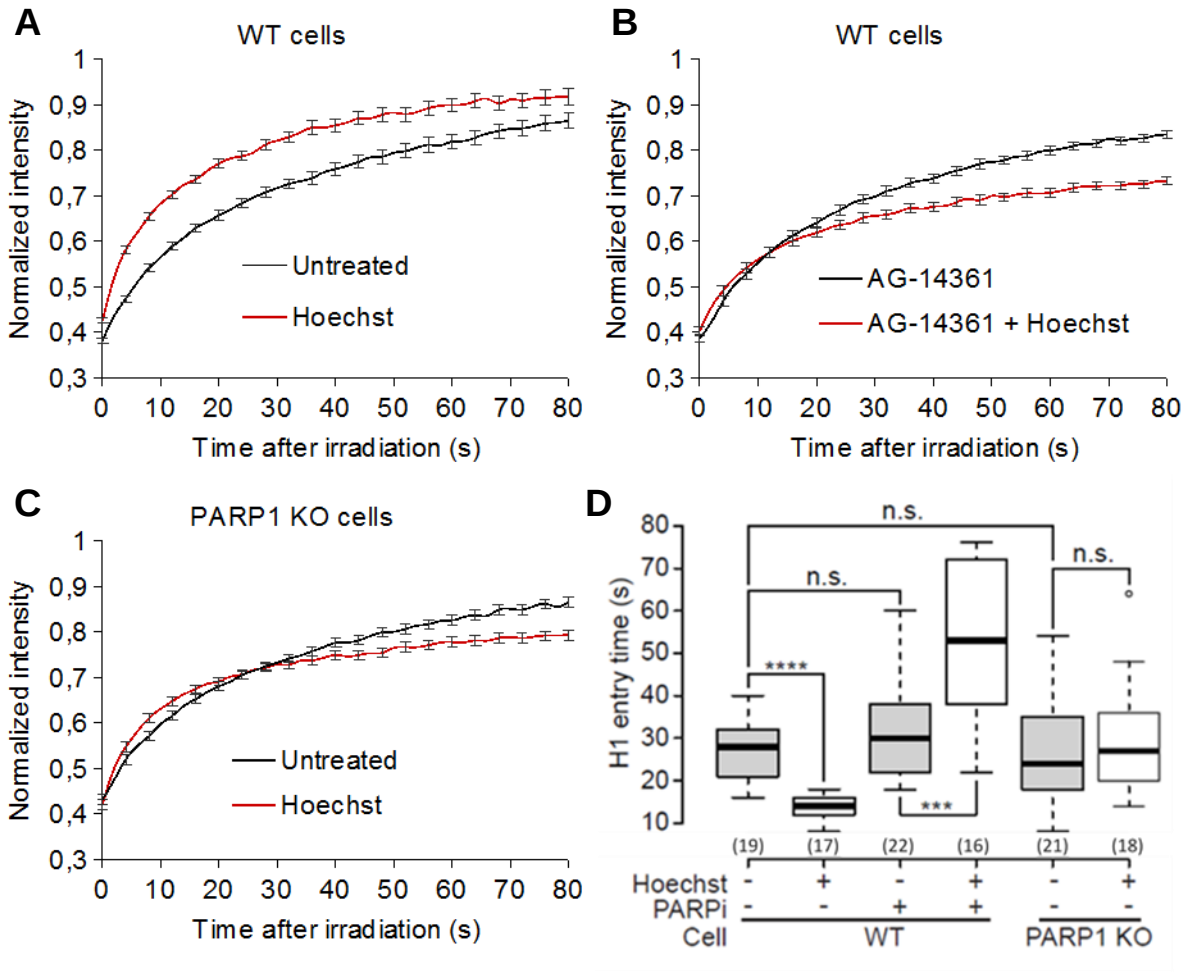

Figure 33: The speed of recovery of H1 is increased upon DNA damage.
(A - C) Kinetics of the release of the H1 proteins localized at the DNA lesions at the time of laser micro-irradiation in WT cells or PARP1 KO cells co-expressing H2B-PATagRFP and H1.1-GFP, pre-sensitized or not with Hoechst and treated or not with the PARP inhibitor AG-14361 (mean ± SEM). (D) Characteristic recovery time for H1, measured at half fluorescence recovery, in WT and PARP1 KO cells.

DNA accessibility and the functional role of chromatin relaxation

In order to better characterize the environment that damaged, relaxed, chromatin constitutes, I firstly wanted to investigate the possible impact of chromatin relaxation and PARylation on the macromolecular crowding levels at the DNA damage sites. To this end, I studied the volume occupation of GFP monomers, dimers and pentamers inside damaged and undamaged chromatin areas, as well as their dynamics before and after DNA damage induction using fluorescence correlation spectroscopy (FCS). Those three molecules were chosen as they do not interact with any nuclear components and should, therefore, diffuse freely, only according to their molecular weight, conformation, and the possible hindrance in diffusion due to macromolecular crowding. Moreover, different sized GFP arrays are used as crowding should affect proteins behavior differentially according to their molecular weight. Using our recruitment assay, which allows to simultaneously follow the recruitment of proteins while taking into account and measuring chromatin relaxation using tagged H2B proteins, I also investigated the behavior of chromatin-interacting proteins to test whether or not chromatin relaxation could lead to enhanced interaction with DNA-binding molecules.

Chromatin relaxation and volume exclusion

The first effect of macromolecular crowding, as described in the introduction, is volume exclusion. The volume occupied by a large number of surrounding molecules is not accessible. I wanted to investigate the possibility that chromatin relaxation upon DNA damage, *i.e.* a same amount of chromatin spread over a larger area, would diminish macromolecular crowding, and thus, volume exclusion, in that damaged area. This theory would fit well with speculations proposing that the purpose of chromatin relaxation is to increase access for repair proteins to damaged DNA [Smerdon, 1991]. In order to test this hypothesis, I compared the average fluorescence signal of GFP arrays composed of one, two or five GFPs inside a damaged chromatin area with their average fluorescence signal inside the undamaged neighboring area. Since GFPs should not interact with any nuclear component, their concentration in any given space should only lie on the accessible volume.

GFP monomers and GFP dimers actually display a higher concentration in damaged chromatin areas compared to their concentration in undamaged conditions (fig. 34, A, B, C, and D). These results show that chromatin relaxation leads to a slight, yet very significant, increase in accessible volume for those two proteins. This effect is dependent on PARylation and chromatin relaxation as PARP inhibited cells do not display this increase (fig. 34, C and D). However, since only around a 5% gain in accessible volume is observed, freeing accessible volume does not appear to be the purpose, or the only purpose, of relaxation upon DNA damage as chromatin occupies an area 40 to 50% percent larger after relaxation upon DNA damage (fig. 20, C). Surprisingly, no change in accessible volume is observed for the GFP pentamer tracer (fig. 34, E). This result is counter-intuitive as theoretical predictions suggest that the volume exclusion effect caused by macromolecular crowding should have a greater impact on larger molecules [Mourão *et al.*, 2014]. In those conditions, it would seem that the complex chromatin architecture reorganization that occurs upon DNA damage will confine this newly accessible volume to narrow regions.

Altogether, it would seem that chromatin relaxation does slightly reduce macromolecular crowding, even if this effect seems limited compared to the extent of the chromatin decondensation and even if the topology and 3-dimensional organization of chromatin might restrict this newly accessible volume to small probes with sizes below 60 kDa.

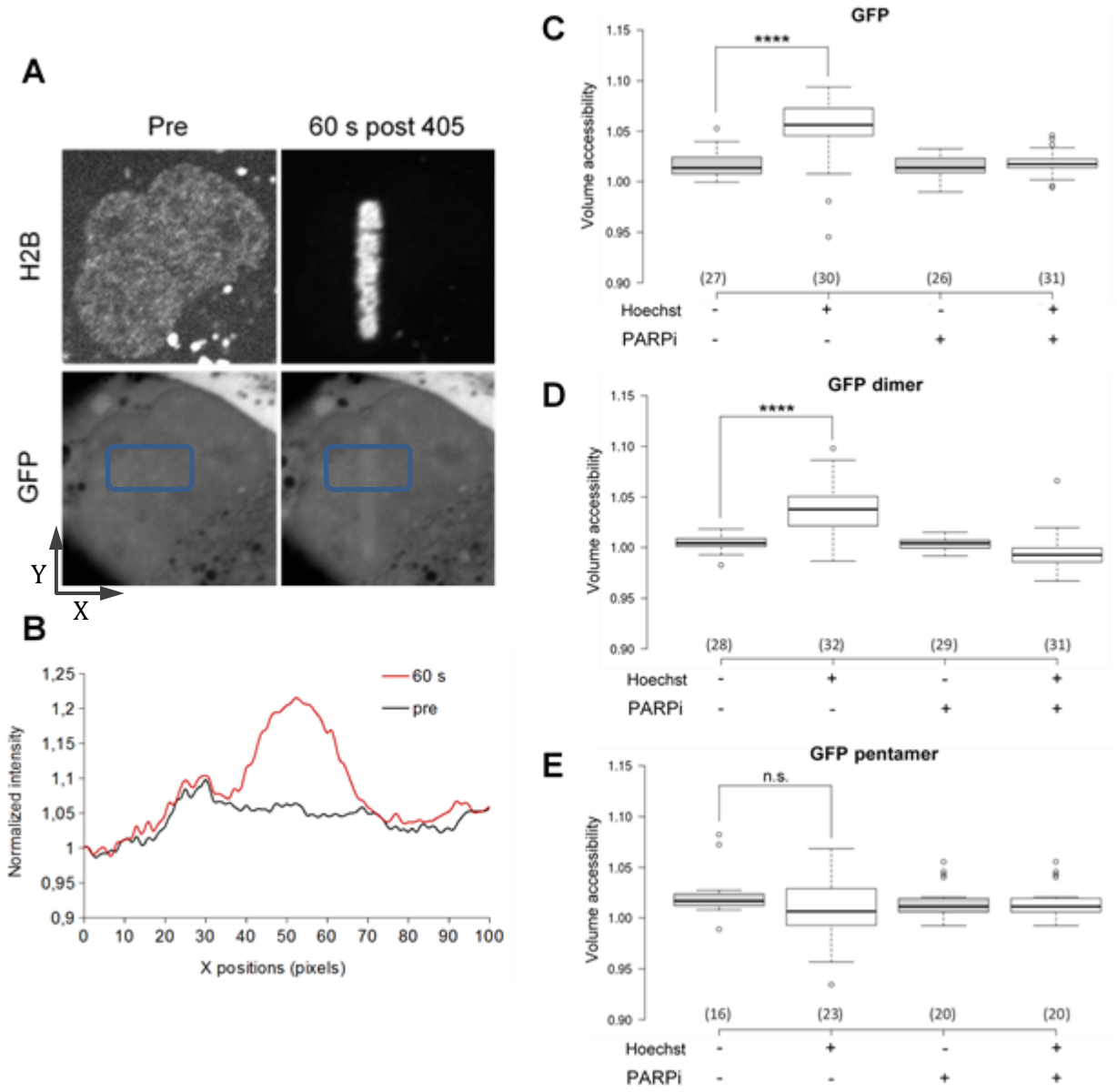

Figure 34: Impact of the DNA damage-induced chromatin relaxation on the volume exclusion effect caused by macromolecular crowding.

(A) Confocal images of a nucleus transfected with H2B-PATagRFP and GFP before or 60 seconds after DNA damage induction. Measurements of background-subtracted intensity are performed within the region of interest displayed on the GFP images, averaged in Y positions and normalized to obtain the graph (B). (C, D, E) Volume accessibility measured inside the photo-activated chromatin region for GFP, GFP dimer and GFP pentamer tracers fused to EGFP in cells co-expressing H2B-PATagRFP to identify the irradiated chromatin area. Cells are either treated with Hoechst, AG-14361, both, or are left untreated. The accessible volume inside the damaged area is calculated as a ratio between the averaged signal intensity inside the damaged area and the average of two same-sized neighboring regions.

Chromatin relaxation doesn't lead to enhanced diffusion at the site of DNA damage

Following those first interesting results regarding the volume exclusion effect induced by macromolecular crowding, I investigated the possible impact of DNA damage-induced chromatin relaxation on the diffusion hindrance caused by macromolecular crowding in the nucleus. Thus, I followed the dynamics of GFP monomers, dimers and pentamers using fluorescence correlation spectroscopy inside damaged and undamaged area with or without applying PARP inhibitor treatment. By focusing a laser on a single point and studying the flow of molecules coming in and out of the small focal volume enlightened, and through the fitting of the autocorrelation curve obtained plotted through time (fig. 35, A), FCS allows to study very accurately the diffusion kinetics of GFPs in a very precise location of the cell. Thus, if macromolecular crowding is reduced, even slightly, as suggested by the volume exclusion effect reduction, diffusion of those non-binding proteins should be enhanced in damaged areas as compared to undamaged ones, and suppressed upon PARP inhibition.

For those three proteins, no significant difference in the diffusion kinetics was observed between measurements performed in damaged and undamaged areas (fig. 35, B). The same conclusions are drawn regarding the results in PARylation inhibited conditions (fig. 35, B). Taking those results together with the previous experiments regarding the volume exclusion effect, two hypotheses can emerge. One is that macromolecular crowding is actually not reduced inside the damaged and relaxed chromatin area, and that the newly accessible volume to GFP monomers and dimers upon DNA damage and chromatin relaxation does not arise from a decreased macromolecular crowding in the area, but from a restructuration of chromatin inside the area. The second theory is that macromolecular crowding inside damaged chromatin areas is indeed slightly reduced, but this decrease is not sufficient to produce a visible effect on the diffusion kinetics of GFP monomers and dimers. Also important to note is that these results also suggest that chromatin over-compaction upon simultaneous DNA damage induction and PARP inhibition does not lead to a higher level of crowding in the photoactivated region.

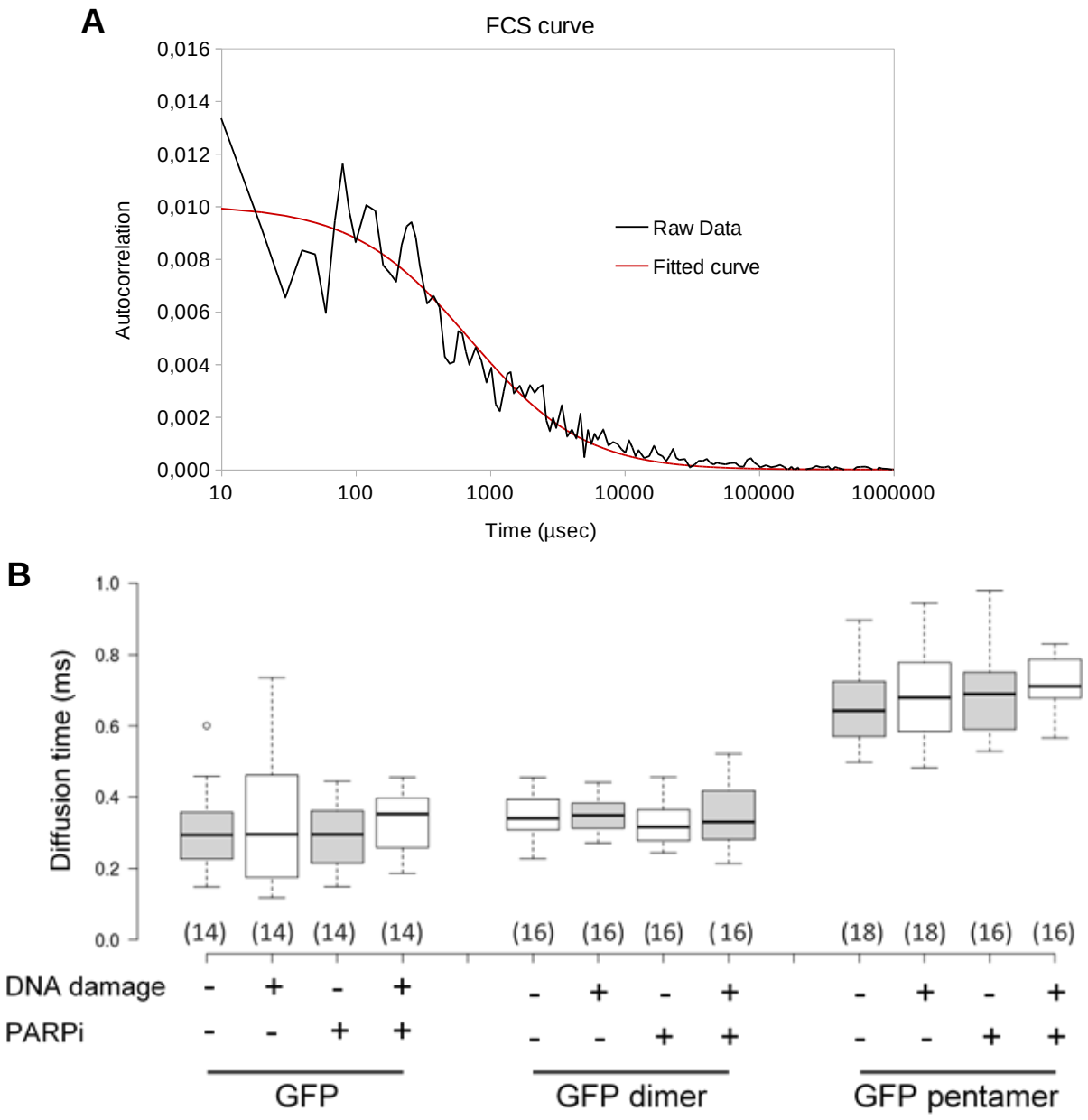

Figure 35: Impact of the DNA damage-induced chromatin relaxation on the diffusion hindrance effect caused by macromolecular crowding.

(A) Here is shown an example autocorrelation curve chosen randomly from one of the experiments fitted with a one-specie model assuming pure diffusion. (B) Diffusion speeds calculated by FCS for GFP, GFP dimers and pentamers obtained in cells cotransfected with H2B-PATagRFP. For each cell and each condition, three measurements are performed and averaged. FCS measurements are performed either before damage induction or two minutes after DNA damage induction. No significative difference was observed between damaged and undamaged conditions.

Chromatin relaxation at DNA breaks leads to enhanced interaction between DNA and its interacting factors

The last predicted effect of a modulation of the crowding level inside the damaged, relaxed chromatin area is the modification of the reaction kinetics in this area. More precisely in this case, a decrease in the crowding level should weaken interactions with chromatin and its binding partners. Even if the modulation of the macromolecular crowding levels in the damaged area is probably not the purpose of chromatin relaxation, it is still interesting to understand if this modified relaxed and PARylated environment has an impact on chromatin interactions. In order to quantify chromatin interactions in this context, I chose to look at the binding of chromatin interactors that should not be in any way recruited to DNA damage sites or play a role in the overall DNA damage response. Thus, using our recruitment assay, I followed the dynamics inside and outside of the damaged chromatin area of proteins that are not found in mammalian nuclei, namely two proteins of bacteria, LacI and TetR, that bind DNA in their respective operon, *lac* and *tet*, and the DNA binding domain of CEBP (CCAAT enhancer-binding protein) alone (BZip). Those three molecules have been shown to display a tendency to bind nonspecifically to DNA [Furini *et al.*, 2010; Normanno *et al.*, 2015; Tsekouras *et al.*, 2015], making their diffusive properties sensitive to change in DNA accessibility.

Surprisingly, all three proteins displayed a very strong "recruitment" to DNA damage sites (fig. 36). This enhanced-binding behavior is dependent on PARylation and/or decondensation as the "recruitment" of these DNA-binding probes is suppressed upon PARP inhibition (fig. 36). Changes in macromolecular crowding levels are therefore not likely to play a role regarding the binding kinetics of DNA interactors upon DNA damage, as the predicted effect of a decreased crowding level would be a reduction of the proportion of partners interacting together. However, changes are observed in the volume accessible to molecules in the damaged chromatin region, considering small proteins, and chromatin interactors there appear to display enhanced binding, suggesting that DNA accessibility is indeed modified upon DNA damage, possibly to facilitate access for repair proteins, even if the mechanisms driving this phenomenon remain, for now, unclear.

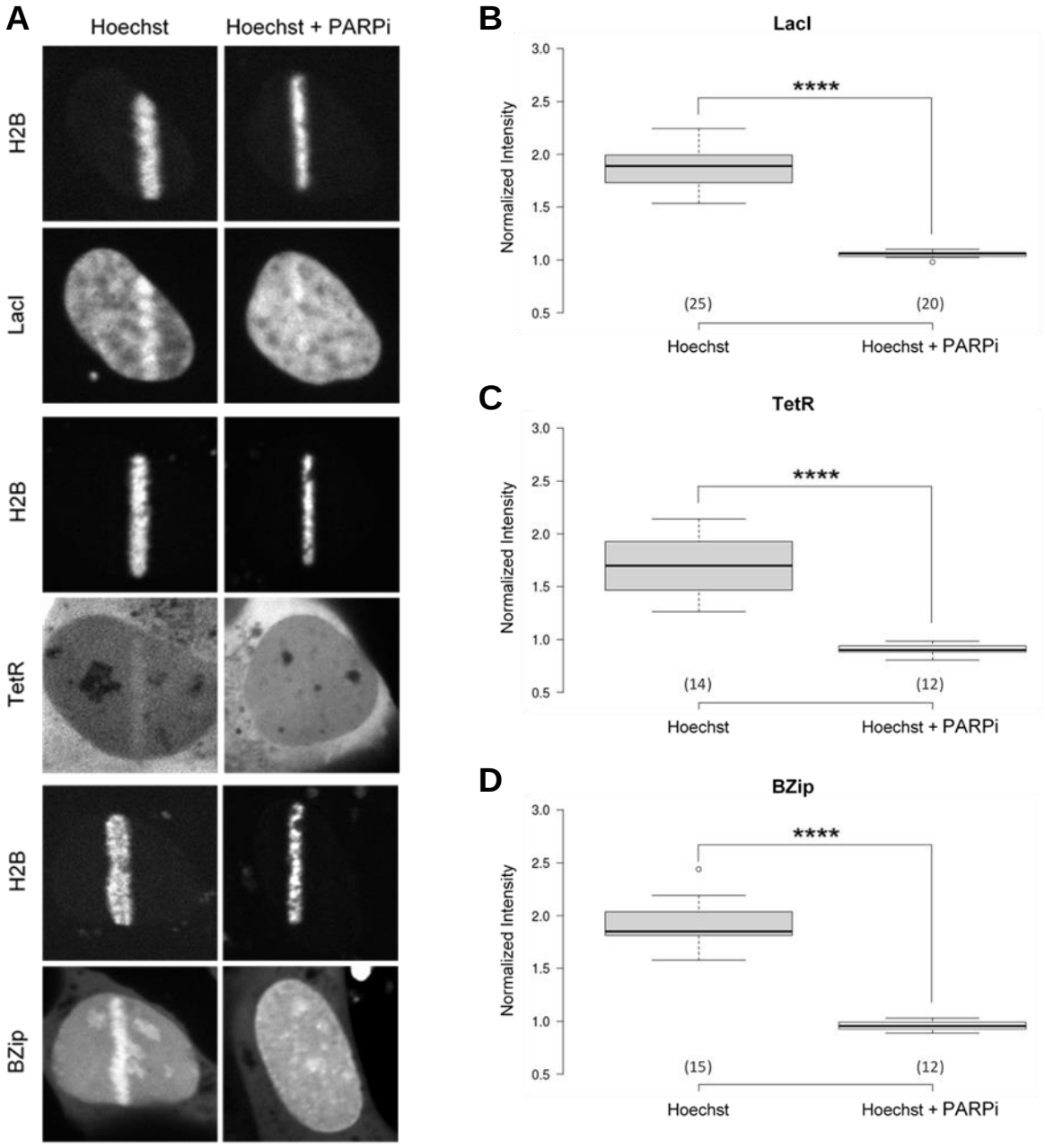

Figure 36: Impact of the DNA damage-induced chromatin relaxation on the interactions between chromatin and its binding partners.

(A) Confocal images of nuclei transfected either with H2B-PATagRFP and LacI-GFP, H2BPATagRFP and TetR-GFP, or H2B-PAGFP and BZip-Ruby2 60 seconds after photo-irradiation and treated with Hoechst alone or along AG-14361. (B, C, D) Quantification of the background-subtracted and normalized integrated signal intensity inside the damaged chromatin area for LacI, TetR and BZip in Hoechst treated conditions with or without PARP inhibitor treatment with AG-14361 60 seconds after DNA damage induction.

DISCUSSION

PARylation by PARP1 is the main force driving chromatin relaxation upon DNA damage

This work helped to gain hindsight on the role of PARP1 and PARylation in the DNA damage-induced chromatin relaxation. Indeed, PARP1 is, in our conditions, recruited within seconds at the site of DNA damage (fig. 20), as shown by others [Ahel *et al.*, 2009; Timinszky *et al.*, 2009]. It would, by interaction with chromatin, most likely take the place of H1 at the entry and exit sites of DNA on the nucleosome, and induce chromatin over-compaction [Kim *et al.*, 2004; Clark *et al.*, 2012], if it was catalytically inactive (fig. 23). However, the presence of DNA damage indeed triggers PARP1 catalytic activity which then leads to its auto-modification and chromatin relaxation [Ahel *et al.*, 2009]. The mechanisms driving this shift in PARP1 interaction with chromatin and catalytic activation are not fully understood, but it was proposed that PARP1 could bind damaged chromatin, in this case single-stranded DNA or DSBs, in a very different way, involving different domains, than its binding on undamaged chromatin [Langelier *et al.*, 2012]. The conformation in which PARP1 would bind damaged DNA would, in this model, trigger its catalytic activity while its binding to the entry and exit sites of DNA on the nucleosome would not [Altmeyer *et al.*, 2009].

This model fits nicely with our experimental data showing that recruitment of PARP1 without catalytic activity leads to chromatin over-compaction, while PARylation activation triggered by DNA damage leads to chromatin relaxation (fig. 23). The fact that PARP1 binds to chromatin or to damaged DNA in two different ways could also help explaining data suggesting that PARP1 auto-modification, which occurs almost instantly after DNA damage recognition, leads to PARP1 detachment from chromatin [Ogata *et al.*, 1981; Kim *et al.*, 2004]. Yet, PARP1 in our conditions remains at the site of the breaks after the initial phase of chromatin relaxation and is not released from the damaged area (fig. 19). To clarify these contradictions and fit those results in the model, it was shown recently that PARP1 auto-modification indeed weakens its affinity for chromatin, but not for DNA [Muthurajan *et al.*, 2014], hinting at the possibility that PARylated PARP1 would actually have a higher binding affinity for damaged DNA than unmodified PARP1, amplifying PARP1 pro-decondensation response to DNA damage.

It was also suggested that PARP1 could have a role in maintaining damaged chromatin fragments closer together [Ali *et al.*, 2012], explaining PARP1 lingering presence at the site of DNA damage after its initial PARylation response. Here, PARP1 would have the dual role of keeping broken ends together by direct binding, while keeping neighboring DNA, damaged or undamaged, away from the break of interest through

PARylation (fig. 37) [Ali *et al.*, 2012]. This would appear especially essential in the case of multiple DSBs in which the cell needs to puzzle together chromatin pieces before restoring the initial conformation and sequence of DNA. An interesting comparison to the situation in yeast cells can help strengthen this theory. Yeast cells predominantly use homologous recombination to repair DSBs [Seeber and Gasser, 2016], while human cells restrict the use of HR to specific phases of the cell cycle in which a sister chromatid template is readily accessible for recombination and repair, and use therefore non-homologous end-joining most of the time to repair DSBs [Brandsma and Gent, 2012]. One of the causes for this difference in repair pathway choice might simply be the difference in nuclear volume between those two species that renders any homology search without sister chromatid really difficult in human cells. But one of the molecular reasons for these differences might be the presence of PARP1 in human cells keeping DNA ends together to be rejoined, and its absence in yeast cells letting free DNA ends roam the nucleus in search for a homologous sequence. This would also go along with two recent studies, one showing that expression of PARP1 in yeast actually reduces UV-induced homologous recombination [La Ferla *et al.*, 2015], and the other suggesting that PARP1 can actually covalently modify free DNA ends [Talhaoui *et al.*, 2016].

A question still lingers, however: Why such a dual and complex role for a single protein switching its action on chromatin compaction from one opposite end to the other upon DNA damage and how are those two opposite effects regulated? We have shown here that the amplitude of chromatin relaxation upon DNA damage is dependent on the level of damage, but is also dependent on the level of recruitment and activation of PARP1 at the site of the lesions, as an inappropriate amount of PARP1, either way, will lead to an impaired chromatin relaxation (fig. 25), and thus potentially improper DNA repair [Rank *et al.*, 2016; Sellou *et al.*, 2016]. The regulation of this pivotal actor in the DNA damage response remains largely unknown and should be, in my opinion, the focus of future research in the field. However, this might not be an easy task, as its regulation might depend on the regulation of its expression levels, the regulation of NAD^+ availability, as well as the simultaneous regulation of the activity of PARG or other PAR erasers.

The role of other DDR-PARPs in chromatin relaxation upon DNA damage

While PARP2 and PARP3 have been shown to be recruited to sites of DNA damage (fig. 24), their actions in DNA damage repair and signalization, as well as their targets, are widely unknown [Barkauskaite *et al.*, 2015]. Interestingly, neither one of those two proteins possess any proper DNA-binding site (fig. 17), and the question of the mechanism of their recruitment to DNA breaks has remained unanswered for a long

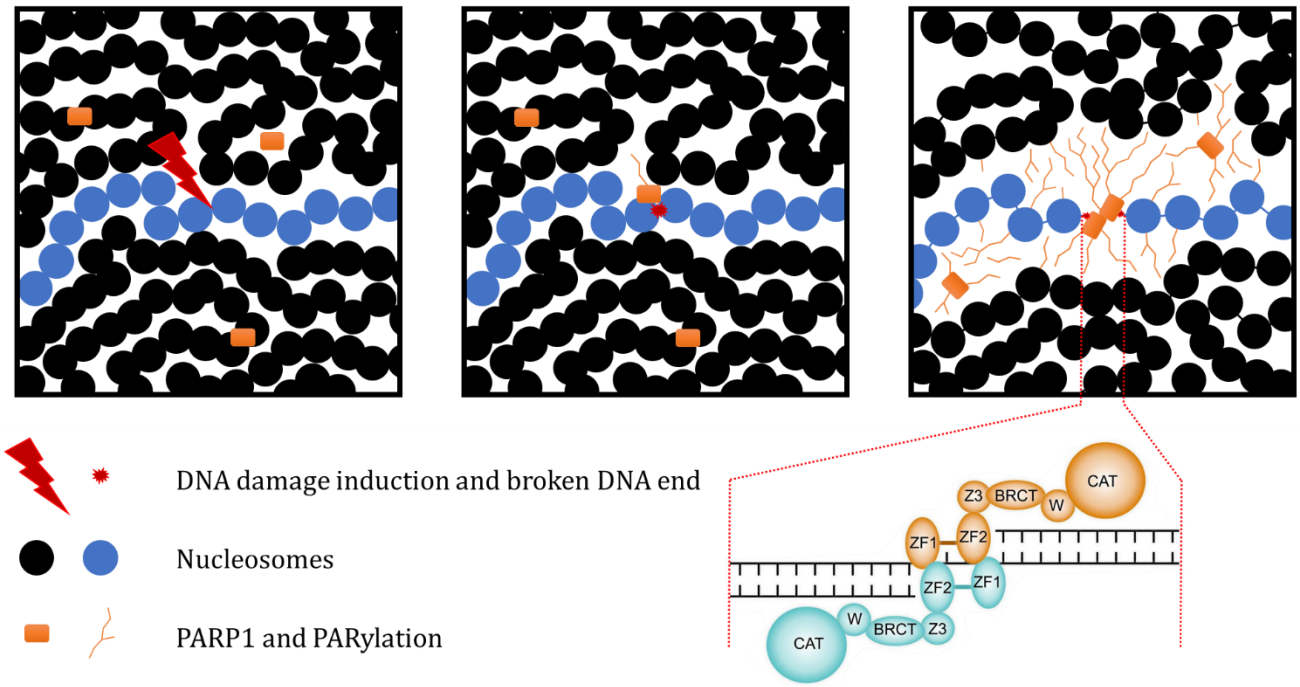

Figure 37: PARP1 tether broken DNA ends together while keeping other chromatin fibers away.
Adapted from Ali *et al.*, 2012.

time [Langelier *et al.*, 2014]. Unlike the long N-terminal region of PARP1 that encompasses three Zn fingers domains (among others, fig. 17) able to bind DNA and that has been shown to be essential for DNA binding, PARP2 and 3 display a very short N-terminal region (NTR) with no known domain characterized [Langelier *et al.*, 2012]. The C-terminal domains of those three enzymes are, however, very similar containing the same domains (fig. 17). The NTR of PARP2, slightly longer and of a different composition than the one of PARP3, has been proposed to play a role in DNA binding due to the high number of basic residues in this domain [Amé *et al.*, 1999]. However, it was shown more recently that PARP2 and 3 NTR do not play a crucial role in DNA binding for these proteins and are not even thought to be essential for their DNA-dependent activation [Langelier *et al.*, 2014].

Based on these facts, one might have wondered if the recruitment of these two proteins might have been linked to PARP1 recruitment and PARylation at the site of DNA damage. We have shown here, for the first time, to my knowledge, that PARP2 and 3 do not require prior PARP1 recruitment and activation to be localized at DNA damage sites rapidly after damage induction, ruling out this possibility (fig. 24). Since it was proposed that the WGR domain of PARP1, along with its Zn fingers and CAT domains drove the DNA-dependent activation of PARP1 [Langelier *et al.*, 2012], we can hypothesize that the WGR domain of PARP2 and PARP3 may also play a role in their binding and recruitment to damaged DNA and their possible subsequent activation.

This said, their functions in DNA damage repair remain unknown. Since the double knockout of both PARP1 and PARP2 induces embryonic lethality in mice [Boehler *et al.*, 2011] while simple knockouts of those two proteins allow survival of the individual, some redundant functions exist between those two proteins. However, in our experiments and in the context of DNA damage, no apparent compensation for the lack of PARP1 has been observed regarding PARP2 or PARP3 (fig. 24). This suggests that PARP2 and 3 might function independently of PARP1 in the context of DNA damage. Moreover, I may add that, since a highly weakened chromatin relaxation of the same amplitude is observed in PARP1 KO cells both with and without applying PARP inhibitory treatment (fig. 23), PARylation by any other PARP than PARP1, including PARP2 and PARP3, is therefore not likely to play a role in chromatin relaxation upon DNA damage. It would be interesting in future studies to precisely identify the role of those two proteins in the DDR, as well as their targets and mechanism of action.

What are the molecular causes responsible for chromatin relaxation?

As demonstrated during these experiments, PARP1 is the key player responsible, directly or indirectly, for chromatin relaxation upon DNA damage. However, it is interesting to note that in no experiments presented above is chromatin decondensation fully abolished, except under PARP inhibitory conditions where PARP1 over-condensation action might hide other pro-decondensation mechanisms (fig. 23). This implies that other cellular pathways independent from PARP1 and PARylation are activated upon DNA damage to fulfill the same role and may work in synergy with the action of PARP1 and PARylation to induce a proper chromatin relaxation.

As any integration of epigenetic marks such as DNA modification, post-translational modification of chromatin components or histone variant integration could potentially, to some extent, modify the compaction state of chromatin, candidates likely to play a role in chromatin decondensation upon DNA damage are numerous. Among them, recent findings suggest a crucial role for the phosphorylation of KAP-1 (KRAB-associated protein 1) at damaged chromatin areas. KAP-1 is known to be a co-repressor in transcription and its association with chromatin is correlated with higher compaction states [Ziv *et al.*, 2006]. Its phosphorylation, which occurs only at DNA damage sites and mostly performed by ATM, leads to its departure from the damaged area. Moreover, ablation of its phosphorylation site has been shown to lead to a highly impaired chromatin relaxation upon DNA damage [Ziv *et al.*, 2006; Iyengar and Farnham, 2011]. Another factor that has drawn more attention these last years in the field is Tip60. Indeed, Tip60 is recruited within seconds to DNA damage sites and has been shown to be able to acetylate histones H2A and H4 [Murr *et al.*, 2006; Sun *et al.*, 2010], modifications thought to lead to a more opened chromatin compaction state [de Wit and van Steensel, 2009], as well as other DDR factors such as p53 or ATM [Sykes *et al.*, 2006; Sun *et al.*, 2010]. Moreover, the inactivation of Tip60 has been shown to greatly impact chromatin relaxation upon DNA damage [Murr *et al.*, 2006; Xu *et al.*, 2010; Xu *et al.*, 2012]. Modification of DNA at damage sites is also a subject of investigations and the recent findings of interplay between Tet enzymes, responsible for cytosine hydroxymethylation at DNA damage sites [Kafer *et al.*, 2016], and PARP1 [Ciccarone *et al.*, 2015] place the labeling of DNA with hydroxymethylated cytosines, modification associated with more opened chromatin conformations [Kafer *et al.*, 2016], as a potential actor in chromatin decondensation upon DNA damage.

Moreover, we have shown in this work that ATP is another factor that is essential for a proper chromatin decondensation upon DNA damage to occur (fig. 26). I have not personally established the link between PAR- and ATP-dependent processes, but this work has been conducted in the team and led to the

characterization of two other players in the DNA damage-induced chromatin relaxation, Alc1 (Amplified in Liver Cancer 1) and CHD4 (Chromodomain Helicase DNA Binding Protein 4). Those two chromatin remodelers have been shown to be recruited to DNA damage sites in a PAR-dependent manner and act on chromatin conformation using the energy provided by ATP [Sellou *et al.*, 2016; unpublished data from H. Sellou]. PAR- and ATP-dependent mechanisms are therefore tightly linked, even if there might also be ATP-dependent pro-decondensation processes occurring without the need for a prior PARylation event at the site of the breaks. Interestingly, impairment of the activity or recruitment capacity of either Alc1 or CHD4 leads to a severely hindered chromatin relaxation. This suggests that several processes are occurring, either simultaneously or sequentially, and acting in synergy to allow the proper response of chromatin to DNA damage [Sellou *et al.*, 2016]. Based on these facts and knowing that chromatin relaxation never reaches lower levels than in the absence of PARP1, one can imagine that PARylation by PARP1 acts as a pioneering pro-decondensation event to initiate chromatin relaxation in any case, while other factors may be important to perform particular remodeling processes in specific chromatin areas (fig. 38). The list of those secondary specific factors might include Alc1 [Sellou *et al.*, 2016], CHD-4 [unpublished data from H. Sellou], CHD-2 [Luijsterburg *et al.*, 2016], the Tet enzymes [Ciccarone *et al.*, 2015], SMARCA5 [Smeenk *et al.*, 2013], Tip60 [Ikura *et al.*, 2016], and probably many others. I would find it particularly interesting if, in future studies, a network of proteins could be identified working in concert or sometimes in opposite ways to allow the regulation of chromatin relaxation upon DNA damage.

Altogether, PARP1 still appears to be among the first key DNA damage sensors allowing, upon PARylation, the recruitment of DDR factors and their subsequent actions leading to chromatin relaxation upon DNA damage. But is the role of PARylation limited to a mere scaffold, or does it alter chromatin conformation on its own like it was long ago predicted to [Mathis and Althaus, 1987]? This question remains unanswered for now, but it would appear interesting to gain a better understanding of this peculiar post-translational modification and the chromatin conformation changes it might induce. Can PARylation alone disrupt contacts between adjacent nucleosomes *in vivo*? Can it modify completely the electrostatic conditions and create a new and transient sub-nuclear compartment at damaged chromatin sites? Does the recruitment of PARP1 to DNA damage sites hinder its role at insulator regions, participating in chromatin relaxation?

The behavior of linker histone H1 at DNA damage sites

Based on earlier studies depicting the relationship between PARP1 and H1, the linker histone was my first candidate as a possible mediator of chromatin relaxation, playing its role either upon PARP1 recruitment and competition for binding [Kim *et al.*, 2004; Clark *et al.*, 2012] or upon PARylation by PARP1 [Shan *et al.*,

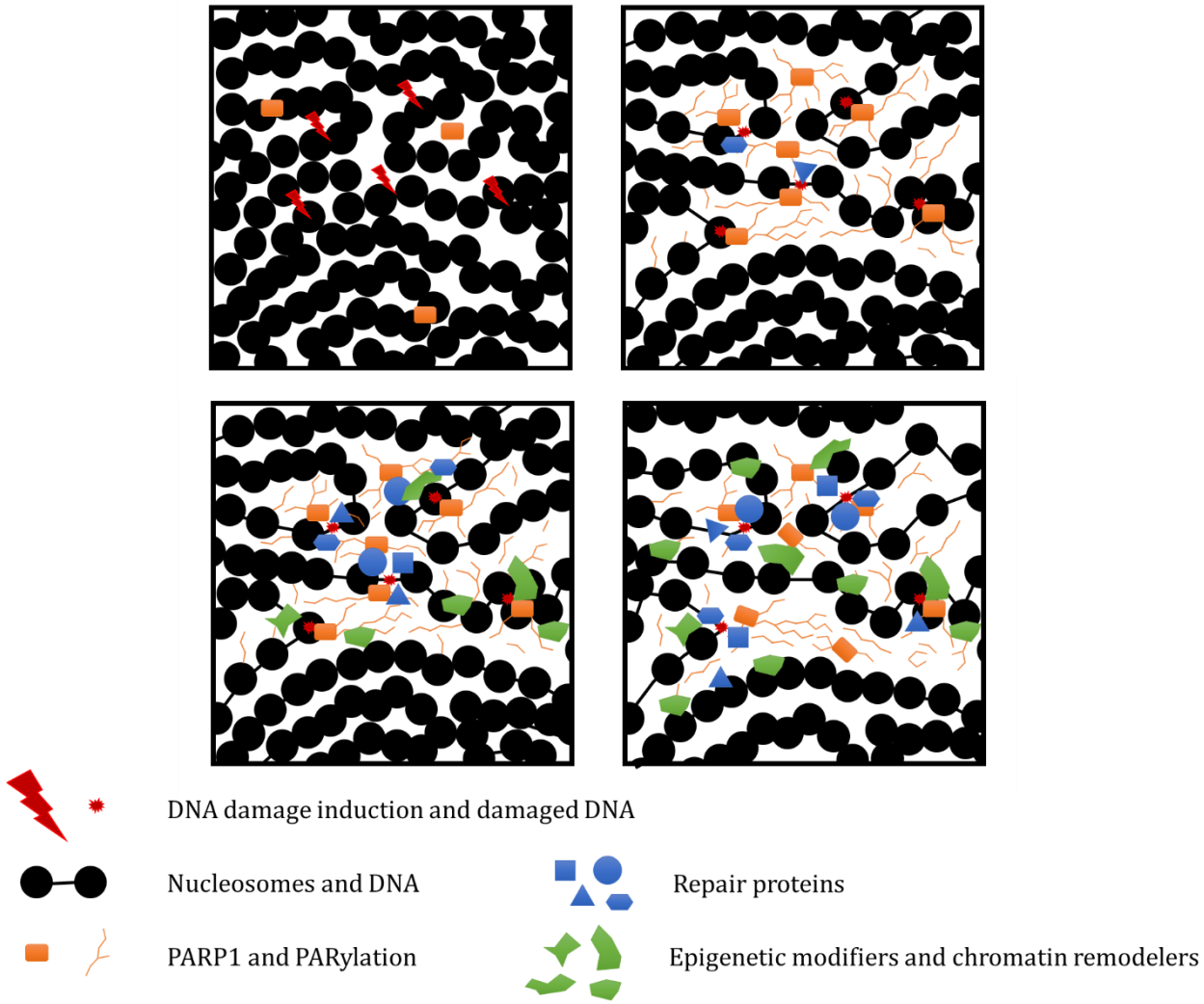

Figure 38: PARP1 initiates chromatin relaxation and helps in the recruitment of specific factors that will extend relaxation dealing with specific DNA damage or specific chromatin areas.

2014] at DNA damage sites. Both those mechanisms could decrease H1 binding on chromatin, which could consecutively lead to chromatin relaxation. Indeed, I found that H1 release from DNA damage sites is accelerated (fig. 27). This is in agreement with a recent study in which it was suggested that the displacement of H1 upon PARylation could be behind chromatin decondensation [Strickfaden *et al.*, 2016]. Moreover, I found that this accelerated release was not specific to this particular isoform since four others display the same behavior (fig. 27). Surprisingly, however, we observed that inhibiting PARylation by AG-14361 treatment or by knocking-out PARP1, while blocking chromatin relaxation, did not suppress the accelerated H1 release at DNA breaks (fig. 29). Those results exclude both mechanisms of H1 displacement by PARP1 previously reported in the context of transcriptional regulation, either through PARylation [Shan *et al.*, 2014] or through competition for binding [Krishnakumar *et al.*, 2008].

Searching further for the cause of H1 accelerated release, and knowing that H1 has been shown to be the potential target of almost every PTM currently known [Wisniewski *et al.*, 2007; Christophorou *et al.*, 2014; Hergeth and Schneider, 2015], I focused my attention on ATM and DNA-PK as both those enzymes are recruited very rapidly to DNA damage sites and trigger major PTM cascades [Uematsu *et al.*, 2007; Caron *et al.*, 2015]. However, blocking their activity with specific inhibitors did not lead to any change in H1 behavior (fig. 31). Testing the requirement for ATP, with or without performing hypotonic shock to restore the chromatin compaction state, led to the same conclusions (fig. 30). This suggests that phosphorylation of H1, or other chromatin components such as H2AX, is unlikely to be the key factor responsible for its eviction from DNA damage sites. Moreover, since ATP is not only required for phosphorylation but also serves as an energy provider for pre-modification steps of other PTMs, several modifications are less likely to play a role in its release, such as its ubiquitylation [Thorslund *et al.*, 2015], even if this should be properly tested to confirm it. Acetylation [Wisniewski *et al.*, 2007; Kamieniarz *et al.*, 2012] or citrullination [Christophorou *et al.*, 2014], possibly among others, still represent potential candidates of PTM that could participate in H1 release from DNA damage sites.

Other than post-translational modifications of H1, a competition mechanism for binding on the nucleosome could also be responsible for H1 behavior. The first option that comes to mind when considering this idea would be the replacement of the linker histone present at the site of DNA damage by another, DNA damage specific, isoform. However, since five out of the seven somatic H1 isoforms display the same behavior, namely H1.1 to H1.5 (fig. 27), one may think the other two will share this behavior as well [Izzo and Schneider, 2015]. Nevertheless, H1.0 and H1X are the isoforms that differ from the other five sharing less sequence homology and being expressed independently of the cell cycle

[Marzluff, 2005]. Even if no study, to my knowledge, has tried to address this particular question, they could potentially possess specific and unpredicted functions during DNA damage repair. Its different isoforms are not the only proteins capable of competing for binding with H1 since multiple chromatin-associated proteins have been shown to interact with the entry and exit sites of DNA on the nucleosome. Indeed, in addition to PARP1, MeCP2, HMGD1 and several HMGN proteins have been shown *in vivo* or *in vitro* to compete for binding with the linker histone [Riedmann and Fondufe-Mittendorf, 2016; Catez *et al.*, 2004; Nalabothula *et al.*, 2014]. Even if HMG proteins have been shown to play a role in DNA repair [Gerlitz, 2010], no study interested in a possible competition for binding with H1 was performed in the context of DNA damage, to my knowledge. It might be interesting to focus, in future work, on the relationship between those proteins and H1 upon DNA damage.

H1 eviction could be necessary for chromatin relaxation

Whether it arises from a direct post-translational modification of H1 itself or its interacting partners in chromatin or a competition or sequestration mechanism, H1 accelerated release from DNA damage sites occurs in all conditions tested in this work. Those results led me to the thought that H1 eviction from DNA damage sites might be necessary for chromatin relaxation to occur and could be the initial step towards chromatin relaxation and DNA damage repair. Based on this work, one can even speculate that H1 eviction from DNA damage sites might be sufficient to induce a small chromatin relaxation on its own, as long as no other chromatin associated protein, such as PARP1, is present at the site of DNA damage to fulfill the role of the linker histone in its absence. The release of H1, in this theory, could be solely responsible for the small decondensation observed after DNA damage induction in PARP1 KO cells (fig. 23). Moreover, if the action of chromatin remodelers such as Alc1 or CHD4 [Sellou *et al.*, 2016], recruited upon PARylation, is indeed the main driving force behind chromatin relaxation upon DNA damage, the presence of H1, or any other protein bound to the entry and exit sites of DNA on the nucleosome, might supposedly hinder or completely prevent their effects [Ramachandran *et al.*, 2003; Maier *et al.*, 2008], making it necessary to remove the linker histone before chromatin relaxation.

Another possibility is that the linker histone release from DNA damage sites might not be related to chromatin decondensation, while still serving a purpose during DNA damage repair, consistent with the fact that H1 release is accelerated upon DNA damage. First experiments conducted on chromatin accessibility in the context of DNA damage stated that nucleosomes induce a sheltering effect on DNA, increasing the proportion of damage in linker DNA and reducing it in nucleosomal DNA [Takata *et al.*, 2013]. Therefore, one might suspect that this more accessible [Smerdon and Lieberman, 1978], more

prone to damage [Mitchell *et al.*, 1990; Takata *et al.*, 2013], DNA would be the first to be recognized by DNA damage sensors and repair might therefore start earlier for linker DNA than for nucleosomal DNA [Meijer and Smerdon, 1999; Hara *et al.*, 2000]. In this theory, eviction of the linker histone would then only reflect the action of the first DNA repair proteins focused on damaged linker DNA and would somehow be independent of the handling of damaged nucleosomal DNA, and possibly the necessary chromatin relaxation required to process DNA damage in those areas, further on. Another possibility that should not be excluded is that, since a very high amount of DNA damage would be occurring on linker DNA [Takata *et al.*, 2013], DNA damage may simply alter the conformation of chromatin in these areas, impairing directly the capacity of binding of H1, forcing its release from chromatin. Future work in this field should aim at understanding the precise purpose of H1 accelerated release upon DNA damage.

Clues gathered from H1 accelerated recovery to DNA damage sites

When H1 release from DNA damage sites may seem like an intuitive event in order to loosen interactions within chromatin and allow relaxation, the linker histone accelerated recovery to DNA damage sites is a bit more puzzling behavior (fig. 33). To reconcile those apparently contradictory results, one can imagine that, upon DNA damage and through some unknown mechanisms, H1 affinity for chromatin is weakened, not only at DNA breaks but all over the nucleus and its speed is therefore increased both inside and outside the damaged area. However, the fact that the increased recovery speed is dependent on PARylation while the increased release speed is not tells us that those two phenomena probably reflect different regulation mechanisms. Moreover, since H1 recovery is actually slowed down upon DNA damage in PARP inhibitory conditions (fig. 33), H1 behavior in FRAP experiments is more likely dependent on the damaged chromatin compaction state, rather than on PARylation itself.

The behavior of H1 in FRAP experiments can help characterizing H1 release from DNA damage sites, and possibly understanding the complex reorganization that chromatin relaxation induces. Firstly, the driving force behind H1 increased release speed from DNA damage sites appears more likely to be a post-translational modification or a direct consequence of DNA damage disrupting the conformation of chromatin, rather than a competition mechanism. Secondly, the fact that H1 recovery is accelerated in the case of DNA damage, and not equivalent to undamaged conditions (fig. 33), might suggest that H1 actually possess a higher affinity for damaged chromatin and possibly binds damaged chromatin in a different way than it binds undamaged chromatin. This peculiar conclusion does not itself lead to a better understanding of the damaged and relaxed chromatin topology but can surely pave the way for future studies that could aim at characterizing the shifts in accessibility, which will be the next topic of this discussion, that

chromatin undergoes upon DNA damage-induced chromatin relaxation. However, it cannot be excluded that this increased recovery speed can actually reflect H1 affinity for PAR chains present at the DNA damage sites, as H1 has been shown *in vitro* to possess high affinity for PAR [Malanga *et al.*, 1998].

Deciphering the link between chromatin relaxation upon DNA damage and macromolecular crowding

After trying to understand the mechanisms driving chromatin relaxation upon DNA damage, I also wanted to study the functional role of this modification of the chromatin compaction state. In order to test the straightforward theory that suggests that chromatin decondensation serves as a mean to increase DNA accessibility, I used the framework of macromolecular crowding. Indeed, the high crowding state of the nucleus, in which at least 30 % of the volume is inaccessible due to the presence of chromatin [Rouquette *et al.*, 2009], has been shown to impact on reaction-diffusion kinetics of nuclear proteins thus potentially affecting all physiological processes in this compartment [Minton, 2006; Görisch *et al.*, 2003]. Then, when looking at damaged chromatin swell up to 150% its original size upon DNA damage, I wondered if the shifts in DNA accessibility at DNA breaks described in early experiments [Smerdon and Lieberman, 1978] could be the result of a change in macromolecular crowding induced by the early chromatin relaxation. I then followed the three major parameters that should vary due to change in crowding levels: volume exclusion, diffusional capacity of molecules and reaction kinetics.

Experiments conducted to study the volume exclusion effect on GFP tracers showed that a small volume percentage is indeed freed upon chromatin relaxation due to DNA damage (fig. 34). This effect is lost after PARP inhibitory treatment stating that this volume becomes accessible upon decondensation and/or PARylation and not upon damage itself (fig. 34). Interestingly, this effect is observed only for the smaller tracers as GFP pentamers display no change in accessible volume upon chromatin relaxation (fig. 34). It is interesting to point out that, in theory, larger molecules should be more affected by macromolecular crowding levels, in terms of volume exclusion, than smaller ones [Minton, 2006], and should, therefore, display an accentuated shift in volume accessibility upon a decrease in crowding levels. This means that the conformation of chromatin, along with its interacting partners, more than its compaction state, plays a crucial role in regulating its surrounding volume accessible to other molecules (fig. 9). This newly accessible volume could reside within chromatin, due to the fact that both intra-nucleosomal and inter-nucleosomal histone contacts are presumed to be loosened, possibly creating newly available space, or outside of chromatin. In this case, one might think that PAR chains, which could, upon DNA damage,

become the main crowder inside this specific chromatin area, might display a specific conformation in which some volume is accessible for small proteins, such as GFPs, but inaccessible to larger ones.

Diffusion properties of the same GFP tracers, in contrast to volume exclusion, showed no change comparing undamaged and damaged chromatin regions (fig. 35). This suggests that the slight reduction of the level of macromolecular crowding within the damaged area observed previously is not sufficient to lead to a change in the diffusion kinetics of the GFP probes, probably due to the fact that diffusion might be more affected by the 3-dimensional structure of the environment than volume accessibility. This result might first seem surprising as a same amount of chromatin indeed occupies a larger volume after DNA damage induced-chromatin decondensation and the GFP probes should logically be able to roam more freely this damaged area. However, considering that PAR chains share more similarities with DNA than with any other post-translational modifications [Miwa *et al.*, 1979; D'Amours *et al.*, 1999], one might wonder if the PARylation levels occurring at the site of the breaks may compensate for the loss of chromatin and thereby "restore" a somehow normal, *i.e.* comparable to undamaged chromatin, level of nucleic acid chains in this damaged area. Moreover, PAR chains are presumed to be the docking bay of an incredible amount of proteins [Gagné *et al.* 2008] that could also compensate for this loss.

Experiments led on the study of reaction kinetics with damaged chromatin areas were performed using DNA-binding molecules that should not be, in any way, recruited to DNA damage sites, namely two bacterial proteins, LacI and TetR, and the DNA-binding domain of CEBP alone, BZip. Very surprisingly, those three molecules displayed a very fast and strong recruitment to DNA damage sites hinting at an enhanced binding affinity upon chromatin relaxation (fig. 36). This effect was completely abolished upon PARylation inhibition (fig. 36). This suggests that, even if the macromolecular crowding level inside the damaged area does not seem to be greatly altered based on the volume exclusion and diffusion kinetics experiments, DNA in this area appears to be more accessible for its binding partners. It is interesting to note that, according to theoretical predictions and *in vivo* data, lowering the crowding level inside a specific crowded area would tend to decrease interactions within this area, rather than increasing it as seen for the observed DNA-binding probes [Minton, 1998; Martin and Cardoso, 2010]. This further supports the fact that the possible regulation of the macromolecular crowding level in the damaged chromatin area may not be the way by which DNA gains higher accessibility.

The purpose of chromatin relaxation upon DNA damage

Following those experiments on macromolecular crowding in the nucleus, the purpose of chromatin relaxation seems to be a gain in DNA accessibility, as shown by the enhanced binding displayed by generic chromatin interactors (fig. 36). This would fit in with the theory that emerged right after the first experiments studying chromatin decondensation upon DNA damage stating that densely packed chromatin would need a way to allow access for repair proteins in order to handle the damage [Smerdon and Lieberman, 1978; Smerdon, 1991]. To my knowledge, this theory regarding the purpose of chromatin relaxation has not been challenged by any other since.

However, it might seem odd that a decrease in the level of crowding inside the damaged area would not be a factor granting higher diffusional capacity and a higher volume fraction accessible for DNA repair proteins. This raises the question of the way chromatin is actually able to display a higher accessibility while staying in what could be defined as an inaccessible environment. Moreover, a recent study showed that more than 70% of all transcription factors (included in the analysis) are rapidly localized at DNA damage sites, strengthening the results we observed using LacI, TetR and BZip [Izhar *et al.*, 2015]. This also adds a new layer of complexity as this collection of chromatin interactors all localized in the same space would intuitively increase the crowding level in the area, and lower access of chromatin. It should, therefore, be a tightly regulated event in order not to overwhelm the DNA repair machinery in this damaged chromatin area, or maybe serve a yet unknown purpose.

It is interesting to point out that chromatin relaxation actually defines two processes occurring at different scales. On the one hand, the enlargement of the damaged chromatin area observed by light microscopy (fig. 23), and on the other hand, the higher accessibility of DNA observed at the molecular scale (fig. 36). While increase in DNA accessibility could surely be achieved upon the action of chromatin remodelers and other epigenetic modifiers recruited through PARylation by PARP1 [Gagné *et al.*, 2008; Clapier and Cairns, 2009], it is difficult to grasp how those events occurring at the nucleosomal scale could induce a global change in the architecture of chromatin at the nuclear scale. Finding the link between those two events would surely increase our knowledge regarding the purpose of chromatin relaxation, and its implications for the global nuclear architecture.

Moreover, the link between chromatin relaxation, DNA accessibility and DNA repair is not well-defined either. Indeed, one might think that handling of DNA damage would occur directly after recruitment of DNA repair proteins achieved through higher DNA accessibility. However, some recent studies have linked

DSB repair to the recruitment of factors associated with repressive, more compacted chromatin conformations, suggesting that DNA repair could actually occur after the initial decondensation step and thus during the subsequent recondensation phenomenon [Ayoub *et al.*, 2008; Khurana *et al.*, 2014; Burgess *et al.*, 2014]. The chromatin compaction state, directed by interactions between chromatin and its binding partners at DNA damage sites, has even been proposed to play a significative role in the choice of the repair pathway regarding specific DNA lesions [Khurana *et al.*, 2014]. This work opens the door for another purpose of the regulation of chromatin compaction state at DNA damage sites, even if only too few studies have tried to study this particular role so far.

GENERAL CONCLUSION

To conclude, this work has helped gain hindsight on the dual role of PARP1 in the DNA damage-induced chromatin relaxation, placing this enzyme as the pioneering factor responsible for chromatin decondensation, as well as for the recruitment of other proteins essential to this process. It would be interesting to follow this study by furthering our understanding of PARP1 regulation, both in its shift from chromatin-associated protein to DNA damage sensor, and in the tight regulation of its activity from which depends the extent of the chromatin relaxation. The interesting behavior of linker histone H1 upon DNA damage induction has also been investigated here. The release of H1 from damage sites may be essential for chromatin decondensation as it has been shown to be a very early and, from what we have seen, systematic, response to DNA damage. This work should be pursued with the goal to unravel the driving force, as well as the purpose, of H1 behavior upon DNA damage. Regarding the functional role of chromatin relaxation, we have excluded here that a reduction of macromolecular crowding could be the mean to increase DNA accessibility. Moreover, we have shown that damaged chromatin is indeed more accessible to DNA-binding molecules in a PARylation and/or relaxation manner. Relating the changes observed in the chromatin compaction state with those observed in DNA accessibility upon DNA damage should, in my opinion, be the main focus of future studies.

Although a lot of pieces of this puzzle of always-increasing complexity are becoming now more and more well-defined, especially during these last few years, we still lack the understanding of how all these pieces fit together, preventing us from totally grasping the entire nature and the true purpose(s) of this phenomenon. A lot of exciting work still awaits us in this field!

REFERENCES

Adam, S., and Polo, S.E. (2014). Blurring the line between the DNA damage response and transcription: the importance of chromatin dynamics. Exp. Cell Res. 329, 148–153.

Ahel, D., Horejsí, Z., Wiechens, N., Polo, S.E., Garcia-Wilson, E., Ahel, I., Flynn, H., Skehel, M., West, S.C., Jackson, S.P., *et al.* (2009). Poly(ADP-ribose)-dependent regulation of DNA repair by the chromatin remodeling enzyme ALC1. Science 325, 1240–1243.

Ahel, I., Ahel, D., Matsusaka, T., Clark, A.J., Pines, J., Boulton, S.J., and West, S.C. (2008). Poly(ADP-ribose)-binding zinc finger motifs in DNA repair/checkpoint proteins. Nature 451, 81–85.

al, H.A., et Quantitative analysis of cell cycle phase durations and PC12 differentiation using fluorescent biosensors. - PubMed - NCBI.

Albig, W., and Doenecke, D. (1997). The human histone gene cluster at the D6S105 locus. Hum. Genet. 101, 284–294.

Ali, A.A.E., Timinszky, G., Arribas-Bosacoma, R., Kozlowski, M., Hassa, P.O., Hassler, M., Ladurner, A.G., Pearl, L.H., and Oliver, A.W. (2012). The zinc-finger domains of PARP1 cooperate to recognize DNA strand breaks. Nat. Struct. Mol. Biol. 19, 685–692.

Allan, J., Hartman, P.G., Crane-Robinson, C., and Aviles, F.X. (1980). The structure of histone H1 and its location in chromatin. Nature 288, 675–679.

Altmeyer, M., Messner, S., Hassa, P.O., Fey, M., and Hottiger, M.O. (2009). Molecular mechanism of poly(ADP-ribosyl)ation by PARP1 and identification of lysine residues as ADP-ribose acceptor sites. Nucleic Acids Res. 37, 3723–3738.

Amé, J.C., Rolli, V., Schreiber, V., Niedergang, C., Apiou, F., Decker, P., Muller, S., Höger, T., Ménissier-de Murcia, J., and de Murcia, G. (1999). PARP-2, A novel mammalian DNA damage-dependent poly(ADP-ribose) polymerase. J. Biol. Chem. 274, 17860–17868.

Aten, J.A., Stap, J., Krawczyk, P.M., van Oven, C.H., Hoebe, R.A., Essers, J., and Kanaar, R. (2004). Dynamics of DNA double-strand breaks revealed by clustering of damaged chromosome domains. Science 303, 92–95.

Ayoub, N., Jeyasekharan, A.D., Bernal, J.A., and Venkitaraman, A.R. (2008). HP1-beta mobilization promotes chromatin changes that initiate the DNA damage response. Nature 453, 682–686.

Ayrapetov, M.K., Gursoy-Yuzugullu, O., Xu, C., Xu, Y., and Price, B.D. (2014). DNA double-strand breaks promote methylation of histone H3 on lysine 9 and transient formation of repressive chromatin. Proc. Natl. Acad. Sci. U.S.A. 111, 9169–9174.

Bancaud, A., Huet, S., Daigle, N., Mozziconacci, J., Beaudouin, J., and Ellenberg, J. (2009). Molecular crowding affects diffusion and binding of nuclear proteins in heterochromatin and reveals the fractal organization of chromatin. EMBO J. 28, 3785–3798.

Banks, D.S., and Fradin, C. (2005). Anomalous diffusion of proteins due to molecular crowding. Biophys. J. 89, 2960–2971.

Bannister, A.J., Zegerman, P., Partridge, J.F., Miska, E.A., Thomas, J.O., Allshire, R.C., and Kouzarides, T. (2001). Selective recognition of methylated lysine 9 on histone H3 by the HP1 chromo domain. Nature 410, 120–124.

Barkauskaite, E., Jankevicius, G., and Ahel, I. (2015). Structures and Mechanisms of Enzymes Employed in the Synthesis and Degradation of PARP-Dependent Protein ADP-Ribosylation. Mol. Cell 58, 935–946.

Beaudouin, J., Mora-Bermúdez, F., Klee, T., Daigle, N., and Ellenberg, J. (2006). Dissecting the contribution of diffusion and interactions to the mobility of nuclear proteins. Biophys. J. 90, 1878–1894.

Bednar, J., and Woodcock, C.L. (1999). Cryoelectron microscopic analysis of nucleosomes and chromatin. Meth. Enzymol. 304, 191–213.

Bednar, J., Horowitz, R.A., Grigoryev, S.A., Carruthers, L.M., Hansen, J.C., Koster, A.J., and Woodcock, C.L. (1998). Nucleosomes, linker DNA, and linker histone form a unique structural motif that directs the higher-order folding and compaction of chromatin. Proc. Natl. Acad. Sci. U.S.A. 95, 14173–14178.

Bednar, J., Hamiche, A., and Dimitrov, S. (2016). H1-nucleosome interactions and their functional implications. Biochim. Biophys. Acta 1859, 436–443.
Berg, H.C. (1993). Random Walks in Biology (Princeton University Press).
Blier, P.R., Griffith, A.J., Craft, J., and Hardin, J.A. (1993). Binding of Ku protein to DNA. Measurement of affinity for ends and demonstration of binding to nicks. J. Biol. Chem. 268, 7594–7601.
Bock, F.J., and Chang, P. (2016). New directions in poly(ADP-ribose) polymerase biology. FEBS J. 283, 4017–4031.
Boehler, C., Gauthier, L., Yelamos, J., Noll, A., Schreiber, V., and Dantzer, F. (2011). Phenotypic characterization of Parp-1 and Parp-2 deficient mice and cells. Methods Mol. Biol. 780, 313–336.
Bornfleth, H., Edelmann, P., Zink, D., Cremer, T., and Cremer, C. (1999). Quantitative motion analysis of subchromosomal foci in living cells using four-dimensional microscopy. Biophys. J. 77, 2871–2886.
Bowen, N.J., Fujita, N., Kajita, M., and Wade, P.A. (2004). Mi-2/NuRD: multiple complexes for many purposes. Biochim. Biophys. Acta 1677, 52–57.
Brandsma, I., and Gent, D.C. (2012). Pathway choice in DNA double strand break repair: observations of a balancing act. Genome Integr 3, 9.
Breslin, C., Hornyak, P., Ridley, A., Rulten, S.L., Hanzlikova, H., Oliver, A.W., and Caldecott, K.W. (2015). The XRCC1 phosphate-binding pocket binds poly (ADP-ribose) and is required for XRCC1 function. Nucleic Acids Res. 43, 6934–6944.
Brochu, G., Duchaine, C., Thibeault, L., Lagueux, J., Shah, G.M., and Poirier, G.G. (1994). Mode of action of poly(ADP-ribose) glycohydrolase. Biochim. Biophys. Acta 1219, 342–350.
Bronshtein, I., Kanter, I., Kepten, E., Lindner, M., Berezin, S., Shav-Tal, Y., and Garini, Y. (2016). Exploring chromatin organization mechanisms through its dynamic properties. Nucleus 7, 27–33.
Bronstein, I., Israel, Y., Kepten, E., Mai, S., Shav-Tal, Y., Barkai, E., and Garini, Y. (2009). Transient anomalous diffusion of telomeres in the nucleus of mammalian cells. Phys. Rev. Lett. 103, 018102.
Burgess, R.C., Burman, B., Kruhlak, M.J., and Misteli, T. (2014). Activation of DNA damage response signaling by condensed chromatin. Cell Rep 9, 1703–1717.
Bustin, M., Catez, F., and Lim, J.-H. (2005). The dynamics of histone H1 function in chromatin. Mol. Cell 17, 617–620.
Cabal, G.G., Genovesio, A., Rodriguez-Navarro, S., Zimmer, C., Gadal, O., Lesne, A., Buc, H., Feuerbach-Fournier, F., Olivo-Marin, J.-C., Hurt, E.C., *et al.* (2006). SAGA interacting factors confine sub-diffusion of transcribed genes to the nuclear envelope. Nature 441, 770–773.
Caiafa, P., Guastafierro, T., and Zampieri, M. (2009). Epigenetics: poly(ADP-ribosyl)ation of PARP-1 regulates genomic methylation patterns. FASEB J. 23, 672–678.
Capelson, M., Doucet, C., and Hetzer, M.W. (2010). Nuclear pore complexes: guardians of the nuclear genome. Cold Spring Harb. Symp. Quant. Biol. 75, 585–597.
Caron, P., Choudjaye, J., Clouaire, T., Bugler, B., Daburon, V., Aguirrebengoa, M., Mangeat, T., Iacovoni, J.S., Álvarez-Quilón, A., Cortés-Ledesma, F., *et al.* (2015). Non-redundant Functions of ATM and DNA-PKcs in Response to DNA Double-Strand Breaks. Cell Rep 13, 1598–1609.
Casolari, J.M., Brown, C.R., Komili, S., West, J., Hieronymus, H., and Silver, P.A. (2004). Genome-wide localization of the nuclear transport machinery couples transcriptional status and nuclear organization. Cell 117, 427–439.
Catez, F., Brown, D.T., Misteli, T., and Bustin, M. (2002). Competition between histone H1 and HMGN proteins for chromatin binding sites. EMBO Rep. 3, 760–766.
Catez, F., Yang, H., Tracey, K.J., Reeves, R., Misteli, T., and Bustin, M. (2004). Network of dynamic interactions between histone H1 and high-mobility-group proteins in chromatin. Mol. Cell. Biol. 24, 4321–4328.
Chakravarthy, S., and Luger, K. (2006). The histone variant macro-H2A preferentially forms "hybrid nucleosomes." J. Biol. Chem. 281, 25522–25531.
Chambeyron, S., and Bickmore, W.A. (2004). Chromatin decondensation and nuclear reorganization of the HoxB locus upon induction of transcription. Genes Dev. 18, 1119–1130.

Chambon, P., Weill, J.D., and Mandel, P. (1963). Nicotinamide mononucleotide activation of new DNA-dependent polyadenylic acid synthesizing nuclear enzyme. Biochem. Biophys. Res. Commun. 11, 39–43.
Chang, H.H.Y., Watanabe, G., and Lieber, M.R. (2015). Unifying the DNA end-processing roles of the artemis nuclease: Ku-dependent artemis resection at blunt DNA ends. J. Biol. Chem. 290, 24036–24050.
Chaumeil, J., Le Baccon, P., Wutz, A., and Heard, E. (2006). A novel role for Xist RNA in the formation of a repressive nuclear compartment into which genes are recruited when silenced. Genes Dev. 20, 2223–2237.
Cheutin, T., McNairn, A.J., Jenuwein, T., Gilbert, D.M., Singh, P.B., and Misteli, T. (2003). Maintenance of stable heterochromatin domains by dynamic HP1 binding. Science 299, 721–725.
Cho, E.J., and Kim, J.S. (2012). Crowding effects on the formation and maintenance of nuclear bodies: insights from molecular-dynamics simulations of simple spherical model particles. Biophys. J. 103, 424–433.
Choi, J.K., and Howe, L.J. (2009). Histone acetylation: truth of consequences? Biochem. Cell Biol. 87, 139–150.
Chou, D.M., Adamson, B., Dephoure, N.E., Tan, X., Nottke, A.C., Hurov, K.E., Gygi, S.P., Colaiácovo, M.P., and Elledge, S.J. (2010). A chromatin localization screen reveals poly (ADP ribose)-regulated recruitment of the repressive polycomb and NuRD complexes to sites of DNA damage. Proc. Natl. Acad. Sci. U.S.A. 107, 18475–18480.
Christophorou, M.A., Castelo-Branco, G., Halley-Stott, R.P., Oliveira, C.S., Loos, R., Radzisheuskaya, A., Mowen, K.A., Bertone, P., Silva, J.C.R., Zernicka-Goetz, M., *et al.* (2014). Citrullination regulates pluripotency and histone H1 binding to chromatin. Nature 507, 104–108.
Chuang, C.-H., Carpenter, A.E., Fuchsova, B., Johnson, T., de Lanerolle, P., and Belmont, A.S. (2006). Long-range directional movement of an interphase chromosome site. Curr. Biol. 16, 825–831.
Chubb, J.R., Boyle, S., Perry, P., and Bickmore, W.A. (2002). Chromatin motion is constrained by association with nuclear compartments in human cells. Curr. Biol. 12, 439–445.
Ciccarone, F., Valentini, E., Zampieri, M., and Caiafa, P. (2015). 5mC-hydroxylase activity is influenced by the PARylation of TET1 enzyme. Oncotarget 6, 24333–24347.
Ciccarone, F., Zampieri, M., and Caiafa, P. (2017). PARP1 orchestrates epigenetic events setting up chromatin domains. Semin. Cell Dev. Biol. 63, 123–134.
Ciccia, A., and Elledge, S.J. (2010). The DNA damage response: making it safe to play with knives. Mol. Cell 40, 179–204.
Clapier, C.R., and Cairns, B.R. (2009). The biology of chromatin remodeling complexes. Annu. Rev. Biochem. 78, 273–304.
Clark, N.J., Kramer, M., Muthurajan, U.M., and Luger, K. (2012). Alternative modes of binding of poly(ADP-ribose) polymerase 1 to free DNA and nucleosomes. J. Biol. Chem. 287, 32430–32439.
Clausell, J., Happel, N., Hale, T.K., Doenecke, D., and Beato, M. (2009). Histone H1 subtypes differentially modulate chromatin condensation without preventing ATP-dependent remodeling by SWI/SNF or NURF. PLoS ONE 4, e0007243.
Coleman-Derr, D., and Zilberman, D. (2012). DNA methylation, H2A.Z, and the regulation of constitutive expression. Cold Spring Harb. Symp. Quant. Biol. 77, 147–154.
Cosgrove, M.S., Boeke, J.D., and Wolberger, C. (2004). Regulated nucleosome mobility and the histone code. Nat. Struct. Mol. Biol. 11, 1037–1043.
Cravens, S.L., and Stivers, J.T. (2016). Comparative Effects of Ions, Molecular Crowding, and Bulk DNA on the Damage Search Mechanisms of hOGG1 and hUNG. Biochemistry 55, 5230–5242.
Cremer, T., Küpper, K., Dietzel, S., and Fakan, S. (2004). Higher order chromatin architecture in the cell nucleus: on the way from structure to function. Biol. Cell 96, 555–567.
Cushman, I., Stenoien, D., and Moore, M.S. (2004). The dynamic association of RCC1 with chromatin is modulated by Ran-dependent nuclear transport. Mol. Biol. Cell 15, 245–255.
Cutter, A.R., and Hayes, J.J. (2015). A brief review of nucleosome structure. FEBS Letters 589, 2914–2922.
Dahm, R. (2008). Discovering DNA: Friedrich Miescher and the early years of nucleic acid research. Hum. Genet. 122, 565–581.

Dai, L., Peng, C., Montellier, E., Lu, Z., Chen, Y., Ishii, H., Debernardi, A., Buchou, T., Rousseaux, S., Jin, F., *et al.* (2014). Lysine 2-hydroxyisobutyrylation is a widely distributed active histone mark. Nat. Chem. Biol. 10, 365–370.

D'Amours, D., Desnoyers, S., D'Silva, I., and Poirier, G.G. (1999). Poly(ADP-ribosyl)ation reactions in the regulation of nuclear functions. Biochem. J. 342 (Pt 2), 249–268.

Danielsen, J.M.R., Sylvestersen, K.B., Bekker-Jensen, S., Szklarczyk, D., Poulsen, J.W., Horn, H., Jensen, L.J., Mailand, N., and Nielsen, M.L. (2011). Mass spectrometric analysis of lysine ubiquitylation reveals promiscuity at site level. Mol. Cell Proteomics 10, M110.003590.

Davey, C.A., Sargent, D.F., Luger, K., Maeder, A.W., and Richmond, T.J. (2002). Solvent mediated interactions in the structure of the nucleosome core particle at 1.9 a resolution. J. Mol. Biol. 319, 1097–1113.

Deaton, A.M., and Bird, A. (2011). CpG islands and the regulation of transcription. Genes Dev. 25, 1010–1022.

Deng, X., Zhironkina, O.A., Cherepanynets, V.D., Strelkova, O.S., Kireev, I.I., and Belmont, A.S. (2016). Cytology of DNA Replication Reveals Dynamic Plasticity of Large-Scale Chromatin Fibers. Curr. Biol. 26, 2527–2534.

Deterding, L.J., Bunger, M.K., Banks, G.C., Tomer, K.B., and Archer, T.K. (2008). Global changes in and characterization of specific sites of phosphorylation in mouse and human histone H1 Isoforms upon CDK inhibitor treatment using mass spectrometry. J. Proteome Res. 7, 2368–2379.

Dion, V., and Gasser, S.M. (2013). Chromatin movement in the maintenance of genome stability. Cell 152, 1355–1364.

Dion, V., Kalck, V., Horigome, C., Towbin, B.D., and Gasser, S.M. (2012). Increased mobility of double-strand breaks requires Mec1, Rad9 and the homologous recombination machinery. Nat. Cell Biol. 14, 502–509.

Dixon, J.R., Selvaraj, S., Yue, F., Kim, A., Li, Y., Shen, Y., Hu, M., Liu, J.S., and Ren, B. (2012). Topological domains in mammalian genomes identified by analysis of chromatin interactions. Nature 485, 376–380.

Dixon, J.R., Jung, I., Selvaraj, S., Shen, Y., Antosiewicz-Bourget, J.E., Lee, A.Y., Ye, Z., Kim, A., Rajagopal, N., Xie, W., *et al.* (2015). Chromatin architecture reorganization during stem cell differentiation. Nature 518, 331–336.

Doil, C., Mailand, N., Bekker-Jensen, S., Menard, P., Larsen, D.H., Pepperkok, R., Ellenberg, J., Panier, S., Durocher, D., Bartek, J., *et al.* (2009). RNF168 binds and amplifies ubiquitin conjugates on damaged chromosomes to allow accumulation of repair proteins. Cell 136, 435–446.

Dunstan, M.S., Barkauskaite, E., Lafite, P., Knezevic, C.E., Brassington, A., Ahel, M., Hergenrother, P.J., Leys, D., and Ahel, I. (2012). Structure and mechanism of a canonical poly(ADP-ribose) glycohydrolase. Nat Commun 3, 878.

Ea, V., Baudement, M.-O., Lesne, A., and Forné, T. (2015). Contribution of Topological Domains and Loop Formation to 3D Chromatin Organization. Genes (Basel) 6, 734–750.

Ellis, R.J. (2001). Macromolecular crowding: obvious but underappreciated. Trends Biochem. Sci. 26, 597–604.

Elsaesser, S.J., and Allis, C.D. (2010). HIRA and Daxx constitute two independent histone H3.3-containing predeposition complexes. Cold Spring Harb. Symp. Quant. Biol. 75, 27–34.

Eltsov, M., Maclellan, K.M., Maeshima, K., Frangakis, A.S., and Dubochet, J. (2008). Analysis of cryo-electron microscopy images does not support the existence of 30-nm chromatin fibers in mitotic chromosomes in situ. Proc. Natl. Acad. Sci. U.S.A. 105, 19732–19737.

Erdel, F., Schubert, T., Marth, C., Längst, G., and Rippe, K. (2010). Human ISWI chromatin-remodeling complexes sample nucleosomes via transient binding reactions and become immobilized at active sites. Proc. Natl. Acad. Sci. U.S.A. 107, 19873–19878.

Erdel, F., Krug, J., Längst, G., and Rippe, K. (2011). Targeting chromatin remodelers: signals and search mechanisms. Biochim. Biophys. Acta 1809, 497–508.

Erener, S., Hesse, M., Kostadinova, R., and Hottiger, M.O. (2012). Poly(ADP-ribose)polymerase-1 (PARP1) controls adipogenic gene expression and adipocyte function. Mol. Endocrinol. 26, 79–86.

Ettig, R., Kepper, N., Stehr, R., Wedemann, G., and Rippe, K. (2011). Dissecting DNA-histone interactions in the nucleosome by molecular dynamics simulations of DNA unwrapping. Biophys. J. 101, 1999–2008.

Fan, Y., Nikitina, T., Morin-Kensicki, E.M., Zhao, J., Magnuson, T.R., Woodcock, C.L., and Skoultchi, A.I. (2003). H1 linker histones are essential for mouse development and affect nucleosome spacing *in vivo*. Mol. Cell. Biol. 23, 4559–4572.

Fan, Y., Nikitina, T., Zhao, J., Fleury, T.J., Bhattacharyya, R., Bouhassira, E.E., Stein, A., Woodcock, C.L., and Skoultchi, A.I. (2005). Histone H1 depletion in mammals alters global chromatin structure but causes specific changes in gene regulation. Cell 123, 1199–1212.

Farrell, A.W., Halliday, G.M., and Lyons, J.G. (2011). Chromatin structure following UV-induced DNA damage-repair or death? Int J Mol Sci 12, 8063–8085.

Filion, G.J., van Bemmel, J.G., Braunschweig, U., Talhout, W., Kind, J., Ward, L.D., Brugman, W., de Castro, I.J., Kerkhoven, R.M., Bussemaker, H.J., *et al.* (2010). Systematic protein location mapping reveals five principal chromatin types in Drosophila cells. Cell 143, 212–224.

Finch, J.T., and Klug, A. (1976). Solenoidal model for superstructure in chromatin. Proc. Natl. Acad. Sci. U.S.A. 73, 1897–1901.

Fontana, P., Bonfiglio, J.J., Palazzo, L., Bartlett, E., Matic, I., and Ahel, I. (2017). Serine ADP-ribosylation reversal by the hydrolase ARH3. Elife 6.

Frado, L.L., Mura, C.V., Stollar, B.D., and Woodcock, C.L. (1983). Mapping of histone H5 sites on nucleosomes using immunoelectron microscopy. J. Biol. Chem. 258, 11984–11990.

Friedberg, E.C. (2001). How nucleotide excision repair protects against cancer. Nat. Rev. Cancer 1, 22–33.

Furini, S., Domene, C., and Cavalcanti, S. (2010). Insights into the sliding movement of the lac repressor nonspecifically bound to DNA. J Phys Chem B 114, 2238–2245.

Fussner, E., Strauss, M., Djuric, U., Li, R., Ahmed, K., Hart, M., Ellis, J., and Bazett-Jones, D.P. (2012). Open and closed domains in the mouse genome are configured as 10-nm chromatin fibres. EMBO Rep. 13, 992–996.

Gagné, J.-P., Hunter, J.M., Labrecque, B., Chabot, B., and Poirier, G.G. (2003). A proteomic approach to the identification of heterogeneous nuclear ribonucleoproteins as a new family of poly(ADP-ribose)-binding proteins. Biochem. J. 371, 331–340.

Gagné, J.-P., Isabelle, M., Lo, K.S., Bourassa, S., Hendzel, M.J., Dawson, V.L., Dawson, T.M., and Poirier, G.G. (2008). Proteome-wide identification of poly(ADP-ribose) binding proteins and poly(ADP-ribose)-associated protein complexes. Nucleic Acids Res. 36, 6959–6976.

García-Giménez, J.L., Ledesma, A.M.V., Esmoris, I., Romá-Mateo, C., Sanz, P., Viña, J., and Pallardó, F.V. (2012). Histone carbonylation occurs in proliferating cells. Free Radic. Biol. Med. 52, 1453–1464.

Gartenberg, M.R., Neumann, F.R., Laroche, T., Blaszczyk, M., and Gasser, S.M. (2004). Sir-mediated repression can occur independently of chromosomal and subnuclear contexts. Cell 119, 955–967.

Geiman, T.M., and Robertson, K.D. (2002). Chromatin remodeling, histone modifications, and DNA methylation-how does it all fit together? J. Cell. Biochem. 87, 117–125.

van Gent, D.C., Hoeijmakers, J.H., and Kanaar, R. (2001). Chromosomal stability and the DNA double-stranded break connection. Nat. Rev. Genet. 2, 196–206.

Gerlich, D., Beaudouin, J., Kalbfuss, B., Daigle, N., Eils, R., and Ellenberg, J. (2003). Global chromosome positions are transmitted through mitosis in mammalian cells. Cell 112, 751–764.

Gerlitz, G. (2010). HMGNs, DNA repair and cancer. Biochim. Biophys. Acta 1799, 80–85.

Golia, B., Moeller, G.K., Jankevicius, G., Schmidt, A., Hegele, A., Preißer, J., Tran, M.L., Imhof, A., and Timinszky, G. (2017). ATM induces MacroD2 nuclear export upon DNA damage. Nucleic Acids Res. 45, 244–254.

Görisch, S.M., Richter, K., Scheuermann, M.O., Herrmann, H., and Lichter, P. (2003). Diffusion-limited compartmentalization of mammalian cell nuclei assessed by microinjected macromolecules. Exp. Cell Res. 289, 282–294.

Gottschalk, A.J., Timinszky, G., Kong, S.E., Jin, J., Cai, Y., Swanson, S.K., Washburn, M.P., Florens, L., Ladurner, A.G., Conaway, J.W., *et al.* (2009). Poly(ADP-ribosyl)ation directs recruitment and activation of an ATP-dependent chromatin remodeler. Proc. Natl. Acad. Sci. U.S.A. 106, 13770–13774.

Gräff, J., and Mansuy, I.M. (2008). Epigenetic codes in cognition and behaviour. Behav. Brain Res. 192, 70–87.

Green, C.M., and Almouzni, G. (2002). When repair meets chromatin. First in series on chromatin dynamics. EMBO Rep. 3, 28–33.
Grigoryev, S.A., and Woodcock, C.L. (2012). Chromatin organization - the 30 nm fiber. Exp. Cell Res. 318, 1448–1455.
Gruenbaum, Y., Margalit, A., Goldman, R.D., Shumaker, D.K., and Wilson, K.L. (2005). The nuclear lamina comes of age. Nat. Rev. Mol. Cell Biol. 6, 21–31.
Guastafierro, T., Cecchinelli, B., Zampieri, M., Reale, A., Riggio, G., Sthandier, O., Zupi, G., Calabrese, L., and Caiafa, P. (2008). CCCTC-binding factor activates PARP-1 affecting DNA methylation machinery. J. Biol. Chem. 283, 21873–21880.
Guelen, L., Pagie, L., Brasset, E., Meuleman, W., Faza, M.B., Talhout, W., Eussen, B.H., de Klein, A., Wessels, L., de Laat, W., *et al.* (2008). Domain organization of human chromosomes revealed by mapping of nuclear lamina interactions. Nature 453, 948–951.
Guo, C.Y., Wang, Y., Brautigan, D.L., and Larner, J.M. (1999). Histone H1 dephosphorylation is mediated through a radiation-induced signal transduction pathway dependent on ATM. J. Biol. Chem. 274, 18715–18720.
Gutiyama, L.M., da Cunha, J.P.C., and Schenkman, S. (2008). Histone H1 of Trypanosoma cruzi is concentrated in the nucleolus region and disperses upon phosphorylation during progression to mitosis. Eukaryotic Cell 7, 560–568.
Haince, J.-F., McDonald, D., Rodrigue, A., Déry, U., Masson, J.-Y., Hendzel, M.J., and Poirier, G.G. (2008). PARP1-dependent kinetics of recruitment of MRE11 and NBS1 proteins to multiple DNA damage sites. J. Biol. Chem. 283, 1197–1208.
Hajjoul, H., Mathon, J., Ranchon, H., Goiffon, I., Mozziconacci, J., Albert, B., Carrivain, P., Victor, J.-M., Gadal, O., Bystricky, K., *et al.* (2013). High-throughput chromatin motion tracking in living yeast reveals the flexibility of the fiber throughout the genome. Genome Res. 23, 1829–1838.
Hakim, O., Sung, M.-H., Voss, T.C., Splinter, E., John, S., Sabo, P.J., Thurman, R.E., Stamatoyannopoulos, J.A., de Laat, W., and Hager, G.L. (2011). Diverse gene reprogramming events occur in the same spatial clusters of distal regulatory elements. Genome Res. 21, 697–706.
Hall, D., and Minton, A.P. (2003). Macromolecular crowding: qualitative and semiquantitative successes, quantitative challenges. Biochim. Biophys. Acta 1649, 127–139.
Hamiche, A., Schultz, P., Ramakrishnan, V., Oudet, P., and Prunell, A. (1996). Linker histone-dependent DNA structure in linear mononucleosomes. J. Mol. Biol. 257, 30–42.
Hancock, R. (2004). A role for macromolecular crowding effects in the assembly and function of compartments in the nucleus. J. Struct. Biol. 146, 281–290.
Hancock, R. (2008). Self-association of polynucleosome chains by macromolecular crowding. Eur. Biophys. J. 37, 1059–1064.
Hancock, R. (2014). The crowded nucleus. Int Rev Cell Mol Biol 307, 15–26.
Happel, N., Schulze, E., and Doenecke, D. (2005). Characterisation of human histone H1x. Biol. Chem. 386, 541–551.
Haqqani, A.S., Kelly, J.F., and Birnboim, H.C. (2002). Selective nitration of histone tyrosine residues *in vivo* in mutatect tumors. J. Biol. Chem. 277, 3614–3621.
Hara, R., Mo, J., and Sancar, A. (2000). DNA damage in the nucleosome core is refractory to repair by human excision nuclease. Mol. Cell. Biol. 20, 9173–9181.
Hassa, P.O., and Hottiger, M.O. (2008). The diverse biological roles of mammalian PARPS, a small but powerful family of poly-ADP-ribose polymerases. Front. Biosci. 13, 3046–3082.
Heermann, D.W., Jerabek, H., Liu, L., and Li, Y. (2012). A model for the 3D chromatin architecture of pro and eukaryotes. Methods 58, 307–314.
Heo, K., Kim, H., Choi, S.H., Choi, J., Kim, K., Gu, J., Lieber, M.R., Yang, A.S., and An, W. (2008). FACT-mediated exchange of histone variant H2AX regulated by phosphorylation of H2AX and ADP-ribosylation of Spt16. Mol. Cell 30, 86–97.
Hergeth, S.P., and Schneider, R. (2015). The H1 linker histones: multifunctional proteins beyond the nucleosomal core particle. EMBO Rep. 16, 1439–1453.

Heun, P., Laroche, T., Shimada, K., Furrer, P., and Gasser, S.M. (2001). Chromosome dynamics in the yeast interphase nucleus. Science 294, 2181–2186.
Heyer, W.-D., Ehmsen, K.T., and Liu, J. (2010). Regulation of homologous recombination in eukaryotes. Annu. Rev. Genet. 44, 113–139.
Hinde, E., Kong, X., Yokomori, K., and Gratton, E. (2014). Chromatin dynamics during DNA repair revealed by pair correlation analysis of molecular flow in the nucleus. Biophys. J. 107, 55–65.
Höfling, F., Franosch, T., and Frey, E. (2006). Localization transition of the three-dimensional lorentz model and continuum percolation. Phys. Rev. Lett. 96, 165901.
Hota, S.K., and Bartholomew, B. (2011). Diversity of operation in ATP-dependent chromatin remodelers. Biochim. Biophys. Acta 1809, 476–487.
Hottiger, M.O. (2011). ADP-ribosylation of histones by ARTD1: an additional module of the histone code? FEBS Lett. 585, 1595–1599.
Hottiger, M.O., Hassa, P.O., Lüscher, B., Schüler, H., and Koch-Nolte, F. (2010). Toward a unified nomenclature for mammalian ADP-ribosyltransferases. Trends Biochem. Sci. 35, 208–219.
Hu, Y., Kireev, I., Plutz, M., Ashourian, N., and Belmont, A.S. (2009). Large-scale chromatin structure of inducible genes: transcription on a condensed, linear template. J. Cell Biol. 185, 87–100.
Huen, M.S.Y., Grant, R., Manke, I., Minn, K., Yu, X., Yaffe, M.B., and Chen, J. (2007). RNF8 transduces the DNA-damage signal via histone ubiquitylation and checkpoint protein assembly. Cell 131, 901–914.
Huet, S., Lavelle, C., Ranchon, H., Carrivain, P., Victor, J.-M., and Bancaud, A. (2014). Relevance and limitations of crowding, fractal, and polymer models to describe nuclear architecture. Int Rev Cell Mol Biol 307, 443–479.
Hutchinson, J.B., Cheema, M.S., Wang, J., Missiaen, K., Finn, R., Gonzalez Romero, R., Th'ng, J.P.H., Hendzel, M., and Ausió, J. (2015). Interaction of chromatin with a histone H1 containing swapped N- and C-terminal domains. Biosci. Rep. 35.
Hyman, A.A., Weber, C.A., and Jülicher, F. (2014). Liquid-liquid phase separation in biology. Annu. Rev. Cell Dev. Biol. 30, 39–58.
Ikura, M., Furuya, K., Fukuto, A., Matsuda, R., Adachi, J., Matsuda, T., Kakizuka, A., and Ikura, T. (2016). Coordinated Regulation of TIP60 and Poly(ADP-Ribose) Polymerase 1 in Damaged-Chromatin Dynamics. Mol. Cell. Biol. 36, 1595–1607.
Isogai, S., Kanno, S.-I., Ariyoshi, M., Tochio, H., Ito, Y., Yasui, A., and Shirakawa, M. (2010). Solution structure of a zinc-finger domain that binds to poly-ADP-ribose. Genes Cells 15, 101–110.
Iyengar, S., and Farnham, P.J. (2011). KAP1 protein: an enigmatic master regulator of the genome. J. Biol. Chem. 286, 26267–26276.
Iyer, L.M., Abhiman, S., and Aravind, L. (2011). Natural history of eukaryotic DNA methylation systems. Prog Mol Biol Transl Sci 101, 25–104.
Izhar, L., Adamson, B., Ciccia, A., Lewis, J., Pontano-Vaites, L., Leng, Y., Liang, A.C., Westbrook, T.F., Harper, J.W., and Elledge, S.J. (2015). A Systematic Analysis of Factors Localized to Damaged Chromatin Reveals PARP-Dependent Recruitment of Transcription Factors. Cell Rep 11, 1486–1500.
Izzo, A., and Schneider, R. (2016). The role of linker histone H1 modifications in the regulation of gene expression and chromatin dynamics. Biochim. Biophys. Acta 1859, 486–495.
Izzo, A., Kamieniarz, K., and Schneider, R. (2008). The histone H1 family: specific members, specific functions? Biol. Chem. 389, 333–343.
Jakob, B., Splinter, J., Durante, M., and Taucher-Scholz, G. (2009). Live cell microscopy analysis of radiation-induced DNA double-strand break motion. Proc. Natl. Acad. Sci. U.S.A. 106, 3172–3177.
Jakob, B., Splinter, J., Conrad, S., Voss, K.-O., Zink, D., Durante, M., Löbrich, M., and Taucher-Scholz, G. (2011). DNA double-strand breaks in heterochromatin elicit fast repair protein recruitment, histone H2AX phosphorylation and relocation to euchromatin. Nucleic Acids Res. 39, 6489–6499.
Jenuwein, T., and Allis, C.D. (2001). Translating the histone code. Science 293, 1074–1080.
Ježková, L., Falk, M., Falková, I., Davídková, M., Bačíková, A., Štefančíková, L., Vachelová, J., Michaelidesová, A., Lukášová, E., Boreyko, A., *et al.* (2014). Function of chromatin structure and

dynamics in DNA damage, repair and misrepair: γ-rays and protons in action. Appl Radiat Isot 83 Pt B, 128–136.
Jiang, X., Xu, Y., and Price, B.D. (2010). Acetylation of H2AX on lysine 36 plays a key role in the DNA double-strand break repair pathway. FEBS Lett. 584, 2926–2930.
Jin, F., Li, Y., Dixon, J.R., Selvaraj, S., Ye, Z., Lee, A.Y., Yen, C.-A., Schmitt, A.D., Espinoza, C.A., and Ren, B. (2013). A high-resolution map of the three-dimensional chromatin interactome in human cells. Nature 503, 290–294.
Jones, P.A., and Baylin, S.B. (2007). The epigenomics of cancer. Cell 128, 683–692.
Joti, Y., Hikima, T., Nishino, Y., Kamada, F., Hihara, S., Takata, H., Ishikawa, T., and Maeshima, K. (2012). Chromosomes without a 30-nm chromatin fiber. Nucleus 3, 404–410.
Kafer, G.R., Li, X., Horii, T., Suetake, I., Tajima, S., Hatada, I., and Carlton, P.M. (2016). 5-Hydroxymethylcytosine Marks Sites of DNA Damage and Promotes Genome Stability. Cell Rep 14, 1283–1292.
Kalocsay, M., Hiller, N.J., and Jentsch, S. (2009). Chromosome-wide Rad51 spreading and SUMO-H2A.Z-dependent chromosome fixation in response to a persistent DNA double-strand break. Mol. Cell 33, 335–343.
Kamieniarz, K., Izzo, A., Dundr, M., Tropberger, P., Ozretic, L., Kirfel, J., Scheer, E., Tropel, P., Wisniewski, J.R., Tora, L., *et al.* (2012). A dual role of linker histone H1.4 Lys 34 acetylation in transcriptional activation. Genes Dev. 26, 797–802.
Kassner, I., Andersson, A., Fey, M., Tomas, M., Ferrando-May, E., and Hottiger, M.O. (2013). SET7/9-dependent methylation of ARTD1 at K508 stimulates poly-ADP-ribose formation after oxidative stress. Open Biol 3, 120173.
Kaufmann, S., Fuchs, C., Gonik, M., Khrameeva, E.E., Mironov, A.A., and Frishman, D. (2015). Inter-chromosomal contact networks provide insights into Mammalian chromatin organization. PLoS ONE 10, e0126125.
Khanna, N., Hu, Y., and Belmont, A.S. (2014). HSP70 transgene directed motion to nuclear speckles facilitates heat shock activation. Curr. Biol. 24, 1138–1144.
Khurana, S., Kruhlak, M.J., Kim, J., Tran, A.D., Liu, J., Nyswaner, K., Shi, L., Jailwala, P., Sung, M.-H., Hakim, O., *et al.* (2014). A macrohistone variant links dynamic chromatin compaction to BRCA1-dependent genome maintenance. Cell Rep 8, 1049–1062.
Kim, M.Y., Mauro, S., Gévry, N., Lis, J.T., and Kraus, W.L. (2004). NAD+-dependent modulation of chromatin structure and transcription by nucleosome binding properties of PARP-1. Cell 119, 803–814.
Kizilyaprak, C., Spehner, D., Devys, D., and Schultz, P. (2011). The linker histone H1C contributes to the SCA7 nuclear phenotype. Nucleus 2, 444–454.
Kleine, H., Poreba, E., Lesniewicz, K., Hassa, P.O., Hottiger, M.O., Litchfield, D.W., Shilton, B.H., and Lüscher, B. (2008). Substrate-assisted catalysis by PARP10 limits its activity to mono-ADP-ribosylation. Mol. Cell 32, 57–69.
Koh, D.W., Lawler, A.M., Poitras, M.F., Sasaki, M., Wattler, S., Nehls, M.C., Stöger, T., Poirier, G.G., Dawson, V.L., and Dawson, T.M. (2004). Failure to degrade poly(ADP-ribose) causes increased sensitivity to cytotoxicity and early embryonic lethality. Proc. Natl. Acad. Sci. U.S.A. 101, 17699–17704.
van Koningsbruggen, S., Gierlinski, M., Schofield, P., Martin, D., Barton, G.J., Ariyurek, Y., den Dunnen, J.T., and Lamond, A.I. (2010). High-resolution whole-genome sequencing reveals that specific chromatin domains from most human chromosomes associate with nucleoli. Mol. Biol. Cell 21, 3735–3748.
Kornberg, R.D. (1974). Chromatin structure: a repeating unit of histones and DNA. Science 184, 868–871.
Koschmann, C., Nunez, F.J., Mendez, F., Brosnan-Cashman, J.A., Meeker, A.K., Lowenstein, P.R., and Castro, M.G. (2017). Mutated Chromatin Regulatory Factors as Tumor Drivers in Cancer. Cancer Res. 77, 227–233.
Kouzarides, T. (2007). Chromatin modifications and their function. Cell 128, 693–705.
Krasikova, Y.S., Rechkunova, N.I., Maltseva, E.A., Petruseva, I.O., and Lavrik, O.I. (2010). Localization of xeroderma pigmentosum group A protein and replication protein A on damaged DNA in nucleotide excision repair. Nucleic Acids Res. 38, 8083–8094.

Krawczyk, P.M., Borovski, T., Stap, J., Cijsouw, T., ten Cate, R., Medema, J.P., Kanaar, R., Franken, N. a. P., and Aten, J.A. (2012). Chromatin mobility is increased at sites of DNA double-strand breaks. J. Cell. Sci. 125, 2127–2133.

Krishnakumar, R., Gamble, M.J., Frizzell, K.M., Berrocal, J.G., Kininis, M., and Kraus, W.L. (2008). Reciprocal binding of PARP-1 and histone H1 at promoters specifies transcriptional outcomes. Science 319, 819–821.

Kruhlak, M.J., Celeste, A., Dellaire, G., Fernandez-Capetillo, O., Müller, W.G., McNally, J.G., Bazett-Jones, D.P., and Nussenzweig, A. (2006). Changes in chromatin structure and mobility in living cells at sites of DNA double-strand breaks. J. Cell Biol. 172, 823–834.

Kulms, D., and Schwarz, T. (2000). Molecular mechanisms of UV-induced apoptosis. Photodermatol Photoimmunol Photomed 16, 195–201.

Kysela, B., Chovanec, M., and Jeggo, P.A. (2005). Phosphorylation of linker histones by DNA-dependent protein kinase is required for DNA ligase IV-dependent ligation in the presence of histone H1. Proc. Natl. Acad. Sci. U.S.A. 102, 1877–1882.

La Ferla, M., Mercatanti, A., Rocchi, G., Lodovichi, S., Cervelli, T., Pignata, L., Caligo, M.A., and Galli, A. (2015). Expression of human poly (ADP-ribose) polymerase 1 in Saccharomyces cerevisiae: Effect on survival, homologous recombination and identification of genes involved in intracellular localization. Mutat. Res. 774, 14–24.

Lachner, M., and Jenuwein, T. (2002). The many faces of histone lysine methylation. Curr. Opin. Cell Biol. 14, 286–298.

Lachner, M., O'Carroll, D., Rea, S., Mechtler, K., and Jenuwein, T. (2001). Methylation of histone H3 lysine 9 creates a binding site for HP1 proteins. Nature 410, 116–120.

Langelier, M.-F., Planck, J.L., Roy, S., and Pascal, J.M. (2012). Structural basis for DNA damage-dependent poly(ADP-ribosyl)ation by human PARP-1. Science 336, 728–732.

Langelier, M.-F., Riccio, A.A., and Pascal, J.M. (2014). PARP-2 and PARP-3 are selectively activated by 5' phosphorylated DNA breaks through an allosteric regulatory mechanism shared with PARP-1. Nucleic Acids Res. 42, 7762–7775.

Längst, G., and Manelyte, L. (2015). Chromatin Remodelers: From Function to Dysfunction. Genes (Basel) 6, 299–324.

Laurent, T.C. (1963). THE INTERACTION BETWEEN POLYSACCHARIDES AND OTHER MACROMOLECULES. 5. THE SOLUBILITY OF PROTEINS IN THE PRESENCE OF DEXTRAN. Biochem. J. 89, 253–257.

Lesne, A., Riposo, J., Roger, P., Cournac, A., and Mozziconacci, J. (2014). 3D genome reconstruction from chromosomal contacts. Nat. Methods 11, 1141–1143.

Levi, V., Ruan, Q., Plutz, M., Belmont, A.S., and Gratton, E. (2005). Chromatin dynamics in interphase cells revealed by tracking in a two-photon excitation microscope. Biophys. J. 89, 4275–4285.

Li, M., and Yu, X. (2013). Function of BRCA1 in the DNA damage response is mediated by ADP-ribosylation. Cancer Cell 23, 693–704.

Li, A., Yu, Y., Lee, S.-C., Ishibashi, T., Lees-Miller, S.P., and Ausió, J. (2010). Phosphorylation of histone H2A.X by DNA-dependent protein kinase is not affected by core histone acetylation, but it alters nucleosome stability and histone H1 binding. J. Biol. Chem. 285, 17778–17788.

Li, Q., Barkess, G., and Qian, H. (2006). Chromatin looping and the probability of transcription. Trends Genet. 22, 197–202.

Li, Y., Huang, W., Niu, L., Umbach, D.M., Covo, S., and Li, L. (2013). Characterization of constitutive CTCF/cohesin loci: a possible role in establishing topological domains in mammalian genomes. BMC Genomics 14, 553.

Li, Z., Gadue, P., Chen, K., Jiao, Y., Tuteja, G., Schug, J., Li, W., and Kaestner, K.H. (2012). Foxa2 and H2A.Z mediate nucleosome depletion during embryonic stem cell differentiation. Cell 151, 1608–1616.

Liang, Y., and Hetzer, M.W. (2011). Functional interactions between nucleoporins and chromatin. Curr. Opin. Cell Biol. 23, 65–70.

Lieber, M.R. (2010). The mechanism of double-strand DNA break repair by the nonhomologous DNA end-joining pathway. Annu. Rev. Biochem. 79, 181–211.
Lieberman-Aiden, E., van Berkum, N.L., Williams, L., Imakaev, M., Ragoczy, T., Telling, A., Amit, I., Lajoie, B.R., Sabo, P.J., Dorschner, M.O., *et al.* (2009). Comprehensive mapping of long-range interactions reveals folding principles of the human genome. Science 326, 289–293.
Lisby, M., Mortensen, U.H., and Rothstein, R. (2003). Colocalization of multiple DNA double-strand breaks at a single Rad52 repair centre. Nat. Cell Biol. 5, 572–577.
Llères, D., James, J., Swift, S., Norman, D.G., and Lamond, A.I. (2009). Quantitative analysis of chromatin compaction in living cells using FLIM-FRET. J. Cell Biol. 187, 481–496.
Lone, I.N., Shukla, M.S., Charles Richard, J.L., Peshev, Z.Y., Dimitrov, S., and Angelov, D. (2013). Binding of NF-κB to nucleosomes: effect of translational positioning, nucleosome remodeling and linker histone H1. PLoS Genet. 9, e1003830.
López-Velázquez, G., Márquez, J., Ubaldo, E., Corkidi, G., Echeverría, O., and Vázquez Nin, G.H. (1996). Three-dimensional analysis of the arrangement of compact chromatin in the nucleus of G0 rat lymphocytes. Histochem. Cell Biol. 105, 153–161.
Lottersberger, F., Karssemeijer, R.A., Dimitrova, N., and de Lange, T. (2015). 53BP1 and the LINC Complex Promote Microtubule-Dependent DSB Mobility and DNA Repair. Cell 163, 880–893.
Lou, Z., Minter-Dykhouse, K., Franco, S., Gostissa, M., Rivera, M.A., Celeste, A., Manis, J.P., van Deursen, J., Nussenzweig, A., Paull, T.T., *et al.* (2006). MDC1 maintains genomic stability by participating in the amplification of ATM-dependent DNA damage signals. Mol. Cell 21, 187–200.
Luger, K., Mäder, A.W., Richmond, R.K., Sargent, D.F., and Richmond, T.J. (1997). Crystal structure of the nucleosome core particle at 2.8 A resolution. Nature 389, 251–260.
Luijsterburg, M.S., de Krijger, I., Wiegant, W.W., Shah, R.G., Smeenk, G., de Groot, A.J.L., Pines, A., Vertegaal, A.C.O., Jacobs, J.J.L., Shah, G.M., *et al.* (2016). PARP1 Links CHD2-Mediated Chromatin Expansion and H3.3 Deposition to DNA Repair by Non-homologous End-Joining. Mol. Cell 61, 547–562.
Luk, E., Ranjan, A., Fitzgerald, P.C., Mizuguchi, G., Huang, Y., Wei, D., and Wu, C. (2010). Stepwise histone replacement by SWR1 requires dual activation with histone H2A.Z and canonical nucleosome. Cell 143, 725–736.
Lukas, C., Melander, F., Stucki, M., Falck, J., Bekker-Jensen, S., Goldberg, M., Lerenthal, Y., Jackson, S.P., Bartek, J., and Lukas, J. (2004). Mdc1 couples DNA double-strand break recognition by Nbs1 with its H2AX-dependent chromatin retention. EMBO J. 23, 2674–2683.
Ma, C.J., Gibb, B., Kwon, Y., Sung, P., and Greene, E.C. (2017). Protein dynamics of human RPA and RAD51 on ssDNA during assembly and disassembly of the RAD51 filament. Nucleic Acids Res. 45, 749–761.
Ma, Y., Lu, H., Tippin, B., Goodman, M.F., Shimazaki, N., Koiwai, O., Hsieh, C.-L., Schwarz, K., and Lieber, M.R. (2004). A biochemically defined system for mammalian nonhomologous DNA end joining. Mol. Cell 16, 701–713.
Maeshima, K., Hihara, S., and Eltsov, M. (2010). Chromatin structure: does the 30-nm fibre exist *in vivo*? Curr. Opin. Cell Biol. 22, 291–297.
Maeshima, K., Imai, R., Tamura, S., and Nozaki, T. (2014a). Chromatin as dynamic 10-nm fibers. Chromosoma 123, 225–237.
Maeshima, K., Imai, R., Hikima, T., and Joti, Y. (2014b). Chromatin structure revealed by X-ray scattering analysis and computational modeling. Methods 70, 154–161.
Maeshima, K., Ide, S., Hibino, K., and Sasai, M. (2016). Liquid-like behavior of chromatin. Curr. Opin. Genet. Dev. 37, 36–45.
Mahaney, B.L., Meek, K., and Lees-Miller, S.P. (2009). Repair of ionizing radiation-induced DNA double-strand breaks by non-homologous end-joining. Biochem. J. 417, 639–650.
Maier, V.K., Chioda, M., Rhodes, D., and Becker, P.B. (2008). ACF catalyses chromatosome movements in chromatin fibres. EMBO J. 27, 817–826.
Malanga, M., Atorino, L., Tramontano, F., Farina, B., and Quesada, P. (1998). Poly(ADP-ribose) binding properties of histone H1 variants. Biochim. Biophys. Acta 1399, 154–160.

Maréchal, A., and Zou, L. (2013). DNA Damage Sensing by the ATM and ATR Kinases. Cold Spring Harb Perspect Biol 5.
Marfella, C.G.A., and Imbalzano, A.N. (2007). The Chd family of chromatin remodelers. Mutat. Res. 618, 30–40.
Marion, C., Roche, J., Roux, B., and Gorka, C. (1985). Differences in the condensation of chromatin by individual subfractions of histone H1: implications for the role of H1(0) in the structural organization of chromatin. Biochemistry 24, 6328–6335.
Marshall, W.F., Straight, A., Marko, J.F., Swedlow, J., Dernburg, A., Belmont, A., Murray, A.W., Agard, D.A., and Sedat, J.W. (1997). Interphase chromosomes undergo constrained diffusional motion in living cells. Curr. Biol. 7, 930–939.
Martin, R.M., and Cardoso, M.C. (2010). Chromatin condensation modulates access and binding of nuclear proteins. FASEB J. 24, 1066–1072.
Marzluff, W.F., Gongidi, P., Woods, K.R., Jin, J., and Maltais, L.J. (2002). The human and mouse replication-dependent histone genes. Genomics 80, 487–498.
Mathis, G., and Althaus, F.R. (1987). Release of core DNA from nucleosomal core particles following (ADP-ribose)n-modification *in vitro*. Biochem. Biophys. Res. Commun. 143, 1049–1054.
Mazumder, A., Roopa, T., Kumar, A., Iyer, K.V., Ramdas, N.M., and Shivashankar, G.V. (2010). Prestressed nuclear organization in living cells. Methods Cell Biol. 98, 221–239.
McDowall, A.W., Smith, J.M., and Dubochet, J. (1986). Cryo-electron microscopy of vitrified chromosomes in situ. EMBO J. 5, 1395–1402.
Mearini, G., and Fackelmayer, F.O. (2006). Local chromatin mobility is independent of transcriptional activity. Cell Cycle 5, 1989–1995.
Meas, R., and Mao, P. (2015). Histone ubiquitylation and its roles in transcription and DNA damage response. DNA Repair (Amst.) 36, 36–42.
Meijer, M., and Smerdon, M.J. (1999). Accessing DNA damage in chromatin: insights from transcription. Bioessays 21, 596–603.
Meister, P., Poidevin, M., Francesconi, S., Tratner, I., Zarzov, P., and Baldacci, G. (2003). Nuclear factories for signalling and repairing DNA double strand breaks in living fission yeast. Nucleic Acids Res. 31, 5064–5073.
Messner, S., Altmeyer, M., Zhao, H., Pozivil, A., Roschitzki, B., Gehrig, P., Rutishauser, D., Huang, D., Caflisch, A., and Hottiger, M.O. (2010). PARP1 ADP-ribosylates lysine residues of the core histone tails. Nucleic Acids Res. 38, 6350–6362.
Meyer, B., Bénichou, O., Kafri, Y., and Voituriez, R. (2012). Geometry-induced bursting dynamics in gene expression. Biophys. J. 102, 2186–2191.
Mills, K.D., Ferguson, D.O., and Alt, F.W. (2003). The role of DNA breaks in genomic instability and tumorigenesis. Immunol. Rev. 194, 77–95.
Mimitou, E.P., and Symington, L.S. (2009). Nucleases and helicases take center stage in homologous recombination. Trends Biochem. Sci. 34, 264–272.
Min, W., Bruhn, C., Grigaravicius, P., Zhou, Z.-W., Li, F., Krüger, A., Siddeek, B., Greulich, K.-O., Popp, O., Meisezahl, C., *et al.* (2013). Poly(ADP-ribose) binding to Chk1 at stalled replication forks is required for S-phase checkpoint activation. Nat Commun 4, 2993.
Miné-Hattab, J., and Rothstein, R. (2012). Increased chromosome mobility facilitates homology search during recombination. Nat. Cell Biol. 14, 510–517.
Minton, A.P. (1997). Influence of excluded volume upon macromolecular structure and associations in "crowded" media. Curr. Opin. Biotechnol. 8, 65–69.
Minton, A.P. (1998). Molecular crowding: analysis of effects of high concentrations of inert cosolutes on biochemical equilibria and rates in terms of volume exclusion. Meth. Enzymol. 295, 127–149.
Minton, A.P. (2006). How can biochemical reactions within cells differ from those in test tubes? J. Cell. Sci. 119, 2863–2869.
Misteli, T., Gunjan, A., Hock, R., Bustin, M., and Brown, D.T. (2000). Dynamic binding of histone H1 to chromatin in living cells. Nature 408, 877–881.

Mitchell, D.L., Nguyen, T.D., and Cleaver, J.E. (1990). Nonrandom induction of pyrimidine-pyrimidone (6-4) photoproducts in ultraviolet-irradiated human chromatin. J. Biol. Chem. 265, 5353–5356.
Miwa, M., Saikawa, N., Yamaizumi, Z., Nishimura, S., and Sugimura, T. (1979). Structure of poly(adenosine diphosphate ribose): identification of 2'-[1''-ribosyl-2''-(or 3''-)(1'''-ribosyl)]adenosine-5',5'',5'''-tris(phosphate) as a branch linkage. Proc. Natl. Acad. Sci. U.S.A. 76, 595–599.
Mohammad, D.H., and Yaffe, M.B. (2009). 14-3-3 proteins, FHA domains and BRCT domains in the DNA damage response. DNA Repair (Amst.) 8, 1009–1017.
Mohrmann, L., and Verrijzer, C.P. (2005). Composition and functional specificity of SWI2/SNF2 class chromatin remodeling complexes. Biochim. Biophys. Acta 1681, 59–73.
Mourão, M.A., Hakim, J.B., and Schnell, S. (2014). Connecting the dots: the effects of macromolecular crowding on cell physiology. Biophys. J. 107, 2761–2766.
Muramatsu, N., and Minton, A.P. (1988). Tracer diffusion of globular proteins in concentrated protein solutions. Proc. Natl. Acad. Sci. U.S.A. 85, 2984–2988.
Murr, R., Loizou, J.I., Yang, Y.-G., Cuenin, C., Li, H., Wang, Z.-Q., and Herceg, Z. (2006). Histone acetylation by Trrap-Tip60 modulates loading of repair proteins and repair of DNA double-strand breaks. Nat. Cell Biol. 8, 91–99.
Muthurajan, U.M., Hepler, M.R.D., Hieb, A.R., Clark, N.J., Kramer, M., Yao, T., and Luger, K. (2014). Automodification switches PARP-1 function from chromatin architectural protein to histone chaperone. Proc. Natl. Acad. Sci. U.S.A. 111, 12752–12757.
Nagai, S., Dubrana, K., Tsai-Pflugfelder, M., Davidson, M.B., Roberts, T.M., Brown, G.W., Varela, E., Hediger, F., Gasser, S.M., and Krogan, N.J. (2008). Functional targeting of DNA damage to a nuclear pore-associated SUMO-dependent ubiquitin ligase. Science 322, 597–602.
Nalabothula, N., McVicker, G., Maiorano, J., Martin, R., Pritchard, J.K., and Fondufe-Mittendorf, Y.N. (2014). The chromatin architectural proteins HMGD1 and H1 bind reciprocally and have opposite effects on chromatin structure and gene regulation. BMC Genomics 15, 92.
Nelms, B.E., Maser, R.S., MacKay, J.F., Lagally, M.G., and Petrini, J.H. (1998). In situ visualization of DNA double-strand break repair in human fibroblasts. Science 280, 590–592.
Németh, A., Conesa, A., Santoyo-Lopez, J., Medina, I., Montaner, D., Péterfia, B., Solovei, I., Cremer, T., Dopazo, J., and Längst, G. (2010). Initial genomics of the human nucleolus. PLoS Genet. 6, e1000889.
Neumann, F.R., Dion, V., Gehlen, L.R., Tsai-Pflugfelder, M., Schmid, R., Taddei, A., and Gasser, S.M. (2012). Targeted INO80 enhances subnuclear chromatin movement and ectopic homologous recombination. Genes Dev. 26, 369–383.
Nick McElhinny, S.A., Snowden, C.M., McCarville, J., and Ramsden, D.A. (2000). Ku recruits the XRCC4-ligase IV complex to DNA ends. Mol. Cell. Biol. 20, 2996–3003.
Nie, Y., Cheng, X., Chen, J., and Sun, X. (2014). Nucleosome organization in the vicinity of transcription factor binding sites in the human genome. BMC Genomics 15, 493.
Nobrega, M.A., Ovcharenko, I., Afzal, V., and Rubin, E.M. (2003). Scanning human gene deserts for long-range enhancers. Science 302, 413.
Nora, E.P., Lajoie, B.R., Schulz, E.G., Giorgetti, L., Okamoto, I., Servant, N., Piolot, T., van Berkum, N.L., Meisig, J., Sedat, J., *et al.* (2012). Spatial partitioning of the regulatory landscape of the X-inactivation centre. Nature 485, 381–385.
Normanno, D., Boudarène, L., Dugast-Darzacq, C., Chen, J., Richter, C., Proux, F., Bénichou, O., Voituriez, R., Darzacq, X., and Dahan, M. (2015). Probing the target search of DNA-binding proteins in mammalian cells using TetR as model searcher. Nat Commun 6, 7357.
Nott, T.J., Petsalaki, E., Farber, P., Jervis, D., Fussner, E., Plochowietz, A., Craggs, T.D., Bazett-Jones, D.P., Pawson, T., Forman-Kay, J.D., *et al.* (2015). Phase transition of a disordered nuage protein generates environmentally responsive membraneless organelles. Mol. Cell 57, 936–947.
Öberg, C., Izzo, A., Schneider, R., Wrange, Ö., and Belikov, S. (2012). Linker histone subtypes differ in their effect on nucleosomal spacing *in vivo*. J. Mol. Biol. 419, 183–197.

Oberoi, J., Richards, M.W., Crumpler, S., Brown, N., Blagg, J., and Bayliss, R. (2010). Structural basis of poly(ADP-ribose) recognition by the multizinc binding domain of checkpoint with forkhead-associated and RING Domains (CHFR). J. Biol. Chem. 285, 39348–39358.

Ogata, N., Ueda, K., Kawaichi, M., and Hayaishi, O. (1981). Poly(ADP-ribose) synthetase, a main acceptor of poly(ADP-ribose) in isolated nuclei. J. Biol. Chem. 256, 4135–4137.

Ogiwara, H., Ui, A., Otsuka, A., Satoh, H., Yokomi, I., Nakajima, S., Yasui, A., Yokota, J., and Kohno, T. (2011). Histone acetylation by CBP and p300 at double-strand break sites facilitates SWI/SNF chromatin remodeling and the recruitment of non-homologous end joining factors. Oncogene 30, 2135–2146.

Oka, S., Kato, J., and Moss, J. (2006). Identification and characterization of a mammalian 39-kDa poly(ADP-ribose) glycohydrolase. J. Biol. Chem. 281, 705–713.

O'Sullivan Coyne, G., Chen, A., and Kummar, S. (2015). Delivering on the promise: poly ADP ribose polymerase inhibition as targeted anticancer therapy. Curr Opin Oncol 27, 475–481.

Pacchierotti, F., and Spanò, M. (2015). Environmental Impact on DNA Methylation in the Germline: State of the Art and Gaps of Knowledge. Biomed Res Int 2015.

Pack, C., Saito, K., Tamura, M., and Kinjo, M. (2006). Microenvironment and effect of energy depletion in the nucleus analyzed by mobility of multiple oligomeric EGFPs. Biophys. J. 91, 3921–3936.

Panier, S., and Boulton, S.J. (2014). Double-strand break repair: 53BP1 comes into focus. Nat. Rev. Mol. Cell Biol. 15, 7–18.

Parseghian, M.H., and Hamkalo, B.A. (2001). A compendium of the histone H1 family of somatic subtypes: an elusive cast of characters and their characteristics. Biochem. Cell Biol. 79, 289–304.

Peric-Hupkes, D., Meuleman, W., Pagie, L., Bruggeman, S.W.M., Solovei, I., Brugman, W., Gräf, S., Flicek, P., Kerkhoven, R.M., van Lohuizen, M., *et al.* (2010). Molecular maps of the reorganization of genome-nuclear lamina interactions during differentiation. Mol. Cell 38, 603–613.

Peters, A.H.F.M., Mermoud, J.E., O'Carroll, D., Pagani, M., Schweizer, D., Brockdorff, N., and Jenuwein, T. (2002). Histone H3 lysine 9 methylation is an epigenetic imprint of facultative heterochromatin. Nat. Genet. 30, 77–80.

Phair, R.D., Scaffidi, P., Elbi, C., Vecerová, J., Dey, A., Ozato, K., Brown, D.T., Hager, G., Bustin, M., and Misteli, T. (2004). Global nature of dynamic protein-chromatin interactions *in vivo*: three-dimensional genome scanning and dynamic interaction networks of chromatin proteins. Mol. Cell. Biol. 24, 6393–6402.

Phillies, G.D.J. (1985). Diffusion of bovine serum albumin in a neutral polymer solution. Biopolymers 24, 379–386.

Phillips, J.E., and Corces, V.G. (2009). CTCF: master weaver of the genome. Cell 137, 1194–1211.

Phillips-Cremins, J.E., Sauria, M.E.G., Sanyal, A., Gerasimova, T.I., Lajoie, B.R., Bell, J.S.K., Ong, C.-T., Hookway, T.A., Guo, C., Sun, Y., *et al.* (2013). Architectural protein subclasses shape 3D organization of genomes during lineage commitment. Cell 153, 1281–1295.

Platani, M., Goldberg, I., Lamond, A.I., and Swedlow, J.R. (2002). Cajal body dynamics and association with chromatin are ATP-dependent. Nat. Cell Biol. 4, 502–508.

Pleschke, J.M., Kleczkowska, H.E., Strohm, M., and Althaus, F.R. (2000). Poly(ADP-ribose) binds to specific domains in DNA damage checkpoint proteins. J. Biol. Chem. 275, 40974–40980.

Pliss, A., Malyavantham, K., Bhattacharya, S., Zeitz, M., and Berezney, R. (2009). Chromatin dynamics is correlated with replication timing. Chromosoma 118, 459–470.

Pliss, A., Malyavantham, K.S., Bhattacharya, S., and Berezney, R. (2013). Chromatin dynamics in living cells: identification of oscillatory motion. J. Cell. Physiol. 228, 609–616.

Poirier, G.G., de Murcia, G., Jongstra-Bilen, J., Niedergang, C., and Mandel, P. (1982). Poly(ADP-ribosyl)ation of polynucleosomes causes relaxation of chromatin structure. Proc. Natl. Acad. Sci. U.S.A. 79, 3423–3427.

Polo, S.E., Kaidi, A., Baskcomb, L., Galanty, Y., and Jackson, S.P. (2010). Regulation of DNA-damage responses and cell-cycle progression by the chromatin remodelling factor CHD4. EMBO J. 29, 3130–3139.

Price, B.D., and D'Andrea, A.D. (2013). Chromatin remodeling at DNA double-strand breaks. Cell 152, 1344–1354.

Prioleau, M.-N., and MacAlpine, D.M. (2016). DNA replication origins-where do we begin? Genes Dev. 30, 1683–1697.

Pruss, D., Bartholomew, B., Persinger, J., Hayes, J., Arents, G., Moudrianakis, E.N., and Wolffe, A.P. (1996). An asymmetric model for the nucleosome: a binding site for linker histones inside the DNA gyres. Science 274, 614–617.

Qiu, H., Chereji, R.V., Hu, C., Cole, H.A., Rawal, Y., Clark, D.J., and Hinnebusch, A.G. (2016). Genome-wide cooperation by HAT Gcn5, remodeler SWI/SNF, and chaperone Ydj1 in promoter nucleosome eviction and transcriptional activation. Genome Res. 26, 211–225.

Ramachandran, A., Omar, M., Cheslock, P., and Schnitzler, G.R. (2003). Linker histone H1 modulates nucleosome remodeling by human SWI/SNF. J. Biol. Chem. 278, 48590–48601.

Rank, L., Veith, S., Gwosch, E.C., Demgenski, J., Ganz, M., Jongmans, M.C., Vogel, C., Fischbach, A., Buerger, S., Fischer, J.M.F., *et al.* (2016). Analyzing structure-function relationships of artificial and cancer-associated PARP1 variants by reconstituting TALEN-generated HeLa PARP1 knock-out cells. Nucleic Acids Res. 44, 10386–10405.

Rasmussen, T.P., Huang, T., Mastrangelo, M.A., Loring, J., Panning, B., and Jaenisch, R. (1999). Messenger RNAs encoding mouse histone macroH2A1 isoforms are expressed at similar levels in male and female cells and result from alternative splicing. Nucleic Acids Res. 27, 3685–3689.

Rea, S., Eisenhaber, F., O'Carroll, D., Strahl, B.D., Sun, Z.W., Schmid, M., Opravil, S., Mechtler, K., Ponting, C.P., Allis, C.D., *et al.* (2000). Regulation of chromatin structure by site-specific histone H3 methyltransferases. Nature 406, 593–599.

Ricci, M.A., Manzo, C., García-Parajo, M.F., Lakadamyali, M., and Cosma, M.P. (2015). Chromatin fibers are formed by heterogeneous groups of nucleosomes *in vivo*. Cell 160, 1145–1158.

Richmond, T.J., Finch, J.T., Rushton, B., Rhodes, D., and Klug, A. (1984). Structure of the nucleosome core particle at 7 A resolution. Nature 311, 532–537.

Richter, K., Nessling, M., and Lichter, P. (2008). Macromolecular crowding and its potential impact on nuclear function. Biochim. Biophys. Acta 1783, 2100–2107.

Riedmann, C., and Fondufe-Mittendorf, Y.N. (2016). Comparative analysis of linker histone H1, MeCP2, and HMGD1 on nucleosome stability and target site accessibility. Sci Rep 6, 33186.

Roadmap Epigenomics Consortium, Kundaje, A., Meuleman, W., Ernst, J., Bilenky, M., Yen, A., Heravi-Moussavi, A., Kheradpour, P., Zhang, Z., Wang, J., *et al.* (2015). Integrative analysis of 111 reference human epigenomes. Nature 518, 317–330.

Robinett, C.C., Straight, A., Li, G., Willhelm, C., Sudlow, G., Murray, A., and Belmont, A.S. (1996). *In vivo* localization of DNA sequences and visualization of large-scale chromatin organization using lac operator/repressor recognition. J. Cell Biol. 135, 1685–1700.

Robinson, P.J.J., and Rhodes, D. (2006). Structure of the "30 nm" chromatin fibre: a key role for the linker histone. Curr. Opin. Struct. Biol. 16, 336–343.

Robinson, P.J.J., Fairall, L., Huynh, V.A.T., and Rhodes, D. (2006). EM measurements define the dimensions of the "30-nm" chromatin fiber: evidence for a compact, interdigitated structure. Proc. Natl. Acad. Sci. U.S.A. 103, 6506–6511.

Rogakou, E.P., Boon, C., Redon, C., and Bonner, W.M. (1999). Megabase chromatin domains involved in DNA double-strand breaks *in vivo*. J. Cell Biol. 146, 905–916.

Rosenthal, F., Feijs, K.L.H., Frugier, E., Bonalli, M., Forst, A.H., Imhof, R., Winkler, H.C., Fischer, D., Caflisch, A., Hassa, P.O., *et al.* (2013). Macrodomain-containing proteins are new mono-ADP-ribosylhydrolases. Nat. Struct. Mol. Biol. 20, 502–507.

Roth, S.Y., and Allis, C.D. (1992). Chromatin condensation: does histone H1 dephosphorylation play a role? Trends Biochem. Sci. 17, 93–98.

Roukos, V., Voss, T.C., Schmidt, C.K., Lee, S., Wangsa, D., and Misteli, T. (2013). Spatial dynamics of chromosome translocations in living cells. Science 341, 660–664.

Rouleau, M., McDonald, D., Gagné, P., Ouellet, M.-E., Droit, A., Hunter, J.M., Dutertre, S., Prigent, C., Hendzel, M.J., and Poirier, G.G. (2007). PARP-3 associates with polycomb group bodies and with components of the DNA damage repair machinery. J. Cell. Biochem. 100, 385–401.

Rouquette, J., Genoud, C., Vazquez-Nin, G.H., Kraus, B., Cremer, T., and Fakan, S. (2009). Revealing the high-resolution three-dimensional network of chromatin and interchromatin space: a novel electron-microscopic approach to reconstructing nuclear architecture. Chromosome Res. 17, 801–810.

Ruf, A., Mennissier de Murcia, J., de Murcia, G., and Schulz, G.E. (1996). Structure of the catalytic fragment of poly(AD-ribose) polymerase from chicken. Proc. Natl. Acad. Sci. U.S.A. 93, 7481–7485.

Rulten, S.L., Fisher, A.E.O., Robert, I., Zuma, M.C., Rouleau, M., Ju, L., Poirier, G., Reina-San-Martin, B., and Caldecott, K.W. (2011). PARP-3 and APLF function together to accelerate nonhomologous end-joining. Mol. Cell 41, 33–45.

Runge, J.S., Raab, J.R., and Magnuson, T. (2016). Epigenetic Regulation by ATP-Dependent Chromatin-Remodeling Enzymes: SNF-ing Out Crosstalk. Curr. Top. Dev. Biol. 117, 1–13.

Saad, H., Gallardo, F., Dalvai, M., Tanguy-le-Gac, N., Lane, D., and Bystricky, K. (2014). DNA dynamics during early double-strand break processing revealed by non-intrusive imaging of living cells. PLoS Genet. 10, e1004187.

Sanyal, A., Lajoie, B.R., Jain, G., and Dekker, J. (2012). The long-range interaction landscape of gene promoters. Nature 489, 109–113.

Saxton, M.J. (2012). Wanted: a positive control for anomalous subdiffusion. Biophys. J. 103, 2411–2422.

Schärer, O.D. (2013). Nucleotide excision repair in eukaryotes. Cold Spring Harb Perspect Biol 5, a012609.

Schermelleh, L., Solovei, I., Zink, D., and Cremer, T. (2001). Two-color fluorescence labeling of early and mid-to-late replicating chromatin in living cells. Chromosome Res. 9, 77–80.

Schou, K.B., Schneider, L., Christensen, S.T., and Hoffmann, E.K. (2008). Early-stage apoptosis is associated with DNA-damage-independent ATM phosphorylation and chromatin decondensation in NIH3T3 fibroblasts. Cell Biol. Int. 32, 107–113.

Seeber, A., and Gasser, S.M. (2016). Chromatin organization and dynamics in double-strand break repair. Curr. Opin. Genet. Dev. 43, 9–16.

Seeber, A., Dion, V., and Gasser, S.M. (2013). Checkpoint kinases and the INO80 nucleosome remodeling complex enhance global chromatin mobility in response to DNA damage. Genes Dev. 27, 1999–2008.

Seksek, O., Biwersi, J., and Verkman, A.S. (1997). Translational diffusion of macromolecule-sized solutes in cytoplasm and nucleus. J. Cell Biol. 138, 131–142.

Sellou, H., Lebeaupin, T., Chapuis, C., Smith, R., Hegele, A., Singh, H.R., Kozlowski, M., Bultmann, S., Ladurner, A.G., Timinszky, G., *et al.* (2016). The poly(ADP-ribose)-dependent chromatin remodeler Alc1 induces local chromatin relaxation upon DNA damage. Mol. Biol. Cell 27, 3791–3799.

Sexton, T., and Cavalli, G. (2015). The role of chromosome domains in shaping the functional genome. Cell 160, 1049–1059.

Shan, L., Li, X., Liu, L., Ding, X., Wang, Q., Zheng, Y., Duan, Y., Xuan, C., Wang, Y., Yang, F., *et al.* (2014). GATA3 cooperates with PARP1 to regulate CCND1 transcription through modulating histone H1 incorporation. Oncogene 33, 3205–3216.

Sharifi, R., Morra, R., Appel, C.D., Tallis, M., Chioza, B., Jankevicius, G., Simpson, M.A., Matic, I., Ozkan, E., Golia, B., *et al.* (2013). Deficiency of terminal ADP-ribose protein glycohydrolase TARG1/C6orf130 in neurodegenerative disease. EMBO J. 32, 1225–1237.

Shen, Y., Yue, F., McCleary, D.F., Ye, Z., Edsall, L., Kuan, S., Wagner, U., Dixon, J., Lee, L., Lobanenkov, V.V., *et al.* (2012). A map of the cis-regulatory sequences in the mouse genome. Nature 488, 116–120.

Shi, L., and Oberdoerffer, P. (2012). Chromatin dynamics in DNA double-strand break repair. Biochim. Biophys. Acta 1819, 811–819.

Shimada, M., Niida, H., Zineldeen, D.H., Tagami, H., Tanaka, M., Saito, H., and Nakanishi, M. (2008). Chk1 is a histone H3 threonine 11 kinase that regulates DNA damage-induced transcriptional repression. Cell 132, 221–232.

Shivji, M.K., Podust, V.N., Hübscher, U., and Wood, R.D. (1995). Nucleotide excision repair DNA synthesis by DNA polymerase epsilon in the presence of PCNA, RFC, and RPA. Biochemistry 34, 5011–5017.

Simonis, M., Klous, P., Splinter, E., Moshkin, Y., Willemsen, R., de Wit, E., van Steensel, B., and de Laat, W. (2006). Nuclear organization of active and inactive chromatin domains uncovered by chromosome conformation capture-on-chip (4C). Nat. Genet. 38, 1348–1354.

Simonis, M., Kooren, J., and de Laat, W. (2007). An evaluation of 3C-based methods to capture DNA interactions. Nat. Methods 4, 895–901.

Simpson, R.T. (1978). Structure of the chromatosome, a chromatin particle containing 160 base pairs of DNA and all the histones. Biochemistry 17, 5524–5531.

Slade, D., Dunstan, M.S., Barkauskaite, E., Weston, R., Lafite, P., Dixon, N., Ahel, M., Leys, D., and Ahel, I. (2011). The structure and catalytic mechanism of a poly(ADP-ribose) glycohydrolase. Nature 477, 616–620.

Smeenk, G., Wiegant, W.W., Marteijn, J.A., Luijsterburg, M.S., Sroczynski, N., Costelloe, T., Romeijn, R.J., Pastink, A., Mailand, N., Vermeulen, W., *et al.* (2013). Poly(ADP-ribosyl)ation links the chromatin remodeler SMARCA5/SNF2H to RNF168-dependent DNA damage signaling. J. Cell. Sci. 126, 889–903.

Smerdon, M.J. (1991). DNA repair and the role of chromatin structure. Curr. Opin. Cell Biol. 3, 422–428.

Smerdon, M.J., and Lieberman, M.W. (1978). Nucleosome rearrangement in human chromatin during UV-induced DNA- reapir synthesis. Proc. Natl. Acad. Sci. U.S.A. 75, 4238–4241.

Smith, O.K., and Aladjem, M.I. (2014). Chromatin Structure and Replication Origins: Determinants Of Chromosome Replication And Nuclear Organization. J Mol Biol 426, 3330–3341.

Smith-Roe, S.L., Nakamura, J., Holley, D., Chastain, P.D., Rosson, G.B., Simpson, D.A., Ridpath, J.R., Kaufman, D.G., Kaufmann, W.K., and Bultman, S.J. (2015). SWI/SNF complexes are required for full activation of the DNA-damage response. Oncotarget 6, 732–745.

Sonoda, E., Hochegger, H., Saberi, A., Taniguchi, Y., and Takeda, S. (2006). Differential usage of non-homologous end-joining and homologous recombination in double strand break repair. DNA Repair (Amst.) 5, 1021–1029.

Soria, G., Polo, S.E., and Almouzni, G. (2012). Prime, repair, restore: the active role of chromatin in the DNA damage response. Mol. Cell 46, 722–734.

Soutoglou, E., and Misteli, T. (2007). Mobility and immobility of chromatin in transcription and genome stability. Curr. Opin. Genet. Dev. 17, 435–442.

Soutoglou, E., Dorn, J.F., Sengupta, K., Jasin, M., Nussenzweig, A., Ried, T., Danuser, G., and Misteli, T. (2007). Positional stability of single double-strand breaks in mammalian cells. Nat. Cell Biol. 9, 675–682.

Speicher, M.R., and Carter, N.P. (2005). The new cytogenetics: blurring the boundaries with molecular biology. Nat. Rev. Genet. 6, 782–792.

Staynov, D.Z. (2008). DNase I footprinting of the nucleosome in whole nuclei. Biochem. Biophys. Res. Commun. 372, 226–229.

van Steensel, B., and Dekker, J. (2010). Genomics tools for unraveling chromosome architecture. Nat. Biotechnol. 28, 1089–1095.

Steffen, J.D., Brody, J.R., Armen, R.S., and Pascal, J.M. (2013). Structural Implications for Selective Targeting of PARPs. Front Oncol 3, 301.

Steffen, J.D., Tholey, R.M., Langelier, M.-F., Planck, J.L., Schiewer, M.J., Lal, S., Bildzukewicz, N.A., Yeo, C.J., Knudsen, K.E., Brody, J.R., *et al.* (2014). Targeting PARP-1 allosteric regulation offers therapeutic potential against cancer. Cancer Res. 74, 31–37.

Stracker, T.H., and Petrini, J.H.J. (2011). The MRE11 complex: starting from the ends. Nat. Rev. Mol. Cell Biol. 12, 90–103.

Strahl, B.D., and Allis, C.D. (2000). The language of covalent histone modifications. Nature 403, 41–45.

Strickfaden, H., McDonald, D., Kruhlak, M.J., Haince, J.-F., Th'ng, J.P.H., Rouleau, M., Ishibashi, T., Corry, G.N., Ausio, J., Underhill, D.A., *et al.* (2016). Poly(ADP-ribosyl)ation-dependent Transient Chromatin Decondensation and Histone Displacement following Laser Microirradiation. J. Biol. Chem. 291, 1789–1802.

Subach, O.M., Malashkevich, V.N., Zencheck, W.D., Morozova, K.S., Piatkevich, K.D., Almo, S.C., and Verkhusha, V.V. (2010). Structural characterization of acylimine-containing blue and red chromophores in mTagBFP and TagRFP fluorescent proteins. Chem. Biol. 17, 333–341.

Sugasawa, K., Ng, J.M., Masutani, C., Iwai, S., van der Spek, P.J., Eker, A.P., Hanaoka, F., Bootsma, D., and Hoeijmakers, J.H. (1998). Xeroderma pigmentosum group C protein complex is the initiator of global genome nucleotide excision repair. Mol. Cell 2, 223–232.

Sun, Y., Jiang, X., Xu, Y., Ayrapetov, M.K., Moreau, L.A., Whetstine, J.R., and Price, B.D. (2009). Histone H3 methylation links DNA damage detection to activation of the tumour suppressor Tip60. Nat. Cell Biol. 11, 1376–1382.

Sun, Y., Jiang, X., and Price, B.D. (2010). Tip60: connecting chromatin to DNA damage signaling. Cell Cycle 9, 930–936.

Suzuki, K., Ojima, M., Kodama, S., and Watanabe, M. (2006). Delayed activation of DNA damage checkpoint and radiation-induced genomic instability. Mutat. Res. 597, 73–77.

Syed, S.H., Goutte-Gattat, D., Becker, N., Meyer, S., Shukla, M.S., Hayes, J.J., Everaers, R., Angelov, D., Bednar, J., and Dimitrov, S. (2010). Single-base resolution mapping of H1-nucleosome interactions and 3D organization of the nucleosome. Proc. Natl. Acad. Sci. U.S.A. 107, 9620–9625.

Sykes, S.M., Mellert, H.S., Holbert, M.A., Li, K., Marmorstein, R., Lane, W.S., and McMahon, S.B. (2006). Acetylation of the p53 DNA-binding domain regulates apoptosis induction. Mol. Cell 24, 841–851.

Taddei, A., Van Houwe, G., Hediger, F., Kalck, V., Cubizolles, F., Schober, H., and Gasser, S.M. (2006). Nuclear pore association confers optimal expression levels for an inducible yeast gene. Nature 441, 774–778.

Tagami, H., Ray-Gallet, D., Almouzni, G., and Nakatani, Y. (2004). Histone H3.1 and H3.3 complexes mediate nucleosome assembly pathways dependent or independent of DNA synthesis. Cell 116, 51–61.

Tajik, A., Zhang, Y., Wei, F., Sun, J., Jia, Q., Zhou, W., Singh, R., Khanna, N., Belmont, A.S., and Wang, N. (2016). Transcription upregulation via force-induced direct stretching of chromatin. Nat Mater 15, 1287–1296.

Takata, H., Matsunaga, S., Morimoto, A., Ono-Maniwa, R., Uchiyama, S., and Fukui, K. (2007). H1.X with different properties from other linker histones is required for mitotic progression. FEBS Letters 581, 3783–3788.

Takata, H., Hanafusa, T., Mori, T., Shimura, M., Iida, Y., Ishikawa, K., Yoshikawa, K., Yoshikawa, Y., and Maeshima, K. (2013). Chromatin compaction protects genomic DNA from radiation damage. PLoS ONE 8, e75622.

Talasz, H., Sapojnikova, N., Helliger, W., Lindner, H., and Puschendorf, B. (1998). *In vitro* binding of H1 histone subtypes to nucleosomal organized mouse mammary tumor virus long terminal repeat promotor. J. Biol. Chem. 273, 32236–32243.

Talhaoui, I., Lebedeva, N.A., Zarkovic, G., Saint-Pierre, C., Kutuzov, M.M., Sukhanova, M.V., Matkarimov, B.T., Gasparutto, D., Saparbaev, M.K., Lavrik, O.I., *et al.* (2016). Poly(ADP-ribose) polymerases covalently modify strand break termini in DNA fragments *in vitro*. Nucleic Acids Res. 44, 9279–9295.

Tallis, M., Morra, R., Barkauskaite, E., and Ahel, I. (2014). Poly(ADP-ribosyl)ation in regulation of chromatin structure and the DNA damage response. Chromosoma 123, 79–90.

Talwar, S., Kumar, A., Rao, M., Menon, G.I., and Shivashankar, G.V. (2013). Correlated spatio-temporal fluctuations in chromatin compaction states characterize stem cells. Biophys. J. 104, 553–564.

Tan, M., Luo, H., Lee, S., Jin, F., Yang, J.S., Montellier, E., Buchou, T., Cheng, Z., Rousseaux, S., Rajagopal, N., *et al.* (2011). Identification of 67 histone marks and histone lysine crotonylation as a new type of histone modification. Cell 146, 1016–1028.

Tapias, A., Auriol, J., Forget, D., Enzlin, J.H., Schärer, O.D., Coin, F., Coulombe, B., and Egly, J.-M. (2004). Ordered conformational changes in damaged DNA induced by nucleotide excision repair factors. J. Biol. Chem. 279, 19074–19083.

Tark-Dame, M., Jerabek, H., Manders, E.M.M., van der Wateren, I.M., Heermann, D.W., and van Driel, R. (2014). Depletion of the chromatin looping proteins CTCF and cohesin causes chromatin compaction: insight into chromatin folding by polymer modelling. PLoS Comput. Biol. 10, e1003877.

Taverna, S.D., Li, H., Ruthenburg, A.J., Allis, C.D., and Patel, D.J. (2007). How chromatin-binding modules interpret histone modifications: lessons from professional pocket pickers. Nat. Struct. Mol. Biol. 14, 1025–1040.

Teloni, F., and Altmeyer, M. (2016). Readers of poly(ADP-ribose): designed to be fit for purpose. Nucleic Acids Res. 44, 993–1006.
Thakar, A., Gupta, P., Ishibashi, T., Finn, R., Silva-Moreno, B., Uchiyama, S., Fukui, K., Tomschik, M., Ausio, J., and Zlatanova, J. (2009). H2A.Z and H3.3 histone variants affect nucleosome structure: biochemical and biophysical studies. Biochemistry 48, 10852–10857.
Th'ng, J.P., Guo, X.W., Swank, R.A., Crissman, H.A., and Bradbury, E.M. (1994). Inhibition of histone phosphorylation by staurosporine leads to chromosome decondensation. J. Biol. Chem. 269, 9568–9573.
Thorslund, T., Ripplinger, A., Hoffmann, S., Wild, T., Uckelmann, M., Villumsen, B., Narita, T., Sixma, T.K., Choudhary, C., Bekker-Jensen, S., *et al.* (2015). Histone H1 couples initiation and amplification of ubiquitin signalling after DNA damage. Nature 527, 389–393.
Timinszky, G., Till, S., Hassa, P.O., Hothorn, M., Kustatscher, G., Nijmeijer, B., Colombelli, J., Altmeyer, M., Stelzer, E.H.K., Scheffzek, K., *et al.* (2009). A macrodomain-containing histone rearranges chromatin upon sensing PARP1 activation. Nat. Struct. Mol. Biol. 16, 923–929.
Tóth, K.F., Knoch, T.A., Wachsmuth, M., Frank-Stöhr, M., Stöhr, M., Bacher, C.P., Müller, G., and Rippe, K. (2004). Trichostatin A-induced histone acetylation causes decondensation of interphase chromatin. J. Cell. Sci. 117, 4277–4287.
Tsekouras, K., Siegel, A.P., Day, R.N., and Pressé, S. (2015). Inferring diffusion dynamics from FCS in heterogeneous nuclear environments. Biophys. J. 109, 7–17.
Tsouroula, K., Furst, A., Rogier, M., Heyer, V., Maglott-Roth, A., Ferrand, A., Reina-San-Martin, B., and Soutoglou, E. (2016). Temporal and Spatial Uncoupling of DNA Double Strand Break Repair Pathways within Mammalian Heterochromatin. Mol. Cell 63, 293–305.
Uematsu, N., Weterings, E., Yano, K., Morotomi-Yano, K., Jakob, B., Taucher-Scholz, G., Mari, P.-O., van Gent, D.C., Chen, B.P.C., and Chen, D.J. (2007). Autophosphorylation of DNA-PKCS regulates its dynamics at DNA double-strand breaks. J. Cell Biol. 177, 219–229.
Vaňková Hausnerová, V., and Lanctôt, C. (2017). Chromatin decondensation is accompanied by a transient increase in transcriptional output. Biol. Cell 109, 65–79.
Vaquerizas, J.M., Kummerfeld, S.K., Teichmann, S.A., and Luscombe, N.M. (2009). A census of human transcription factors: function, expression and evolution. Nat. Rev. Genet. 10, 252–263.
Vaquero, A., Scher, M., Lee, D., Erdjument-Bromage, H., Tempst, P., and Reinberg, D. (2004). Human SirT1 interacts with histone H1 and promotes formation of facultative heterochromatin. Mol. Cell 16, 93–105.
Verdone, L., La Fortezza, M., Ciccarone, F., Caiafa, P., Zampieri, M., and Caserta, M. (2015). Poly(ADP-Ribosyl)ation Affects Histone Acetylation and Transcription. PLoS ONE 10, e0144287.
Verschure, P.J., van der Kraan, I., Manders, E.M.M., Hoogstraten, D., Houtsmuller, A.B., and van Driel, R. (2003). Condensed chromatin domains in the mammalian nucleus are accessible to large macromolecules. EMBO Rep. 4, 861–866.
Vivelo, C.A., and Leung, A.K.L. (2015). Proteomics approaches to identify mono-(ADP-ribosyl)ated and poly(ADP-ribosyl)ated proteins. Proteomics 15, 203–217.
Volker, M., Moné, M.J., Karmakar, P., van Hoffen, A., Schul, W., Vermeulen, W., Hoeijmakers, J.H., van Driel, R., van Zeeland, A.A., and Mullenders, L.H. (2001). Sequential assembly of the nucleotide excision repair factors *in vivo*. Mol. Cell 8, 213–224.
Vyas, S., Matic, I., Uchima, L., Rood, J., Zaja, R., Hay, R.T., Ahel, I., and Chang, P. (2014). Family-wide analysis of poly(ADP-ribose) polymerase activity. Nat Commun 5, 4426.
Walter, A., Chapuis, C., Huet, S., and Ellenberg, J. (2013). Crowded chromatin is not sufficient for heterochromatin formation and not required for its maintenance. J. Struct. Biol. 184, 445–453.
Walter, J., Schermelleh, L., Cremer, M., Tashiro, S., and Cremer, T. (2003). Chromosome order in HeLa cells changes during mitosis and early G1, but is stably maintained during subsequent interphase stages. J. Cell Biol. 160, 685–697.
Wang, Y., Kim, N.S., Haince, J.-F., Kang, H.C., David, K.K., Andrabi, S.A., Poirier, G.G., Dawson, V.L., and Dawson, T.M. (2011). Poly(ADP-ribose) (PAR) binding to apoptosis-inducing factor is critical for PAR polymerase-1-dependent cell death (parthanatos). Sci Signal 4, ra20.

Wang, Z., Michaud, G.A., Cheng, Z., Zhang, Y., Hinds, T.R., Fan, E., Cong, F., and Xu, W. (2012). Recognition of the iso-ADP-ribose moiety in poly(ADP-ribose) by WWE domains suggests a general mechanism for poly(ADP-ribosyl)ation-dependent ubiquitination. Genes Dev. 26, 235–240.
Watson, J.D., and Crick, F.H. (1953). Molecular structure of nucleic acids; a structure for deoxyribose nucleic acid. Nature 171, 737–738.
Weber, S.C., Spakowitz, A.J., and Theriot, J.A. (2012). Nonthermal ATP-dependent fluctuations contribute to the *in vivo* motion of chromosomal loci. Proc. Natl. Acad. Sci. U.S.A. 109, 7338–7343.
Wei, H., and Yu, X. (2016). Functions of PARylation in DNA Damage Repair Pathways. Genomics Proteomics Bioinformatics 14, 131–139.
Whitlock, J.P., and Simpson, R.T. (1976). Removal of histone H1 exposes a fifty base pair DNA segment between nucleosomes. Biochemistry 15, 3307–3314.
Wielckens, K., Schmidt, A., George, E., Bredehorst, R., and Hilz, H. (1982). DNA fragmentation and NAD depletion. Their relation to the turnover of endogenous mono(ADP-ribosyl) and poly(ADP-ribosyl) proteins. J. Biol. Chem. 257, 12872–12877.
Williams, R.S., Williams, J.S., and Tainer, J.A. (2007). Mre11-Rad50-Nbs1 is a keystone complex connecting DNA repair machinery, double-strand break signaling, and the chromatin template. Biochem. Cell Biol. 85, 509–520.
Wisniewski, J.R., Zougman, A., Krüger, S., and Mann, M. (2007). Mass spectrometric mapping of linker histone H1 variants reveals multiple acetylations, methylations, and phosphorylation as well as differences between cell culture and tissue. Mol. Cell Proteomics 6, 72–87.
de Wit, E., and van Steensel, B. (2009). Chromatin domains in higher eukaryotes: insights from genome-wide mapping studies. Chromosoma 118, 25–36.
Woodcock, C.L., Frado, L.L., and Rattner, J.B. (1984). The higher-order structure of chromatin: evidence for a helical ribbon arrangement. J. Cell Biol. 99, 42–52.
Woodcock, C.L., Skoultchi, A.I., and Fan, Y. (2006). Role of linker histone in chromatin structure and function: H1 stoichiometry and nucleosome repeat length. Chromosome Res. 14, 17–25.
Wu, S., Shi, Y., Mulligan, P., Gay, F., Landry, J., Liu, H., Lu, J., Qi, H.H., Wang, W., Nickoloff, J.A., *et al.* (2007). A YY1-INO80 complex regulates genomic stability through homologous recombination-based repair. Nat. Struct. Mol. Biol. 14, 1165–1172.
Xu, Y., Sun, Y., Jiang, X., Ayrapetov, M.K., Moskwa, P., Yang, S., Weinstock, D.M., and Price, B.D. (2010). The p400 ATPase regulates nucleosome stability and chromatin ubiquitination during DNA repair. J. Cell Biol. 191, 31–43.
Xu, Y., Ayrapetov, M.K., Xu, C., Gursoy-Yuzugullu, O., Hu, Y., and Price, B.D. (2012). Histone H2A.Z controls a critical chromatin remodeling step required for DNA double-strand break repair. Mol. Cell 48, 723–733.
Yaneva, M., Kowalewski, T., and Lieber, M.R. (1997). Interaction of DNA-dependent protein kinase with DNA and with Ku: biochemical and atomic-force microscopy studies. EMBO J. 16, 5098–5112.
Yoda, K., Ando, S., Morishita, S., Houmura, K., Hashimoto, K., Takeyasu, K., and Okazaki, T. (2000). Human centromere protein A (CENP-A) can replace histone H3 in nucleosome reconstitution *in vitro*. Proc Natl Acad Sci U S A 97, 7266–7271.
Yu, W., Ginjala, V., Pant, V., Chernukhin, I., Whitehead, J., Docquier, F., Farrar, D., Tavoosidana, G., Mukhopadhyay, R., Kanduri, C., *et al.* (2004). Poly(ADP-ribosyl)ation regulates CTCF-dependent chromatin insulation. Nat. Genet. 36, 1105–1110.
Yuan, J. (1996). Evolutionary conservation of a genetic pathway of programmed cell death. J. Cell. Biochem. 60, 4–11.
Zampieri, M., Ciccarone, F., Calabrese, R., Franceschi, C., Bürkle, A., and Caiafa, P. (2015). Reconfiguration of DNA methylation in aging. Mechanisms of Ageing and Development 151, 60–70.
Zhang, F., Shi, J., Chen, S.-H., Bian, C., and Yu, X. (2015). The PIN domain of EXO1 recognizes poly(ADP-ribose) in DNA damage response. Nucleic Acids Res. 43, 10782–10794.
Zhang, Y., Wang, J., Ding, M., and Yu, Y. (2013). Site-specific characterization of the Asp- and Glu-ADP-ribosylated proteome. Nat. Methods 10, 981–984.

Zhao, Y.-Q., Jordan, I.K., and Lunyak, V.V. (2013). Epigenetics components of aging in the central nervous system. Neurotherapeutics 10, 647–663.

Zhu, P., and Li, G. (2016). Higher-order structure of the 30-nm chromatin fiber revealed by cryo-EM. IUBMB Life 68, 873–878.

Zidovska, A., Weitz, D.A., and Mitchison, T.J. (2013). Micron-scale coherence in interphase chromatin dynamics. Proc. Natl. Acad. Sci. U.S.A. 110, 15555–15560.

Ziv, Y., Bielopolski, D., Galanty, Y., Lukas, C., Taya, Y., Schultz, D.C., Lukas, J., Bekker-Jensen, S., Bartek, J., and Shiloh, Y. (2006). Chromatin relaxation in response to DNA double-strand breaks is modulated by a novel ATM- and KAP-1 dependent pathway. Nat. Cell Biol. 8, 870–876.

Zlatanova, J., and Doenecke, D. (1994). Histone H1 zero: a major player in cell differentiation? FASEB J. 8, 1260–1268.

Zlatanova, J., Caiafa, P., and Van Holde, K. (2000). Linker histone binding and displacement: versatile mechanism for transcriptional regulation. FASEB J. 14, 1697–1704.

Zuin, J., Dixon, J.R., van der Reijden, M.I.J.A., Ye, Z., Kolovos, P., Brouwer, R.W.W., van de Corput, M.P.C., van de Werken, H.J.G., Knoch, T.A., van IJcken, W.F.J., *et al.* (2014). Cohesin and CTCF differentially affect chromatin architecture and gene expression in human cells. Proc. Natl. Acad. Sci. U.S.A. 111, 996–1001.

APPENDICES

Lebeaupin, T., Sellou, H., Timinszky, G., Huet, S. (2015). Chromatin dynamics at DNA breaks: what, how and why? AIMS Biophysics 2, 458–475.

Sellou, H., Lebeaupin, T., Chapuis, C., Smith, R., Hegele, A., Singh, H.R., Kozlowski, M., Bultmann, S., Ladurner, A.G., Timinszky, G., *et al.* (2016). The poly(ADP-ribose)-dependent chromatin remodeler Alc1 induces local chromatin relaxation upon DNA damage. Mol. Biol. Cell 27, 3791–3799.

Lebeaupin, T., Smith, R., Huet, S., and Timinszky, G. (2017). Poly(ADP-Ribose)-Dependent Chromatin Remodeling in DNA Repair. Methods Mol. Biol. 1608, 165–183.

Lebeaupin, T., Smith, R., Huet, S. (to be published in “Nuclear Architecture and Dynamics" of the "Translational Epigenetics Series”, Elsevier). The multiple effects of molecular crowding in the cell nucleus: from molecular dynamics to the regulation of nuclear architecture. (preprint manuscript)

AIMS Biophysics, 2(4): 458-475.
DOI: 10.3934/biophy.2015.4.458
Received date 15 July 2015,
Accepted date 06 September 2015,
Published date 10 September 2015

http://www.aimspress.com/

Review

Chromatin dynamics at DNA breaks: what, how and why?

Théo Lebeaupin [1,2,3], Hafida Sellou [1,2,3], Gyula Timinszky [3], and Sébastien Huet [1,2,*]

[1] CNRS, UMR 6290, Institut Génétique et Développement de Rennes, Rennes, France
[2] Université de Rennes 1, Structure fédérative de recherche Biosit, Rennes, France
[3] Department of Physiological Chemistry, Adolf Butenandt Institute, Ludwig-Maximilians-Universität München, Munich, Germany

* **Correspondence:** Email: sebastien.huet@univ-rennes1.fr; Tel: +33-223234557.

Abstract: Chromatin has a complex, dynamic architecture in the interphase nucleus, which regulates the accessibility of the underlying DNA and plays a key regulatory role in all the cellular functions using DNA as a template, such as replication, transcription or DNA damage repair. Here, we review the recent progresses in the understanding of the interplay between chromatin architecture and DNA repair mechanisms. Several reports based on live cell fluorescence imaging show that the activation of the DNA repair machinery is associated with major changes in the compaction state and the mobility of chromatin. We discuss the functional consequences of these changes in yeast and mammals in the light of the different repair pathways utilized by these organisms. In the final section of this review, we show how future developments in high-resolution light microscopy and chromatin modelling by polymer physics should contribute to a better understanding of the relationship between the structural changes in chromatin and the activity of the repair processes.

Keywords: chromatin; nucleus; DNA repair; double strand break; homologous recombination; non-homologous end joining; fluorescence microscopy; single particle tracking; anomalous diffusion; polymer physics

1. Introduction

Chromatin, one of the most complex supramolecular structures in the cell, displays several organizational levels spanning over four orders of magnitudes in size from the 2-nm diameter of the DNA double helix to the few tens of micrometers of chromosome territories in the nucleus [1]. This

packing state of chromatin is thought to influence all cellular functions acting on DNA. For example, even though the causal link between these two processes remains unclear, the modulation of transcription is associated with major changes in the chromatin organization [2]. While we have a relatively good understanding of nucleosome structure and function and that of the chromosome territories, the multiple organizational levels between these two extreme structures remain poorly understood and are the subject of intense research.

In the present review, we will focus on the interplay between chromatin and DNA repair, which has been receiving growing attention over the last years. Recent studies have shown that major chromatin remodeling events occur in the vicinity of DNA lesions [3,4]. However, it is still largely unknown whether these remodeling events are a mere consequence of the repair processes or play an active role in the resolution of DNA breaks. We will first review our current knowledge about chromatin structure and dynamics in the absence of DNA damage and in response to the induction of such damage. Second, we will examine the potential functional roles of chromatin dynamics during the DNA repair processes. Finally, we will speculate on how recent chromatin polymer models combined with high-resolution spatio-temporal data could help to bridge the gap between the modifications of the internal organization of the chromatin fiber induced by the DNA repair machinery and the changes in chromatin dynamics assessed by light microscopy.

2. The Organizational Levels of Chromatin: from the Nucleosome to Chromosome Territories

Similar to proteins, chromatin displays a hierarchical organization [2]. The primary structure encompasses the nucleosome architecture and the internal packing of the chromatin fiber, meaning the spatial distribution of the nucleosomes along this fiber. For many years, the classical view has been that the beads-on-a-string fiber composed of nucleosomes alternating with linker DNA spontaneously folds into a thicker 30-nm fiber [5,6]. However, the existence of this folding level was recently questioned by several studies that failed to identify the 30-nm fiber in the interphase nucleus using different high resolution imaging methods [7,8]. More recently, data obtained in yeast with a new chromosome conformation capture approach leading to mono-nucleosome resolution [9] suggested the existence of small compact tetranucleosome structures similar to those previously observed in-vitro [6], but did not demonstrate the presence of longer regular 30-nm fibers.

The secondary structuring level of the chromatin fiber relies on the formation of loops due to long-distance interactions along this fiber. Although the existence of chromatin loops of kilobase-to-megabase sizes has been widely documented [9,10], their distribution along the fiber and their stability remain debated [11]. These loops may be the elementary component of a recently identified structural unit: the topologically associated domains (TADs) [12,13,14], which correspond to compact structures encompassing ~1Mb of DNA and characterized by a high probability of contacts along the chromatin fiber.

Finally, the ternary structure of the chromatin corresponds to the spatial distributions of the TADs and, at larger scales, of the whole chromosomes, within the nucleus. The TADs associate to form larger compartments sharing similar features, such as an opened chromatin state or a defined gene density [15], reminiscent of the original definition of euchromatin and heterochromatin areas. Studies analyzing the spatial distributions of whole chromosomes showed that they were not widespread over the nuclear volume but occupy compact and largely mutually exclusive areas called

chromosome territories [16,17]. The positioning of these territories in the nucleus is not random and is probably partially defined by interactions with the inner nuclear membranes [18].

So far, we only described a snapshot of chromatin architecture. However, several studies have reported rapid chromatin motions at scales up to ~1 μm [19–22], which would suggest that chromatin architecture is highly dynamic at all the organizational levels below chromosome territories [23]. These local chromatin motions probably originate both from passive thermal fluctuations and active remodeling mechanisms but the relative contributions of each component is still a subject of investigations [24,25].

3. Current Methodologies Available to Analyze Chromatin Dynamics

Chromatin dynamics in the living interphase nucleus can be directly analyzed at multiple scales in space and time using different fluorescence-based imaging methods. The main difference between these approaches resides in the size of the assessed chromatin area. The movements of chromosome territories within the nucleus can be followed by confocal microscopy using fluorescently tagged histones [26,27]. Single chromosomes or sub-chromosomal areas can be identified by local photobleaching or photoactivation of the fluorescent proteins [28]. This approach can also be used to characterize chromatin compaction, in the context of the DNA damage response [29]. The minimal chromatin area that can be studied with this approach is defined by the size of the laser spot used to photobleach or photoconvert the tagged histones, which probably encompasses several Mb of DNA wrapped around thousands of nucleosomes.

To study the dynamics of smaller chromatin areas, DNA can be directly labeled by the incorporation of fluorescent nucleotides during replication [30]. The labeled areas thus correspond to replication foci that contain ~0.8Mb of DNA [31]. Another common labeling approach uses repeated bacterial sequences, such as the Lac or the Tet operator, integrated into the genome. The binding of the associated repressor proteins tagged by fluorescent dyes to this DNA stretch, whose size is approximately 100 kb, generates a fluorescent spot whose trajectory can be followed under the microscope [32]. Although this strategy has demonstrated its usefulness in analyzing chromatin motion (see below), it is known to suffer from several pitfalls. For instance, the integration of these DNA arrays containing a large number of repeated sequences tightly bound to repressor proteins induce the formation of fragile sites and the transcriptional silencing of the surrounding genes [33,34]. Interestingly, it was recently reported that shorter DNA recognition sequences of only one kilobase can be used to assess chromatin motions [35]. Moreover, the newly developed tools for genome editing such as the TALEs or CRISPR/Cas systems can also be applied to fluorescently tag short target DNA sequences in living cells [36,37]. These new approaches would allow not only to solve the issues related to the repetitive nature of the Lac or Tet arrays but also to follow the dynamics of smaller chromatin regions. The different methods mentioned so far to assess chromatin dynamics were based on the local labeling of predefined chromatin regions. An alternative is to label uniformly the chromatin, using for example fluorescently tagged core histones, and to use image correlation methods to characterize the local chromatin movements [38,39].

4. Chromatin Dynamics in the Absence of DNA Damage

Although the global architecture of chromatin is stable during interphase [26,27], local movements with amplitudes of 0.3 to 1 μm have been reported in multiple organisms: bacteria [22], yeast [19] and higher eukaryotes [40,41]. Most of the reports studying chromatin motion are based on the analysis of the mean squared displacement (MSD) curves calculated from the tracks of fluorescently labeled chromatin foci [42]. Diffusion coefficients derived from these MSDs range between 10^{-5} and 10^{-3} $\mu m^2/s$ [40,41]. By comparison, the diffusion coefficient of a 30 kD globular protein in mammalian nuclei is several magnitudes higher, 10–40 $\mu m^2/s$. Interestingly, chromatin mobility is usually higher in yeast than in mammals, maybe due to the fact that mammalian chromosomes are longer than the yeast ones and thus more difficult to move [43]. The analysis of the MSD curves also indicates that chromatin dynamics do not correspond to pure diffusion but rather to anomalous diffusion or subdiffusion [44] (Figure 1). Such diffusion patterns arise either when molecules diffuse in complex heterogeneous media [45] or when studying thermal fluctuations within a polymer [46], both of which could explain the observed chromatin dynamics. Interestingly, the subdiffusive motion of the chromatin seems homogeneous within a large range of timescale from 10^{-2} to 10^2 s [44,47], suggesting that the components responsible for these chromatin motions act at multiple timescales. In rare cases, transient directional chromatin movements have been also reported [20].

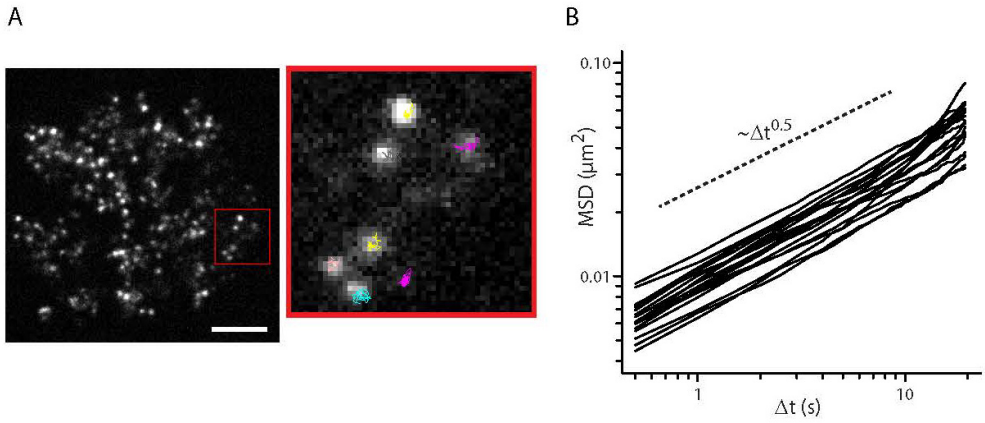

Figure 1. (A) Nucleus of a U2OS cell with its DNA labeled using fluorescent nucleotides. Bar = 5μm. The inset shows examples of trajectories displayed by the labeled chromatin foci. The trajectories were recorded for 30s at 2 frames per second. (B) Curves of the mean square displacement (MSD) calculated from the trajectories of the labeled foci. Each curve corresponds to the averaged chromatin dynamics within one nucleus (21 nuclei, 40 to 180 track per nucleus). The fact that the curves show a slope of ~0.5 in the log-log representation indicates that the chromatin dynamics is subdiffusive at the studied timescales.

Although contradictory results have been reported [25,40], several studies indicate that local chromatin motions are principally due to ATP-dependent processes rather than thermal fluctuations [19,24,38]. Multiple active processes are probably responsible for chromatin dynamics.

While the influence of the DNA replication status is unclear [19,25,48], modulations of transcription levels correlate with changes in chromatin motions [49,50]. In this context, the ATP-dependent chromatin remodeler INO80 is an important regulator of chromatin dynamics [51]. In the case of directed motion related to transcription activation, the involvement of actin dependent transport has been reported [52,53]. Besides these active processes directly acting on chromatin, the nuclear environment surrounding chromatin also influences its movements. The tethering of chromatin to stable nuclear structures such as the lamina or the nucleoli reduces chromatin motions [54]. Moreover, a recent report revealed that the viscoelastic properties of the complex and heterogeneous nuclear environment also modulate chromatin dynamics [55].

5. Chromatin Dynamics upon DNA Damage

Chromatin dynamics in the context of DNA repair mechanisms has been mainly analyzed for the most deleterious form of DNA damage: double strand breaks (DSBs). Eukaryotic organisms activate two main mechanisms to repair DSBs (Figure 2): homologous recombination (HR) and non-homologous end joining (NHEJ). HR requires the pairing between the broken DNA and an intact homologous sequence, which is used as a template for the faithful repair [56]. Instead, NHEJ directly religates the broken ends without the need for an intact template, making this type of repair more error-prone [57]. The changes in chromatin architecture associated with the activation of these DSB repair pathways have been studied mostly in yeast and mammalian nuclei. While chromatin dynamics is in the same range in yeast and mammals in the absence of DNA damage, the induction of DSBs is associated with a very different response of the chromatin architecture in the two model systems. This observation may be related to the fact that HR is the major DSB repair pathway in yeast while NHEJ dominates in differentiated mammalian cell lines [58].

5.1. The yeast paradigm

In yeast, chromatin dynamics was assessed by tracking fluorescently labeled chromosomal loci during two different steps of the DSB repair by HR: the early resection process and the later homologous pairing phase. During resection, a strong inhibition of the chromatin motions was observed [35]. Chromatin dynamics associated with homologous pairing was characterized mainly in terms of confinement radius, which corresponds to the size of the region explored by the tracked locus. The induction of DSBs by restriction enzymes or pharmacological treatment was associated with an expansion of the nuclear area explored by the mobile damaged locus, even if the amplitude of this expansion varies depending on the locus of interest and the ploidy of the cell [59,60]. Surprisingly, the induction of DNA damage not only affects the dynamics of the damaged site but also induces an overall increase of chromatin mobility in diploid cells [3]. The fact that this global effect was not observed in haploid cells under similar conditions [59] suggests that it only occurs when a damaged chromosome needs to explore the nucleus to find and pair with its homologue. It is also important to note that the modulation of chromatin movements at DNA breaks depends on the type of DNA damage since spontaneous breaks occurring during DNA replication display decreased mobility compared to undamaged DNA [48]. Several members of the DNA repair machinery are implicated in the modulation of the chromatin dynamics in relation to DNA damage: the recombinase protein Rad51, the ATR mediator Mec1 and the INO80 nucleosome remodeling

complex [59,60], but the exact mechanism by which these repair proteins regulate chromatin motions remains unknown.

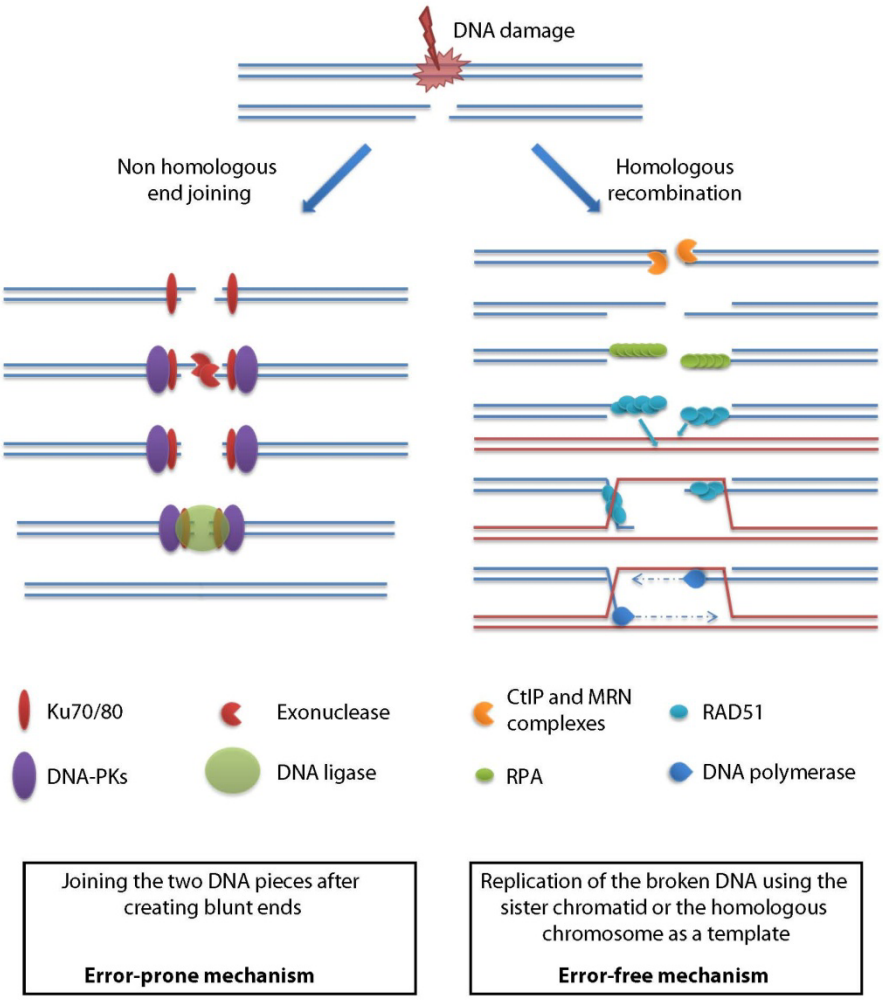

Figure 2. Schematic description of the two main pathways for repairing DNA double strand breaks.

In addition to the increased chromatin mobility, several studies describe the clustering of multiple DSBs. Lisby et al. showed the co-localization of DNA lesions in foci containing the repair factor Rad52 suggesting that these multiple DSBs are driven to a shared location, the so-called "repair centers" or "repair factories" [61]. When no homology is found and DSBs persist, Rad51, a protein involved in homology pairing, remains on the broken DNA indicating persistent homology search which ultimately leads to the relocation of the DSBs to the nuclear periphery [62,63]. Altogether, the different data obtained in yeast thus suggest a global picture in which the enhancement of the mobility of DNA breaks is a key step for their efficient repair (Figure 3).

5.2. The mammalian paradigm

While recent publications allowed us to draw a relatively clear picture of the modulation of chromatin dynamics in yeast upon induction of DSBs, the situation in mammalian nuclei appears much more complex. On the one hand, there are several findings similar to the yeast-like model in which damaged DNA gains mobility and, in some cases, relocates to repair-competent areas. After irradiation by α-particles, the damaged chromatin displays enhanced mobility compared to undamaged DNA [64] and tends to fuse into clusters [65]. Similarly increased dynamics was also found for uncapped telomeres, which can be recognized as DSBs [66]. Finally, damaged DNA in heterochromatin tends to move into euchromatin where γH2AX foci are formed, suggesting that this relocation step is necessary for proper signaling and repair [67,68]. This mechanism, which is also observed in Drosophila melanogaster [69], may limit the risk of deleterious chromosomal rearrangements within the highly repetitive heterochromatin. However, there are numerous reports that do not observe pronounced changes in chromatin mobility upon damage induced by γ or UV-laser irradiation [29], X-ray irradiation [70], ion irradiation [71] or enzymatically-induced DSBs [72,73].

Besides the analysis of chromatin movements, many publications also investigated the modulation of the chromatin compaction state at DNA breaks. Smerdon and Lieberman showed in 1978 that UV-induced DNA damage gives rise to an increased sensitivity of chromatin to nucleases [74]. This higher accessibility at the nucleosomal level upon DNA damage is correlated with chromatin decondensation at the micrometer scales accessible by light microscopy [29,75], even though the causal link between these two remodeling events occurring at different scales is still unclear (Figure 3). Following this initial fast decondensation, the damaged chromatin area slowly recondenses [4], potentially reaching higher compaction levels than before damage induction [76].

Currently, we have no precise clue about the molecular mechanisms regulating chromatin packing upon DNA damage. Multiple proteins are recruited to the DNA breaks. Some of them, such as PARP1, promote chromatin decondensation [4,77], while others, such as HP1, induce the formation of a closed chromatin state [78,79]. It is unclear how the action of these proteins with opposite effects on chromatin packing is coordinated. Khurana and colleagues proposed that chromatin decondensation and compaction occur sequentially through a balance between the factors intervening in these two processes, this coordination being a key determinant of the choice of the repair pathway [4]. Alternatively, Hinde et al. suggested a model in which both chromatin expansion and compaction processes happen at the same time but in distinct regions of the chromatin in the vicinity of the DNA breaks [39].

6. Functional Roles of Chromatin Dynamics at the DNA Breaks

The data reviewed so far identify major changes in both chromatin mobility and compaction state during the DNA damage response. In this section, we will investigate the functional roles of these chromatin-remodeling processes.

Regarding the yeast model, it has been postulated that the increased mobility of DSBs may promote homology search, which is the limiting factor in HR (Figure 3). This is supported by the fact that the increased chromatin mobility upon DNA damage is absent in yeast depleted for proteins involved in homology search [59,60]. The increased chromatin movements may also promote the

merging of multiple DSBs in repair foci [61]. The formation of nuclear bodies is a classical cellular response to promote different functions due to the local accumulation of specific proteins [80].

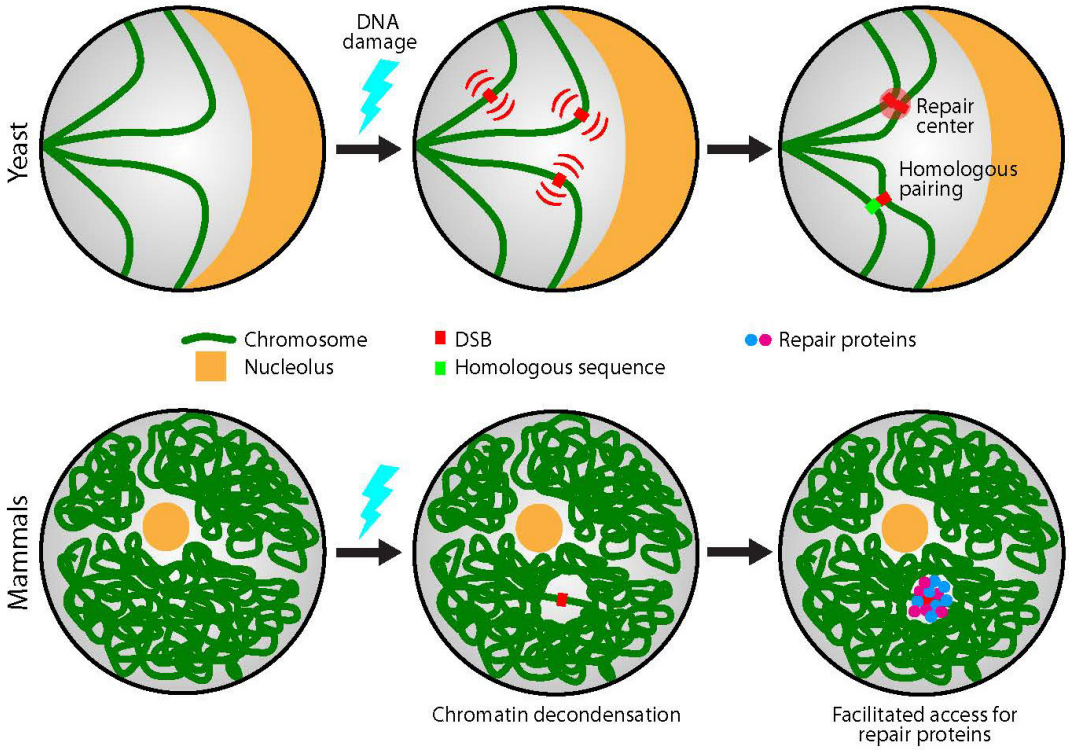

Figure 3. Schematic description of the changes in chromatin motions and compaction state observed at DNA breaks for yeast and mammals.

In this context, the DSB clusters may constitute areas highly favorable for efficient repair. However, it is interesting to note that increased chromatin mobility at the DNA breaks is not generally observed in mammalian nuclei. Two reasons may explain these differences between yeast and mammals. The first is the amplitude of the nuclear movements relative to the size of the nucleus. In the yeast nucleus characterized by a 2 µm diameter, chromatin loci already explore a significant fraction, about 10–20 %, of the nuclear volume in the absence of DNA damage [81]. Following a modest increase in chromatin mobility, this value increases to ~50 % upon DNA damage [59], allowing the efficient search for the intact homologous sequence required in HR. In mammalian nuclei, the amplitude of chromatin motions in the absence of damage is in the same range than in yeast but the volume to explore is two orders of magnitude bigger. Consequently, the efficient exploration of the nucleus for homologous pairing would require a strong increase in chromatin movements, which may only be achieved by major unfolding of the chromatin fiber. Nevertheless, long-range chromatin displacements can occur in mammalian nuclei as observed in the case of transcriptional activation [52]. Thus, rather than the potential inefficiency of the nuclear exploration for homologous pairing, chromatin may not display increased mobility at DNA breaks in mammalian cells to limit the risk of deleterious chromosome translocations, which could ultimately lead to cancer development [51,73,82]. Indeed, a recent genome-wide analysis of chromosomal rearrangements in mammalian nuclei shows that the physical proximity to the DSB is a key

determinant in the probability of translocation events [83]. Altogether, the potentially inefficient and risky pairing step with the homologous chromosome required for HR in unreplicated genomes may explain why mammalian cells rather use NHEJ to repair DSBs in G1 and only switch to HR when a close-by sister chromatid is available. It remains however unclear why the risk of ectopic translocation inherent to HR might be more tolerable in unicellular organisms such as yeast than in multicellular higher eukaryotes.

In addition to the modulation of chromatin movements, the activation of the DNA repair machinery is also associated with changes in chromatin compaction. It is assumed that chromatin decondensation following DNA damage is a necessary step and its impairment greatly inhibits the repair process [84]. A straightforward model is that chromatin decondensation facilitates DNA access to repair proteins (Figure 3) as illustrated by the hypersensitivity of the chromatin to nucleases at the DNA breaks. However, this simple model should be considered with caution because several studies reported that molecular tracers of sizes up to a few hundred kDa can easily diffuse through the nucleus and penetrate even the densely packed heterochromatin [85,86]. It was also proposed that the chromatin packing state may influence the way that proteins scan for binding sites, which correspond to DNA breaks in the case of repair proteins, along the chromatin fiber [86]. In addition, it was recently suggested that it is the over-compaction of chromatin at DNA breaks rather than its decondensation that may trigger the recruitment of some repair components [76]. The chromatin over-condensation or recondensation following DNA damage in association to the recruitment of heterochromatin proteins [4,76,79] may originate from the necessity to both inhibit transcription of the damaged DNA and keep the loose broken DNA ends in close proximity to facilitate repair.

To reconcile these different and sometimes contradictory observations, we will require a better understanding of the types of DNA lesions created with the different DNA damaging methods [87,88]. Other parameters such as the differential activation of distinct DNA repair pathways depending on the cell type or the cell cycle, or the time-window at which the chromatin movements are assessed, must be also analyzed carefully.

7. The Future Step: Relating the Changes in Chromatin Dynamics at DNA Breaks to the Activity of the DNA Repair Machinery

The changes in the chromatin architecture at DNA breaks described in the previous sections may be the direct consequence of the modifications of the physical properties of the DNA polymer upon damage. DSBs occurring in particular in the linker DNA could dramatically destabilize the chromatin fiber. Single and double strand DNA breaks may also lead to a local release of topological constraints, a key component of the chromatin packing state [89,90]. However, the fact that the chromatin remodeling mechanisms observed at DNA breaks are inhibited when impairing specific DNA repair pathways [59,60,77] suggest that these remodeling mechanisms are not the mere physical consequences of breaks along the DNA but are rather driven by the activity of the DNA repair machinery.

The DNA repair machinery directly acts on the chromatin fiber via three major mechanisms: i) nucleosome destabilization, ii) alteration of the nucleosome-nucleosome interactions within the fiber and iii) nucleosome repositioning [91]. These chromatin remodeling processes involve a complex choreography of molecular actors. The most canonical post-transcriptional modification found at DSBs is the phosphorylation of the H2AX histone variant, which is a major signal controlling the

recruitment of several members of the DNA repair machinery. It may also play a structural role by promoting chromatin relaxation [92] or nucleosome destabilization [93,94] at DNA breaks. The formation of negatively charged chains of poly-ADP-ribose, another post-transcriptional modification often found at DNA breaks [95], on the linker histone H1 is thought to induce the relaxation of the chromatin fiber due to the repulsion between the neighboring nucleosomes within the fiber [96,97]. The histone variant H2A.Z also appears as a key regulator of the nucleosome stability at DNA breaks [98]. Finally, multiple ATP-dependent chromatin remodeling enzymes are recruited at DNA damage sites. These enzymes are often part of multi-subunits complexes, fuelled by the energy provided by ATP hydrolysis to actively alter histone-DNA interactions leading to nucleosome sliding, eviction or histone exchange [99]. Altogether, these different molecular actors of the DNA repair machinery acting on the nucleosomes will have a major impact on the internal organization of the chromatin fiber, which we identified in the first section of this review as the primary structure of chromatin. It remains however largely unknown how these changes occurring on this primary structure will influence the higher hierarchical folding steps of the chromatin to ultimately lead to the modifications of the chromatin movements or compaction levels that were reviewed above .In the following, we will show how recent developments in high-resolution fluorescence microscopy and in the modeling of chromatin architecture by polymer physics may help in building an integrated description of the interplay between chromatin architecture and DNA repair mechanisms.

Chromatin dynamics in living nuclei is usually studied by tracking diffraction-limited fluorescent spots corresponding to defined tagged chromatin areas. This approach allows to assess chromatin movements as small as a few tens of nanometer, well below the nominal spatial resolution of optical microscopy, provided that the signal-to-noise ratio (SNR) of the tracked spots is sufficiently high [100]. For many years, reaching high SNR required the labeling of chromatin regions containing about 0.1 to 1 Mb of DNA, thus preventing the direct characterization of the dynamics of the smaller structural units of chromatin [54]. The recent progress in single-molecule imaging abolished this limitation since single fluorescently labeled nucleosomes [101] or single dyes incorporated in the DNA [102] can be detected in living cells, allowing to follow their local movements [103]. When used in fixed samples for ultrastructure reconstruction, these single-molecule imaging approaches also further our understanding of the fine-scale organization of chromatin [104,105,106]. These new methodologies will refine our description of the dynamic chromatin architecture in the absence of and following DNA breaks. To study the dynamic structural information of chromatin at an even smaller scale, the analysis of fluorescence resonance energy transfer (FRET) signals between fluorophores attached to chromatin components, such as histones, appears to be a promising method [107]. Because FRET is sensitive to variations of few nanometers in the distance between the two fluorophores, the recording of the variations of FRET signals upon DNA damage should help to identify subtle changes in the packing state of chromatin.

Given the complexity of chromatin architecture and the diversity of experimental approaches to study chromatin structure and dynamics, the precise understanding of the interplay between the chromatin state and DNA repair mechanisms would clearly benefit from an integrated multiscale model describing the spatial organization of chromatin in the interphase nucleus. In 2009, Emanuel et al. made the provocative statement that, with the resolution of the experimental methods available at the time, any of the structural models could fit the data [108]. Nevertheless, since then, we gained significant quantitative understanding about the dynamic chromatin architecture. Based on these new

findings, different models have been proposed. A very simple polymer model was introduced by Rouse in 1953 [109]. The polymer is modeled as a chain of beads connected with springs and the contributions of volume exclusion and hydrodynamic interactions are neglected. Surprisingly, this model agrees very well with the experimental data describing chromatin movements in bacteria [110] and yeast [44]. Nevertheless, fitting these data with the Rouse model leads to an unrealistic highly flexible chromatin fiber with a persistence length of only few nanometer [44]. In addition, while the subdiffusive motion displayed by chromatin in bacteria and yeast appears homogeneous over the assessed timescales in agreement with the predictions of the Rouse model [44,110], the situation in mammalian nuclei is more complex with different subdiffusive regimes depending on the timescales [47]. These different results call for polymer models more complex than the Rouse chain to describe the subdiffusive chromatin movements [111].

In 2009, based on the spatial proximity maps obtained by Hi-C methods (high throughput sequencing combined to chromosome conformation capture), it was proposed that chromatin adopts a particular metastable compact configuration: the fractal globule [15,112]. Noteworthy, this fractal feature nicely agrees with data obtained using different methods [113]. Yet, this model suffers from several limitations. In particular, it fails to predict the compact structure of chromosome territories [114]. To obtain this compact configuration, multiple models have been proposed to take into account the formation of dynamic chromatin loops [114,115,116]. One interesting feature associated with the presence of loops is that they allow the generation of chromatin structures that agree with the fluorescence in-situ hybridization (FISH) data, while limiting the formation of knots, which are thought to be deleterious for the cells [117]. Despite not being a necessary condition [43], these loops may also contribute to the spontaneous unmixing of chromosomes, which could explain the existence of chromosome territories [118,119]. It remains, however, unclear whether the loop formation requires specific interactions along the chromatin fiber [114,120] or if non-specific, entropy driven, contacts are sufficient [121]. Very recently, Zhang et al. have used Hi-C contact maps to define an effective energy landscape for the chromatin fiber [122]. Based on this energy function, they could simulate chromatin architectures that recapitulate the formation of loops and their assembling into topologically associated domains. Besides the chromatin polymer itself, a global model should also include its surrounding heterogeneous environment. For example, the crowding induced by the numerous macromolecules (proteins, RNA...) diffusing through the nucleus seems to have a major impact on chromatin architecture [113].

8. Conclusion

Even though if it is now clear that complex chromatin remodeling events occur at DNA breaks, we still have some difficulties to draw a clear picture of the interplay between the DNA repair processes and the dynamic chromatin architecture. Among others, two elements would help to make significant progress in this direction. First, we would need a global and integrated description of the chromatin architecture in the absence and upon DNA damage. Second, we should investigate more precisely the impact of the multiscale chromatin organization on the ability of DNA repair proteins navigating through the nucleus to find their target and bind to it. The recent technical breakthroughs achieved to investigate chromatin structure at high resolution and the development of complex polymer models of the chromatin will definitely help to answer these questions in the future. Altogether, we foresee that advances in the establishment of an integrated chromatin polymer model

together with the improving spatial and temporal resolution of the methods used to analyze chromatin architecture should greatly refine the description of chromatin organization. Once such a refined picture will be available, it will perhaps be possible to better understand how remodeling events occurring at the fiber level such as those induced by molecular actors of the DNA repair machinery, can influence chromatin architecture at multiple space scales.

Acknowledgments

This work was supported by grants from the Agence National de la Recherche (JCJC-SVSE2-2011, ChromaTranscript project) and from the European Union (FP7-PEOPLE-2011-CIG, ChromaTranscript project). G.T. acknowledges the financial support from the Deutsche Forschungsgemeinschaft (TI 817/2-1) and from the Worldwide Cancer Research (#14-1315).

Conflict of Interest

The authors declare no conflict of interest.

References

1. Woodcock CL, Ghosh RP (2010) Chromatin higher-order structure and dynamics. *Cold Spring Harb Perspect Biol* 2: a000596.
2. Sexton T, Cavalli G (2015) The role of chromosome domains in shaping the functional genome. *Cell* 160: 1049–1059.
3. Miné-Hattab J, Rothstein R (2012) Increased chromosome mobility facilitates homology search during recombination. *Nat Cell Biol* 14: 510–517.
4. Khurana S, Kruhlak MJ, Kim J, et al. (2014) A macrohistone variant links dynamic chromatin compaction to BRCA1-dependent genome maintenance. *Cell Rep* 8: 1049–1062.
5. Robinson PJJ, Fairall L, Huynh VAT, et al. (2006) EM measurements define the dimensions of the "30-nm" chromatin fiber: evidence for a compact, interdigitated structure. *Proc Natl Acad Sci U S A* 103: 6506–6511.
6. Schalch T, Duda S, Sargent DF, et al. (2005) X-ray structure of a tetranucleosome and its implications for the chromatin fibre. *Nature* 436: 138–141.
7. Joti Y, Hikima T, Nishino, et al. (2012) Chromosomes without a 30-nm chromatin fiber. *Nucl Austin Tex* 3: 404–410.
8. Fussner E, Ahmed K, Dehghani, et al. (2010) Changes in chromatin fiber density as a marker for pluripotency. *Cold Spring Harb Symp Quant. Biol* 75: 245–249.
9. Yokota H, van den Engh G, Hearst JE, et al. (1995) Evidence for the organization of chromatin in megabase pair-sized loops arranged along a random walk path in the human G0/G1 interphase nucleus. *J Cell Biol* 130: 1239–1249.
10. Petrascheck M, Escher D, Mahmoudi T et al. (2005) DNA looping induced by a transcriptional enhancer in vivo. *Nucleic Acids Res.* 33: 3743–3750.
11. Pombo A, Dillon N (2015) Three-dimensional genome architecture: players and mechanisms. *Nat Rev Mol Cell Biol* 16: 245–257.

12. Dixon JR, Selvaraj S, Yue F, et al. (2012) Topological domains in mammalian genomes identified by analysis of chromatin interactions. *Nature* 485: 376–380.
13. Nora EP, Lajoie BR, Schulz EG, et al. (2012) Spatial partitioning of the regulatory landscape of the X-inactivation centre. *Nature* 485: 381–385.
14. Sexton T, Yaffe E, Kenigsberg E, et al. (2012) Three-dimensional folding and functional organization principles of the Drosophila genome. *Cell* 148: 458–472.
15. Lieberman-Aiden E, van Berkum NL, Williams L, et al. (2009) Comprehensive mapping of long-range interactions reveals folding principles of the human genome. *Science* 326: 289–293.
16. Bolzer A, Kreth G, Solovei I, et al. (2005) Three-dimensional maps of all chromosomes in human male fibroblast nuclei and prometaphase rosettes. *PLoS Biol* 3: e157.
17. Cremer T, Cremer M (2010) Chromosome territories. *Cold Spring Harb Perspect Biol* 2: a003889.
18. Kinney NA, Onufriev AV, Sharakhov IV (2015) Quantified effects of chromosome-nuclear envelope attachments on 3D organization of chromosomes. *Nucl Austin Tex* 6: 212–224.
19. Heun P, Laroche T, Shimada K, et al. (2001) Chromosome dynamics in the yeast interphase nucleus. *Science* 294: 2181–2186.
20. Levi V, Ruan Q, Plutz M, et al. (2005) Chromatin dynamics in interphase cells revealed by tracking in a two-photon excitation microscope. *Biophys J* 89: 4275–4285.
21. Hubner M, Spector D (2010) Chromatin Dynamics. *Annu Rev Biophys* 39: 471–489.
22. Javer A, Long Z, Nugent E, et al. (2013) Short-time movement of E. coli chromosomal loci depends on coordinate and subcellular localization. *Nat Commun.* 4: 3003.
23. Gibcus JH, Dekker J (2013) The hierarchy of the 3D genome. *Mol Cell* 49: 773–782.
24. Weber SC, Spakowitz AJ, Theriot JA (2012) Nonthermal ATP-dependent fluctuations contribute to the in vivo motion of chromosomal loci. *Proc Natl Acad Sci U S A* 109: 7338–7343.
25. Pliss A, Malyavantham KS, Bhattacharya S, et al. (2013) Chromatin dynamics in living cells: identification of oscillatory motion. *J Cell Physiol* 228, 609–616.
26. Gerlich D, Beaudouin J, Kalbfuss B, et al. (2003) Global chromosome positions are transmitted through mitosis in mammalian cells. *Cell* 112: 751–764.
27. Walter J, Schermelleh L, Cremer M, et al. (2003) Chromosome order in HeLa cells changes during mitosis and early G1, but is stably maintained during subsequent interphase stages. *J Cell Biol* 160: 685–697.
28. Müller I, Boyle S, Singer RH, et al. (2010) Stable morphology, but dynamic internal reorganisation, of interphase human chromosomes in living cells. *PloS One* 5: e11560.
29. Kruhlak MJ, Celeste A, Dellaire G, et al. (2006) Changes in chromatin structure and mobility in living cells at sites of DNA double-strand breaks. *J Cell Biol* 172: 823–834.
30. Zink D, Cremer T, Saffrich R, et al. (1998) Structure and dynamics of human interphase chromosome territories in vivo. *Hum Genet* 102: 241–251.
31. Jackson DA, Pombo A (1998) Replicon clusters are stable units of chromosome structure: evidence that nuclear organization contributes to the efficient activation and propagation of S phase in human cells. *J Cell Biol* 140: 1285–1295.
32. Robinett CC, Straight A, Li G, et al. (1996) In vivo localization of DNA sequences and visualization of large-scale chromatin organization using lac operator/repressor recognition. *J Cell Biol* 135: 1685–1700.

33. Jacome A, Fernandez-Capetillo O (2011) Lac operator repeats generate a traceable fragile site in mammalian cells. *EMBO Rep* 12: 1032–1038.
34. Dubarry M, Loïodice I, Chen CL, et al. (2011) Tight protein-DNA interactions favor gene silencing. *Genes Dev* 25: 1365–1370.
35. Saad H, Gallardo F, Dalvai M, et al. (2014) DNA dynamics during early double-strand break processing revealed by non-intrusive imaging of living cells. *PLoS Genet* 10: e1004187.
36. Chen B, Gilbert LA, Cimini BA, et al. (2013) Dynamic imaging of genomic loci in living human cells by an optimized CRISPR/Cas system. *Cell* 155: 1479–1491.
37. Miyanari Y, Ziegler-Birling C, Torres-Padilla M-E (2013) Live visualization of chromatin dynamics with fluorescent TALEs. *Nat Struct Mol Biol* 20: 1321–1324.
38. Zidovska A, Weitz DA, Mitchison TJ (2013) Micron-scale coherence in interphase chromatin dynamics. *Proc Natl Acad Sci U S A* 110: 15555–15560.
39. Hinde E, Kong X, Yokomori K, et al. (2014) Chromatin dynamics during DNA repair revealed by pair correlation analysis of molecular flow in the nucleus. *Biophys J* 107: 55–65.
40. Marshall WF, Straight A, Marko JF, et al. (1997) Interphase chromosomes undergo constrained diffusional motion in living cells. *Curr Biol CB* 7: 930–939.
41. Bornfleth H, Edelmann P, Zink D, et al. (1999) Quantitative motion analysis of subchromosomal foci in living cells using four-dimensional microscopy. *Biophys J* 77: 2871–2886.
42. Qian H, Sheetz MP, Elson EL (1991) Single particle tracking. Analysis of diffusion and flow in two-dimensional systems. *Biophys J* 60: 910–921.
43. Rosa A, Everaers R (2008) Structure and dynamics of interphase chromosomes. *PLoS Comput Biol* 4: e1000153.
44. Hajjoul H, Mathon J, Ranchon H, et al. (2013) High-throughput chromatin motion tracking in living yeast reveals the flexibility of the fiber throughout the genome. *Genome Res* 23: 1829–1838.
45. Havlin S, Ben-Avraham D (2002) Diffusion in disordered media. *Adv Phys* 51: 187–292.
46. Doi M (1996) *Introduction to polymer physics* Oxford University Press.
47. Bronstein I, Israel Y, Kepten E, et al. (2009) Transient anomalous diffusion of telomeres in the nucleus of mammalian cells. *Phys Rev Lett* 103: 018102.
48. Dion V, Kalck V, Seeber A, et al. (2013) Cohesin and the nucleolus constrain the mobility of spontaneous repair foci. *EMBO Rep* 14: 984–991.
49. Gartenberg MR, Neumann FR, Laroche T, et al. (2004) Sir-mediated repression can occur independently of chromosomal and subnuclear contexts. *Cell* 119: 955–967.
50. Hu Y, Kireev I, Plutz M, et al. (2009) Large-scale chromatin structure of inducible genes: transcription on a condensed, linear template. *J Cell Biol* 185: 87–100.
51. Neumann FR, Dion V, Gehlen LR, et al. (2012) Targeted INO80 enhances subnuclear chromatin movement and ectopic homologous recombination. *Genes Dev* 26: 369–383.
52. Chuang C-H, Carpenter AE, Fuchsova B, et al. (2006) Long-range directional movement of an interphase chromosome site. *Curr Biol* 16: 825–831.
53. Khanna N, Hu Y, Belmont AS (2014) HSP70 transgene directed motion to nuclear speckles facilitates heat shock activation. *Curr Biol* 24: 1138–1144.
54. Chubb JR, Boyle S, Perry P, et al. (2002) Chromatin motion is constrained by association with nuclear compartments in human cells. *Curr Biol* 12: 439–445.

55. Lucas JS, Zhang Y, Dudko OK, et al. (2014) 3D trajectories adopted by coding and regulatory DNA elements: first-passage times for genomic interactions. *Cell* 158: 339–352.
56. Daley JM, Gaines WA, Kwon Y, et al. (2014) Regulation of DNA pairing in homologous recombination. *Cold Spring Harb Perspect Biol* 6: a017954.
57. Lieber MR (2010) The mechanism of double-strand DNA break repair by the nonhomologous DNA end-joining pathway. *Annu Rev Biochem* 79: 181–211.
58. Sonoda E, Hochegger H, Saberi A, et al. (2006) Differential usage of non-homologous end-joining and homologous recombination in double strand break repair. *DNA Repair* 5: 1021–1029.
59. Dion V, Kalck V, Horigome C, et al. (2012) Increased mobility of double-strand breaks requires Mec1, Rad9 and the homologous recombination machinery. *Nat Cell Biol* 14: 502–509.
60. Seeber A, Dion V, Gasser SM (2013) Checkpoint kinases and the INO80 nucleosome remodeling complex enhance global chromatin mobility in response to DNA damage. *Genes Dev* 27: 1999–2008.
61. Lisby M, Mortensen UH, Rothstein R (2003) Colocalization of multiple DNA double-strand breaks at a single Rad52 repair centre. *Nat Cell Biol* 5: 572–577.
62. Nagai S, Dubrana K, Tsai-Pflugfelder M, et al. (2008) Functional targeting of DNA damage to a nuclear pore-associated SUMO-dependent ubiquitin ligase. *Science* 322: 597–602.
63. Kalocsay M, Hiller NJ, Jentsch S (2009) Chromosome-wide Rad51 spreading and SUMO-H2A.Z-dependent chromosome fixation in response to a persistent DNA double-strand break. *Mol Cell* 33: 335–343.
64. Krawczyk PM, Borovski T, Stap J, et al. (2012) Chromatin mobility is increased at sites of DNA double-strand breaks. *J Cell Sci* 125: 2127–2133.
65. Aten JA, Stap J, Krawczyk PM, et al. (2004) Dynamics of DNA double-strand breaks revealed by clustering of damaged chromosome domains. *Science* 303: 92–95.
66. Dimitrova N, Chen Y-CM, Spector DL, et al. (2008) 53BP1 promotes non-homologous end joining of telomeres by increasing chromatin mobility. *Nature* 456: 524–528.
67. Jakob B, Splinter J, Conrad S, et al. (2011) DNA double-strand breaks in heterochromatin elicit fast repair protein recruitment, histone H2AX phosphorylation and relocation to euchromatin. *Nucleic Acids Res* 39: 6489–6499.
68. Ježková L, Falk M, Falková I, et al. (2014) Function of chromatin structure and dynamics in DNA damage, repair and misrepair: γ-rays and protons in action. *Appl Radiat Isot Data Instrum Methods Use Agric Ind Med* 83: 128–136.
69. Chiolo I, Minoda A, Colmenares SU, et al. (2011) Double-strand breaks in heterochromatin move outside of a dynamic HP1a domain to complete recombinational repair. *Cell* 144: 732–744.
70. Nelms BE, Maser RS, MacKay JF, et al. (1998) In situ visualization of DNA double-strand break repair in human fibroblasts. *Science* 280: 590–592.
71. Jakob B, Splinter J, Durante M, et al. (2009) Live cell microscopy analysis of radiation-induced DNA double-strand break motion. *Proc Natl Acad Sci U S A* 106: 3172–3177.
72. Soutoglou E, Dorn JF, Sengupta K, et al. (2007) Positional stability of single double-strand breaks in mammalian cells. *Nat Cell Biol* 9: 675–682.
73. Roukos V, Voss TC, Schmidt CK, et al. (2013) Spatial dynamics of chromosome translocations in living cells. *Science* 341: 660–664.

74. Smerdon MJ, Lieberman MW (1978) Nucleosome rearrangement in human chromatin during UV-induced DNA- reapir synthesis. *Proc Natl Acad Sci U S A* 75: 4238–4241.
75. Ziv Y, Bielopolski D, Galanty Y, et al. (2006) Chromatin relaxation in response to DNA double-strand breaks is modulated by a novel ATM- and KAP-1 dependent pathway. *Nat Cell Biol* 8: 870–876.
76. Burgess RC, Burman B, Kruhlak MJ, et al. (2014) Activation of DNA damage response signaling by condensed chromatin. *Cell Rep* 9: 1703–1717.
77. Smeenk G, Wiegant WW, Marteijn JA, et al. (2013) Poly(ADP-ribosyl)ation links the chromatin remodeler SMARCA5/SNF2H to RNF168-dependent DNA damage signaling. *J Cell Sci* 126: 889–903.
78. Baldeyron C, Soria G, Roche D, et al. (2011) HP1alpha recruitment to DNA damage by p150CAF-1 promotes homologous recombination repair. *J Cell Biol* 193: 81–95.
79. Ayrapetov MK, Gursoy-Yuzugullu O, Xu C, et al. (2014) DNA double-strand breaks promote methylation of histone H3 on lysine 9 and transient formation of repressive chromatin. *Proc Natl Acad Sci U S A* 111: 9169–9174.
80. Zhu L, Brangwynne CP (2015) Nuclear bodies: the emerging biophysics of nucleoplasmic phases. *Curr Opin Cell Biol* 34: 23–30.
81. Chubb JR, Bickmore WA (2003) Considering nuclear compartmentalization in the light of nuclear dynamics. *Cell* 112: 403–406.
82. Lemaître C, Soutoglou E (2015) DSB (Im)mobility and DNA repair compartmentalization in mammalian cells. *J Mol Biol* 427: 652–658.
83. Klein IA, Resch W, Jankovic M, et al. (2011) Translocation-capture sequencing reveals the extent and nature of chromosomal rearrangements in B lymphocytes. *Cell* 147: 95–106.
84. Murr R, Loizou JI, Yang Y-G, et al. (2006) Histone acetylation by Trrap-Tip60 modulates loading of repair proteins and repair of DNA double-strand breaks. *Nat Cell Biol* 8: 91–99.
85. Verschure PJ, van der Kraan I, Manders EMM, et al. (2003) Condensed chromatin domains in the mammalian nucleus are accessible to large macromolecules. *EMBO Rep* 4: 861–866.
86. Bancaud A, Huet S, Daigle N, et al. (2009) Molecular crowding affects diffusion and binding of nuclear proteins in heterochromatin and reveals the fractal organization of chromatin. *EMBO J* 28: 3785–3798.
87. Dinant C, de Jager M, Essers J, et al. (2007) Activation of multiple DNA repair pathways by sub-nuclear damage induction methods. *J Cell Sci* 120: 2731–2740.
88. Kong X, Mohanty SK, Stephens J, et al. (2009) Comparative analysis of different laser systems to study cellular responses to DNA damage in mammalian cells. *Nucleic Acids Res* 37: e68.
89. Gilbert N, Allan J (2014) Supercoiling in DNA and chromatin. *Curr Opin Genet Dev* 25: 15–21.
90. Elbel T, Langowski J (2015) The effect of DNA supercoiling on nucleosome structure and stability. *J Phys Condens Matter Inst Phys J* 27: 064105.
91. Polo SE (2015) Reshaping chromatin after DNA damage: the choreography of histone proteins. *J Mol Biol* 427: 626–636.
92. Downs JA, Lowndes NF, Jackson SP (2000) A role for Saccharomyces cerevisiae histone H2A in DNA repair. *Nature* 408: 1001–1004.
93. Heo K, Kim H, Choi SH, et al. (2008) FACT-mediated exchange of histone variant H2AX regulated by phosphorylation of H2AX and ADP-ribosylation of Spt16. *Mol Cell* 30: 86–97.

94. Li A, Yu Y, Lee S-C, et al. (2010) Phosphorylation of histone H2A.X by DNA-dependent protein kinase is not affected by core histone acetylation, but it alters nucleosome stability and histone H1 binding. *J Biol Chem* 285: 17778–17788.
95. Golia B, Singh HR, Timinszky G (2015) Poly-ADP-ribosylation signaling during DNA damage repair. *Front Biosci Landmark Ed* 20: 440–457.
96. Poirier GG, de Murcia G, Jongstra-Bilen J, et al. (1982) Poly(ADP-ribosyl)ation of polynucleosomes causes relaxation of chromatin structure. *Proc Natl Acad Sci U S A* 79: 3423–3427.
97. de Murcia G, Huletsky A, Lamarre D, et al. (1986) Modulation of chromatin superstructure induced by poly(ADP-ribose) synthesis and degradation. *J Biol Chem* 261: 7011–7017.
98. Xu Y, Ayrapetov MK, Xu C, et al. (2012) Histone H2A.Z controls a critical chromatin remodeling step required for DNA double-strand break repair. *Mol Cell* 48: 723–733.
99. Clapier CR, Cairns BR (2009) The biology of chromatin remodeling complexes. *Annu Rev Biochem* 78: 273–304.
100. Cheezum MK, Walker WF, Guilford WH (2001) Quantitative comparison of algorithms for tracking single fluorescent particles. *Biophys J* 81: 2378–2388.
101. Wombacher R, Heidbreder M, van de Linde S, et al. (2010) Live-cell super-resolution imaging with trimethoprim conjugates. *Nat Methods* 7: 717–719.
102. Benke A, Manley S (2012) Live-cell dSTORM of cellular DNA based on direct DNA labeling. *Chembiochem Eur J Chem Biol* 13: 298–301.
103. Hihara S, Pack C-G, Kaizu K, et al. (2012) Local nucleosome dynamics facilitate chromatin accessibility in living mammalian cells. *Cell Rep* 2: 1645–1656.
104. Récamier V, Izeddin I, Bosanac L, et al. (2014) Single cell correlation fractal dimension of chromatin: a framework to interpret 3D single molecule super-resolution. *Nucl Austin Tex* 5: 75–84.
105. Ricci MA, Manzo C, García-Parajo MF, et al. (2015) Chromatin fibers are formed by heterogeneous groups of nucleosomes in vivo. *Cell* 160: 1145–1158.
106. Zhang Y, Máté G, Müller P, et al. (2015) Radiation induced chromatin conformation changes analysed by fluorescent localization microscopy, statistical physics, and graph theory. *PloS One* 10: e0128555.
107. Llères D, James J, Swift S, et al. (2009) Quantitative analysis of chromatin compaction in living cells using FLIM-FRET. *J Cell Biol* 187: 481–496.
108. Emanuel M, Radja NH, Henriksson A, et al. (2009) The physics behind the larger scale organization of DNA in eukaryotes. *Phys Biol* 6: 025008.
109. Rouse P (1953) A Theory of the Linear Viscoelastic Properties of Dilute Solutions of Coiling Polymers. *J Chem Phys* 21: 1272–1280.
110. Weber SC, Spakowitz AJ, Theriot JA (2010) Bacterial chromosomal loci move subdiffusively through a viscoelastic cytoplasm. *Phys Rev Lett* 104: 238102.
111. Metzler R, Jeon J-H, Cherstvy AG, et al. (2014) Anomalous diffusion models and their properties: non-stationarity, non-ergodicity, and ageing at the centenary of single particle tracking. *Phys Chem Chem Phys* 16: 24128–24164.
112. Mirny LA (2011) The fractal globule as a model of chromatin architecture in the cell. *Chromosome Res Int J Mol Supramol Evol Asp Chromosome Biol* 19: 37–51.

113. Huet S, Lavelle C, Ranchon H, et al. (2014) Relevance and limitations of crowding, fractal, and polymer models to describe nuclear architecture. *Int Rev Cell Mol Biol* 307: 443–479.
114. Barbieri M, Chotalia M, Fraser J, et al. (2012) Complexity of chromatin folding is captured by the strings and binders switch model. *Proc Natl Acad Sci U S A* 109: 16173–16178.
115. Mateos-Langerak J, Bohn M, de Leeuw W, et al. (2009) Spatially confined folding of chromatin in the interphase nucleus. *Proc Natl Acad Sci U S A* 106: 3812–3817.
116. Bohn M, Heermann DW (2010) Diffusion-driven looping provides a consistent framework for chromatin organization. *PloS One* 5: e12218.
117. Jerabek H, Heermann DW (2014) How chromatin looping and nuclear envelope attachment affect genome organization in eukaryotic cell nuclei. *Int Rev Cell Mol Biol* 307: 351–381.
118. Cook PR, Marenduzzo D (2009) Entropic organization of interphase chromosomes. *J Cell Biol* 186: 825–834.
119. Bohn M, Heermann DW (2011) Repulsive forces between looping chromosomes induce entropy-driven segregation. *PloS One* 6: e14428.
120. Jost D, Carrivain P, Cavalli G, et al. (2014) Modeling epigenome folding: formation and dynamics of topologically associated chromatin domains. *Nucleic Acids Res* 42: 9553–9561.
121. Finan K, Cook PR, Marenduzzo D (2011) Non-specific (entropic) forces as major determinants of the structure of mammalian chromosomes. *Chromosome Res Int J Mol Supramol Evol Asp Chromosome Biol* 19: 53–61.
122. Zhang B, Wolynes PG (2015) Topology, structures, and energy landscapes of human chromosomes. *Proc Natl. Acad Sci U S A* 112: 6062–6067.

AIMS Press

The poly(ADP-ribose)-dependent chromatin remodeler Alc1 induces local chromatin relaxation upon DNA damage

Hafida Sellou[a,b,c,†], Théo Lebeaupin[a,b,c,†], Catherine Chapuis[a,b], Rebecca Smith[c], Anna Hegele[c], Hari R. Singh[c], Marek Kozlowski[c], Sebastian Bultmann[d,e], Andreas G. Ladurner[c,e,f], Gyula Timinszky[c,*], and Sébastien Huet[a,b,*]

[a]CNRS, UMR 6290, Institut Génétique et Développement de Rennes, 35043 Rennes, France; [b]Université de Rennes 1, Structure fédérative de recherche Biosit, 35043 Rennes, France; [c]Department of Physiological Chemistry, Biomedical Center Munich, and [d]Department of Biology II, Ludwig-Maximilians-Universität München, 82152 Planegg-Martinsried, Germany; [e]Center for Integrated Protein Science Munich (CIPSM), Department of Chemistry and Biochemistry, Ludwig-Maximilians-Universität München, 81377 Munich, Germany; [f]Munich Cluster for Systems Neurology (SyNergy), Biomedical Center Munich, Ludwig-Maximilians-Universität München, 81377 Munich, Germany

ABSTRACT **Chromatin relaxation is one of the earliest cellular responses to DNA damage. However, what determines these structural changes, including their ATP requirement, is not well understood. Using live-cell imaging and laser microirradiation to induce DNA lesions, we show that the local chromatin relaxation at DNA damage sites is regulated by PARP1 enzymatic activity. We also report that H1 is mobilized at DNA damage sites, but, since this mobilization is largely independent of poly(ADP-ribosyl)ation, it cannot solely explain the chromatin relaxation. Finally, we demonstrate the involvement of Alc1, a poly(ADP-ribose)- and ATP-dependent remodeler, in the chromatin-relaxation process. Deletion of Alc1 impairs chromatin relaxation after DNA damage, while its overexpression strongly enhances relaxation. Altogether our results identify Alc1 as an important player in the fast kinetics of the NAD$^+$- and ATP-dependent chromatin relaxation upon DNA damage in vivo.**

Monitoring Editor
William P. Tansey
Vanderbilt University

Received: May 4, 2016
Revised: Sep 15, 2016
Accepted: Oct 5, 2016

INTRODUCTION

The complex multiscale architecture of chromatin poses a formidable challenge for the DNA repair machinery, which requires regulated access to DNA lesions. Early steps of the DNA damage response involve chromatin remodeling, leading to an increased sensitivity of chromatin to nucleases (Smerdon and Lieberman, 1978). Experiments in living cells have shown that DNA damage induced by laser microirradiation leads to an ATP-dependent but ataxia telangiectasia mutated (ATM)-independent chromatin relaxation at sites of DNA damage (Kruhlak *et al.*, 2006). While the dense packing of chromatin may hinder the efficiency of DNA repair (Schuster-Böckler and Lehner, 2012), recent reports also show that chromatin overcompaction at DNA lesions may also be important to inhibit transcription during repair and to keep the broken DNA ends in close proximity (Ayrapetov *et al.*, 2014; Burgess *et al.*, 2014).

One of the earliest events upon DNA damage is the recruitment and activation of poly(ADP-ribose) polymerase 1 (PARP1), a key regulator of chromatin structure during DNA repair and transcription (Lebeaupin *et al.*, 2015). It is activated by DNA lesions and attaches poly(ADP-ribose) (PAR) to itself and other chromatin factors, including histones. The binding of PARP1 to chromatin modifies its compaction state through multiple, sometimes opposite, mechanisms. Inactive PARP1 competes with the linker histone H1, leading to the formation of compact and transcriptionally repressed genomic regions (Kim *et al.*, 2004). In contrast, PARylated polynucleosomes appear as a loose, beads-on-a-string fiber, on electron micrographs

This article was published online ahead of print in MBoC in Press (http://www.molbiolcell.org/cgi/doi/10.1091/mbc.E16-05-0269) on October 12, 2016.

The authors declare no competing financial interests.

†These authors contributed equally to this work.

*Address correspondence to: Gyula Timinszky (gyula.timinszky@med.lmu.de) and Sébastien Huet (sebastien.huet@univ-rennes1.fr).

Abbreviations used: GFP, green fluorescent protein; HRP, horseradish peroxidase; IgG, immunoglobulin G; KO, knockout; PAR, poly(ADP-ribose); PARP1, poly(ADP-ribose) polymerase 1; PBS, phosphate-buffered saline; RNAi, RNA interference; siRNA, small interfering RNA; YFP, yellow fluorescent protein.

Supplemental Material can be found at:
http://www.molbiolcell.org/content/suppl/2016/10/10/mbc.E16-05-0269v1.DC1

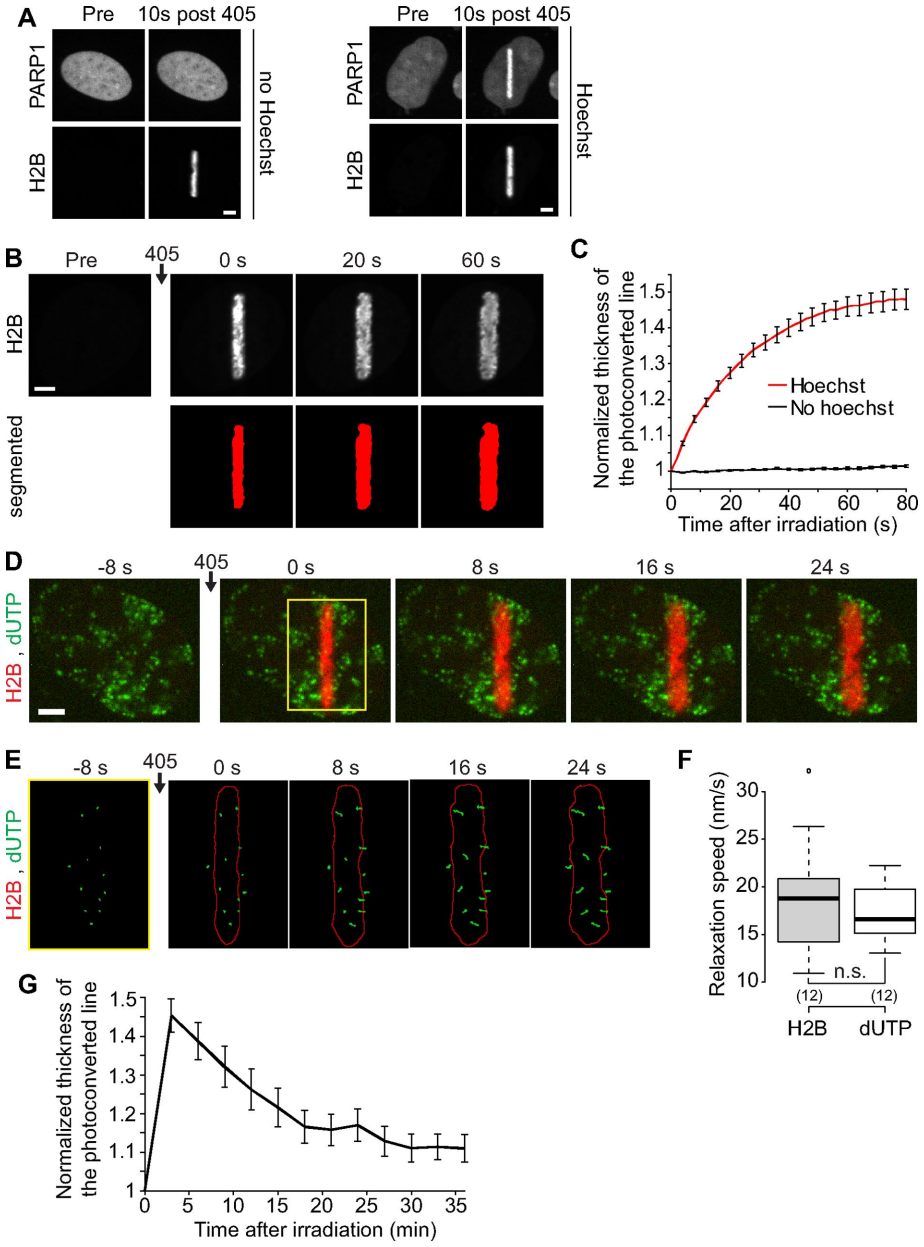

FIGURE 1: DNA damage induced by laser microirradiation induces transient chromatin relaxation. (A) Recruitment of PARP1 at the microirradiated area in cells coexpressing PARP1-mCherry and H2B-PAGFP. Scale bar: 4 μm. In cells not presensitized with Hoechst, the 405 nm irradiation induces local photoactivation of the H2B-PAGFP but no recruitment of PARP1-mCherry. In contrast, in the case of Hoechst presensitization, the 405 nm irradiation induces both photoactivation of the H2B-PAGFP and a marked recruitment of PARP1-mCherry, indicating the presence of DNA lesions. Similarly, we observed the recruitment of 53BP1 only in cells presensitized with Hoechst (unpublished data). (B) Confocal image sequence of a human U2OS nucleus expressing H2B-PAGFP. Scale bar: 4 μm. The automatic segmentation of the histone H2B channel is shown in red below the raw images. The average thickness of the segmented line can be plotted as a function of time after irradiation, as shown in C for cells presensitized ($n = 17$) or not ($n = 23$) with Hoechst (mean ± SEM). Based on this analysis, the ratio between the thicknesses of the photoconverted line at time = 60 s and time = 0 s can be calculated to estimate the relative relaxation of the irradiated region. (D) Confocal image sequence of a U2OS cell expressing H2B-PATagRFP (red) and labeled with fluorescent nucleotides dUTP-ATTO633 (green). Scale bar: 4 μm. (E) Enlarged view of the region overlaid in yellow on the previous panel. The segmentation of the photoconverted chromatin area (red outline) and trajectories of individual foci labeled with fluorescent nucleotides (green) are shown. For this experiment, the power of the 405 nm laser used for simultaneous photoactivation and microirradiation was set to 250 μW at the sample level, instead of 125 μW, to induce an enhanced chromatin relaxation, allowing an easier identification of the phase of directed motion for the dUTP-labeled foci. (F) Comparison between the speed at which the width of the H2B-labeled region is growing and the speed of the dUTP-labeled foci perpendicular to the irradiation line. We show the average speed for the 30 s subsequent to laser microirradiation. *p* Values were calculated by paired *t* test. (G) Dynamics of the chromatin compaction state at DNA damage sites over long timescales measured in wild-type U2OS cell expressing H2B-PATagRFP (mean ± SEM, $n = 16$).

(Poirier *et al.*, 1982). It was suggested that the PARylation of chromatinized H1 could counteract its ability to condense chromatin (Huletsky *et al.*, 1989). Additionally, PARylation is also involved in the recruitment and the regulation of several chromatin-remodeling enzymes whose ATP-dependent activity could promote chromatin relaxation (Chou *et al.*, 2010; Polo *et al.*, 2010; Smeenk *et al.*, 2013).

In the present work, we sought to address the impact of PARP1 on chromatin structure and dynamics following DNA damage. Using photoactivated histones, live-cell imaging, and laser microirradiation in human cells, we analyzed the contributions of PARylation, linker histone H1, ATP, and the nucleosome remodeler Alc1 during the transient chromatin relaxation observed upon DNA damage.

RESULTS AND DISCUSSION

DNA damage induction by laser microirradiation induces a rapid chromatin relaxation at the DNA lesions

To assess large-scale chromatin reorganization at sites of DNA damage in living cells, we established an assay using human U2OS cells expressing the core histone H2B labeled with the photoconvertible dyes PAGFP or PATagRFP. By irradiating a predefined nuclear area with a 405 nm laser, we simultaneously photoconvert the tagged histones and, if cells have been Hoechst-presensitized, induce DNA lesions, allowing us to compare chromatin dynamics in the presence or absence of DNA damage (Figure 1A).

On microirradiation at 405 nm of cells expressing photoactivatable H2B and presensitized with Hoechst, we observed a rapid increase of the size of the photoconverted chromatin area (Figure 1, B and C), indicating chromatin relaxation at DNA damage sites, as previously reported (Kruhlak *et al.*, 2006). However, an alternative interpretation could be the local release

of photoconverted H2B through nucleosome remodeling induced upon DNA damage (Polo, 2015). To distinguish between these two possibilities, we labeled DNA by incorporating fluorescent nucleotides (Schermelleh *et al.*, 2001). On irradiation, we observed the directional movement of fluorescent spots away from the irradiated line (Figure 1, D and E, and Supplemental Movie 1), with a speed similar to the one characterizing the expansion of the H2B photoconverted area (Figure 1F). These results indicate that the changes in the size of the photoactivated H2B area upon DNA damage reflect the relaxation of chromatinized DNA, rather than the local release of photoactivated H2B. This fast initial chromatin relaxation upon DNA damage is followed by a slow recondensation with chromatin recovering a compaction state close to its predamage level in ~20 min (Figure 1G).

Chromatin relaxation at DNA damage sites is controlled by PARP1 activation

In agreement with recent reports (Khurana *et al.*, 2014; Strickfaden *et al.*, 2016), we observed that chromatin relaxation at DNA lesions is PARylation dependent (Figures 2A and Supplemental Figure S1, A–D). Interestingly, inhibiting PARylation not only abolished chromatin relaxation at DNA damage sites but also induced a small but significant chromatin overcompaction upon laser microirradiation (Figure 2A). The human PARP enzyme family has multiple members, and we found that PARP1, PARP2, and PARP3 are all recruited at DNA damage sites (Supplemental Figure S1E). PARP1 is responsible for ~85% of PARylation activity (Woodhouse and Dianov, 2008). Therefore, to address the specific role of PARP1 in chromatin relaxation, we generated PARP1 knockout (KO) U2OS cell lines. While PARP1 was absent from these cells, we could detect similar amounts of PARP2 and PARP3 as compared with wild type (Supplemental Figure S1F). Chromatin relaxation at DNA lesions was dramatically reduced in PARP1 KO cells (Figure 2, A and B), a phenotype that could be partially rescued by reexpressing wild-type PARP1 (Figure 2C). Remarkably, laser irradiation in the PARP1 KOs did not lead to chromatin overcompaction, even after inhibition of PARylation (Figure 2A). Instead, we observed a residual chromatin relaxation independent of PARylation activity, suggesting that it was not triggered by the activity of other PARPs, such as PARP2 or PARP3. Altogether, since PARP inhibitors do not block the recruitment of PARP1 to DNA damage (Timinszky *et al.*, 2009), our data suggest that chromatin overcompaction when inhibiting PARylation is due to PARP1 binding to DNA lesions, whereas its product, PAR, is responsible for chromatin relaxation. These findings reconcile oppositely reported effects of PARP1 on chromatin structure (Poirier *et al.*, 1982; Kim *et al.*, 2004).

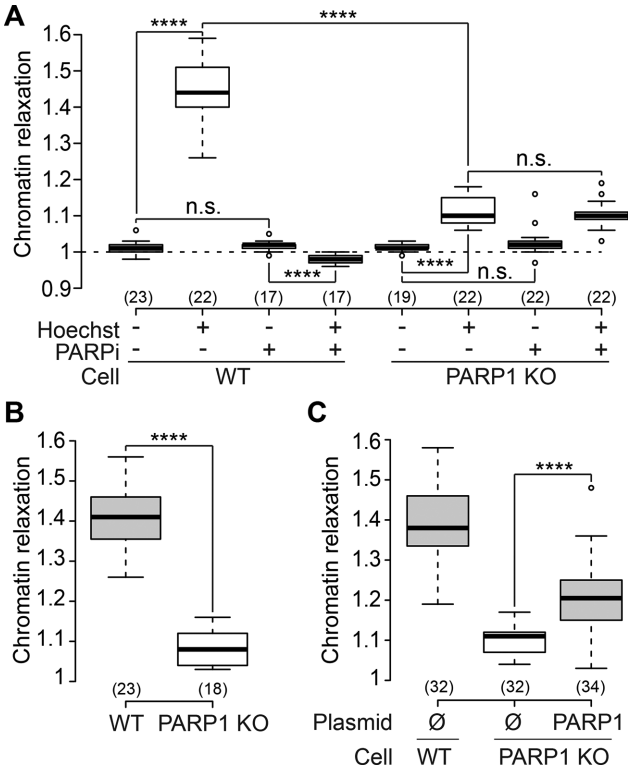

FIGURE 2: PARP1 activity controls chromatin relaxation at DNA damage sites. (A) Relative chromatin relaxation at 60 s after laser microirradiation in wild-type and PARP1 KO cells (clone C8) transfected with H2B-PAGFP and treated or not with the PARP inhibitor AG14361 (30 µM, 1 h; PARPi). (B) Similar results were obtained with a second PARP1 KO cell clone (clone C12). (C) Partial rescue of the impairment of chromatin relaxation in the PARP1 KO cells (clone C8) by reexpression of wild-type PARP1 fused to mCherry.

Chromatin relaxation at DNA lesions is not directly triggered by the mobilization of linker histone H1

In vitro studies identified the linker histone H1 to be crucial for the formation of compact chromatin (Thoma *et al.*, 1979). Because H1 is a substrate of PARP1, PARylation of H1 could trigger its dissociation from chromatin, as shown for regulated transcription (Ju *et al.*, 2006), and lead to chromatin relaxation. To test this hypothesis, we analyzed H1 (H1.1 variant) dynamics at DNA lesions in cells coexpressing H2B-PATagRFP and H1-PAGFP, allowing us to simultaneously label the damaged chromatin area and follow the dynamics of the H1 proteins localized within this area at the time of irradiation (Figure 3A and Supplemental Movie 2). For quantification of the redistribution of photoactivated H1 from the irradiated area independently of the co-occurring chromatin-relaxation process, the integrated fluorescence signal for H1 was measured within the irradiated area defined by the segmentation of the H2B channel (Figure 3B).

We found that H1 initially localized within the irradiated area is released faster in the presence of DNA damage (Figure 3, B and C). Knowing that most H1 molecules are bound to chromatin at any given time (Beaudouin *et al.*, 2006), this can only reflect impaired binding to chromatin. Once the photoconverted H1 proteins are redistributed over the entire nucleus, the DNA damage area appears to be depleted for H1 (Supplemental Figure S1G). This depletion progressively disappears as chromatin slowly recondenses. At the same time, we observed no significant release of the core histone H2B from the irradiated region (Supplemental Figure S1H).

Inhibiting PARylation reduced H1 dynamics both in the presence and absence of DNA damage, while deleting PARP1 only slowed H1 dynamics in the presence of DNA damage (Figure 3C). These data are consistent with the observation that the PARylation of H1 increases its dynamics (Ju *et al.*, 2006). Nevertheless, even in the presence of PARP inhibitor or in the PARP1 KO cells, H1 dynamics were always much faster after DNA damage as compared with the dynamics observed when no damage was induced (Figure 3C). Because chromatin relaxation was abolished in cells treated with PARP inhibitors and strongly reduced in the PARP1 KOs (Figure 2A), this indicates that chromatin loosening at DNA lesions is not the direct consequence of PAR-driven H1 mobilization at DNA lesions. This result contrasts with a recent report that correlates H1 eviction and PAR-dependent chromatin relaxation at DNA lesions (Strickfaden *et al.*, 2016). The discrepancy with our findings may arise from the

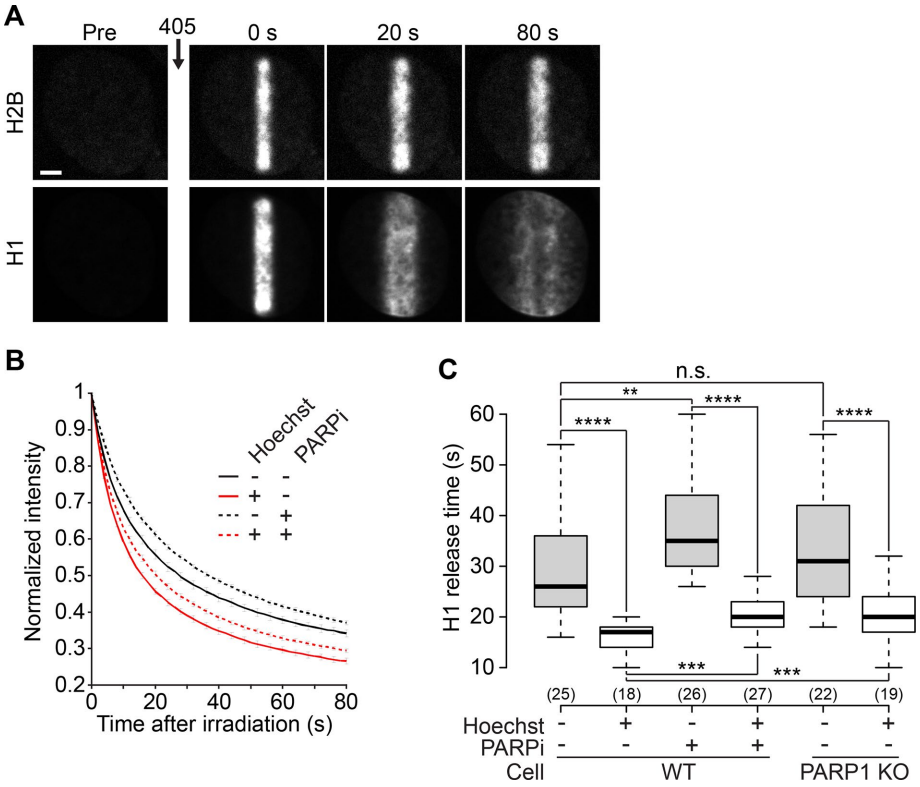

FIGURE 3: The linker histone H1 is mobilized at DNA lesions. (A) Confocal image sequence of a U2OS nucleus coexpressing H2B-PATagRFP and H1.1-PAGFP. For the H1 channel, the image contrast was enhanced to allow the visualization of H1 redistribution over the entire nucleus following laser microirradiation. This led to an apparent saturation of the image at time = 0 s. Scale bar: 4 μm. (B) Kinetics of the release of the H1 proteins localized at the DNA lesions at the time of laser microirradiation in wild-type cells coexpressing H2B-PATagRFP and H1.1-PAGFP, presensitized or not with Hoechst and treated or not with the PARP1 inhibitor AG14361 (30 μM, 1 h; PARPi) (mean ± SEM, for each condition, 17 < *n* < 28). (C) Characteristic release time for H1, measured at half fluorescence decay, in wild-type and PARP1 KO cells.

difference in laser-irradiation methods, which could lead to different DNA damage (Kong *et al.*, 2009). Nevertheless, we cannot exclude that the PARylation-dependent chromatin relaxation requires concomitant H1 mobilization, which is always observed upon DNA damage independent of PARP1 activation. Furthermore, it is possible that the DNA damage–induced H1 mobilization accounts for the observed residual chromatin relaxation observed in the PARP1 KOs.

Contribution of ATP-dependent processes in chromatin relaxation at DNA lesions

In vitro PARP1 activation results in chromatin loosening in the absence of ATP (Poirier *et al.*, 1982), whereas ATP depletion abolishes chromatin relaxation at DNA lesions in live cells (Kruhlak *et al.*, 2006; Luijsterburg *et al.*, 2012). To establish the role of ATP in our assays, we quantified chromatin relaxation and PARylation levels upon laser microirradiation in cells depleted for ATP. We found that ATP depletion significantly impaired chromatin relaxation upon DNA damage (Figure 4A) while not affecting the level of PARylation at the lesions, as shown by the similar accumulation of the PAR-binder WWE domain of RNF146 at DNA damage sites (Figure 4B) (Wang *et al.*, 2012). Nevertheless, ATP depletion did not fully abolish chromatin relaxation, its amplitude corresponding to approximately half of the control situation. This result suggests that PARylation may act on chromatin in both ATP-dependent and ATP-independent ways but it may also be due to only partial depletion of ATP. A confounding effect of ATP inhibition is chromatin hypercondensation (Figure 4C). To test whether chromatin hypercondensation could explain the inhibition of chromatin relaxation seen upon ATP depletion, we induced chromatin tightening in another way. Cells were bathed in hypertonic medium to induce a shrinking of the nuclear volume (Figure 4, D and E), which in turn leads to chromatin hypercondensation. The chromatin patterns in hypertonic cells visually resembled those obtained after ATP depletion (Figure 4C). The hypertonic treatment itself does not activate the PARylation signaling pathway (Figure 4, F and G). In hypertonic cells, chromatin loosening upon DNA damage was slightly increased compared with isotonic controls (Figure 4H), while PARylation at the site of damage was unchanged (Figure 4I). Thus the reduction of chromatin relaxation at DNA lesions observed upon ATP depletion does not seem to be the mere consequence of a tighter chromatin packing before damage induction.

The ATP-dependent remodeler Alc1 contributes to chromatin relaxation at DNA damage sites

Several ATP-dependent chromatin-remodeling enzymes have been shown to be regulated by PARP activation (Chou *et al.*, 2010; Polo *et al.*, 2010; Smeenk *et al.*, 2013). However, the only chromatin-remodeling enzyme with an ADP-ribose–binding domain that actively remodels nucleosomes upon PARP1 activation is Alc1 (Ahel *et al.*, 2009; Gottschalk *et al.*, 2009; Pines *et al.*, 2012). To address the role of Alc1, also known as CHD1L, in chromatin relaxation, we generated an Alc1 KO U2OS cell line (Supplemental Figure S2A). By coexpressing a fluorescently tagged version of Alc1 together with H2B-PAGFP in these cells, we followed the recruitment of this protein at DNA damage sites together with the relaxation process (Figure 5, A and B). The fast accumulation of Alc1 observed at the site of DNA damage, with a maximum recruitment a few seconds after laser microirradiation, is compatible with a role for Alc1 in chromatin relaxation at DNA breaks, a process that lasts approximately 60 s. Moreover, the recruitment of Alc1 at DNA damage sites was abolished by PARP inhibitor treatment or for Alc1 lacking the PAR-binding macrodomain (Supplemental Figure S2, B and C), indicating that Alc1 recruitment, similar to chromatin relaxation, is fully controlled by PARP1 activation at DNA lesions.

The loss of Alc1 had no detectable effect on chromatin architecture in the absence of DNA damage (Figure 5C and Supplemental Figure S2, D and E) but led to impaired chromatin relaxation upon laser irradiation (Figure 5D and Supplemental Figure S2, F and G). Expression of wild-type Alc1 in Alc1 KOs fully restored chromatin relaxation at DNA lesions in contrast to the expression of ATPase-dead Alc1 mutants (Alc1-E175Q or Alc1-K77R) despite their efficient recruitment at DNA damage sites (Supplemental Figure S2, B and H). Cells depleted for Alc1 using RNA interference (RNAi) behaved in a similar manner (Supplemental Figure S2, I and J). While ATP depletion only slightly reduced chromatin relaxation in the Alc1

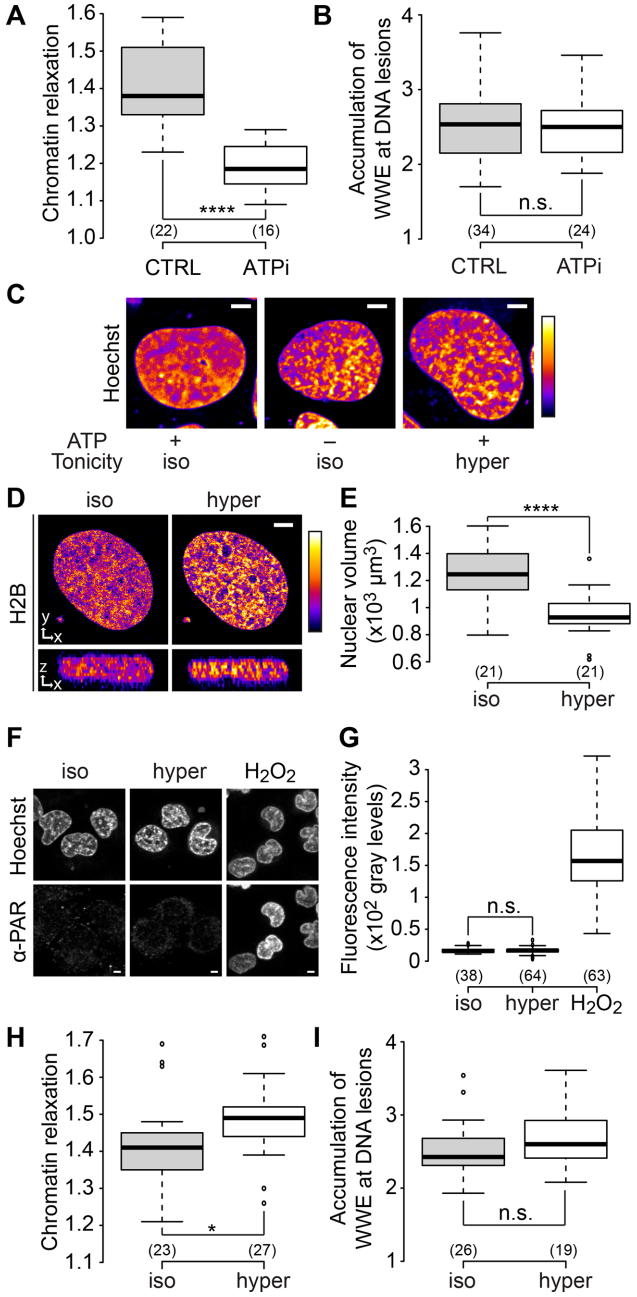

FIGURE 4: Chromatin relaxation at DNA damage sites partially depends on ATP. (A) Relative chromatin relaxation at 60 s after laser microirradiation in wild-type cells expressing H2B-PAGFP and depleted or not for ATP. (B) Accumulation of the WWE domain of RNF146 at the DNA lesions estimated 60 s after laser microirradiation in wild-type cells expressing an EGFP-tagged version of WWE and depleted or not for ATP. (C) Confocal image of U2OS cell nuclei stained with Hoechst and left untreated, depleted for ATP, or bathed with hypertonic medium. Scale bar: 4 µm. (D) Middle *x,y* and *x,z* sections of raw confocal image stacks of a U2OS cell expressing H2B-EGFP before and after the change of the bathing medium from isotonic to hypertonic. Scale bar: 4 µm. For C and D, fluorescence signals are pseudocolored using the lookup table shown on the right of the images. (E) Change in nuclear volumes of U2OS cells expressing H2B-EGFP upon hypertonic treatment. The nuclear volumes were estimated by automatic segmentation of confocal image stacks. (F, G) Images and quantification of immunofluorescence staining with anti-PAR (10H) antibody performed in U2OS cells left untreated, subjected to hypertonic shock, or treated with H_2O_2 (1 mM in PBS for 10 min). (H) Relative chromatin relaxation at 60 s after laser microirradiation in wild-type cells expressing H2B-PAGFP and bathed in isotonic or hypertonic media. (I) Accumulation of the WWE domain of RNF146 at the DNA lesions estimated 60 s after laser microirradiation in wild-type cells bathed in isotonic or hypertonic medium.

KO cells (Figure 5E), the inhibition of PARylation completely suppressed the relaxation process (Figure 5F), suggesting that the remaining chromatin relaxation observed at DNA damage sites in the absence of Alc1 is mediated mainly by the ATP-independent loosening effect of PARylation. Importantly, the overexpression of Alc1 in wild-type cells strongly increased chromatin relaxation at DNA lesions, while overexpressing the ATPase-dead Alc1-E175Q had no effect (Figure 5G). Altogether these results identify Alc1 as a mediator of PARylation-dependent chromatin relaxation through its ATP-dependent remodeling activity. A recent publication also reported the role of the remodeler CHD2 in the chromatin relaxation at DNA lesions (Luijsterburg *et al.*, 2016). Because CHD2 appears to be recruited at the DNA damage sites slightly later than Alc1, the two remodelers may act sequentially to allow chromatin loosening. Further work is required to understand how the activities of these two remodelers are coordinated.

In conclusion, our present work extends our understanding of the contribution of the PARylation signaling pathway in the early chromatin remodeling at DNA lesions. We demonstrate the dual impact of PARP1 on the chromatin structure. In line with in vitro observations (Kim *et al.*, 2004), our data in living cells indicate that PARP1 binding to DNA breaks leads to chromatin overcompaction while the formation of PAR chains due to PARP1 activity triggers its relaxation, in agreement with a recent report (Strickfaden *et al.*, 2016). Moreover, our data show for the first time the direct contribution of the ATP-dependent chromatin-remodeling activity of the remodeler Alc1 in the rapid chromatin relaxation observed upon DNA damage induction. We also found that the absence of either PARP1 or Alc1 reduces cell survival capacity upon X-ray irradiation (Figure 5H). This result, which corroborates other reports showing that several members of the PARylation signaling pathway are important for efficient DNA repair (Khurana *et al.*, 2014; Nagy *et al.*, 2016), argues for a key regulatory role of the PARylation-dependent modulation of the chromatin compaction state during the DNA damage response. In addition, we propose that the dramatic increase in chromatin relaxation together with the cell hypersensitivity to X-ray irradiation observed in the case of Alc1 overexpression (Figure 5, G and H) might underlie the oncogenic potential of this remodeler, which has been shown to promote cancer progression and metastasis (Cheng *et al.*, 2013).

MATERIALS AND METHODS

Plasmids

The core histone H2B, subcloned from the pH2B-mCherry vector was a gift from J. Ellenberg, European Molecular Biology Laboratory, Heidelberg, Germany (Neumann *et al.*, 2010; Euroscarf accession number P30632), was cloned into pPATagRFP-N1 using *Nde*I and *Bam*HI restriction sites. pPATagRFP-N1 was a gift from V. Verkhusha, Albert Einstein College of Medicine, Bronx, NY (Subach *et al.*, 2010; Addgene plasmid #31941). The histone H2B-PAGFP and histone H1.1-PAGFP were gifts from J. Ellenberg (Beaudouin *et al.*, 2006; Euroscarf accession numbers P30499 and P30503, respectively). Another construct of H1.1-PAGFP was produced with the PAGFP tag on the other side of the protein to ensure that similar

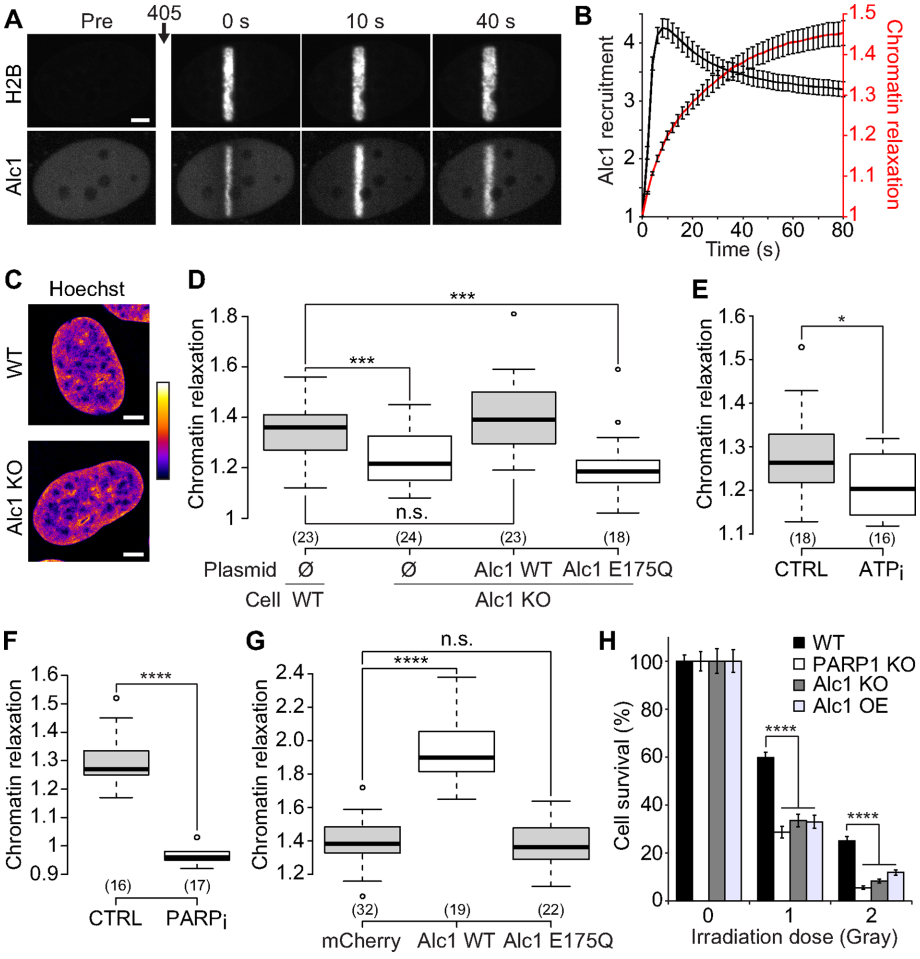

FIGURE 5: The chromatin remodeler Alc1 contributes to chromatin relaxation upon DNA damage. (A) Confocal image sequence of a U2OS nucleus coexpressing H2B-PAGFP and Alc1-mCherry. Scale bar: 4 µm. (B) Relative kinetics of Alc1 recruitment and chromatin relaxation at the DNA lesions measured in Alc1 KO cells coexpressing H2B-PAGFP and Alc1-mCherry (mean ± SEM, $n = 20$). (C) Confocal images of wild-type and Alc KO U2OS cells labeled with Hoechst. Scale bar: 4 µm. Fluorescence signals are pseudocolored using the lookup table shown on the right of the images. (D) Relative chromatin relaxation at 60 s after laser microirradiation for wild-type vs. Alc1 KO cells cotransfected with H2B-PAGFP and an empty plasmid (Ø), wild-type Alc1 or the catalytic-dead mutant Alc1 E175Q, both fused to mCherry. Cells with comparable expression levels of the wild-type or mutant Alc1 constructs were chosen, as assessed by similar fluorescence signals in the mCherry channel. (E) Relative chromatin relaxation at 60 s after laser microirradiation in Alc1 KO cells expressing H2B-PAGFP and depleted or not for ATP. (F) Relative chromatin relaxation at 60 s after laser microirradiation in Alc1 KO cells expressing H2B-PAGFP and treated or not with the PARP1 inhibitor AG14361 (30 µM, 1 h). (G) Relative chromatin relaxation at 60 s after laser microirradiation for wild-type cells expressing H2B-PAGFP and transfected with uncoupled mCherry, wild-type Alc1 fused to mCherry, or the catalytic-dead mutant Alc1 E175Q fused to mCherry. Cells with comparable expression levels of the transfected constructs were chosen, as assessed by similar fluorescence signals in the mCherry channel. (H) Clonogenic survival after different doses of X-ray irradiation for wild-type U2OS cells, KOs for Alc1 and PARP1, and wild-type cells overexpressing Alc1 fused to YFP.

fused to YFP was described previously (Gottschalk *et al.*, 2009).The Alc1-K77R construct fused to mCherry was obtained by first mutating a wild-type ALC1 construct fused to YFP (Gottschalk *et al.*, 2009), using QuikChange in vitro mutagenesis (Agilent, Santa Clara, CA), and then exchanging YFP for mCherry. The WWE domain of RNF146 (amino acids 99–183) was cloned into pmEGFP-C1 using *Bgl*II and *Eco*RI by PCR amplifying it from a cDNA library. PARP1-mCherry was described previously (Timinszky *et al.*, 2009). This construct was also used to generate PARP1-EGFP by exchanging mCherry with EGFP. PARP2-EGFP was generated by PCR amplification of PARP2, digestion with *Nhe*I/*Sma*I, and ligation into pmEGFPC1. PARP3-EGFP (short isoform) was a gift from C. Prigent, Institut de Génétique et Développement de Rennes, CNRS, France (Rouleau *et al.*, 2007). Mammalian expression was under the control of cytomegalovirus (CMV) promoter. All constructs were sequence verified.

Cell culture, inhibitor treatments, and osmotic shocks

Cells used for this work were wild-type U2OS cells or KO cells made from parental U2OS cells. Cells were routinely cultured in DMEM (with 4.5 g/l glucose) supplemented with 10% fetal bovine serum (FBS), 2 mM glutamine, 100 µg/ml penicillin, and 100 U/ml streptomycin in 5% CO_2 at 37°C. For microscopy, cells were plated on Lab-Tek II chambered coverglass (Thermo Fisher Scientific, Waltham, MA). Presensitization was achieved by bathing cells for 1 h in culture medium containing 0.3 µg/ml Hoechst 33342 (Life Technologies, Carlsbad, CA). Immediately before imaging, the growth medium was replaced by Leibovitz's L-15 medium (Life Technologies) supplemented with 20% FBS, 2 mM glutamine, 100 µg/ml penicillin, and 100 U/ml streptomycin. The PARP1 inhibitors AG14361 and Olaparib (Euromedex, Souffelweyersheim, France) were used at 30 and 50 µM, respectively. ATP depletion was achieved as previously described (Platani *et al.*, 2002). The osmotic shock procedure was as previously described (Walter *et al.*, 2013). All experiments presented in this work were performed on unsynchronized cells.

results could be obtained with both constructs (Hutchinson *et al.*, 2015). H1.1 was PCR amplified from the H1.1-PAGFP plasmid and subcloned into pmEGFP-N1 using *Bgl*II and *Apa*I to obtain the H1.1-EGFP construct. Wild-type Alc1 and E175Q Alc1 mutant fused to the C-terminus of enhanced green fluorescent protein (EGFP) or mCherry were obtained by exchanging yellow fluorescent protein (YFP) for the respective fluorescent protein in the constructs described previously (Gottschalk *et al.*, 2009). The Alc1-Δmacro mutant

Live-cell DNA labeling with fluorescent nucleotides

U2OS cells expressing H2B-PATagRFP were synchronized at the G_1/S phase transition by treating the cells with aphidicolin (Sigma-Aldrich, St. Louis, MO) at 5 µg/ml for 18 h. After aphidicolin release, the cell layer, bathed with growing medium containing 10 µM of dUTP-ATTO633 (Jena Bioscience, Jena, Germany), was scraped using a silicon stick to allow nucleotide loading and integration to the DNA during replication (Schermelleh *et al.*, 2001).

Transfections and generation of stable and KO cell lines

Transient transfections were performed 12–24 h after cells were plated, using XtremeGENE HP (Roche, Basel, Switzerland) or JetPRIME (Polyplus Transfection, Illkirch, France) according to the manufacturers' instructions. Cells were imaged 48–72 h after transfection.

To establish cell lines stably expressing H2B-PATagRFP or Alc1-YFP (construct described in Gottschalk *et al.*, 2009), wild-type U2OS cells were transfected with the appropriate DNA construct and grown in culture medium containing Geneticin (PAA Laboratories, Pasching, Austria) for selection. Clones with stably integrated H2B-PATagRFP or Alc1-YFP were picked after 2 wk of Geneticin selection. Once selected, these cells were cultured in normal medium supplemented with 500 µg/ml Geneticin.

The KO cell lines were made according to the protocol described by the Zhang lab (Ran *et al.*, 2013). The target sequence for *ALC1* (5′-GACTTCCCTCAAGTACGTTAG-3′) and PARP1 (5′-GTCCAACAG-AAGTACGTGCAA-3′) was chosen according to the Web-based CRISPR design tool from the Zhang lab (www.genome-engineering.org). The sgRNA oligos were introduced into pX458 expressing Cas9 nuclease fused to green fluorescent protein (GFP; Addgene #48138). pSpCas9(BB)-2A-GFP (PX458) was a gift from Feng Zhang (Broad Institute of MIT and Harvard, Cambridge, MA; Addgene plasmid #48138). We transfected the plasmids using the transfection reagent XtremeGENE HP (Roche) according to the manufacturer's protocol. Single GFP-positive cells were sorted into 96-well plates using FACS. The KO cell lines grown from the single cells were identified by Western blot using specific antibodies against PARP1 or Alc1.

Small interfering RNA (siRNA) knockdown

For RNAi-mediated knockdown, we used SilencerSelect Negative Control No. 2 (ref. 4390846) and siRNA against Alc1 (CHD1L; ref. s18358) from Ambion (Thermo Fisher Scientific). Cells grown in normal culture medium were transfected with 500 nM siRNA using Oligofectamine (Life Technologies) according to the manufacturer's instructions. After 48 h, cells were used for imaging or harvested for protein analysis.

Western blot

Cell lysates were separated using SDS–PAGE, transferred to nitrocellulose membranes (GE Healthcare, Little Chalfont, UK), and blocked in 5% (wt/vol) milk powder in 0.05% (vol/vol) phosphate-buffered saline (PBS)-Tween 20 at room temperature. The primary antibodies were diluted in 5% (wt/vol) milk powder in 0.05% (vol/vol) PBS-Tween 20 and used at the following concentrations: affinity-purified anti-Alc1 rabbit polyclonal, 1:2500; anti-actin (Sigma-Aldrich; A5060), 1:1000; anti-PARP1 rabbit polyclonal, 1:10,000; anti-PARP2 polyclonal rabbit antibody (Active Motif, Carlsbad, CA; #39743), 1:1000; anti-PARP3 polyclonal rabbit (Thermo Fisher Scientific; PA5-21478), 2 µg/ml; and the mouse monoclonal (DM1A) anti-tubulin (Sigma-Aldrich; T9026), 1:20,000. Horseradish peroxidase (HRP)-conjugated secondary antibodies were used to detect primary antibodies. The HRP-conjugated anti-rabbit immunoglobulin G (IgG) and anti-mouse IgG antibodies (BioRad, Hercules, CA) were used at 1:10,000, and the blot was developed using the ELC reagent (Merck Millipore, Billerica, MA).

Immunofluorescence staining

Cells were washed once in PBS and incubated in serum-free DMEM containing either dimethyl sulfoxide, Olaparib (50 µM), or AG14631 (30 µM) for 1 h. Cells were then exposed to H_2O_2 (0.5 mM) in serum-free DMEM for 10 min and fixed in ice-cold methanol:acetone (1:1) for 10 min. After being washed once with PBS and then blocked for 1 h (5% milk in PBS + 0.05% Tween-20), cells were incubated with anti–poly-ADPr mouse monoclonal 10H antibody (ascites) diluted (1:800) in blocking buffer overnight at 4°C. They were then washed three times with PBS + 0.1% Triton X-100 before being incubated with Alexa Fluor 488 anti-mouse IgG (4 µg/ml; Life Technologies) in blocking buffer for 1 h, after which they were washed three times with PBS + 0.1% Triton X-100, and nuclei were stained using Hoescht (1 µg/ml) for 10 min. Cells were washed twice with PBS + 0.1% Triton X-100 before imaging.

Quantification of cell viability upon X-ray irradiation

Cells were seeded at a density of 500 cells per well in a 12-well plate. Plates were immediately treated with X-ray irradiation (1 or 2 Gy) (Faxitron, Tucson, AZ) and returned to the incubator for 11 d to allow colony formation. Cells were washed once with PBS before being fixed and stained for 30 min with a 4% paraformaldehyde and 0.5% crystal violet solution. Staining solution was removed, and plates were immersed in water to remove excess stain. The colony area percentage was calculated using the ColonyArea plug-in for ImageJ according to Guzmán *et al.* (2014). Average colony area percentage was normalized to an untreated control.

Live-cell imaging and laser microirradiation

Live-cell imaging was performed on an inverted confocal spinning disk (imaging scan head CSU-X1 from Yokogawa [Tokyo, Japan] and microscope body Ti-E from Nikon [Tokyo, Japan]) equipped with a single-point scanning head to allow laser microirradiation and local photoactivation using a 405 nm laser. We used a Plan APO 63×, oil-immersion objective lens (numerical aperture [N.A.] 1.4) and a sCMOS ORCA Flash 4.0 camera (Hamamatsu, Hamamatsu, Japan) for imaging the cells. The pixel resolution at the object plane was 108 nm. The fluorescence of EGFP and the activated form of PAGFP was excited with a laser at 488 nm, and the fluorescence of mCherry and the activated form of PATagRFP was excited with a laser at 561 nm. For fluorescence detection, we used band-pass filters adapted to the fluorophores. Laser powers were adjusted to minimize bleaching during the time-lapse acquisitions. Photoactivation and DNA damage were induced simultaneously using a 405 nm laser. The power of the 405 nm laser used for photoactivation and, for cells presensitized with Hoechst, induction of DNA lesions, was set to 125 µW at the sample level, unless stated otherwise. Cells were irradiated along a 16-µm-long line crossing the nucleus. The microscope was equipped with a heating chamber to maintain cells at 37°C during the imaging experiments. When long time-lapse experiments of 30–60 min to study chromatin remodeling in response to DNA damage were performed, premature cell death that would indicate a phototoxic effect due to imaging was never observed.

Images shown in Supplemental Figure S1, A and C, were taken on an inverted AxioObserver Z1 confocal spinning-disk microscope (Zeiss, Oberkochen, Germany) equipped with a single-point scanning head for laser microirradiation and local photoactivation using a 405 nm laser (Rapp OptoElectronic). We used a C-Apo 63×, water-immersion objective lens (N.A. 1.2), and the images were acquired on a AxioCam HRm CCD camera (Zeiss). The pixel resolution at the object plane was 171 nm. The fluorescence of EGFP and YFP was excited with a laser at 488 nm, and the fluorescence of the activated form of PATagRFP was excited with a laser at 561 nm. For fluorescence detection, we used band-pass filters adapted to the fluorophores. The microirradiation conditions at 405 nm were adjusted to obtain amplitudes of the chromatin relaxation at DNA lesions that were similar to those obtained with the system described above. A heating chamber was used to maintain the cells at 37°C.

Image analysis

The time-lapse sequences were analyzed automatically using custom-made routines written in Matlab (Mathworks, Natick, MA) to quantify chromatin relaxation at DNA lesions. The chromatin area microirradiated at 405 nm and tagged with photoactivatable H2B was segmented by *k*-means segmentation. An ellipsoid was fitted to the segmented area, and its minor axis length was used to estimate the width of the microirradiated chromatin area and thus assess changes in the chromatin compaction level.

To analyze the release of the photoactivatable H1 proteins from the area irradiated at 405 nm, we measured the H1 integrated intensity inside the segmented microirradiated chromatin area in cells coexpressing H1 and H2B tagged with two different photoactivatable dyes. This intensity was divided by the H1 intensity integrated over the whole nucleus to correct for bleaching and small focus drifts. For this step, whole nuclei were segmented using the low fluorescence signal coming from the nonactivated tagged H2B proteins. The same approach was used to analyze the release of the H2B proteins from DNA lesions and to characterize Alc1 recruitment kinetics.

When necessary, nuclei movements occurring during the time-lapse experiments were corrected using the ImageJ plug-in StackReg (Thévenaz *et al.*, 1998).

The accumulation of the fluorescently tagged WWE domain of RNF146 at the DNA lesions was quantified as follows. The mean fluorescence intensity in three areas was estimated by manual segmentation: at the site of DNA damage (I_d), in a region of the nucleus not subjected to laser irradiation (I_{nd}), and outside the cells (I_{bg}). The accumulation of the WWE domain at the DNA lesions A_{WWE} was then calculated as

$$A_{WWE} = \frac{I_d - I_{bg}}{I_{nd} - I_{bg}}$$

For quantifying the immunofluorescence staining with anti-PAR (10H) antibody, the nuclei were segmented using Hoechst staining, and the mean fluorescence intensity for the anti-PAR antibody was measured inside each nucleus after background subtraction.

For chromatin texture analysis, wild-type and Alc1 KO U2OS cells were plated on Lab-Tek II chambered coverglasses, fixed with 4% paraformaldehyde for 10 min at room temperature, and stained with Hoechst 33342 (1 µg/ml) for 1 h. Confocal images were captured on a Leica SP8 confocal microscope using a Plan APO 63×, oil-immersion objective lens (N.A. 1.4). Hoechst staining was excited with a 405-nm laser, and the emission band was chosen to optimize fluorescence collection. The pinhole was set to one Airy unit, and we used a pixel size of 60 nm. The GLCM ImageJ texture plug-in written by Julio E. Cabrera was used to analyze chromatin texture. The correlation and contrast parameters were chosen to characterize chromatin texture using a pixel-to-pixel distance of 7 pixels, which allowed maximizing the differences measured between the cells bathed with the isotonic medium and those subjected to osmotic stress.

In cells labeled with fluorescent nucleotides, the chromatin dynamics was assessed by tracking the fluorescently labeled DNA replication foci using the plug-in Particle Tracker from ImageJ (Sbalzarini and Koumoutsakos, 2005).

Statistics

In the figure legends, *n* refers to the number of cells used for a given experimental condition. Box plots were generated using a Web tool developed by the Tyers and Rappsilber labs (http://boxplot.tyerslab.com). The box limits correspond to the 25th and 75th percentiles, and the bold line indicates the median value. The whiskers extend 1.5 times the interquartile range, and outliers are shown by dots. The numbers in parentheses refers to the number of cells for each condition. Unless stated otherwise, *p* values were calculated using an unpaired Student's *t* test, assuming unequal variances. On the box plots: *, $p < 0.05$; **, $p < 0.01$; ***, $p < 0.001$; ****, $p < 0.0001$; n.s., not significant.

ACKNOWLEDGMENTS

We thank the Microscopy Rennes Imaging Center (BIOSIT, Université Rennes 1) for technical assistance. This work was supported by the Agence National de la Recherche (JCJC-SVSE2-2011, ChromaTranscript project to S.H.), the Ligue contre le Cancer du Grand-Ouest (commitees 35 and 72 to S.H.), the European Union (FP7-PEOPLE-2011-CIG, ChromaTranscript project to S.H.; and Marie Curie Initial Training Network, Nucleosome4D to A.G.L.), the Deutsche Forschungsgemeinschaft (TI 817/2-1 to G.T.; and SFB collaborative research center 1064 to A.G.L.), and Worldwide Cancer Research (14-1315 to G.T.). H.S.'s PhD fellowship was funded by the Centre National de la Recherche Scientifique and the Région Bretagne. Our collaboration benefited from funding from the Hubert Curien partnership/German Academic Exchange Service–DAAD (28486ZD to S.H.; 55934632 to G.T.) and the Deutsche Forschungsgemeinschaft CIPSM and SyNergy excellence clusters (to A.G.L.).

REFERENCES

Ahel D, Horejsí Z, Wiechens N, Polo SE, Garcia-Wilson E, Ahel I, Flynn H, Skehel M, West SC, Jackson SP, *et al.* (2009). Poly(ADP-ribose)-dependent regulation of DNA repair by the chromatin remodeling enzyme ALC1. Science 325, 1240–1243.

Ayrapetov MK, Gursoy-Yuzugullu O, Xu C, Xu Y, Price BD (2014). DNA double-strand breaks promote methylation of histone H3 on lysine 9 and transient formation of repressive chromatin. Proc Natl Acad Sci USA 111, 9169–9174.

Beaudouin J, Mora-Bermúdez F, Klee T, Daigle N, Ellenberg J (2006). Dissecting the contribution of diffusion and interactions to the mobility of nuclear proteins. Biophys J 90, 1878–1894.

Burgess RC, Burman B, Kruhlak MJ, Misteli T (2014). Activation of DNA damage response signaling by condensed chromatin. Cell Rep 9, 1703–1717.

Cheng W, Su Y, Xu F (2013). CHD1L: a novel oncogene. Mol Cancer 12, 170.

Chou DM, Adamson B, Dephoure NE, Tan X, Nottke AC, Hurov KE, Gygi SP, Colaiácovo MP, Elledge SJ (2010). A chromatin localization screen reveals poly (ADP ribose)-regulated recruitment of the repressive polycomb and NuRD complexes to sites of DNA damage. Proc Natl Acad Sci USA 107, 18475–18480.

Gottschalk AJ, Timinszky G, Kong SE, Jin J, Cai Y, Swanson SK, Washburn MP, Florens L, Ladurner AG, Conaway JW, *et al.* (2009). Poly(ADP-ribosyl)ation directs recruitment and activation of an ATP-dependent chromatin remodeler. Proc Natl Acad Sci USA 106, 13770–13774.

Guzmán C, Bagga M, Kaur A, Westermarck J, Abankwa D (2014). ColonyArea: an ImageJ plugin to automatically quantify colony formation in clonogenic assays. PLoS One 9, e92444.

Huletsky A, de Murcia G, Muller S, Hengartner M, Ménard L, Lamarre D, Poirier GG (1989). The effect of poly(ADP-ribosyl)ation on native and H1-depleted chromatin. A role of poly(ADP-ribosyl)ation on core nucleosome structure. J Biol Chem 264, 8878–8886.

Hutchinson JB, Cheema MS, Wang J, Missiaen K, Finn R, Gonzalez Romero R, Th'ng JPH, Hendzel M, Ausió J (2015). Interaction of chromatin with a histone H1 containing swapped N- and C-terminal domains. Biosci Rep 35, e00209.

Ju B-G, Lunyak VV, Perissi V, Garcia-Bassets I, Rose DW, Glass CK, Rosenfeld MG (2006). A topoisomerase IIβ-mediated dsDNA break required for regulated transcription. Science 312, 1798–1802.

Khurana S, Kruhlak MJ, Kim J, Tran AD, Liu J, Nyswaner K, Shi L, Jailwala P, Sung MH, Hakim O, *et al.* (2014). A macrohistone variant links dynamic

chromatin compaction to BRCA1-dependent genome maintenance. Cell Rep 8, 1049–1062.
Kim MY, Mauro S, Gévry N, Lis JT, Kraus WL (2004). NAD^+-dependent modulation of chromatin structure and transcription by nucleosome binding properties of PARP-1. Cell 119, 803–814.
Kong X, Mohanty SK, Stephens J, Heale JTGomez-Godinez V, Shi LZ, Kim J-S, Yokomori K, Berns MW (2009). Comparative analysis of different laser systems to study cellular responses to DNA damage in mammalian cells. Nucleic Acids Res 37, e68.
Kruhlak MJ, Celeste A, Dellaire G, Fernandez-Capetillo O, Müller WG, McNally JG, Bazett-Jones DP, Nussenzweig A (2006). Changes in chromatin structure and mobility in living cells at sites of DNA double-strand breaks. J Cell Biol 172, 823–834.
Lebeaupin T, Sellou H, Timinszky G, Huet S (2015). Chromatin dynamics at DNA breaks: what, how and why? AIMS Biophys 2, 458–475.
Luijsterburg MS, Lindh M, Acs K, Vrouwe MG, Pines A, van Attikum H, Mullenders LH, Dantuma NP (2012). DDB2 promotes chromatin decondensation at UV-induced DNA damage. J Cell Biol 197, 267–281.
Luijsterburg MS, de Krijger I, Wiegant WW, Shah RG, Smeenk G, de Groot AJ, Pines A, Vertegaal AC, Jacobs JJ, Shah GM, *et al*. (2016). PARP1 links CHD2-mediated chromatin expansion and H3.3 deposition to DNA repair by non-homologous end-joining. Mol Cell 61, 547–562.
Nagy Z, Kalousi A, Furst A, Koch M, Fischer B, Soutoglou E (2016). Tankyrases promote homologous recombination and check point activation in response to DSBs. PLoS Genetics 12, e1005791.
Neumann B, Walter T, Hériché JK, Bulkescher J, Erfle H, Conrad C, Rogers P, Poser I, Held M, Liebel U, *et al*. (2010). Phenotypic profiling of the human genome by time-lapse microscopy reveals cell division genes. Nature 464, 721–727.
Pines A, Vrouwe MG, Marteijn JA, Typas D, Luijsterburg MS, Cansoy M, Hensbergen P, Deelder A, de Groot A, Matsumoto S, *et al.* (2012). PARP1 promotes nucleotide excision repair through DDB2 stabilization and recruitment of ALC1. J Cell Biol 199, 235–249.
Platani M, Goldberg I, Lamond AI, Swedlow JR (2002). Cajal body dynamics and association with chromatin are ATP-dependent. Nat Cell Biol 4, 502–508.
Polo SE (2015). Reshaping chromatin after DNA damage: the choreography of histone proteins. J Mol Biol 427, 626–636.
Polo SE, Kaidi A, Baskcomb L, Galanty Y, Jackson SP (2010). Regulation of DNA-damage responses and cell-cycle progression by the chromatin remodelling factor CHD4. EMBO J 29, 3130–3139.
Poirier GG, de Murcia G, Jongstra-Bilen J, Niedergang C, Mandel P (1982). Poly(ADP-ribosyl)ation of polynucleosomes causes relaxation of chromatin structure. Proc Natl Acad Sci USA 79, 3423–3427.
Ran FA, Hsu PD, Wright J, Agarwala V, Scott DA, Zhang F (2013). Genome engineering using the CRISPR-Cas9 system. Nat Protoc 8, 2281–2308.
Rouleau M, McDonald D, Gagné P, Ouellet M-E, Droit A, Hunter JM, Dutertre S, Prigent C, Hendzel MJ, Poirier GG (2007). PARP-3 associates with polycomb group bodies and with components of the DNA damage repair machinery. J Cell Biochem 100, 385–401.
Sbalzarini IF, Koumoutsakos P (2005). Feature point tracking and trajectory analysis for video imaging in cell biology. J Struct Biol 151, 182–195.
Schermelleh L, Solovei I, Zink D, Cremer T (2001). Two-color fluorescence labeling of early and mid-to-late replicating chromatin in living cells. Chromosome Res 9, 77–80.
Schuster-Böckler B, Lehner B (2012). Chromatin organization is a major influence on regional mutation rates in human cancer cells. Nature 488, 504–507.
Smeenk G, Wiegant WW, Marteijn JA, Luijsterburg MS, Sroczynski N, Costelloe T, Romeijn RJ, Pastink A, Mailand N, Vermeulen W, *et al*. (2013). Poly(ADP-ribosyl)ation links the chromatin remodeler SMARCA5/SNF2H to RNF168-dependent DNA damage signaling. J Cell Sci 126, 889–903.
Smerdon MJ, Lieberman MW (1978). Nucleosome rearrangement in human chromatin during UV-induced DNA-repair synthesis. Proc Natl Acad Sci USA 75, 4238–4241.
Strickfaden H, McDonald D, Kruhlak MJ, Haince JF, Th'ng JP, Rouleau M, Ishibashi T, Corry GN, Ausio J, Underhill DA, *et al*. (2016). Poly(ADP-ribosyl)ation-dependent transient chromatin decondensation and histone displacement following laser micro-irradiation. J Biol Chem 291, 1789-802.
Subach FV, Patterson GH, Renz M, Lippincott-Schwartz J, Verkhusha VV (2010). Bright monomeric photoactivatable red fluorescent protein for two-color super-resolution sptPALM of live cells. J Am Chem Soc 132, 6481–6491.
Thévenaz P, Ruttimann UE, Unser M (1998). A pyramid approach to subpixel registration based on intensity. IEEE Trans Image Process 7, 27–41.
Thoma F, Koller T, Klug A (1979). Involvement of histone H1 in the organization of the nucleosome and of the salt-dependent superstructures of chromatin. J Cell Biol 83, 403–427.
Timinszky G, Till S, Hassa PO, Hothorn M, Kustatscher G, Nijmeijer B, Colombelli J, Altmeyer M, Stelzer EH, Scheffzek K, *et al*. (2009). A macrodomain-containing histone rearranges chromatin upon sensing PARP1 activation. Nat Struct Mol Biol 16, 923–929.
Walter A, Chapuis C, Huet S, Ellenberg J (2013). Crowded chromatin is not sufficient for heterochromatin formation and not required for its maintenance. J Struct Biol 184, 445–53.
Wang Z, Michaud GA, Cheng Z, Zhang Y, Hinds TR, Fan E, Cong F, Xu W (2012). Recognition of the iso-ADP-ribose moiety in poly(ADP-ribose) by WWE domains suggests a general mechanism for poly(ADP-ribosyl)ation-dependent ubiquitination. Genes Dev 26, 235–240.
Woodhouse BC, Dianov GL (2008). Poly ADP-ribose polymerase-1: an international molecule of mystery. DNA Repair (Amst) 7, 1077–1086.

Supplemental Materials

Molecular Biology of the Cell

Sellou et al.

The poly(ADP-ribose)-dependent chromatin remodeler Alc1 induces local chromatin relaxation upon DNA damage

Hafida Sellou, Théo Lebeaupin, Catherine Chapuis, Rebecca Smith, Anna Hegele, Hari R. Singh, Marek Kozlowski, Sebastian Bultmann, Andreas G. Ladurner, Gyula Timinszky, and Sébastien Huet

SUPPLEMENTAL INFORMATION

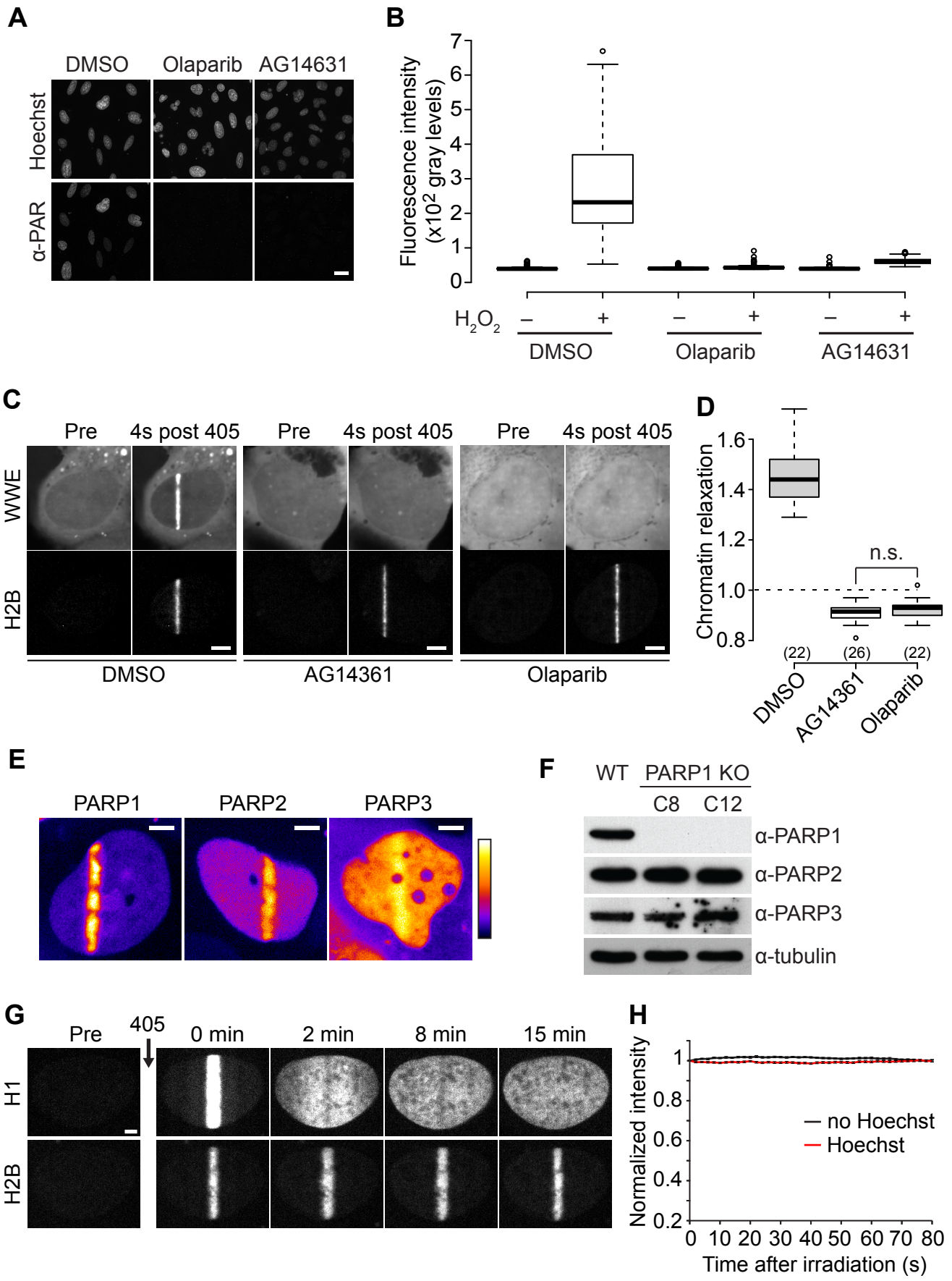

Sellou et al., Figure S1

Figure S1: PARP1-dependent chromatin dynamics at DNA damage sites. (A) Confocal images of immunofluorescence staining with anti-PAR (10H) antibody performed in U2OS cells treated or not with PARP inhibitors. The PARP1 inhibitors AG14361 and Olaparib were used at 30 μM and 50 μM, respectively for 1 hour before H_2O_2 treatment. DNA damage was induced by treating the cells with 0.5 mM H_2O_2 in PBS for 10 min. Bar = 25 μm. For the fluorescence quantification (B), nuclei were segmented using Hoechst staining and the mean fluorescence intensity for the anti-PAR antibody was measured inside each nucleus. (C) Recruitment at DNA damage sites of the PAR-binder WWE domain of RNF146 in cells co-expressing WWE-EGFP and H2B-PATagRFP, pre-sensitized with Hoechst and treated or not with the PARP inhibitors AG14361 (30 μM, 1h) or Olaparib (50 μM, 1h). Bar = 4 μm. The strong recruitment of the WWE domain observed at DNA lesions in the control cells was completely abolished upon treatment with AG14361 or Olaparib, demonstrating the efficiency of these inhibitors. (D) Relative chromatin relaxation at 60s after laser micro-irradiation in U2OS cells expressing H2B-PAGFP and treated or not with the PARP inhibitors AG14361 (30 μM, 1h) or Olaparib (50 μM, 1h). (E) Recruitment of human PARP1, PARP2 and PARP3 at DNA damage sites induced by laser micro-irradiation. U2OS cells were transfected with GFP-tagged PARP proteins. Images were taken 2 minutes after laser irradiation. Bar = 4 μm. Fluorescence signals are pseudocolored using the lookup table shown on the right of the images. (F) Western-blot of wild type U2OS cells and the two knockout cell lines showing the relative amount of PARP1, PARP2 and PARP3 in the different cell lines. (G) Confocal image sequence acquired at long time scales for a U2OS cell co-expressing H2B-PATagRFP and H1-PAGFP. For the H1 channel, the image contrast was enhanced to allow the visualization of H1 redistribution over the entire nucleus following laser micro-irradiation. This led to an apparent saturation of the image at time = 0s. Bar = 4 μm. (H) Kinetics of H2B release from the irradiated line in wild-type U2OS cells expressing H2B-PATagRFP and pre-sensitized (n=18) or not (n=20) with Hoechst (mean ± SEM).

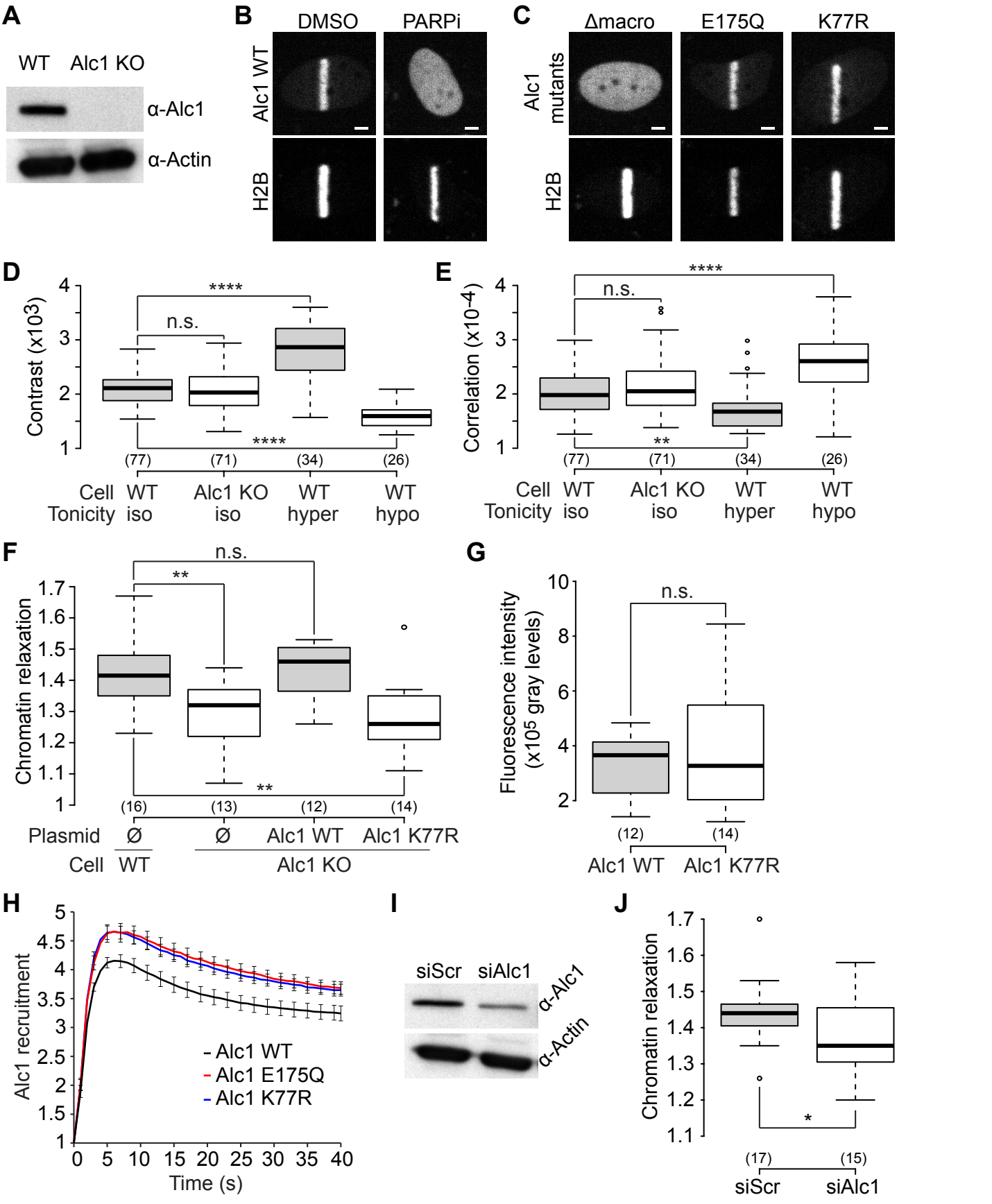

Sellou et al., Figure S2

Figure S2. The chromatin remodeler Alc1 is involved in chromatin relaxation at DNA damage sites. (A) Western-blot of wild type U2OS cells and the Alc1 knockout cell line. (B) Recruitment of Alc1 at the DNA damage sites in cells co-expressing the wild-type version of Alc1 fused to mCherry and H2B-PAGFP. Cells were pre-sensitized with Hoechst and treated or not with the PARP inhibitor AG14361 (30 μM, 1h). Images were acquired 10 s after laser micro-irradiation. Bar = 4 μm. The recruitment of Alc1 at DNA lesions was fully abolished upon treatment with AG14361. (C) Recruitment of Alc1 mutants at the DNA damage sites in cells co-expressing Alc1 mutants fused to GFP or YFP and H2B-PATagRFP. The Alc1-Δmacro is lacking the macro domain and the Alc1-E175Q and Alc1-K77R are two ATPase-dead mutants. Cells were pre-sensitized with Hoechst. Images were acquired 10 s after laser micro-irradiation Bar = 4 μm. The recruitment of Alc1 at DNA lesions was fully abolished for the Alc1 mutant lacking the macro domain but not for the ATPase-dead mutants. (D-E) Quantitative analysis of the Hoechst patterns in wild-type and Alc knockout U2OS cells. Two parameters were assessed to characterize the chromatin compaction state: the contrast (D) and the pixel-to-pixel correlation (E). As positive controls, we analyzed the chromatin patterns in cells bathed with hypertonic or hypotonic medium to induce chromatin hyper-compaction or decompaction, respectively. (F) Relative chromatin relaxation at 60s after laser micro-irradiation for wild type cells versus Alc1 knockout cells co-transfected with H2B-PAGFP and an empty plasmid (Ø), wild-type Alc1 or the catalytic-dead mutant Alc1 K77R, both fused to mCherry. (G) Integrated fluorescence signals in the mCherry channel measured for the nuclei studied in (F) and expressing the wild-type and K77R Alc1 constructs fused to mCherry. (H) Kinetics of Alc1 recruitment at the DNA lesions measured in Alc1 knockout cells co-expressing H2B-PATagRFP and different Alc1 constructs fused to GFP. Three Alc1 constructs were analyzed: a wild-type version and two ATP-ase dead mutants E175Q and K77R (mean ± SEM, $26<n<34$). (I) Western-blot of U2OS cells treated with a scrambled siRNA or with a siRNA directed against Alc1. (J) Relative chromatin relaxation at 60s after laser micro-irradiation for wild type U2OS cells stably expressing H2B-PATagRFP and transfected with a scrambled siRNA or a siRNA directed against Alc1.

Chapter 12

Poly(ADP-Ribose)-Dependent Chromatin Remodeling in DNA Repair

Théo Lebeaupin, Rebecca Smith, Sébastien Huet, and Gyula Timinszky

Abstract

The tightly packed and dynamic structure of chromatin can undergo major reorganization in response to endogenous or exogenous stimuli, such as the regulation of transcription or the cell cycle, or following DNA damage. A fast and local chromatin decondensation is observed upon DNA damage induced by laser micro-irradiation. This decondensation is under the control of poly(ADP-ribosyl)ation (PARylation) by PARP1, one of the first proteins recruited at the DNA damage sites. This chapter provides a step-by-step guide to perform and analyze chromatin decondensation upon DNA damage induction. The protocol is based on fluorescence microscopy of live cells expressing a core histone tagged with a photoactivatable fluorophore. Laser micro-irradiation is used to simultaneously induce DNA damage and activate the fluorescence signal within the irradiated area. This photo-perturbation experiment can be easily implemented on any confocal laser-scanning microscope equipped with a photoperturbation module. The experimental framework can also be used to follow chromatin relaxation in parallel with the recruitment kinetics of a protein of interest at DNA lesions in cells co-expressing the tagged histones and a second protein of interest fused to a different fluorescent tag.

Key words DNA damage response, Chromatin remodeling, Poly(ADP-ribosyl)ation, PARP1, Live-cell imaging, Photo-activation

1 Introduction

Chromatin has a complex 3-dimensional architecture that allows is to reach the high degree of compaction that is required by the cell. However, chromatin is not a static structure. Instead, it is highly dynamic, altering compaction levels to allow specific DNA accessibility depending on endogenous and exogenous stimuli such as cell cycle, transcriptional changes or in response to DNA damage.

As microscopy techniques have continued to develop, laser micro-irradiation combined with live cell fluorescence microscopy

Electronic supplementary material: The online version of this chapter (doi:10.1007/978-1-4939-6993-7_12) contains supplementary material, which is available to authorized users.

Alexei V. Tulin (ed.), *Poly(ADP-Ribose) Polymerase: Methods and Protocols*, Methods in Molecular Biology, vol. 1608,
DOI 10.1007/978-1-4939-6993-7_12, © Springer Science+Business Media LLC 2017

has become an invaluable tool to analyze the DNA damage response of the cells. Upon DNA lesions induced by laser micro-irradiation, chromatin undergoes a rapid relaxation that is dependent on the activity of the poly(ADP-ribose) polymerase 1 (PARP1). PARP1 recognition of damaged DNA triggers its activation and the synthesis of PAR chains [1]. Over 90% of these PAR chains are linked directly to PARP1 itself and serve as a platform for recruitment of required proteins involved in the DNA damage response and possessing PAR recognition motifs [2]. PAR chains are also attached to a number of proteins involved in chromatin architecture and dynamics such as histones, chromatin remodeling enzymes and a diverse range of transcription factors [3]. Similar to other post-translational modifications, the linkage of ADP-ribose or PAR on those proteins can affect their localization, their activity, or their affinity for different substrates. PARylation at the site of DNA damage leads to fast chromatin relaxation, followed by a slow recondensation process [4, 5], identifying PARP1 as a major coordinator of the early steps of chromatin regulation upon DNA damage.

Using live-cell imaging combined with laser micro-irradiation, we describe here a methodology to study chromatin remodeling in response to PARP1 recruitment and activation at the site of DNA damage (Fig. 1). This relaxation can be assessed through a chromatin marker fused to a photoactivatable protein [6] such as the core histone H2B fused to the PATagRFP or PAGFP proteins, which both switch from a dark state to a florescent state upon illumination at 405 nm. Pretreating cells with Hoechst sensitizes them to UV irradiation allowing simultaneous DNA damage and photoactivation upon irradiation using a 405 nm laser. This experiment can be conducted on any confocal laser-scanning microscope capable of local photoperturbation. Furthermore, the protocol allows the use of two different fluorophores to follow the chromatin remodeling at DNA lesions and the recruitment of a given protein of interest to the damaged chromatin in parallel. We also provide a step-by-step analysis pipeline including tips and advice to help extracting the maximum of information from these experiments.

2 Materials

2.1 Cell Culture Reagents

1. U2OS cells in exponential growth.
2. Dulbecco's Modified Eagle Medium (with 4.5 g/L glucose) supplemented with 10% fetal bovine serum, 2 mM glutamine, 100 μg/mL penicillin and 100 U/mL streptomycin.
3. Lab-Tek II chambered coverglass (Thermo Scientific).
4. Phenol-Red-free Leibovitz's L-15 medium supplemented with 20% fetal bovine serum, 2 mM glutamine, 100 μg/mL penicillin and 100 U/mL streptomycin.

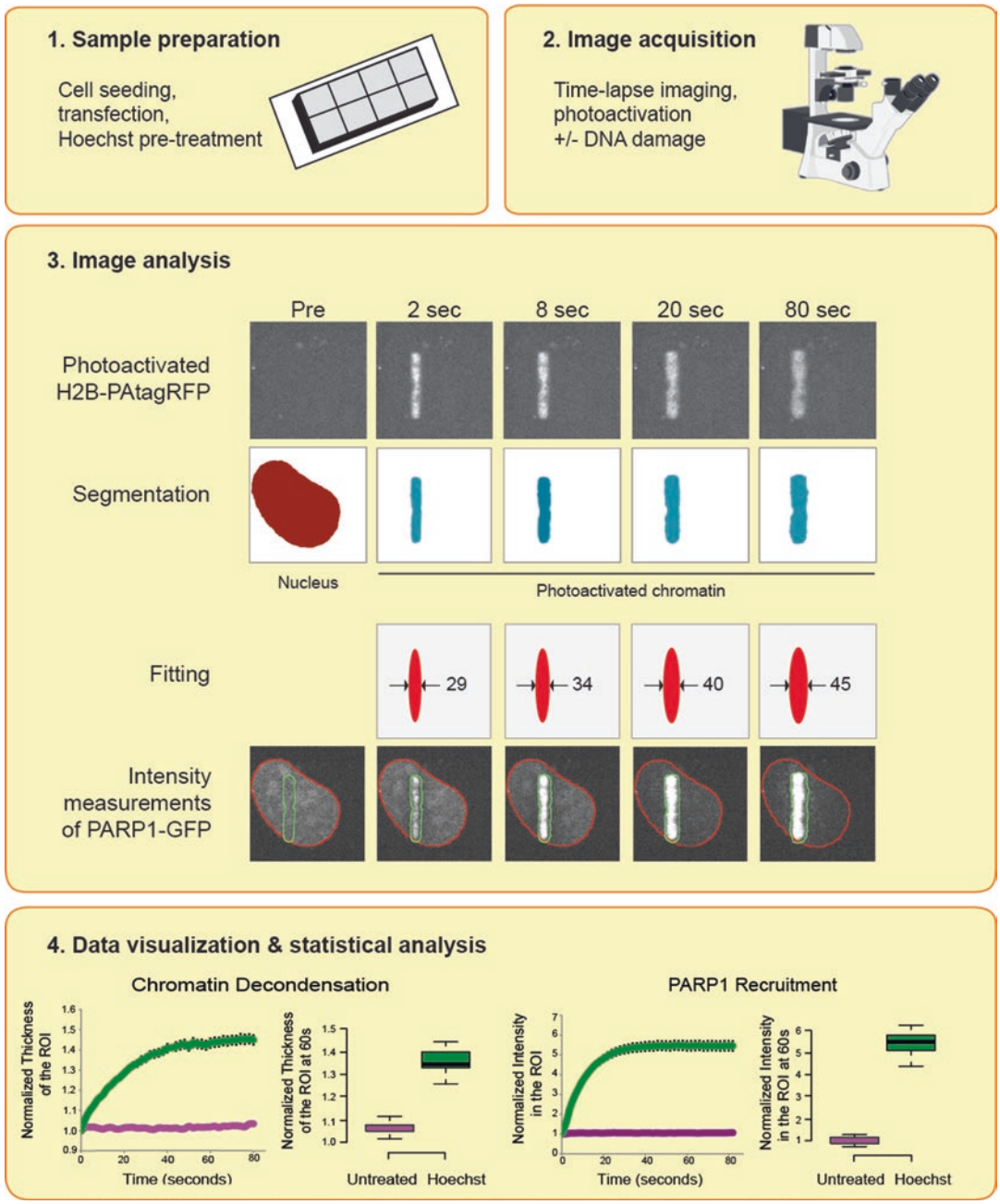

Fig. 1 Workflow of the chromatin decondensation and protein recruitment assay. Cells are prepared for imaging. This includes transfection and DNA pre-sensitization using Hoechst (*1*), followed by live cell imaging and photoperturbation using a confocal microscope (*2*). Image analysis is then performed using provided ImageJ and MatLab programs to extract a maximum of information from the images (*3*). Output files for decondensation and recruitment analysis are used for graphical representation and for statistical analysis (*4*)

5. Phosphate buffered saline (PBS).
6. Trypsin–EDTA.

7. Trypan Blue and Hemocytometer for cell counting.
8. Humidified 37 °C incubator with 5% CO_2.

2.2 Transfections and Treatments

1. H2B-PATagRFP (H2B was made by subcloning H2B from pH2B-mCherry [7] (Euroscarf accession number P30632) into PATag-RFP-N1 [8] (Addgene plasmid # 31941) using NdeI and BamHI restriction sites) or H2B-PAGFP plasmid [9] (Euroscarf accession number P30499).
2. PARP1-mEGFP [10] or PARP1-mCherry plasmid [5].
3. Hoechst 33342.
4. Fugene HD (Promega).
5. OPTI-MEM (Life Technologies).

2.3 Image Acquisition

1. Zeiss AxioObserver Z1 confocal spinning-disk microscope equipped with an AxioCam HRm CCD camera (Zeiss), Yokogawa CXU-X1 scan head and a Zeiss C-Apochromat 63×/1.2 water-immersion objective
2. RAPP DL-405 nm diode laser coupled through the epifluroscence backboard of the microscope.
3. Compact power and energy meter console (Thor Labs) and standard photodiode power sensor, S120VC (Thor Labs)
4. Calibration slide (optional)

2.4 Image Analysis

1. MatLab (MathWorks) - programs: 'tiffread.m', 'findobject.m', 'Chromatin.m'.
2. ImageJ - macros: 'TurboReg.ijm', 'StackReg.ijm', 'QC.ijm', 'Registration.ijm'.

3 Methods

3.1 Cell Culture

The following method has been optimized for U2OS cells. At the time of transfection, cells should be approximately 50–70% confluent. This may vary depending on the cell line used and might require optimization to achieve the desired transfection rates.

Cells are cultured in Dulbecco's Modified Eagle Medium (with 4.5 g/L glucose) supplemented with 10% fetal bovine serum, 2 mM glutamine, 100 μg/mL penicillin and 100 U/mL streptomycin in a 37 °C humidified incubator with 5% CO_2.

1. Aspirate media from cells at approximately 80% confluency.
2. Wash cells with PBS and aspirate.
3. To harvest the cells, incubate them with trypsin–EDTA at 37 °C for 2–3 min until cells begin to detach. Cells should appear

rounded when examined under bright field microscopy. Gently tap the plate/flask to fully detach cells.

4. Neutralize trypsin by adding fresh media and resuspend cells.
5. Count a small aliquot of cells and determine cell density.
6. Dilute cells to 20,000 cells/mL in fresh media and aliquot 300 μL of cell suspension per well into an 8 well Lab-Tek II chambered coverglass. This number is optimized for subsequent transfection of cells. Cells that stably express H2B-PATagRFP or H2B-paGFP should be diluted to 30,000–40,000 cells/mL and can be imaged the following day.
7. Return cells to the incubator and allow them to adhere for a minimum of 4 h before progressing to transfection. Transfection is subject to user preference. Cells can be left for 24 h before transfection, or may be transfected simultaneously with plating.

3.2 Transfection

Transfection of H2B-PATagRFP or H2B-paGFP is described below for two wells of an eight-well Lab-Tek II chambered cover glass using Fugene HD transfection reagent. The protocol can be optimized for alternative transfection reagents. Reactions should be scaled as required. A minimum of two reactions should be made for a control well and a test well.

1. For a single transfection with H2B-PATagRFP or H2B-paGFP, dilute 1.5 μg of DNA in OPTI-MEM for a final volume of 70.5 μL and mix gently. For a co-transfection with H2B-PATagRFP/H2B-paGFP and PARP1-mEGFP/PARP1-mCherry, dilute 1.5 μg of DNA of each plasmid in OPTI-MEM for a final volume of 66 μL and mix gently.
2. Add Fugene HD so there is a 3:1 ratio of Fugene HD to DNA and mix gently. For a single transfection, this is 4.5 μL of Fugene HD and for a co-transfection this is 9 μL of Fugene HD Allow to stand at room temperature for 15 min for complexes to form before adding 30 μL of DNA-Fugene mixture dropwise to each well.
3. Return cells in Lab-Tek II chambered coverglass to the incubator and incubate for 48–72 h. This timing is critical. Cells that are incubated for shorter periods, i.e. 24 h, might not have adequate photoactivable-tagged histone incorporated into chromatin. Unincorporated PA-tagged histones can diffuse throughout the nucleus when photo-activated and may interfere with analysis.

3.3 Microscope Setup, Image Acquisition and DNA Damage

As previously stated, any confocal laser-scanning microscope piloted by software offering a photoperturbation function is suitable for this experiment (*see* **Note 1**). To be able to analyze several cells per condition, and compare different conditions, DNA damage

induction should be as identical as possible for every cell. This means that the pattern of laser micro-irradiation, laser power, position of the laser tracks in the field of view and duration of irradiation, should be maintained constant throughout all the experiment. Due to differences between systems, multiple aspects need to be taken into consideration.

1. All lasers that are in use during this experiment, both for imaging and for photo-perturbation need to be warmed up prior to use. It is suggested that lasers are turned on at least 60 min prior to imaging.
2. The 405 nm laser is used to induce DNA damage in pre-sensitized cells (along a line crossing the nucleus). If this laser enters the microscope through a specific light-path independent from the imaging light-path, it is important to adjust its focus so that it coincides with the imaging focal plane. Defocused micro-irradiation lasers will create inconsistent results as well as light scattering.
3. The efficiency of fluorophore photoactivation (*see* **Note 2**) as well as the amount of DNA damage depends on the light energy per unit area (or light energy density) reaching the irradiated cellular area. Consequently, the size of the irradiation spot will have an impact on the amount of energy required for photo-activation and DNA damage induction. Different microscopes are likely to have varying photopertubation modules; therefore, some values as a starting point for photoactivation and DNA damage are given in Subheading 3.3.3. An example calculation showing how to adapt these values for different microscope systems is also given.
4. We recommend using a power meter to measure the laser settings needed for the micro-irradiation experiment. This step should improve comparability between systems. If a power meter is not available, an initial experiment should be completed to optimize the percentage of laser power that will be needed to photo-activate and induce DNA damage. Importantly, if high laser power is used to induce a large amount of DNA lesions, the center of the photoactivated line may be bleached, preventing further characterization of the chromatin relaxation process using the image analysis routine described below. This problem is more critical when tagging the core histones with PAGFP, which appears to bleach more easily than PATagRFP.
5. The duration of the laser irradiation should be kept constant for each cell to ensure the same level of DNA damage and photoactivation. During irradiation, the laser is scanned along a defined irradiation line using scanning mirrors. Often, the irradiation line needs to be scanned multiple times to induce DNA

lesions. Such scanning can be bidirectional, the laser being kept on for both scanning directions, or unidirectional, the laser being on only for one scanning direction. This parameter will influence the total duration of the irradiation process.

6. The image analysis pipeline has been optimized for images acquired with a 63x objective and a camera characterized by a pixel size of 6.45 μm (classical size for CCD and sCMOS cameras) used at maximum resolution (no pixel binning), thus giving a pixel size at the object plane of 107.5 nm. Increasing the pixel size (due to pixel binning, the use of lower magnification objective or cameras with larger pixels) will degrade the precision of the subsequent image analysis.

3.3.1 Preparing for Imaging

1. One hour prior to imaging, growth media should be aspirated from wells of the LabTek slide and replaced with complete media supplemented with 0.3 μg/mL Hoechst 33342. As two wells per condition are transfected, one well will be treated with Hoechst and the other will not. The 405 nm laser should not induce DNA damage in cells that have not been treated with a sensitizing agent such as Hoechst, however the histones tagged with the photoactivatable protein will be photoactivated.
2. Immediately prior to imaging, replace Hoechst-containing media with fresh imaging media without Hoechst (Phenol-Red-free Leibovitz's L-15 medium supplemented with 20% fetal bovine serum, 2 mM glutamine, 100 μg/mL penicillin and 100 U/mL streptomycin).
3. Switch on the equipment for imaging. This includes the microscope, the lasers used for imaging and micro-irradiation, and the incubator (set to 37 °C). Allow the equipment to equilibrate/warm up for 60 min.
4. Select the 63× water immersion objective. Apply the appropriate immersion fluid.

Note: Before the start of experiments, the 405 nm laser used for micro-irradiation should be calibrated if applicable and its power measured. If the system used does not require or allow the calibration of the two scanners and there is no power meter at hand proceed to Subheading 3.3.4. If no laser power meter is available, the required laser intensities have to be tested and selected experimentally by choosing an intensity setting that allows for reproducible and quantifiable chromatin relaxation.

3.3.2 Calibration of the Photoperturbation System

1. For calibration, apply some fluorescent marker on a slide and cover with a coverslip that is the same thickness as the glass on the Lab-Tek II chambered coverglass. Load the slide and get into focus using bright-field.

2. Proceed to focusing the 405 nm laser in the photoperturbation optical pathway. The following procedure applies for the Zeiss spinning disk equipped with the RAPP laser scanning system.
3. Set the exposure time on the imaging software to 10 ms and set the 488 nm imaging laser to around 1% (or the lowest setting possible) and begin imaging using a continuous imaging mode.
4. On the RAPP software, set the 405 nm laser to around 5% and select manual calibration. A small fluorescent dot should appear in the middle of the screen. A focused laser beam should appear as a small dot. Adjust the focus of the microirradiation laser in order to minimize the spot size.
5. Once in focus, the laser can be calibrated using automatic calibration. The calibration should be done using imaging settings and components that match that wanted for the image collection. Of particular importance is having the correct binning, magnification and camera.
6. Once calibrated, remove the slide and the immersion fluid.
7. Connect the power meter to the sensor and place the sensor on the objective. Select the 405 nm setting on the power meter. In the RAPP software, select manual calibration to turn on the 405 nm laser and change the percentage of laser output until the power level required for the experiment has been reached.
8. Remove the sensor from the objective and reapply immersion fluid.

3.3.3 Determining Power Levels to Use for Decondensation

In general, we suggest using between 0.7–1.1 μJ/μm2 J/m^2 for low levels of DNA damage induction and 1.4–2.2 μJ/μm2 for high levels of DNA damage. To determine the power (in mW) needed to induce the DNA damage two variables are needed; the size of the photoactivated area and the time it takes to draw the line.

1. Focus on cells expressing H2B-PATagRFP or H2B-PAGFP. These cells should not be treated with Hoechst.
2. Using the photoperturbation module, draw a line of defined length. We suggest the length of this line to be around 16 μm. It is important that the length of line is the same as that is going to be used in the decondensation experiment for each cell.
3. On the photoperturbation software, ensure that the number of iterations is set to 70. Drawing a line multiple times at a lower power is the optimal way to photoactivate and induce DNA damage.

4. Less iteration at higher power have a higher chance of causing photobleaching and side scatter which will interfere with the calculations and analysis. Alternatively, if the number of runs on the system cannot be manually changed, it is possible to choose an illumination time instead. In this case, a minimum of 350 ms should be chosen. The laser power for drawing this line should be low enough to not cause photobleaching, however it needs to be high enough for adequate photoactivation.
5. Take note of the time needed to draw the line. If the scanning laser moves in a single direction make sure that the time noted is for object illumination and not total time.
6. Export the image as a TIFF.
7. Using ImageJ, use the line tool to measure the length of the line and the width of the line drawn in pixels. Use these values and the pixel resolution of the camera to determine the area illuminated in m^2.
8. Shown in this step is for 1 $\mu J/\mu m^2$.
   (a) The length of line determined by ImageJ is 16 μm with a width of 2.5 μm.
   (b) Area = 16 μm × 2.5 μm
   = 40 μm^2
   (c) Object illumination =350 ms
   (d) Given that J = Watt (W) × seconds (s)

then	$\mu J/\mu m^2 = (\mu W \times s)/\mu m^2$
	$1\ \mu J/\mu m^2 = (\mu W \times 0.35\ s) / 40\ \mu m^2$
and	$W = (1\ \mu J/\mu m^2 \times 40\ \mu m^2)/0.35\ s$
	$W = \mathbf{114\ \mu W}$

3.3.4 DNA Damage Induction and Imaging

1. Place the Lab-Tek slide containing cells into the slide holder and focus on the cells using bright-field illumination. DO NOT use a DAPI epifluorescence filter cube to look for Hoechst stained nuclei as this will lead to photo-activation impeding further experiments.
2. Once cells are in focus, find nuclei that express tagged histones. Both PAGFP and PATagRFP display a low basal (i.e. pre-activation) fluorescence that can be used to select the cells expressing the tagged histones. Selecting cells with low basal fluorescence will produce a defined line upon photo-activation with the 405 nm laser that is easily detectable with imaging conditions classically used for live cell confocal imaging.
3. Using the RAPP software, select sequence mode and draw a line of a predefined length and change setting to show 70 runs

or a defined object illumination. Change the percentage of laser used to the corresponding power value calculated in Subheading 3.3.3. Copy and paste the line for all the cells in the field of view. Upload the sequence, ready for the experiment.

4. Images should be collected every 2–4 s over a total time of several minutes, according to the demands of your experiment, using the appropriate channels for the experiment. The frequency of image collection can be modified according to the demands of the experiment, as well as the range of the time-lapse acquisition. How often the images are collected is a variable that will be needed for the analysis. However, the frequency of imaging needs to be a compromise between optimal time resolution for the study of chromatin relaxation and protein recruitment at DNA breaks, and minimization of fluorophore photobleaching as well as cell phototoxicity.
5. Start imaging. Ensure to always take a few images before laser micro-irradiation as it will serve during the analysis for normalization and background subtraction. When setting-up the timelapse acquisition, avoid simultaneous image acquisition and micro-irradiation or delete such image frames before analysis since they will perturb the image analysis pipeline.
6. Upon completion of the experiment, rename the experiment with an identifiable name and export images as an OME-TIFF or a Multi-TIFF file. Proceed to Subheading 3.4, image analysis.

3.4 Image Analysis Pipeline

Before starting the image analysis pipeline, some programs and macros need to be downloaded and installed. Two programs were selected for the analysis: ImageJ, an open source image processing program designed for scientific multidimensional images that has become widely popular in the field of image analysis in biology, and MatLab, a powerful and versatile tool used for numerical computation and matrix-based operations that allows fast program writing and execution. ImageJ is used in this analysis during first steps and image visualization, as well as image registration, when needed. The ImageJ scripts were written for version 1.49 k with Java 1.6.0 and will work in any ulterior version. MatLab is used for the main analysis, segmentation, and intensity measurements. The MatLab programs were written for R2012a version (7.14.0.739) but have been shown to work with both older and later versions of MatLab. The code the analysis routines and some sample images can be downloaded at (Electronic Supplementary material). (*See* **Notes 4–10**) provide details regarding the development of an alternative analysis pipeline.

3.4.1 Download and Install Required Software

1. Install ImageJ (https://imagej.nih.gov/ij/download.html) and MatLab (licensed software from MathWorks).

2. The ImageJ plugins TurboReg (http://bigwww.epfl.ch/thevenaz/turboreg/) and StackReg (http://bigwww.epfl.ch/thevenaz/stackreg/) should be installed in ImageJ. To install these plugins, simply extract downloaded archives and cut and paste the '.jar' and .java' files inside the 'ImageJ/Plugins' folder.
3. Download the ImageJ macros 'QC.ijm' and 'Registration.ijm', as well as the 'findobject.m', 'tiffread.m', adapted from [11], and 'Chromatin.m' MatLab routines from (Electronic Supplementary material). Store ImageJ macros in the 'ImageJ/Toolset' folder. The three MatLab programs should be accessible for MatLab thus should be saved inside the default MatLab path.
4. Images to be analyzed should be Tiff stacks. The stack corresponding to the chromatin marker should end with " H2B.tif" and the one associated with the protein recruited at DNA lesions, if applicable, should end with " Rec.tif". For the analysis macro to recognize these labels a space must be before H2B and Rec. Aside from these two labels, names of the two stacks should be identical.

Note: The 'QC' and 'Registration' macros are written for acquisitions containing two channels (chromatin marker and protein recruited at DNA lesions). For two channel acquisition, begin analysis at Subheading 3.4.3. When analyzing chromatin relaxation only, crop individual cells manually (described in Subheading 3.4.2), and move to Subheading 3.4.4.

3.4.2 Quality Control and Cell Cropping for Single Channel Acquisition

1. Open ImageJ.
2. Open the OME-TIFF or Multi-TIFF file.
3. Using the square tool, draw a box around a single cell that has been photoactivated.
4. Duplicate the stack.
5. Repeat **steps 3** and **4** for each cell in the image.
6. Save each stack of images as a '.tif' into a new folder – Note, as these images are going to be used in a MatLab pipeline, the names of the images cannot be excessively long as this would cause the pipeline to crash. Use the saving step to rename each image with a short but identifying name.
7. Repeat **step 3–6** for each condition.
8. Close ImageJ.
9. Proceed to Subheading 3.4.5 MatLab analysis.

3.4.3 Quality Control and Image Cropping for Double Channel Acquisition

If acquisition is performed cell by cell, skip this step and go directly to Registration after performing a quality control step manually, if

necessary. In order for ImageJ macros to run properly, the filepaths should not contain any space characters.

1. Open ImageJ.
2. Drag the 'QC' macro in the 'drag and drop' command bar of ImageJ.
3. Click 'Run' on the macro window that opens.
4. Select the folder where the images for analysis have been saved and press enter.
5. Select a new folder for saving the new stacks of individually cropped cells.
6. For each stack of images, a movie combining both channels will be shown in order to view the photo-activated chromatin lines and the nucleus on the same image. Enter the number of cells you want to keep and press enter. To ensure the accuracy of the subsequent analysis, the cells should display a bright and continuous chromatin photo-activated area after photo-perturbation and the nucleus should be visible. Cells that do not have these qualities should be disregarded.
7. Using the ImageJ rectangular drawing tool, draw a selection around the first cell and press 'OK'. Repeat this for every cell of the movie.
8. Repeat **steps 6** and **7** for all images inside one folder.
9. Repeat **steps 3–8** for all folders/conditions.
10. Close ImageJ.

3.4.4 Registration

1. Open ImageJ.
2. Drag the 'Registration' macro on the 'drag and drop' ImageJ command bar.
3. Click 'Run' on the macro ImageJ window.
4. Select the folder in which the cropped images are saved and press enter.
5. Select a new folder in which stacks of registered images will be saved and press enter. Warning: DO NOT perform any ImageJ function or interfere with the playing movie while registration is running.
6. Once registration is over, repeat **steps 3–5** for every folder/condition.
7. Close ImageJ.

3.4.5 MatLab Analysis

1. Open MatLab.
2. Make sure that the programs 'Chromatin.m', 'tiffread.m' and 'findobject.m' are included inside the default MatLab path. Otherwise, go to 'File', 'Set Path', click on 'Add with sub-

folder', select the folder in which those programs are stored and press 'OK'. Click 'Save' and close window.

3. Click on the 'Current Folder' path to browse the location where the images are saved, press 'OK'.
4. Run the program 'Chromatin.m' by either clicking 'Run' after opening the program in the editor window, or typing the name of the program in the command window (without the '.m' extension, i.e. 'Chromatin').
5. Some user information needs to be specified here. The first window will prompt the user to enter the number of the first frame after photo-perturbation and press 'OK'. In the second one, the pixel size (in μm) and the time between each frame (in seconds) must be entered, respectively, before pressing 'OK'.
6. Next, browse and select all registered stacks ending with " H2B.tif" for one condition and click on 'Open'. MatLab can only integrate a defined number of characters in its file path. If an error message appears right after running the program in the command window, try selecting a smaller number of stacks. However, you need to select at least two movies for the program to run properly.
7. Finally, browse and type a name for the text file in which results of the analysis will be written. Choose a name describing the condition from which stacks are analyzed and click on 'Save'.
8. Click on the appropriate option. "Decondensation Assay (1 channel)" will use only " H2B.tif" files and complete the decondensation analysis. These images should not be processed through to registration. Using registered images for the Decondensation Assay will cause incorrect fitting during analysis and therefore incorrect results. Selecting "Recruitment Assay (2 channels)" will recognize the " H2B.tif" files and the corresponding " Rec.tif" files and complete a decondensation analysis as well as the recruitment analysis. Registered images should be used for the recruitment assay.
9. A 'Segmentation Results' window will appear after each cell analysis. Ensure that the two segmented areas correspond to the photo-activated region and the nucleus throughout the whole movie. If not, remove the results obtained for this cell from the analysis by either re-run the program without the specified cell or deleting the results produced from this cell in the text file. A plot will also appear allowing the user to obtain an initial impression about the experiment.
10. Repeat **steps 4–8** for all wanted conditions.
    The output file is as follows. The first line displays the name of the analyzed stack and the headings describing the results below. After a decondensation assay, only two columns will

Table 1
Descriptions of MatLab output measurements

Headings	Measurement
Name of the stack	In the column which contains the name of the stack is stored the timepoints of the acquisition. First timepoint after photo-perturbation is 0
Rec_ROI	Intensity in the 'Rec channel' inside the photo-activated chromatin area (ROI)
Rec_nucleus	Intensity in the 'Rec channel' inside the whole nucleus
H2B_ROI	Intensity in the 'H2B channel' inside the ROI
H2B_nucleus	Intensity in the 'H2B channel' inside the whole nucleus
Thickness	Normalized thickness of the ellipse fit on the ROI. First timepoint is 1
nRec	Normalized intensity in the 'rec channel'. The signal inside the ROI is divided by the signal inside the whole nucleus, frame by frame. Last timepoint before photo-perturbation is 1
nH2B	Normalized intensity in the 'H2B channel'. The signal inside the ROI is divided by the signal inside the whole nucleus, frame by frame. First timepoint is 1

"Heading" shows the title of each column in the output file. "Measurement" gives a full description of each measurement in the output file. Each row in the text file corresponds to a timepoint. Results from different stack of images analyzed in one program run are below each other separated by headings

appear displaying the time points analyzed and the thickness of the photoactivated line, respectively. After a recruitment assay, several columns are written and each line shows the background-subtracted intensity measurements extracted from a frame starting with the first frame after photo-perturbation. To properly visualize this file, open it using the text import wizard of any spreadsheet selecting 'Space' as a delimiter. Table 1 provides a more detailed description of the extracted data.

4 Notes

1. Photobleaching and photoactivation techniques are nowadays easily implemented on any confocal laser-scanning microscope [12], however the choice of the system is still critical and should be carefully assessed. The major features guiding this choice should be the spatiotemporal resolution of the system and the sensitivity of the detector/camera. The needs, in terms of resolution, strongly depend on the dynamics of the protein

of interest and the properties of the fluorophore. The choice becomes critical when wanting to assess the recruitment of a tagged protein while following the decondensation process. A classical confocal laser-scanning microscope will allow for higher spatial resolution and will offer more options to optimize the acquisition, whereas a spinning-disk confocal microscope should allow for a better temporal resolution as well as reduced fluorophore photobleaching and cell phototoxicity.

2. The use of fluorescent proteins during experiments such as those described in this chapter are highly recommended since the photo-activation of chemical dyes are often associated with the production of toxic free radicals. Additionally the use of fluorescent chemicals usually requires more invasive and more complicated methods.

   The fluorescent probe should display several important characteristics:

   – High brightness to obtain maximal signal with a minimal illumination during the time-lapse acquisition
   – High photostability for reduced photobleaching during the time-lapse acquisition
   – Switch from dark to activated state as instantaneously as possible
   – Little tendency for multimerization to avoid artifacts due to the aggregation of labeled proteins

   Fluorescent proteins are constantly evolving and new ones are discovered regularly. At this time, PAGFP (Ex/Em = 488/517 nm) and PATagRFP (Ex/Em = 562/595 nm) will give the best results regarding photo-activation experiments, while mEGFP (Ex/Em = 488/507 nm) and mCherry (Ex/Em = 587/610 nm) are at the top of the list for tagging proteins to follow their recruitment to DNA damage [13]).

3. Many parameters of photoperturbation and acquisition can only be precisely determined after performing pilot experiments. The parameters mentioned in this chapter can be used to start the empirical optimization steps. Like in any microscopy experiment, phototoxicity during the acquisition should be assessed. This is particularly important for the Hoechst-sensitized cells as they show increased sensitivity to phototoxicity. Fluorophore photobleaching during acquisition should be also carefully assessed and kept to a minimum by reducing the power of the laser used for image acquisition, or the frequency of image acquisition. Photobleaching can be assessed by plotting the intensity over time measured for the chromatin marker inside the whole nucleus.

4. The MatLab routine provided with this protocol is optimized for the system and the conditions described in the Material and

Methods sections. However, this routine should operate correctly on stacks obtained with multiple systems and multiple conditions. Of particular importance are the signal-to-noise ratio and the resolution. To modify the program, open MatLab and click on 'Open' in the 'Editor' window. Browse to find the file 'Chromatin.m' and click on 'OK'. The first thing to test in order to improve segmentation would be to optimize values chosen in the 'Segmentation parameters' section to best fit the experiment. If this does not improve the analysis, adding image filters in the 'Segmentation' or 'Mask cleaning' sections should be considered.

5. Segmentation of the photo-irradiated area is required for developing an analysis pipeline. In order to differentiate the damaged chromatin from undamaged one, as well as to quantify the decondensation of chromatin observed upon DNA damage, a mask must be created frame by frame based on the fluorescent signal displayed by the photo-activated fluorophore fused to the chromatin marker. As the photoactivation by laser irradiation results in a dramatic increase in the fluorescence brightness of photoactivatable proteins, the segmentation of the irradiated area should not be a problem using any kind of intensity thresholding method. A basic Otsu thresholding should be appropriate as long as acquisition photo-bleaching remains at an acceptable level through the whole movie [14].
6. Segmentation of the whole nucleus is required when performing a recruitment assay. Quantifying the total fluorescence within the nucleus will be required for background subtraction, normalizing the recruitment signal at DNA breaks and correcting photo-bleaching induced by image acquisition. The easiest way to segment the whole nucleus is to perform a basic thresholding of the images before irradiation in the channel of the protein of interest, for example using the Otsu algorithm. The same mask will then be applied all over the time-lapse sequence to measure total intensity inside the nucleus. This approach requires that the nuclei do not move over the sequence. If such movement occurs, it can be corrected by image registration. Some commercial tools can perform this alignment such as the Bitplane AutoAligner, or the ImageJ plugin TurboReg [15]. An alternative would be to update the mask of the nucleus for each frame by applying the segmentation algorithm. However, after irradiation, the uneven distribution of the tagged protein due to its recruitment at the DNA lesions may perturb the proper segmentation of the nucleus.
7. Most images obtained with a confocal microscope greatly benefit from a denoising and filtering step that will enhance

the quality of the masks created afterwards. A basic Gaussian blur with a small radius should efficiently smooth high-frequency noise while preserving the structures of interest. The radius can be modified and other, more advanced, filters can be applied on top of the blurred image or in parallel to compare segmentation results. After the segmentation step, it is also recommended to clean up created masks by applying classical opening and closing morphological filters. It can also be useful to "fill the holes" inside masks, if necessary.

8. Every acquisition image contains background fluorescence coming from various sources, such as the medium or the glass coverslip. The camera signal intensities are also usually offset by approximately 100 gray values. Removing the contribution of the background intensity signal that is not due to the tagged protein of interest is critical since it will affect the quantification of the recruitment kinetics when analyzing the accumulation of a given protein at DNA lesions. An average background intensity value should be subtracted from every pixel of every frame of the movie. This assumes that the background fluorescence signal intensity is homogeneous both in space (over the entire image) and in time. This assumption should be verified. The background for the channel corresponding to the protein recruiting at DNA breaks can be estimated by calculating the mean intensity within the complementary mask of the one of whole nucleus (see above segmentation of the whole nucleus).
9. As stated previously, we chose to micro-irradiate cells on a straight vertical line of a fixed and defined length for every cell to ensure that the resulting DNA damage is as identical as possible in terms of quality and quantity from one cell to another. In this case, a way to extract a single parameter of decondensation that is comparable between cells and that reflects the variability of chromatin architecture between different cells as little as possible is to fit an ellipse onto the mask created with the intensity in the chromatin marker channel and measure the thickness of this ellipse. Other photo-irradiation patterns can be chosen in order to best fit the needs of the experiment with another parameter describing the relaxation of chromatin being identified and extracted, such as the total segmented area or, if the damage is induced in a circular region, the radius of the damaged area.
10. The protocol was written to assess the recruitment of a fluorescently-tagged protein while following chromatin decondensation upon DNA damage induced by laser micro-irradiation. This technique can be coupled with any inhibitor or siRNA treatment. It can also be coupled to another photo-perturbation technique to follow the recovery or the release of any protein at, or outside the damaged chromatin. In order to

study the release of a protein from the DNA damage sites, co-transfection must be performed with the chromatin marker tagged to a photoactivatable fluorophore and the protein of interest tagged to another photoactivatable fluorophore. In this case, both fluorophores can be activated by the same 405 nm laser irradiation and the release of the protein of interest from the growing damaged chromatin area can be assessed.

Acknowledgements

Our work was supported by the Ligue contre le Cancer du Grand-Ouest (committees 35 and 72, to S.H.), the European Union (FP7-PEOPLE-2011-CIG, ChromaTranscript project, to S.H. and T.L.) and the Worldwide Cancer Research (#14-1315 to G.T.). Our collaboration benefited from funding from the Hubert Curien partnership/German Academic Exchange Service – DAAD – (28486ZD, to S.H., 55934632; to G.T.). The authors declare no competing financial interests.

References

1. Golia B, Singh HR, Timinszky G (2015) Poly-ADP-ribosylation signaling during DNA damage repair. Front Biosci-Landmark 20:440–457
2. Krishnakumar R, Kraus WL (2010) The PARP side of the nucleus: molecular actions, physiological outcomes, and clinical targets. Mol Cell 39(1):8–24
3. Wei H, Yu X (2016) Functions of PARylation in DNA damage repair pathways. Genomics Proteomics & Bioinformatics 14(3):131-139.
4. Kruhlak MJ, Celeste A, Nussenzweig A (2006) Spatio-temporal dynamics of chromatin containing DNA breaks. Cell Cycle 5(17):1910–1912
5. Timinszky G, Till S, Hassa PO, Hothorn M, Kustatscher G, Nijmeijer B, Colombelli J, Altmeyer M, Stelzer EHK, Scheffzek K, Hottiger MO, Ladurner AG (2009) A macrodomain-containing histone rearranges chromatin upon sensing PARP1 activation. Nat Struct Mol Biol 16(9):923–U941
6. Patterson GH, Lippincott-Schwartz J (2002) A photoactivatable GFP for selective photolabeling of proteins and cells. Science 297(5588):1873–1877
7. Neumann B, Walter T, Heriche JK, Bulkescher J, Erfle H, Conrad C, Rogers P, Poser I, Held M, Liebel U, Cetin C, Sieckmann F, Pau G, Kabbe R, Wunsche A, Satagopam V, Schmitz MHA, Chapuis C, Gerlich DW, Schneider R, Eils R, Huber W, Peters JM, Hyman AA, Durbin R, Pepperkok R, Ellenberg J (2010) Phenotypic profiling of the human genome by time-lapse microscopy reveals cell division genes. Nature 464(7289):721–727
8. Subach FV, Patterson GH, Renz M, Lippincott-Schwartz J, Verkhusha VV (2010) Bright monomeric photoactivatable red fluorescent protein for two-color super-resolution sptPALM of live cells. J Am Chem Soc 132(18): 6481–6491
9. Beaudouin JL, Mora-Bermudez F, Klee T, Daigle N, Ellenberg J (2006) Dissecting the contribution of diffusion and interactions to the mobility of nuclear proteins. Biophys J 90(6):1878–1894
10. Ali AA, Timinszky G, Arribas-Bosacoma R, Kozlowski M, Hassa PO, Hassler M, Ladurner AG, Pearl LH, Oliver AW (2012) The zinc-finger domains of PARP1 cooperate to recognize DNA strand breaks. Nat Struct Mol Biol 19(7):685–692
11. Nedelec F, Surrey T, Maggs AC (2001) Dynamic concentration of motors in microtubule arrays. Phys Rev Lett 86(14):3192–3195
12. McNally JG, Smith CL (2001) Photobleaching by confocal microscopy. In: Diaspro A (ed)

Confocol and two-photon microscopy: foundations, applications and advances. Wiley, Hoboken, NJ, pp 525–538

13. Bancaud A, Huet S, Rabut G, Ellenberg J (2010) Fluorescence perturbation techniques to study mobility and molecular dynamics of proteins in live cells: FRAP, photoactivation, photoconversion, and FLIP. In: Goldman RD, Swedlow JR, Spector DL (eds) Live cell imaging: a laboratory manual, 2nd edn. Cold Spring Harbor Laboratory Press, New York
14. Otsu N (1979) Threshold selection method from gray-level histograms. IEEE Trans Syst Man Cybern 9(1):62–66
15. Thevenaz P, Unser M (1998) An efficient mutual information optimizer for multiresolution image registration. 1998 International Conference on Image Processing - Proceedings, Vol 1. Chicago, IL

The multiple effects of molecular crowding in the cell nucleus: from molecular dynamics to the regulation of nuclear architecture

Théo Lebeaupin[1,2], Rebecca Smith[3], and Sébastien Huet[1,2,*]

[1]CNRS, UMR 6290, Institut Génétique et Développement de Rennes, Rennes, France
[2]Université de Rennes 1, Structure fédérative de recherche Biosit, Rennes, France
[3]Department of Physiological Chemistry, Biomedical Center Munich, Ludwig-Maximilians-Universität München, Planegg-Martinsried, Germany
[#]Correspondence: sebastien.huet@univ-rennes1.fr

Abstract (<200 words)

The cell nucleus is a highly crowded environment. Indeed, this volume of few picoliters accommodates 2 meters of genetic material as well as large amounts of different types of macromolecules such as RNAs or protein complexes. This high degree of macromolecular crowding is expected to strongly impact the dynamic behavior of biomolecules navigating through the nuclear volume. In this review, we present the consequences of crowding on molecular concentration, diffusion and reaction equilibria which are predicted by theoretical and in-vitro data. Next, we describe the experimental data that allowed quantitative assessment of the influence of macromolecular crowding on protein reaction-diffusion dynamics inside the nucleus. Finally, we review the recent findings investigating the different potential physiological roles of crowding. These results suggest that crowding is likely a central player in the control of the nuclear organization by affecting both the chromatin structure, as well as the maintenance of the nuclear sub-compartments. By regulating access to DNA, crowding may also affect all nuclear processes based on DNA transactions.

Keywords (5-10)

Macromolecular crowding, reaction-diffusion dynamics, volume exclusion, anomalous diffusion, phase separation, nucleus, chromatin

Introduction

A classical image which is often used when introducing the question of the spatial organization of the nucleus in eukaryotic cells is the one of the two meter long DNA fiber that needs to fit into a nucleus which is five order of magnitude smaller, namely ~10 μm in diameter. While this

comparison may not be fully relevant since the DNA fiber probably never adopts such an extended, two meter long conformation, it immediately brings forward the question of the level of crowding in the intranuclear environment. This question appears even more crucial when considering that, besides DNA, the nucleus also contains protein complexes, including more than 10 millions nucleosomes, RNAs and multiple other types of biomolecules. These macromolecules occupy a significant fraction of the nuclear volume. Indeed, 30 to 50 % of the nuclear volume is attributed to the chromatin [Lopez-Velazquez et al., 1996; Rouquette et al., 2009] while the contribution of the other types of biomolecules being unclear. This high fraction of occupied volume, which is thus inaccessible to other molecules, clearly defines the intranuclear volume as a strongly crowded environment in which molecular motions as well as chemical reactions will be dramatically different from what is observed in dilute solutions [Minton, JCS, 2006]. Moreover, the nucleus is not simply a crowded bag of randomly diffusing macromolecules. Indeed, while being a continuous environment in contrast to the cytoplasm [Bancaud, EMBOJ, 2009], it displays a multiscale architecture associated with a spatial compartmentalisation of the different nuclear functions [Hemmerich, Chrom Res, 2011]. The macromolecular crowding induced by such complex structure is predicted to have a major impact on nuclear functions by tuning the way biochemical partners meet, interact and react with each others. This influence of crowding has been largely overlooked so far and we are just beginning to understand its biological implications [Huet, Int Rev Cel Mol Biol, 2014].

The main component of the intranuclear volume is the chromatin, which displays a hierarchical architecture spanning over three order of magnitudes in space [Sexton, Cell, 2015]. During interphase, this organization plays an important regulatory role in all cellular functions using the DNA as a template: transcription, DNA replication and DNA repair [Pombo, NatRevMolCellBiol, 2015]. The first structural unit of the chromatin is the nucleosome, whose structure is now well characterized. In contrast, our description of the spatial organization of these nucleosomes along the chromatin fiber remains fuzzy. Although the classical 30-nm fiber model has been challenged by several recent observations [Nishino, EMBOJ, 2012; Maeshima, EMBOJ, 2016], an alternative model has not yet emerged. It was suggested that the highly flexible 10 nm fiber formed by nucleosomes alternating with linker DNA, folds into a compact "polymer melt" in which interactions between nucleosomes located far apart from each other along the fiber dominates over the interactions between neighboring nucleosomes [Maeshima, Chromosoma, 2014]. Within this polymer melt, the existence of small clusters composed of 2 to 10 nucleosomes was reported recently [Hsieh, Cell, 2015; Ricci, Cell, 2015]. Distal interactions along the chromatin fiber are also at the origin of the formation of chromatin loops, which are the elementary component of the

secondary structural unit of the chromatin: the topologically associated domains (TADs) [Dixon, Nature, 2012; Nora, Nature, 2012; Sexton, Cell, 2012]. Each TAD is defined as a compact domain encompassing ~1Mb of DNA in which contacts along the chromatin fiber occur at much higher frequency than with the exterior of this domain. The mechanism driving the formation of the chromatin loops composing the TADs remains unclear. Some author attribute the stabilization of these loops to the involvement of specific molecular actors [Barbieri, PNAS, 2012] while others suggest that chromatin motions by diffusion is sufficient to create transient loops along the fiber [Bohn, Plos One, 2010]. Noteworthy, the packing state of the chromatin fiber within a given domain seems to tightly depend on the epigenetic status of this domain [Boettiger, Nature , 2016]. TADs sharing similar properties in terms of gene density or compaction state tend to associate together to form larger compartments [Bouwman, Genome Biol, 2016] which may overlap at least in part with the euchromatic / heterochromatic domains identified nearly 90 years ago [Heitz, 1928]. Finally, the highest structural level displayed by the chromatin corresponds to the spatial distribution of the chromosomes within the nucleus. Each chromosome occupy a compact volume and show little intermingling with its neighbors. The position of the chromosome territories within the nucleus is not random and seems to depend on the size of the chromosomes [Bolzer, PLOS Biol, 2005] as well as their gene density [Croft, JCB, 1999]. While chromatin is probably the main component of the intranuclear volume, it is not the only one. In fact, this volume is also composed of multiple sub-compartments: nucleoli, cajal bodies, speckles ...[Hemmerich, Chrom Res, 2011], fulfilling specific nuclear functions such as ribosome synthesis or RNA splicing. In contrast to the cytoplasm, these nuclear organelles are not isolated from the rest of the nuclear environment by a lipidic membrane, instead, they are formed by the dynamic accumulation of specific scaffolding proteins via stochastic or hierarchical mechanisms which often use particular chromatin domains as stable seeding platforms [Dundr, Cold Spring Harb Perspect Biol, 2010].

The interphase nuclear organization which was briefly described in the previous paragraph is not static but displays complex dynamics at multiple levels from macromolecules to the nuclear organelles. Diffusion of macromolecules appears surprisingly fast, given the level of crowding within the nucleus. An apparent viscosity only 3 to 4 higher than water was reported for diffusing tracers of 30 to 100 kD [Pack, BJ, 2006] and all nuclear compartments, including the densest ones such as the nucleoli, are readily permeable to macromolecules of sizes up to 500 kD [Gorish, ExpCellRes, 2003; Bancaud, EMBOJ, 2009]. By comparison, the motions displayed by the chromatin polymer are much more restricted, with diffusion coefficients 3 to 4 orders of magnitude lower than for proteins roaming the nucleus [Bornfleth, BJ, 1999; Hajjoul, Genome Res, 2013]. Nevertheless, chromatin displacements over ~0.5 µm have been reported for recording periods of a

few seconds [Heun, Science, 2001; Levi, BJ, 2005]. Such amplitudes of movement, which corresponds to the typical size of the TADs, imply that all chromatin folding levels up to, and including, the TADs undergo constant rapid rearrangements during interphase [Gibcus, MolCell, 2013; Lucas, Cell, 2014]. These chromatin movements, which are mainly driven by ATP-dependent mechanisms [Weber, PNAS, 2012], seems to correlate with the activity of key nuclear functions such as transcription [Khanna, Curr Biol, 2014] or DNA repair [Lebeaupin, AIMS Biophys, 2015]. At higher space scales, the nuclear organization appears stable throughout interphase with chromosome territories showing little changes in terms of their relative positions within the nucleus [Gerlish, Cell, 2003], except perhaps at the beginning of G1 phase [Walter, JCB, 2003]. Similarly, the spatial distribution of most of the nuclear organelles is globally preserved over interphase [Dundr, Cold Spring Harb Perspect Biol, 2010] even if local movements as well as fusion/fission events between organelles have been observed [Platani, NCB, 2002; Brangwynne, PNAS, 2011].

As illustrated in this introduction, the intranuclear volume is filled with a variety of macromolecular objects which are highly heterogeneous in terms of spatial and temporal characteristics. We are currently missing an integrated model that would allow us to define the exact contribution of such heterogeneous crowding on the nuclear structure and functions. In the following, we will first present the theoretical and in-vitro data assessing the consequences of crowding on molecular concentration, diffusion and reaction kinetics. Second, we will describe the experimental results that contributed to the initial assessment of the contribution of molecular crowding on the reaction-diffusion dynamics of nuclear proteins. Finally, we will review the potential physiological roles of molecular crowding in the control of the nuclear architecture as well as in the regulation of the different cellular functions using DNA as a template such as transcription or DNA repair.

1. Macromolecular crowding in the nucleus : the predictions of the theoretical and in-vitro data

The fundamental difference between dilute and crowded solutions is the fraction of the volume which is occupied by inert co-solutes and thus, is not accessible to molecules of interest. A solution is considered crowded when this inaccessible volume fraction is above 20-30 %, which corresponds to concentrations of 200-300 $g.L^{-1}$ for background macromolecules of biological origin [Ellis, Trends Biochem Sci, 2001]. The crowding is not necessarily induced by a single type of macromolecules but can also originate from a mixture of different co-solutes. Based on this definition, the intracellular environment appears as a highly crowded environment. In *Escherichia coli*, the concentration of the biomacromolecules ranges between 250 and 350 $g.L^{-1}$ [Zimmermann,

JMB, 1991; Cayley, Biochem, 2003]. When considering the nucleus of eukaryotic cells, the chromatin itself already occupies 20 % to 50 % of the nuclear volume depending on the cell type [Lopez-Velazquez, Histochem Cell Biol, 1996; Rouquette, Chrom Res, 2009]. In such crowded environments, the reaction-diffusion dynamics of the biological molecules significantly differ from their behavior in dilute solutions [Minton, JCS, 2006]. Thus, macromolecular crowding is likely to impact any intracellular process by affecting the kinetics of the biochemical reactions.

In the following, we will introduce the generic predicted impact of crowding on reaction-diffusion molecular dynamics. At this step, we will consider that the only interaction between the different macromolecules present in the crowded volume is steric repulsion, disregarding any other interactions such as the hydrodynamic or electrostatic ones. The theory predicts that macromolecular crowding has three main consequences on reaction-diffusion dynamics: i) volume exclusion, ii) diffusion slowing down and iii) enhancement of binding rates [Minton, JCS, 2006].

1.2. Molecular crowding leads to volume exclusion

The origin of volume exclusion observed in crowded environments is straightforward. The higher the amount of background co-solutes, the less space is available for molecules of interest, leading to an exclusion of the latter from the crowded area. This means that even freely diffusing tracers will display an uneven steady-state concentration pattern in an environment characterized by an non-homogeneous degree of crowding. This may initially appear counter-intuitive considering that diffusion is supposed to smooth concentration gradients. Importantly, the level of volume exclusion is not only a function of the fraction of the volume occupied by the background macromolecules but also strongly depends on the size and shape of the molecules of interest that one tries to place in such crowded environment. If f_{bg} is the portion of the volume occupied by crowding agents, an infinitely small molecule of interest will have access to a volume fraction equal to $1\text{-}f_{bg}$. However, as the molecule of interest gets larger, the accessible fraction rapidly decreases to eventually reach zero [Hall, BBA, 2003].

1.3. The complex effect of crowding on molecular diffusion

The second predicted consequence of molecular crowding is the impediment of Brownian motion [Zimmerman, Annu Rev Biophys Biomol Struct, 1993]. Indeed, it is more difficult to navigate through a crowded environment in which background macromolecules act as obstacles hindering the movements of diffusive tracers, than in a dilute solution. In contrast to volume exclusion, which

can be estimated theoretically quite precisely based on the characteristics of the background and tracer molecules [Hall, BBA, 2003], it is difficult to quantitatively predict how crowding impacts on the motions of Brownian tracers [Muramatsu, PNAS, 1998 ; Phillies, J Chem Phys, 1985]. Nevertheless, both theoretical and in-vitro studies indicate that the amplitude of the diffusion hindrance, estimated as the ratio between the diffusion coefficient measured in the crowded medium versus in water, depends not only on the concentration of the background molecules but also on their structural characteristics [Phillies, J Chem Phys, 1985]. Most of these works also predicts that the larger the tracer, the more hindered the diffusion is in a given crowded environment [Muramatsu, PNAS, 1998 ; Ando, PNAS, 2010 ; Trovato BJ, 2014].

So far, we assumed that the diffusion in crowded solutions was purely Brownian and thus can be fully characterized by the value of the diffusion coefficient. However, a recurring debate in the field is whether crowding can lead to subdiffusive dynamics, also referred as anomalous diffusion [Dix, Annu Rev Biophys, 2008 ; Saxton, ,Biophys J, 2012 ; Huet Int Rev Cell Mol, Biol, 2014]. The classical way to assess anomalous diffusion is to calculate the mean square displacement (MSD) curves from the tracer trajectories according to the following equation:

$$MSD(n\delta t)=\frac{1}{N-n}\sum_{i=1}^{3}\sum_{j=1}^{n-N}[x_i((j+n)\delta t)-x_i(j\delta t)]^2 \quad , \qquad (1)$$

where the tracer 3-dimensional positions along the trajectory are written as x_i with i =1,...,3, δt is the time interval between consecutive positions and N the total number of positions [Huet, BJ, 2006]. If the tracked object displays anomalous diffusion, the MSD curves follow a power law:

$$MSD(\Delta t)=A(\Delta t)^{\alpha} \qquad (2)$$

where α is called the anomalous coefficient. Pure Brownian motion corresponds to $\alpha = 1$. In this situation the prefactor $A = 6D$ where D is the diffusion coefficient. For subdiffusive behaviors, $0 < \alpha < 1$ and no proper diffusion coefficient value can be defined [Bouchaud, Phys. Rep. Rev. Sec. Phys. Lett., 2010]. In a situation where the crowding agents are immobile, 3-dimensional Monte-Carlo simulations and experimental measurements in *in-vitro* crowded media repeatedly reported anomalous diffusion arising from the "bounce" of the tracer on the fixed obstacles [Fatin-Rouge, BJ, 2004; Höfling, PRL, 2006]. Noteworthy, below the percolation threshold, diffusion is anomalous at intermediate timescales but returns to pure Brownian characteristics at long timescales [Höfling, Rep Prog Phys, 2013]. This crossover to pure diffusion is observed when the area explored by the tracer exceeds the characteristic size of the crowding structures and thus when the medium sensed by the tracer appears as an homogeneous viscous fluid [Banks, Soft Matt, 2016]. While, so far, we only considered fixed crowding structures, it is also important to point out that tracer diffusion is usually much less anomalous if the obstacles are left mobile [Vilaseca, PCCP,

2011]. Thus, the presence of large slow background molecules tends to induce subdiffusive behavior while smaller, more mobile crowders rather lead to a high viscosity, and then slow pure Brownian diffusion [Banks, Biophys J, 2005]. More recently, experiments performed in model crowded media close to the glass transition also demonstrated that the size asymmetry between the tracer and the crowding agents has a critical influence on diffusion anomality [Sentjabrskaja, NatComm, 2016]. Given the complexity and heterogeneity of the cell interior, these *in-silico* and *in-vitro* results predict that crowding will have various effects on diffusion depending on the structural characteristics of the molecules which are considered [Hall, BiophysRev, 2010].

1.4. Macromolecular crowding can tune biochemical reaction rates

The last predicted effect of macromolecular crowding, which deals with reaction equilibria, might be the most relevant for cell physiology. In a crowded environment, freeing an empty space to accommodate a given molecule of interest costs free energy [Hall, BBA, 2003]. Yet, placing two reactants in a crowded medium requires to free a larger empty volume, and thus cost more free energy if the reactants are separated rather than if they are bound to each other. Consequently, the bound state is entropically favored in a crowded media as compared to a dilute one [Minton, Methods Enzymol, 1998]. In the case of a generic reaction A+B↔C characterized by a reaction constant $K=k_a/k_d$ with k_a and k_d the association and dissociation rates, one can usually consider that the activated state complex AB* and the product C occupy similar volumes [Minton, Mol Cell Biochem, 1983]. The presence of crowding agents, assuming only steric interactions with the reaction components, will favor the complex AB* over the separated reactants A+B due to the smaller free volume required to accommodate AB*. This will lead to an increase of k_a. Instead, since the occupied volumes are similar between AB* and C, crowding will not affect k_d. Ultimately, the macromolecular crowding will thus displace the reaction towards the product with a reaction constant K that can be increased by several orders of magnitudes as compared to its value in a dilute environment [Minton, Methods Enzymol, 1998]. Multiple experiments in model environments confirm that crowding strongly influence not only inter-molecular binding kinetics but also macromolecular folding [Zhou, FEBS Lett, 2013].

So far, we have assumed that the kinetics of biochemical reactions are governed solely by the time required to "chemically transform" reactants into products. By doing so, we assumed that the time needed for the reactants to meet each other, which is an obvious prerequisite for the reaction to happen, is negligible. However, this search time might need to be taken into account if reactant diffusion is slowed down, as it occurs in crowded solutions. In the general case, for the generic

reaction A+B↔C mentioned above, the association rate k_a follows the equation:

$$k_a = \frac{k_D k_{react}}{k_D + k_{react}} \quad , \tag{3}$$

where k_D and k_{react} are the association rates obtained in the two extreme cases when the reaction speed is either only limited by diffusion ($k_D >> k_{react}$) or by the chemical reaction ($k_{react} >> k_D$), respectively [Zhou Annu Rev Biophys, 2008]. In a more crowded environment, k_{react} will increase, as discussed in the previous paragraph, but instead, k_D will decrease due to the negative impact of crowding on the mobility of the reactants. Consequently, two regimes are often observed when plotting the association rate k_a as a function of the amount of crowding macromolecules. k_a first increases with crowding but above a certain threshold, the negative impact of crowding on diffusion tends to slow down the association kinetics to ultimately completely prevent any chemical reactions due to the impossibility for the reactants to meet each other [Ellis, Trends Biochem Sci, 2001]. The contribution of diffusion appears particularly relevant to biochemical reactions in the case of the cell nucleus given that the dynamics of many chromatin interacting proteins seems limited by diffusion [Beaudouin, BJ, 2006]. The previous section has also shown that macromolecular crowding may not only slow down diffusion, but also lead to diffusion anomality. Biochemical reactions impacted by the anomalous diffusion of their components are thought to follow particular kinetics often referred as "fractal kinetics" [Kopelman, Science, 1988]. In such situation, the association rates are not constant but decrease with time in relation to the fact that, in the anomalous diffusion regime, it becomes increasingly difficult to explore larger area in comparison to pure Brownian motion.

1.5. The impact of crowding on macromolecular dynamics strongly depends on the physicochemical properties of the crowding agents

In the previous sections, we only considered the influence on reaction-diffusion dynamics of the steric repulsion by the crowding agents. Even though such steric component will always be present, it may be counterbalanced or reinforced by other types of interactions between the molecules of interest and the crowding agents. This is particularly critical when considering the impact of molecular crowding on reaction rates. Indeed, for example, attractive interactions with the crowding agents will lower the free energy of the reactants or products of the reaction as compared to a dilute situation leading to a displacement of the chemical equilibrium [Minton, JCS, 2006]. Due to the high amount of background molecules, even weak short-distance interactions with any of the reaction components can potentially strongly influence not only the reaction rates but also the diffusion of the molecules of interest [Trovato, Biophys J, 2014]. Another aspect that we

disregarded so far is the spatial distribution of the crowding agents. Indeed, we have assumed that the crowded environment is a well-mixed solution in which the background molecules are randomly positioned. Such simplified medium strongly differs from the complex multiscale spatial organization characterizing the intra-nuclear space. Yet, theoretical and in-vitro studies have demonstrated that the spatial distribution of the crowding molecules has a major influence on the diffusion characteristics of mobile tracers [Fatin-Rouge, BJ, 2007; Hofling, RepProgPhys, 2013] and thus on the time required for a given diffusing molecule A to find its target B [Condamin, PNAS, 2008], a mandatory step to initiate the reaction between A and B.

2. Current experimental evidences of the impact of crowding on molecular dynamics in the cell nucleus

While theoretical and in-vitro studies have flourished over the past three decades to describe the impact of crowding on reaction-diffusion kinetics, experimental work exploring this question in the nucleus of living cells remain relatively sparse.

2.1. Assessing volume exclusion inside the nucleus

Chromatin is supposedly the most predominant crowding agent within the nucleus, displaying concentrations ranging from ~ 100 mg/mL to ~ 400 mg/mL [Dahan, Biochemistry, 2000]. Nevertheless, other components, such as transcription complexes and ribosomal subunits in the case of the nucleoli [Andersen, Nature, 2005], are also thought to contribute to crowding. Due to the heterogeneous distribution of these crowding elements, molecules navigating through the nucleus are thought to experience variable levels of macromolecular crowding. Fluorescently labeled dextrans were found partially excluded from chromatin rich regions, as well as in the nucleoli, suggesting enhanced molecular crowding in these areas [Görisch , Exp Cell Res, 2005 ; Verschure, EMBO Rep, 2003]. The volume exclusion was increased with the size of the tracers in agreement with the theoretical predictions [Bancaud, EMBOJ, 2009]. Interestingly, nuclear proteins [Verschure, EMBO Rep, 2003] or highly charged tracers [Görisch, Exp Cell Res, 2005] displayed nuclear distributions markedly different from the ones obtained for neutral dextrans, suggesting that, as discussed in the previous section, the contribution of macromolecular crowding strongly depends on the interactions between the tracers and the crowding agents. Furthermore, the level of exclusion of inert tracers was shown to be modified when altering the level of chromatin compaction by different means [Gorish, JCS 2005; Martin, FASEB J, 2010; Walter, JSB, 2013], confirming that chromatin is the main crowding agent in the nucleus.

2.2. Diffusion hindrance inside the nucleus

The local diffusion of tracers of different molecular weights was assessed in cells by fluorescence recovery after photobleaching (FRAP) [Seksek, JCB, 1997] and fluorescence correlation spectroscopy (FCS) [Pack, BJ, 2006]. By dividing diffusion coefficients measured in cells with those obtained in water, one could estimate the diffusion hindrance due to the intracellular medium. For tracers up to 500 kD, diffusion coefficients measured in cells are three to four times lower than in water [Seksek JCB, 1997; Bancaud, EMBOJ, 2009]. Diffusion hindrance appears slightly more pronounced in the nucleoplasm compared to the cytoplasm, suggesting a higher level of macromolecular crowding in the former compartment [Pack, BJ, 2006]. Assessing the mobility of GFP multimers within the nucleus demonstrated an enhancement of the diffusion hindrance in supposedly highly crowded nuclear areas such as the nucleoli and the heterochromatin foci [Bancaud, EMBOJ, 2009]. In line with the observations regarding volume exclusion, it was also shown that the denser chromatin packing characterizing heterochromatin foci is responsible for the enhanced crowding-induced diffusion hindrance observed in heterochromatin compared to euchromatin [Walter, JSB, 2013]. These results demonstrate that intranuclear crowding, which is induced principally by chromatin, impairs diffusion in agreement with theoretical predictions. Interestingly, while diffusion hindrance varies within the nucleus, it seems largely independent of the tracer size [Pack, BJ, 2006]. This surprising behavior, which appears generic to the intracellular medium since it is also observed in the cytoplasm [Seksek JCB, 1997], contrasts with many theoretical works aiming at simulating the intracellular molecular dynamics which predicts that diffusion hindrance should increase with the size of the tracer [Ando, PNAS, 2010 ; Trovato BJ, 2014]. This discrepancy may arises from the complex spatial organization of the intracellular components impeding diffusion as well as from weak interactions between the tracers and the crowding agents [Ando, PNAS, 2010].

We showed in section 1.2.2. that crowding is predicted to affect diffusion not only quantitatively but also qualitatively by leading to anomalous diffusion. Such anomalous behavior is indeed observed inside the nucleus using FCS, that probes diffusion characteristics within a confocal volume of ~250 nm width and ~1µm height [Wachsmuth , JMolBiol, 2000]. Using fluorescence redistribution after photobleaching or photoactivation (FRAP) methods, anomalous diffusion was also reported in the nucleus when probing local areas similar to those probed by FCS [Daddysman, J PhysChemB, 2013]. Instead, FRAP redistribution kinetics measured for larger nuclear areas rather follow pure diffusion models [Beaudouin, BJ, 2006]. Such crossover from anomalous to pure diffusion fits

nicely with the predictions for spatially organized crowded media and suggests that the largest chromatin structures sensed by the molecules navigating inside the nucleus are ~1 μm in size. Above this characteristic size, the nucleus can be viewed as an homogeneous viscous medium. Importantly, this model is not supported by all results obtained by single particle tracking, which in principle allows access to all space scales. While initial works analyzing the movements of large tracers (quantum-dots, tagged mRNA or nuclear organelles) reported anomalous diffusion followed by pure Brownian motion at long timescales [Platani, JCB, 2000 ; Ishihama, BBRC, 2009 ; Bancaud, EMBOJ, 2009], more recent publications rather suggest that small tracers (size equivalent to a single GFP) follow pure Brownian motion at all timescales [Izeddin, Elife, 2014] and that the anomalous behavior is the consequence of transient unspecific binding to chromatin [Normanno, Nat Comm, 2015]. These discrepancies call for more systematic analysis of the movements of diffusing single molecules inside the nucleus using tools going beyond the classical MSD. In particular, the characterization of the diffusion propagator appears instrumental to establish the exact origin of anomalous behavior: impeded motion in crowded structures with fractal characteristics, transient trapping within short live cages created by mobile crowding agents, unspecific binding, etc. [Mitra, PRL, 1992 ; Szymanski, PRL, 2009 ; Banks, Sof Mat, 2016]. This approach may even uncover anomalous microscopic dynamics despite linear, pure Brownian, MSD curves [Chubynsky, PRL, 2014], a behavior which is observed in colloidal suspensions that are thought to share common traits with the crowded intracellular environment [Kwong, J Phys Chem B, 2014].

2.3. Reaction kinetics in the crowded nucleus

Synthetic data mimicking the complex intracellular medium indicates that macromolecular crowding is a crucial regulator of biochemical reaction kinetics [Tan, NatNanotech, 2013 ; Hansen, ChemBioChem, 2016] but direct experimental evidences confirming this result in living cells remain sparse. While Bancaud et al. reported enhanced binding of generic chromatin-interacting proteins into dense heterochromatin foci as compared to euchromatin [Bancaud, EMBOJ, 2009], other publications studying association kinetics of DNA molecules [Schoen, PNAS, 2009] or proteins [Sudhaharan, JBiolChem, 2009 ; Phillip, PNAS, 2012] reported little differences in the cell nucleus or cytoplasm compared to diluted in-vitro solutions, suggesting that crowding does not significantly affect reaction rates in the cell [Phillip, FEBS Lett, 2013]. One should nevertheless bear in mind that crowding is expected to have two opposite effects on reaction kinetics: the entropy-driven shift towards bound states may be compensated by the slowing-down of encountering rates [Tabaka, Frontiers in Physics, 2014]. Recent work performed on flexible

molecular crowding probes show that compact conformations are favored in the nucleus and, to a smaller extent, in the cytoplasm, compared to dilute solutions [Boersma, NatMeth, 2015 ; Konig, NatMeth, 2015]. Translating this result in the context of bimolecular interactions implies that once two reactants have encountered each other, the intracellular crowding should favor the compact bound state over the, more extended, unbound state. Regarding the encountering rates, the slowing down of diffusion in the intracellular medium compared to water that was described in the previous paragraph will most probably influence the time required for two interacting partners to meet each others. In the case of the nucleus, it was shown that proteins interacting with chromatin can display fractal binding kinetics related to the anomality of the diffusion in the crowded nuclear environment [Bancaud, EMBOJ, 2009].

Considering that the dynamics of many chromatin-interacting proteins is limited by diffusion [Beaudouin et al., 2009], it will be crucial to improve our understanding of the exploration dynamics used by these proteins to find their target in the nucleus. Two types of exploration regimes are possible: compact and non-compact (Figure 4). In a compact regime, a protein searching for a binding site on the chromatin will screen all possible locations before exiting a given area while, in a non-compact situation, the search will leave some locations unvisited to allow exploration of a larger area [Benichou, NatChem, 2010]. A fundamental difference between these two regimes is the dependence of the time required to find an immobile target, often estimated by the mean first passage time (MFTP) towards the initial distance, d_0, between this target and the diffusing seeker. While the MFTP increases with d_0 in a compact regime in agreement to intuitive expectations, it is independent of d_0 for non-compact exploration [Condamin, PNAS, 2008]. This unexpected behavior may have major implications in situations where a given protein has several potential binding sites differentially located within the nucleus [Benichou, NatChem, 2010]. Recent experimental work suggest that the search strategies differ from one chromatin-binding protein to another [Izeddin, ELife, 2015] and also depend on the local chromatin structure, with more compact explorations observed in dense heterochromatin foci [Bancaud, EMBOJ, 2009 ; Knight, Science 2015].

3. A physiological role for macromolecular crowding inside the nucleus ?

We have seen in the last sections that many of the theoretical predictions concerning the consequences of intracellular molecular crowding on molecular reaction-diffusion kinetics have been confirmed experimentally, in particular in the case of the cell nucleus. Nevertheless, one may wonder if this impact of crowding on the way molecules diffuse and interact with partners has

physiological consequences or regulates cellular functions. The easiest way to tune intracellular molecular crowding is to change the cell volume. Such changes can be induced artificially by bathing cells with hypo- or hypertonic media [Walter, J Struct Biol, 2013], but also occur naturally during the cell life via multiple pathways regulating the cellular volume [Finan, J Cell Biochem, 2010]. Tuning the cellular volume is known to have dramatic physiological consequences that cannot be simply explained by mass action laws, but may reveal the non-linear dependence of reaction-diffusion kinetics to molecular crowding [Mourao, BJ, 2014]. A recent example of the potential physiological impact of molecular crowding is the transition from an active to a dormant state in yeast [Joyner, eLife, 2016] and bacteria [Parry, Cell, 2014]. Even if the exact mechanism is still debated [Munder, Elife, 2016], it seems that entry into dormancy is associated with an increase in intracellular crowding induced by cell shrinking, which in turn leads to the freezing of metabolic activities due to slowing down of molecular diffusivity [Joyner, eLife, 2016]. This sharp change in the diffusion properties upon cell shrinking, which is also observed in higher eukaryotes [Zhou, PNAS, 2009], has been interpreted as a glass-transition from a liquid-like to a solid-like state of the intracellular medium [Parry, Cell, 2014]. More specifically, molecular crowding also appear as a key regulator of particular functions such as cell growth [Klumpp, PNAS, 2013] or nucleo-cytoplasmic signaling [Miermont, PNAS, 2013]. In the following, we will review the recent findings demonstrating the role played by molecular crowding in the regulation of nuclear structure and function.

3.1. Molecular crowding influences the nuclear architecture

Several recent findings indicate that the intranuclear crowding has a major influence on the multiple folding levels displayed by chromatin. One recurring debate in the chromatin community is the relevance of the compact 30-nm fiber model to describe the spatial organization of the nucleosomes along the chromatin fiber. While the chromatin spontaneously folds into a 30-nm fiber in dilute *in-vitro* media, this specific conformation is often not observed in the dense nucleus [Fussner, EMBORep, 2012]. To resolve this apparent discrepancy, Maeshima et al. proposed a model in which, in the highly crowded nucleus, inter-fiber nucleosome-nucleosome interactions are favored over intra-fiber interactions leading to a loose 10-nm chromatin fiber instead of the compact 30-nm fiber observed in a dilute medium where intra-fiber interactions dominate [Maeshima, Chromosoma, 2014]. This model is supported by the recent observation that polynucleosome arrays tend to self-assemble into structures lacking 30-nm fibers [Maeshima, EMBOJ, 2016], a process that is promoted by molecular crowding [Hancock EBJ, 2008] and the presence of divalent cations [Hansen, Annu Rev Biophys Biomol Struct, 2002]. At larger scales, it is well established that

modifying the nuclear volume by subjecting cells to osmotic stress has a major impact on the chromatin compaction state [Walter, J Struct Biol, 2013]. Since these osmotic treatments modify both the crowding level and the ionic conditions, it is difficult to properly separate the contribution of these two parameters on the chromatin architecture. Nevertheless, chromatin decondensed by hypotonic treatment can recover its normal compaction state by adding crowding agents [Iborra, Theor Biol Med Mol, 2007], showing that crowding itself influences the chromatin structure.

The second nuclear structural characteristic that to be appears regulated by molecular crowding is the compartmentalization of the intranuclear space. The exact mechanisms driving the formation of the nuclear organelles remain unclear but a physical process that has recently gained interest to address this question is phase separation [Zhu, Curr Opin Cell Biol, 2015]. This concept is very common not only in the field of complex matter but also in our everyday life where it can be used to explain, for example, the progressive demixing of the aqueous and lipidic phases in a vinaigrette. Generally, in a liquid, molecules with different physicochemical characteristics will have the tendency to spontaneously segregate [Hyman, Annu Rev Cell Bio, 2014] thus counteracting diffusive intermingling. Multiple recent evidence strongly suggests that phase separation is a major driving-force in nuclear and cytoplasmic compartmentalization [Weber, Curr Biol, 2015]. If the physicochemical properties of the segregating molecules is the primary factor influencing phase separation [Nott, Mol Cell, 2015], other characteristics of the medium are also important, in particular, molecular crowding. In the context of the nuclear environment, *in-silico* simulations predict that crowding strongly promotes the formation of compartments by phase separation [Cho, BJ, 2012]. Experimentally, it was also shown that molecular crowding contributes to the formation and the maintenance of certain nuclear compartments such as the nucleolus [Hancock, J Struct Biol, 2004]. Nevertheless, this result does not seem generic to all compartments since the accumulation of heterochromatin scaffolding proteins into foci is independent of the crowding status of the nucleus [Walter, J Struct Biol, 2013]. Interestingly, phase separation may not only drive the formation of nuclear compartments composed of elementary diffusing components but could also be involved in the spatial organization of the chromatin fiber within the nucleus considering that polymers with different physicochemical or mechanical properties tend to segregate [Finan, Chrom Res, 2011].

3.2. Molecular crowding influences cellular functions using DNA as a template

Molecular crowding can potentially influence any cellular function requiring the assembly of macro-complexes composed of several partners as it is thought to impact on binding equilibria.

Several recent findings indicates that the impact of molecular crowding may be particularly crucial in nuclear functions involving DNA transactions.

It has been known for more than a decade that the activation of gene transcription is often associated with local chromatin relaxation [Chambeyron, Genes Dev, 2004 ; Hu, JCB, 2009]. Together with the well-known observation that the transcriptionally silent heterochromatin displays a more compact state than the transcriptionally active euchromatin, these different results suggest a straightforward model in which the high crowding due to chromatin compaction prevents transcription factors to access their DNA target sequences thus requiring chromatin relaxation prior to transcription initiation. However, knowing that the transcription machinery actively remodels the chromatin fiber at the molecular level, it is also possible that chromatin relaxation is just the consequence of the transcription process. Definitive evidence to decide between these two alternative models are still missing. Nevertheless, it was recent reported that modulating the chromatin compaction state by osmotic stress or mechanical stretching is sufficient to tune transcription activity [Tajik, Nat Mat, 2016 ; Hausnerov, BiolCell, 2017], demonstrating the crowding induced by chromatin compaction directly influences transcription. Beside this regulatory role, results obtained in synthetic cells also predicts that crowding reduces gene expression cell-to-cell variability and thus contributes to the robustness of the cellular transcriptional pattern [Tan, Nature Nanotech, 2013]. This increased robustness seems related to the impact of crowding on the diffusion of transcription factors [Golkaram, PLOS Comput Biol, 2016] which could influence the mode of exploration used by these transcription factors to find their DNA target sequences [Meyer, BiophysJ, 2012]. Future work performed in living samples should allow validation of this regulation of the gene expression noise by molecular crowding.

Another key cellular function which appears to be influenced by molecular crowding is the DNA repair process. One of the earliest event characterizing the activation of the cellular response to DNA damage is the active remodeling of the chromatin leading to its rapid relaxation in the vicinity of the DNA lesions [Sellou, MBoC, 2016]. Impairing this chromatin relaxation process inhibits the recruitment of some pioneering DNA repair factors to the DNA lesions and reduces DNA repair efficiency [Murr, NCB, 2006], a phenotype that can be rescued by pre-decondensing the chromatin structure prior to DNA damage induction [Murr, NCB, 2006]. If these results clearly support the idea that the early chromatin relaxation allows reducing local molecular crowding to promote access to DNA lesions, this simple generic model is difficult to reconcile with several other findings. First, inhibiting chromatin relaxation at DNA lesions impairs the recruitment of some repair factors while others accumulate normally [Luijsterburg, EMBO J, 2012]. Moreover, Burgess

et al. have shown that the recruitment of some repair factors is actually triggered by the chromatin recondensation process that follows the initial relaxation phase [Burgess, Cell Rep, 2014]. These data imply that increasing accessibility to DNA lesions by lowering local crowding is not a necessary step for the recruitment of all repair proteins. Future work will be necessary to understand this differential impact of the chromatin compaction state on the recruitment of the repair factors at DNA lesions. It might also contribute to validate the interesting possibility that the chromatin relaxation step is involved in the choice of the repair pathway [Khurana, Cell Rep, 2014].

Conclusions and future challenges

Considering the high degree of crowding encountered by biomolecules inside the nucleus, it was not completely unexpected to find that the reaction-diffusion dynamics displayed by these molecules in such crowded environment differ from those measured in dilute medium. However, as shown in this review, it is only recently that we have started to quantitatively assess the specific impact of macromolecular crowding on the diffusion and binding equilibria inside the cell nucleus. Nevertheless, since it is usually very difficult to distinguish the effect of steric hindrance due to molecular crowding from other types of weak attractive or repulsive interactions, more work will be necessary to define whether the impact of molecular crowding on the reaction-diffusion kinetics estimated so far for particular nuclear probes is also relevant other biomolecules. Establishing such a generalized description of the contribution of macromolecular crowding to the dynamics of nuclear biomolecules would be essential to properly interpret the recent findings pointing towards a central role for crowding in the maintenance of the nuclear architecture and in the regulation of several physiological functions occurring inside the nucleus.

Another aspect of this question that would benefit from future in-depth investigations is the assessment of the specific contribution of chromatin to the crowding state of the nucleus compared to other types of macromolecules present inside this organelle. Indeed, if our current simplified view of the nucleus assumes that the chromatin fiber that fills the nucleus is the only crowding agent present in the nucleus, we have currently no idea of the contribution of other biomolecules such as RNAs or diffusing protein complexes. The observation that the nucleolus, that is largely devoid of chromatin but filled with high densities of RNA and proteins, is characterized by a high degree of crowding [Bancaud, EMBOJ, 2009] plaids in favor of such precise analysis of the relative contribution of the main nuclear components to molecular crowding.

Finally, since we have shown in this review that the consequences of molecular crowding on

reaction-diffusion kinetics depend not only on the amount of crowding agents but also on their spatial distribution and dynamic properties, the analysis of the contribution of molecular crowding to nuclear functions would greatly benefit from the drawing of a precise map of the nuclear topography. This question has made tremendous progress over the last years [Sexton, Cell, 2015] and investigating the influence of this refined nuclear organization on the diffusion properties and binding kinetics of biomolecules navigating through the nucleus presents itself as the next important step in furthering our understanding of the functional and structural roles of crowding inside the nucleus.

Figure legends

Figure 1: Molecular crowding induces volume exclusion. (A) The space available in a given volume, represented in light green on the sketch, depends on the amount of background co-solutes present in this volume. For a given probe, the presence of each background molecule creates an exclusion area, represented by the dotted circle, whose radius is the sum of the radii of the background and probe molecules. (B) The volume exclusion is stronger for larger molecular probes.

Figure 2: Molecular crowding slows down diffusion. In the presence of small mobile background molecules, the probe displays pure diffusion with a reduced diffusion coefficient as compared to the one measured in the absence of crowding agents. If the background co-solutes are largely immobile, the diffusion of the probe becomes anomalous as shown by the downward curvature of the MSD curve.

Figure 3: Molecular crowding favors bound states. Energy diagram for a generic bimolecular reaction $A+B \leftrightarrow C$ in a dilute or crowded solution. The increase in free energy of each state in the presence of the background molecules depends on the volume required to accommodate the reaction components in the crowded environment. This volume is equal to V_A+V_B for the reactants, V_{AB*} for transition state and V_C for the product. Since $V_A+V_B > V_{AB*}$ while $V_{AB*} \approx V_C$, the gain in free energy is more pronounced for the reactants than for the transition state or the product. Consequently, the reaction equilibrium is shifted towards the product in the presence of crowding agents.

Figure 4: The architecture of the crowding structures as well as the diffusion characteristics of the chromatin-interacting proteins dictate the exploration regime displayed by the proteins to find their target on the chromatin. The sketch illustrates the two alternative exploration regimes: compact and non-compact.

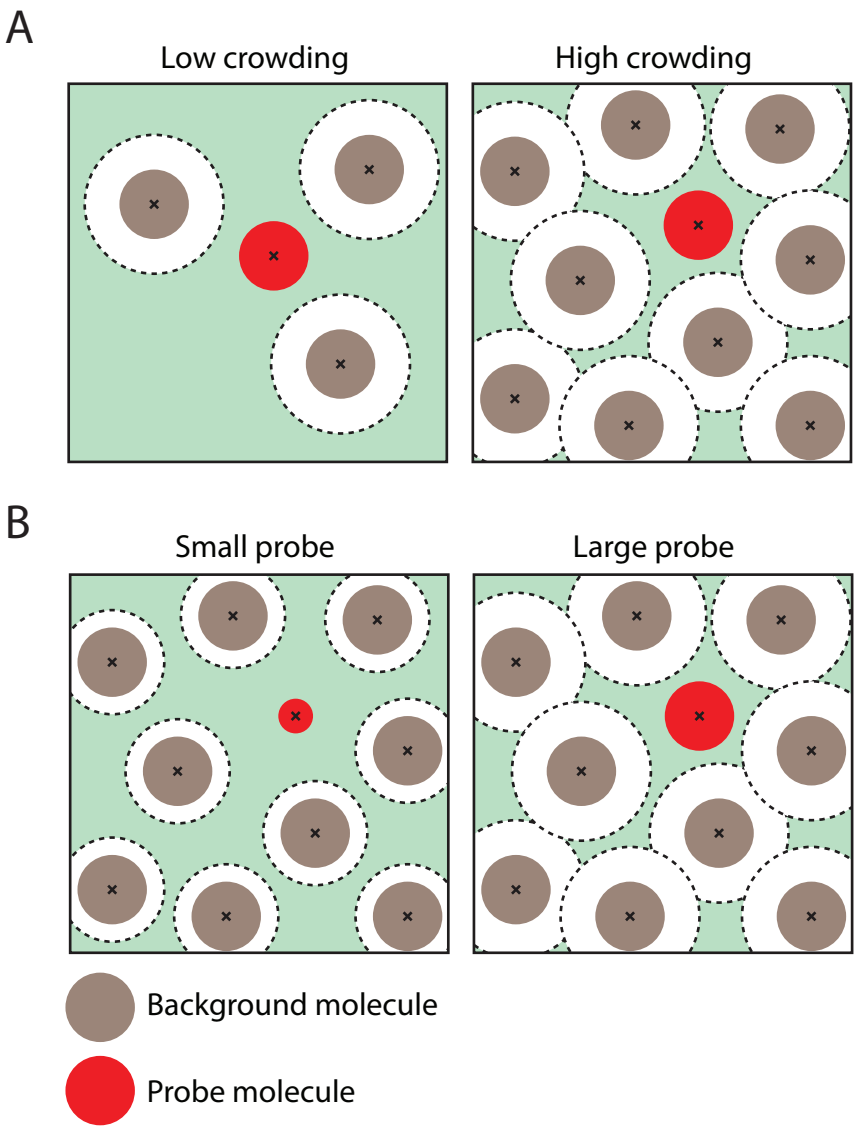
A
Low crowding
High crowding
B
Small probe
Large probe
Background molecule
Probe molecule

Figure 1

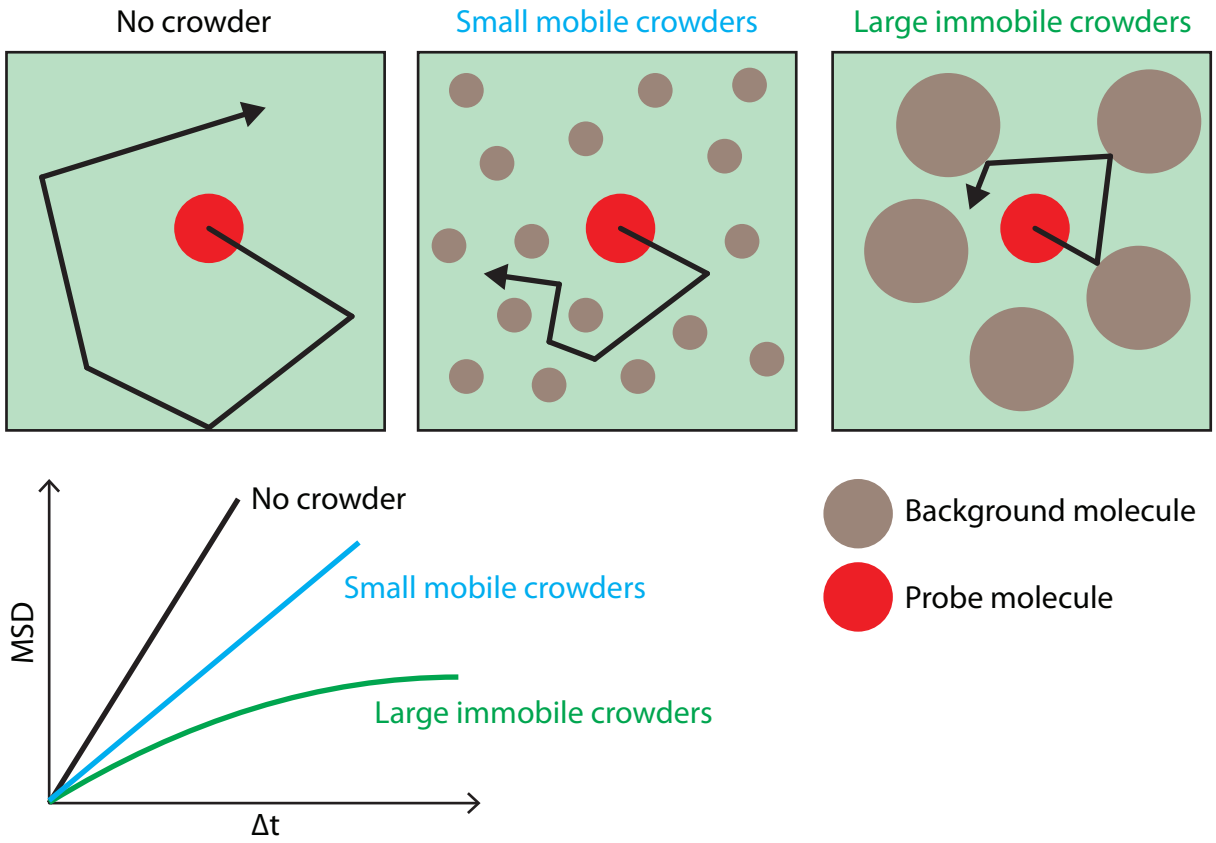
No crowder
Small mobile crowders
Large immobile crowders
MSD
Δt
No crowder
Small mobile crowders
Large immobile crowders
Background molecule
Probe molecule

Figure 2

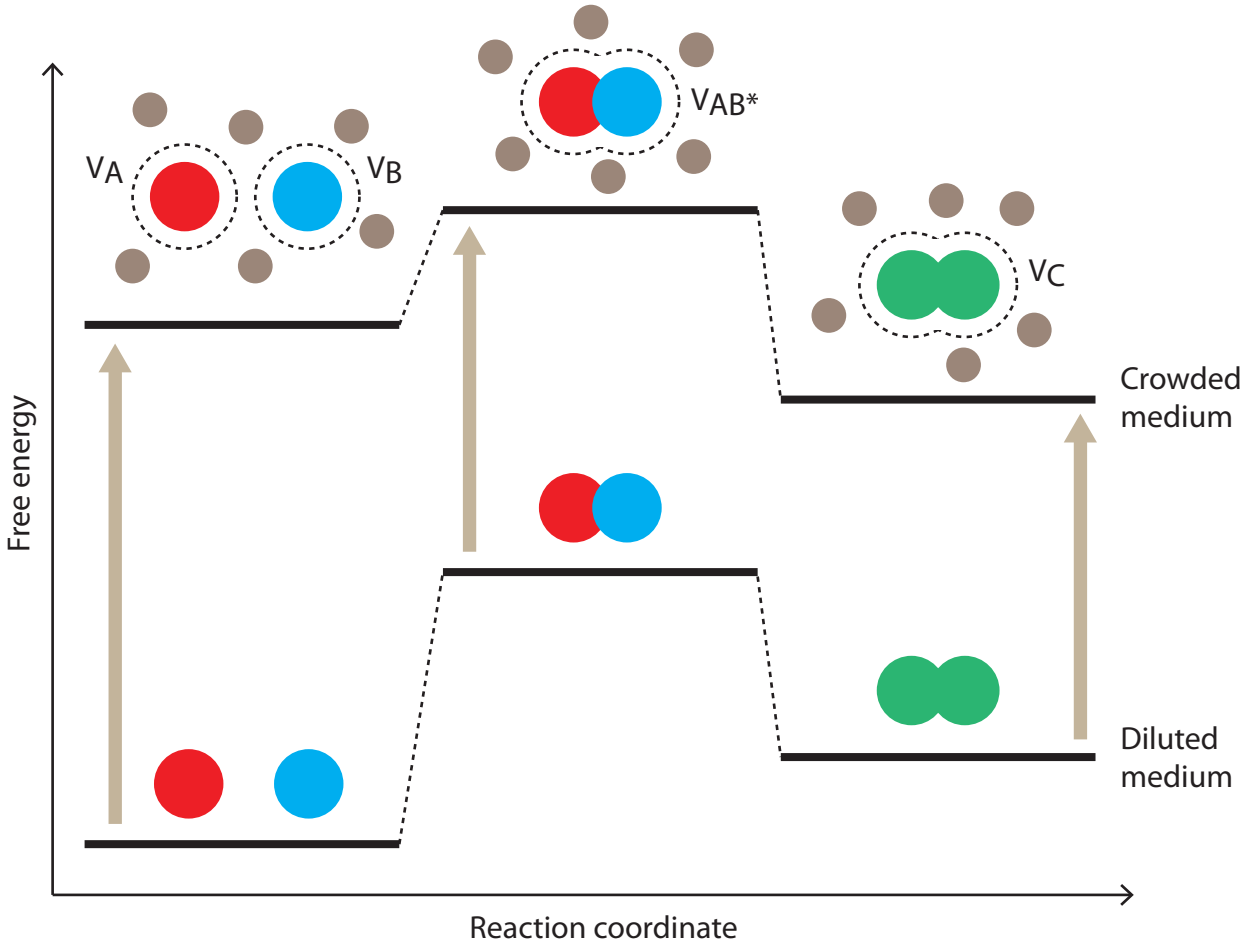
VA
VB
VAB*
VC
Crowded medium
Diluted medium
Free energy
Reaction coordinate

Figure 3

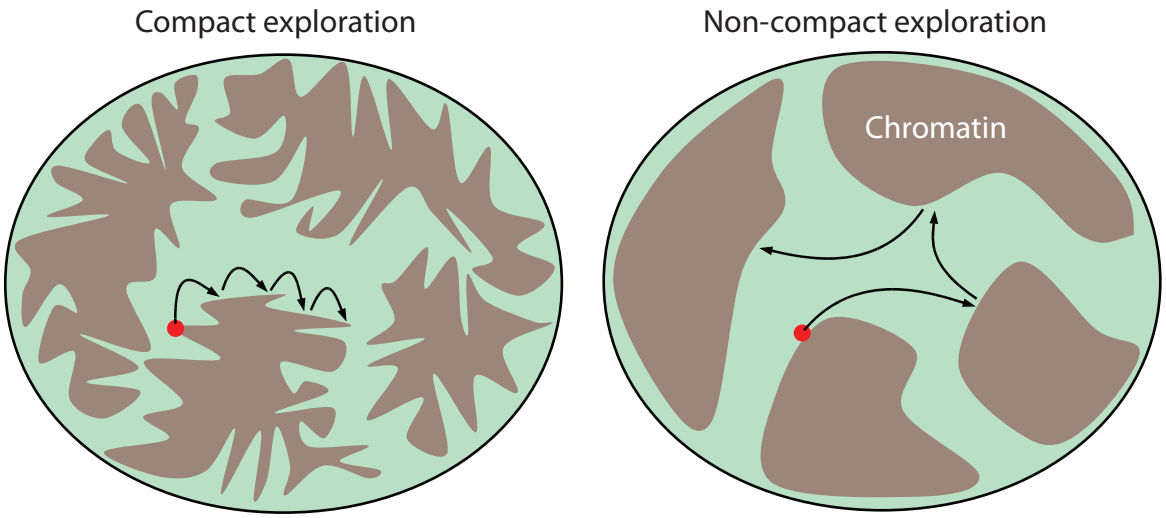

Figure 4